# Amplifying the Innate Immune Response

—

# Cell-Cell Propagation of Proinflammatory Signals during Bacterial Infection

Inauguraldissertation

zur
Erlangung der Würde eines Doktors der Philosophie
vorgelegt der
Philosophisch-Naturwissenschaftlichen Fakultät
der Universität Basel

von
**Christoph Alexander Kasper**
aus Zetzwil AG


BASEL, 2012

Genehmigt von der Philosophisch-Naturwissenschaftlichen Fakultät

auf Antrag von:

Prof. Dr. Cécile Arrieumerlou
*Dissertationsleiterin*
Prof. Dr. Christoph Dehio
*Korreferent*

Basel, den 27.03.2012

Prof. Dr. Martin Spiess
*Dekan*

# Abstract

The enteroinvasive bacterium *Shigella flexneri* uses multiple secreted effector proteins to downregulate interleukin-8 (IL-8) expression in infected epithelial cells. Nevertheless, massive IL-8 secretion is observed in shigellosis. In this thesis, a novel host mechanism of cell-cell communication that circumvents the effectors and strongly amplifies IL-8 expression during bacterial infection is reported. By monitoring proinflammatory signals at the single-cell level during *Shigella* infection, we found that activation of the transcription factor NF-$\kappa$B and the MAP kinases JNK, ERK and p38 rapidly propagates from infected to uninfected adjacent cells leading to massive IL-8 production by uninfected bystander cells. Bystander IL-8 production was also observed during *Listeria monocytogenes* and *Salmonella typhimurium* infection. It was reproduced by microinjection of the Nod1 ligand L-Ala-D-$\gamma$-Glu-meso-diaminopimelic acid and blocked by gap junction inhibitors. Thus, a novel gap junction-mediated mechanism of cell-cell communication was identified that broadly amplifies innate immunity against bacterial infection by rapidly spreading proinflammatory signals to yet uninfected cells.

# Thesis statement

The work presented here was performed in the group of Prof. Cécile Arrieumerlou in the Focal Area of Infection Biology at the Biozentrum of the University of Basel, Switzerland. My PhD was supervised by a thesis committee consisting of:

Prof. Cécile Arrieumerlou
Prof. Christoph Dehio
Prof. Dirk Bumann

The present thesis is written in cumulative format. The first chapter introduces the major topics related to my work, whereas the following chapters illustrate the results of my research consisting of a published article and preliminary results from a second project. Finally, the major aspects of my thesis are discussed and future project directions are provided. An additional publication, to which I have contributed, is contained in the Appendix. For reasons of readability, not all abbreviations are written out in full, but instead a comprehensive glossary of abbreviations can be found at the end of the thesis.

# Contents

# Chapter I

# Introduction

# 1 Preface

Amongst the top ten causes of death worldwide, infectious diseases are prominently represented. In developing countries, lower respiratory infections, diarrhoeal diseases and HIV are the three major causes for death (Fact Sheet N°310, WHO, 2008). At the same time, multi-drug resistances present a severe and progressive problem worldwide. However, the increasing need for new antibiotics is in sharp contrast to the development of such drugs, which has been decreasing since the 1980s and has almost run dry with as little as four new classes of antibiotics approved during the last ten years[1]. The efficient treatment of infectious diseases is therefore likely to be considered one of the major challenges in global health of the coming decades.

The low number of newly available antibiotics in combination with the alarmingly fast emergence of resistances suggests that common principles of antibiotic drug development need to be revised and new strategies have to be exploited. Besides the 'classical' screens for new compounds and the chemical modification of known antibiotics, more effort has been expended in screening natural compounds. The search for drugs, which can support or even potentiate the activity of antibiotics as well holds promise[2]. Still, most of these efforts might result in therapeutics that are rapidly challenged by microbial resistance mechanisms. It seems therefore worth searching for drug targets that are not subject to rapid adaption by the pathogen. Intensive research in the field of infection biology has revealed that bacteria and viruses exploit various host factors to evade the immune system, infect cells and replicate. These host factors, which include receptors and signaling proteins, but also metabolites, represent prime targets for new antimicrobials. Yet, the host pathogen interaction is not a simple interplay between single components, but rather has to be understood as the integration of two complex networks. The identification of new drug targets therefore requires a system-level understanding of the host pathogen interaction. The InfectX project* currently pursues such an objective by identifying the host factors involved during cell invasion by various bacterial and viral pathogens. Chapter III of this thesis summarizes the results obtained so far for one of these pathogens, *Shigella flexneri*.

Besides the search for new antibiotics, the development of vaccines to control infectious diseases represents a main area of research. Vaccinations make use of the strongest and most precise weapon against infectious diseases, our own immune system. The importance of the immune system during infectious diseases is certainly not surprising, but is highlighted by the fact that bacterial and viral pathogens have developed a plethora of mechanisms that downmodulate or shape the host's immune response. Although these mechanisms often form the basis for a successful

*The InfectX project is funded by the Swiss Initiative in Systems Biology. More information about InfectX is available on the project homepage:
http://www.systemsx.ch/projects/systemsxch-projects/research-technology-and-development-projects-rtd/infectx/

infection, they might as well point out the pathogens Achilles' heel. Eventually, the components of the immune system targeted by the pathogen are likely to be the most effective in fighting the infection. Specifically enhancing and shaping the immune response during infection might therefore represent an elegant way of limiting the disease, similarly to how vaccines allow for a rapid response by priming the adaptive immune system. An example for such an approach is the enhancement of the antimicrobial peptide production by the intestinal epithelium[3].

Nonetheless, the precise mechanisms of how the various immune responses are controlled remain only partially understood. Intensive research during the past 20 years has unveiled the molecular mechanisms of pathogen recognition and the signaling cascades that are activated during infection. Nevertheless, a lot more is to be learned, for example how the fine balance between tolerance of commensals and detection of pathogens is achieved. A more complete understanding of the molecular mechanisms that control the immune system will not only have an impact on the field of infection biology, but also provide new insights into inflammatory disorders, autoimmune diseases and cancer. Chapter II of the present work focuses on the topic of inflammatory responses during bacterial infections and demonstrates that uninfected cells also participate in the initiation of immune responses.

# 2 Pathogen recognition by the innate immune system

Recognition of invading pathogens is the essential first step for initializing an immune response. It is therefore not surprising that evolution has brought forth several immune surveillance mechanisms. Central to these systems is the recognition of pathogen-associated molecular patterns (PAMPs). PAMPs are signature molecules, which are essential for pathogen survival and virulence, and are broadly shared among microorganisms. Immune cells, as well as epithelial cells, express several pathogen recognition receptors (PRRs) that can sense the presence of PAMPs. Intensive research over the past three decades has led to the discovery of entire families of PRRs that allow the detection of various PAMPs associated with bacteria and viruses, as well as fungi and parasites[4]. PRRs are generally classified into 4 families: Toll-like receptors (TLRs), C-type lectin receptors (CLRs), which are transmembrane receptors, and the soluble Nod-like receptors (NLRs) and RIG-I-like receptors (RLRs)[4,5]. An overview of PAMPs and their corresponding PRRs is presented in Table I.1.

Binding of PAMPs by the corresponding PRRs leads to downstream signaling events, which will mount an inflammatory response. Depending on the PRR that gets activated, a pathogen-specific immune response will be triggered that facilitates the eradication of the invader. Important mediators of the inflammatory response are cytokines, chemokines and type-I interferons, which get expressed and secreted upon pathogen recognition. These soluble mediators activate cells of the innate immune system and attract them to the site of infection[6,7]. Additionally, they contribute to the initiation of the second line of defense, the adaptive immune system[8]. Finally, certain PRRs also initiate cell death pathways, leading for example to pyroptosis in infected macrophages[9].

In the following sections, pathogen recognition by the different PRRs will be discussed in more detail. Furthermore, the intracellular signaling cascades, which are activated upon pathogen recognition, will be presented.

## 2.1 Pathogen recognition receptors

### 2.1.1 Toll-like receptors

TLRs were the first PRRs to be identified. In Drosophila, the Toll protein was found to play an important role in the antifungal response[10]. Shortly later, a human homologue was found that could induce both NF-$\kappa$B activation and the production of cytokines[11]. To date, 10 functional TLRs (TLR1-10) have been identified in humans covering a wide range of PAMPs[5]. TLR4, for instance, is able to detect bacterial lipopolysaccharide (LPS), TLR5 binds flagellin and TLR9 is able to rec-

**Table I.1 Detection of PAMPs by their corresponding PRR.**

| Species | PAMPs | PRRs |
|---|---|---|
| Bacteria | Lipoproteins | TLR2/1 |
| | LPS | TLR4 |
| | Flagellin | TLR5, NLRC4, NAIP |
| | Lipoteichoic acid | TLR2/6 |
| | RNA | TLR7, NLRP3 |
| | DNA | TLR9, AIM2 |
| | Peptidoglycan | NOD1, NOD2, NLRP1 |
| | T3SS basal body rod component | NLRC4 |
| Viruses | Structural protein | TLR2, TLR4 |
| | RNA | TLR3, TLR7, TLR8, RIG-I, MDA5, NOD2, NLRP3 |
| | DNA | TLR9, AIM2, DAI, IFI16 |
| Fungus | Zymosan | TLR2/6, Dectin-1 |
| | $\beta$-glucan | TLR2/6, Dectin-1, NLRP3 |
| | Mannan | TLR2, TLR4 |
| | DNA | TLR9 |
| | RNA | TLR7 |
| Parasites | tGPI-mutin (*Trypanosoma*) | TLR2 |
| | Glycoinositolphospholipids (*Trypanosoma*) | TLR4 |
| | DNA | TLR9 |
| | Hemozoin (*Plasmodium*) | TLR9, NLRP3 |
| | Profilin-like molecule (*Toxoplasma gondii*) | TLR11 |

*Adapted with modifications from Kawai and Akira*[5] *and Kumar et al.*[4].

ognize DNA. A complete overview of PAMPs recognized by TLRs can be found in Table I.1.

All members of the TLR family are type I transmembrane proteins that have an extracellular domain containing leucine-rich repeats (LRRs). The LRR domain is responsible for the detection of the corresponding PAMP. The cytosolic domain has high similarity to the cytoplasmic domain of the human IL-1 receptor and is therefore also called Toll-IL-1 receptor (TIR) domain[12,13]. Upon ligand binding, TLRs are known to form homo- and heterodimers (in the case of TLR2/1 and TLR2/6). Some TLRs additionally require co-receptors for efficient ligand binding. TLR4, for example, interacts with MD-2 for effective LPS recognition[12,14].

### Localization and signaling of Toll-like receptors

Although all TLR family members are transmembrane proteins, they obtain distinct localizations within the cell. The localization reflects primarily the availability of their ligands. TLR2/1, TLR2/6, TLR4 and TLR5, which are all located in the plasma membrane, detect ligands that are released from the cell surface of

pathogens (e.g. LPS or flagellin). TLR3, TLR7, TLR8 and TLR9 are targeted to intracellular vesicles where they detect nucleic acids that originate from invading viruses or from degradation of bacteria within lysosomes. The localization to intracellular vesicles furthermore prevents the detection of "self" RNA or DNA. For intracellular TLRs, the correct localization is crucial for becoming fully functional[5]. UNC93B1, a membrane protein found in the endoplasmatic reticulum (ER), was shown to interact with TLR3, TLR7 and TLR9 to control their trafficking from the ER to endosomes. Mutations in UNC93B1, which interfere with this function, abrogated cytokine production in response to TLR3, TLR7 and TLR9 ligands[15,16]. Recently, Ewald and colleagues have demonstrated that TLRs get processed by cathepsins and asparagine endopeptidases once reaching endosomal compartments. This processing is essential for generating functional receptors and emphasizes the importance of correct TLR localization[17]. A schematic representation of TLR localization within cells is presented in Figure I.1.

Upon ligand binding, TLRs initiate downstream signaling events that lead to a pathogen-specific inflammatory response. These signaling cascades are triggered by recruitment of a single or several adaptor proteins via TIR-TIR domain interactions [18]. Most TLRs (except for TLR3) recruit the MyD88 adaptor protein. MyD88, in turn, recruits IRAKs, TRAF6 and the TAK1 complex. The TAK1 complex consists of the MAP3 kinase TAK1, TAB1 and TAB2. Upon stimulation, TAK1 will lead to the activation of the IKK complex, which consists of IKK$\alpha$, IKK$\beta$ and NEMO. IKK$\beta$, in turn, will phosphorylate I$\kappa$B$\alpha$, the inhibitor of transcription factor NF-$\kappa$B. Upon phosphorylation, I$\kappa$B$\alpha$ is targeted for proteasomal degradation and NF-$\kappa$B will translocate to the nucleus. Additionally, the IKK complex contributes to the activation of MAP kinases p38, JNK and ERK. In concert, NF-$\kappa$B and the MAP kinases lead to the production and secretion of proinflammatory cytokines[5,19,20]. Alternatively, MyD88 can activate interferon regulatory factors (IRFs) like IRF3 and IRF7. These transcription factors lead to the expression of type I interferons. A similar pathway is initiated by the adaptor protein TRIF that becomes recruited to TLR3 and TLR4. TRIF activates IRF3 via TBK1 and IKK$\epsilon$. The receptor activated thus defines the kinds of cytokines that get produced, ensuring a pathogen-specific inflammatory response[5,19,20]. The downstream signaling cascades of TLRs are summarized in Figure I.1.

### Role of Toll-like receptors during bacterial infections

Bacterial infections can be detected by several TLRs. TLR4 binds LPS released from the surface of Gram-negative bacteria[21]. Heterodimers formed by TLR2 and TLR1 can detect lipopeptides from Gram-negative bacteria, while TLR2 and TLR6 heterodimers recognize lipopeptides released from Gram-positive bacteria[22]. Flagellin, the ligand for TLR5, is a major component of bacterial flagella[23]. TLR7 was reported to bind RNA of certain bacterial pathogens[24] and the ligand for TLR9

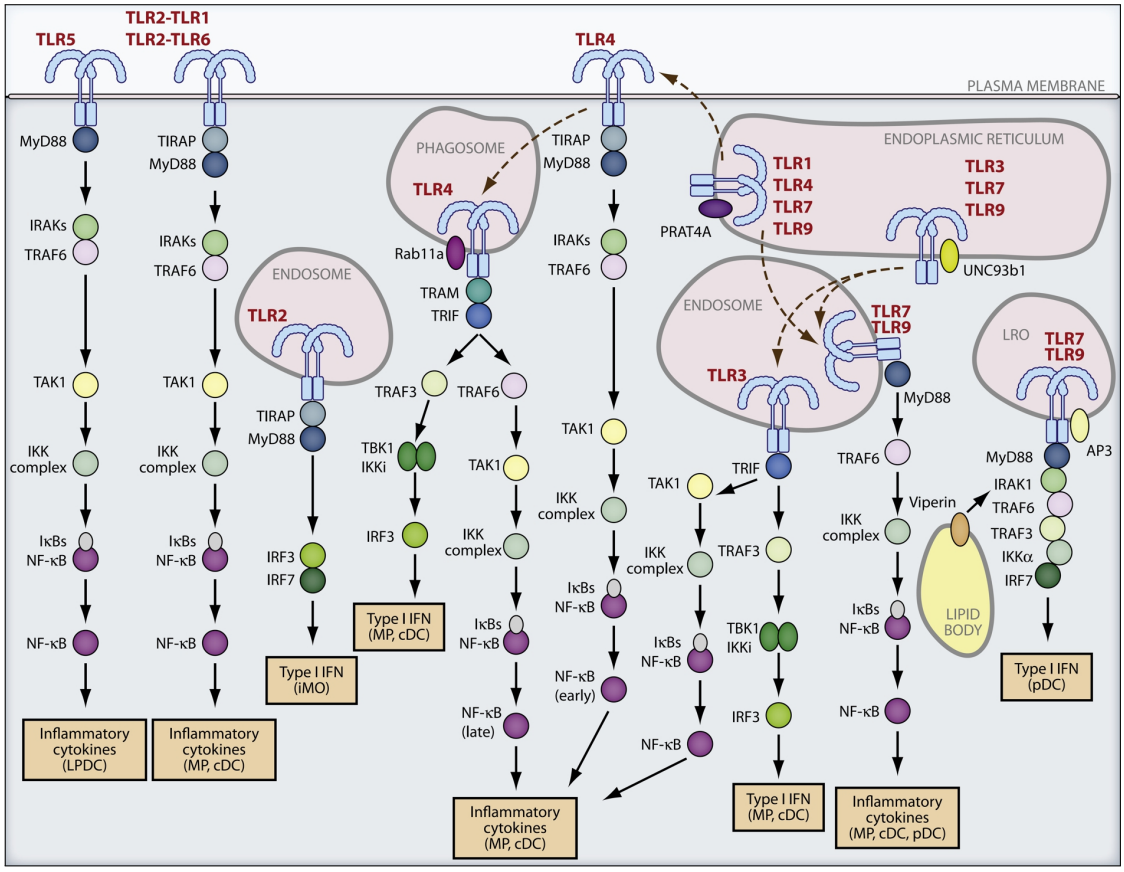


**Figure I.1 Localization, trafficking and signaling of Toll-like receptors.** TLR5, TLR2/1 and TLR2/6 are located in the plasma membrane. Upon ligand binding, they activate the canonical NF-$\kappa$B signaling cascade by interacting with the adaptor proteins MyD88 and TIRAP and by recruiting IRAKs and TRAF6. TLR2 homodimers are found in endosomes where they induce the production of type I interferons via IRF3 and IRF7 in response to viral infections. TLR4 localizes to the plasma membrane where it activates the canonical NF-$\kappa$B pathway via TIRAP and MyD88. Additionally, TLR4 is transported to phagosomes that contain bacteria and are positive for Rab11a. There, TLR4 interacts with the adaptor proteins TRAM and TRIF leading to the activation of IRF3 and NF-$\kappa$B. For the production of inflammatory cytokines, both the early NF-$\kappa$B activation via MyD88 and the late NF-$\kappa$B activation via TRIF are required. TLR3, TLR7 and TLR9 are mainly targeted to the ER during the steady state. UNC93b1 and PRAT4A control the trafficking of these receptors to endosomal compartments where they can engage with their ligands. TLR3 interacts with TRIF activating both NF-$\kappa$B and IRF3. TLR7 and TLR9 located in endosomes lead to the production of inflammatory cytokines via the canonical NF-$\kappa$B pathway. In a process controlled by AP3, TLR7 and TLR9 can be transported to lysosome-related organelles (LRO) where they lead to the activation of IRF7. This signaling cascade is mediated by IRAK1, TRAF6, TRAF3 and IKK$\alpha$ and is facilitated by Viperin expressed in lipid bodies. As receptors and adaptor proteins are differentially expressed in different cell types, not all signaling cascades are active in a specific cell type. Cell types that are able to produce cytokines in response to a specific TLR stimulation are indicated in brackets: LPDC, lamina propria DC; MP, macrophage; cDC, conventional DC; iMO, inflammatory monocytes; pDC, plasmacytoid DC. *Reproduced from Kawai and Akira*[5].

was found to be unmethylated deoxycytidylate-phosphate-deoxyguanylate (CpG) DNA motifs mainly present in bacterial and viral DNA[25]. Finally, *Tlr11* has been associated with the detection of uropathogenic bacteria in mice, but the molecule recognized by the receptor has not yet been identified[26]. Detection of PAMPs from bacteria by TLRs leads to the activation of NF-$\kappa$B and MAP kinases via the TAK1 complex. NF-$\kappa$B and the MAP kinases JNK, ERK and p38 in turn contribute cooperatively to the expression of proinflammatory cytokines[27,28]. Alternatively, detection of DNA and RNA from bacteria, by TLR9 and TLR7 respectively, was shown to lead to the production of type I interferons. This signaling cascade is dependent on the transcription factor IRF7[24].

The importance of bacterial recognition by TLRs is emphasized by several experiments that found a more severe course of disease when components of the signaling cascade were missing. *Tlr4*-deficient mice, for example, are more susceptible to *S. typhimurium* infections[29]. In case of infections by the Gram-positive bacterium *S. aureus*, *Tlr2* was found to be crucial for survival in mice. *MyD88* knockout mice were shown to be even more susceptible to *S. aureus* infections, suggesting that the combined action of several TLRs is required for efficient protection against the pathogen[30]. Mutations that impair TLR signaling could also be linked to immunodeficiency in humans. Autosomal-recessive mutations in IRAK4 or MyD88 predispose patients to recurrent life-threatening bacterial infections during childhood[31,32]. Moreover, polymorphisms in TLR4 are associated with an increased risk of Gram-negative infections and sepsis, asperigillosis and severe malaria[33]. Taken together, intensive research over the past 15 years has established pathogen recognition by TLRs as a central system for initiation and regulation of immune responses during infectious diseases.

### 2.1.2 Nod-like receptors

Nod-like receptors (NLRs) are soluble proteins, which are located in the cell cytoplasm. They are mainly expressed in myeloid cell types, especially antigen-presenting cells (APCs), but are also partially found in cells of the intestinal epithelium[34,35]. Similar to TLRs, NLRs can detect pathogen-associated molecular patterns (PAMPs) originating from bacteria, viruses, fungi and parasites[36]. Detection of PAMPs leads to self-oligomerization of the receptor and recruitment of effector proteins. The effector proteins activate downstream signaling cascades that overlap in part with the signaling downstream of TLRs and contribute to the expression of cytokines, type I interferons and antimicrobial peptides[35,36]. Some NLRs are also able to detect stimuli, which are collectively termed danger-associated molecular patterns (DAMPs). DAMPs originate from both exogenous and endogenous sources (e.g. pore-forming toxins and uric acid, respectively). Upon ligand binding, these NLRs, together with adaptor proteins, form multiprotein complexes called inflammasomes. These signaling platforms process the inactive precursors of cytokines by activating caspase-1[37].

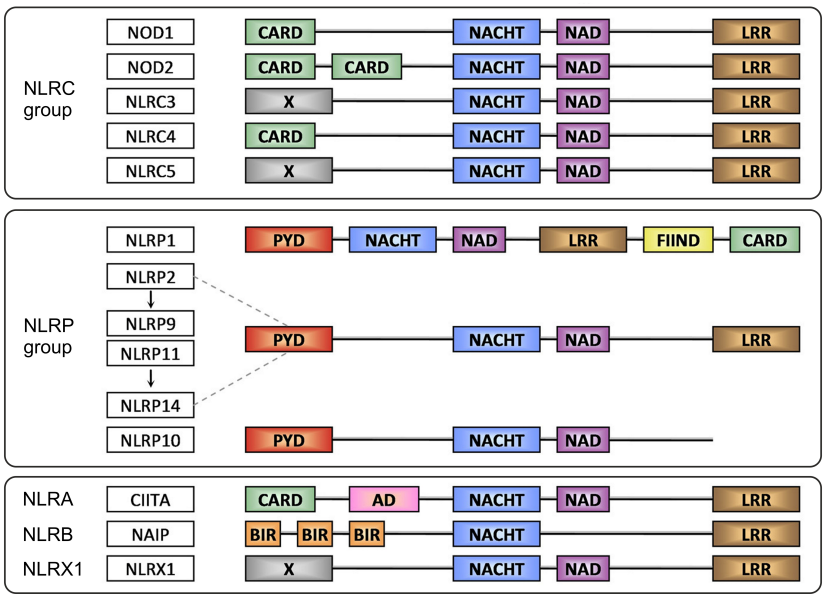


**Figure I.2 Domain organization of the human Nod-like receptor (NLR) family.** The human NLR family consists of 22 proteins that are grouped according to their N-terminal effector domains: CARD domain containing NLR (NLRC) group or pyrin domain containing NLR (NLRP) group. The proteins CIITA, NAIP and NLRX1 have a unique domain organization and are therefore assigned to individual subfamilies: acidic domain containing NLR (NLRA), BIR domain containing NLR (NLRB) and no strong N-terminal homology NLR (NLRX), respectively. Common to all proteins is a central nucleotide-binding domain (NBD) consisting of a NACHT and NAD domain and a C-terminal leucine-rich repeat (LRR) domain. CARD, caspase recruitment domain; PYD, pyrin domain; NAD, NACHT-associated domain; X, undefined domain; FIIND, function-to-find domain; AD, acid transactivation domain; BIR, baculoviral inhibitory repeat. *Adapted with modifications from Werts et al.*[38] and according to naming standards defined by Ting et al.[39].

NLRs constitute a family of proteins sharing a domain architecture that is characterized by a central nucleotide-binding domain (NBD) and a C-terminal leucine-rich repeat (LRR) domain. The LRR domain, which is also found in TLRs, is responsible for the recognition of PAMPs and DAMPs. Ligand binding by NLRs induces a conformational change and self-oligomerization via the NBD domain. Additional domains at the N-terminus allow for recruitment of downstream effector proteins and are the basis for classification of the NLRs into 2 major subfamilies: Proteins containing a caspase recruitment domain (CARD) (NLRC) and proteins containing a pyrin domain (PYD) (NLRP)[36,38]. Protein names for NLRs used in this study comply with the standard nomenclature introduced by Ting et al.[39]. An overview over the domain organization of the human NLR protein family is presented in Figure I.2.

The following paragraphs focus on the NLRs that have been described in detail over the past decade: The Nod proteins and the NLRs being involved in the formation of inflammasomes. A schematic illustration of NLR activation and signaling is presented in Figure I.3.

### Nod1 and Nod2 receptors

The involvement of Nod receptors in innate immunity was first established when Nod1 and Nod2 were found to be activators of NF-$\kappa$B[40–42]. Shortly later, Girardin and colleagues demonstrated that intracellular *S. flexneri* induce NF-$\kappa$B and JNK activation in a Nod1-dependent manner[43]. Initial reports speculated that Nod1 could be an intracellular sensor for LPS, which was rejected when both Nod1 and Nod2 were found to recognize muropeptides originating from bacterial peptidoglycan. Nod1 binds with high affinity peptidoglycan moieties containing the dipeptide $\gamma$-D-glutamyl-meso-diaminopimelic acid (iE-DAP)[44,45]. As iE-DAP is mainly found in peptidoglycan from Gram-negative bacteria, Nod1 can be considered as a specific sensor for Gram-negative pathogens. Nod2 was found to recognize the muramyl dipeptide (MDP) MurNAc-L-Ala-D-isoGln, which is a common motif in all bacterial peptidoglycans[46,47]. Nod1 and Nod2 therefore recognize the presence of cytosolic bacteria, e.g. *S. flexneri* or *L. monocytogenes*, by binding peptidoglycan moieties being shed from the bacterial surface[44,48,49]. Interestingly, several reports have pointed out that Nod1 and Nod2 as well can be stimulated by bacteria residing in phagosomes or even outside of the cell. For example, *H. pylori*, a non-invasive pathogen, delivers peptidoglycan moieties into the cytoplasm through its type IV secretion system[50]. Additionally, cells are able to internalize muropeptides by clathrin-mediated endocytosis[51,52] or through transporter proteins PepT1 and PepT2, which are located in the plasma membrane[51,53,54]. It has further been proven that a fraction of Nod1 and Nod2 is associated with the plasma membrane and can get recruited to sites of bacterial invasion[55,56]. Whether this localization is essential for Nod1/2 signaling or might only facilitate an early recognition of muropeptides is still a matter of debate.

Upon ligand binding, both Nod1 and Nod2 interact with the serine-threonine kinase RIP2 via their CARD domain[40,41,57,58]. Furthermore, members of the IAP protein family get recruited. Among these, cIAP1 and cIAP2 polyubiquitinate RIP2, a modification that is required for downstream signaling[59–61]. RIP2 in turn recruits TRAF6 and the TAK1 complex, that contributes to the activation of the IKK complex[40,41,57,62]. The IKK complex phosphorylates I$\kappa$B$\alpha$, targeting it for proteasomal degradation. In the absence of I$\kappa$B$\alpha$, NF-$\kappa$B translocates to the nucleus[63]. TAK1 represents a MAP3 kinase and hence contributes to the activation of MAP kinases JNK, p38 and ERK, although the precise mechanism of activation has not yet been described[43,48,58,64]. Together, JNK and p38 control the activity of the transcription factor AP-1[27], while p38 and ERK control the access of chromatin to transcription factors (e.g. NF-$\kappa$B or AP-1) via phosphorylation of histone H3[28]. The concerted action of NF-$\kappa$B and MAP kinases induces a robust inflammatory response resulting in the secretion of cytokines and chemokines (e.g. IL-6, IL-8, CXCL1, CXCL2 and CCL2[65,66]), as well as antimicrobial peptides (e.g. $\beta$-defensins and PGRPs[67]). While antimicrobial peptides can directly contribute to bacterial killing, secreted cytokines and chemokines will attract cells of the immune

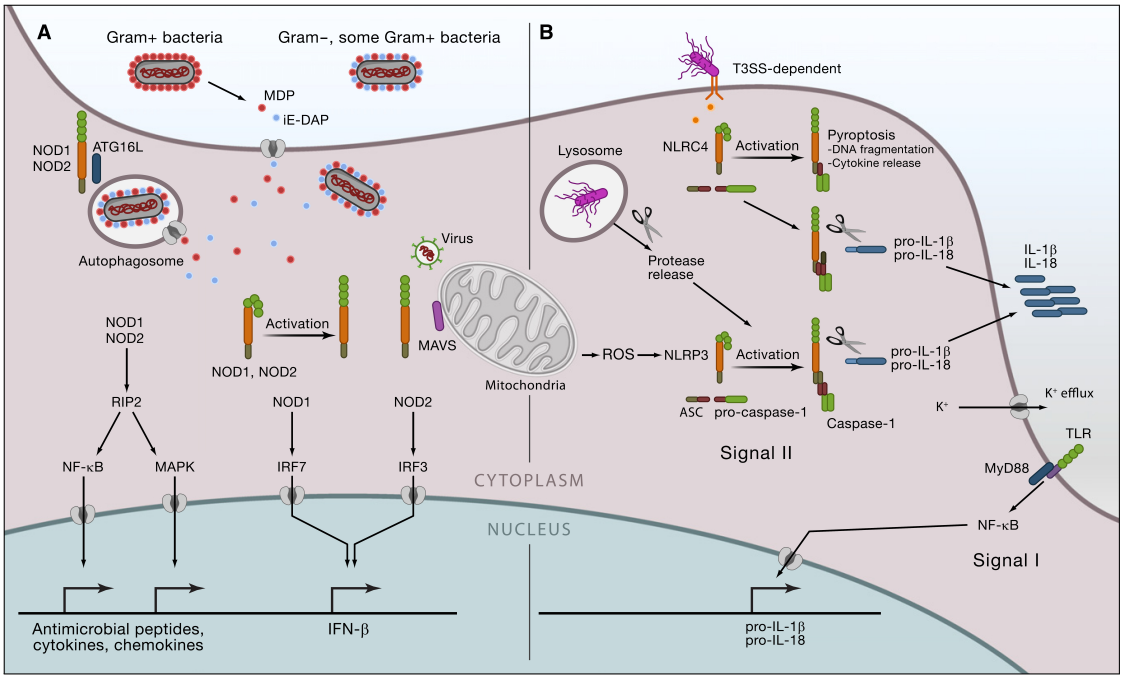


**Figure I.3 Activation and signaling of Nod-like receptors.** LEFT (A): Nod1 and Nod2 get activated by peptidoglycan moieties released from intracellular and extracellular bacteria. iE-DAP, which is mainly present in Gram-negative bacteria, is recognized by Nod1, while Nod2 binds MDP, a common motif of all peptidoglycans. Upon ligand binding, Nod1 and Nod2 recruit RIP2 that stimulates the activation of NF-$\kappa$B and MAP kinases. Collectively, this leads to the expression of cytokines, chemokines and antimicrobial peptides. Additionally, Nod1 and Nod2 were shown to recruit Atg16L to sites of bacterial phagocytosis thereby initiating autophagy. Alternatively, Nod1 was reported to stimulate interferon-$\beta$ expression in response to *H. pylori* infections. Similarly, recognition of viral single-stranded RNA by Nod2 induces transcription of type I interferons in a signaling cascade depending on the protein MAVS. The transcription of type I interferons is mediated by IRF7 and IRF3.
RIGHT (B): Activation of NLRC4 or NLRP3 initiates the formation of inflammasomes. Recognition of bacterial flagellin or components of the T3SS by NLRC4 induces pyroptosis, a form of controlled cell death. At the same time, NLRC4 recruits ASC and caspase-1 to from the so-called NLRC4 inflammasome that processes pro-IL-1$\beta$ and pro-IL-18. NLRP3 is activated by microbial PAMPs or by DAMPs (e.g. increased ROS concentration or lysosomal damage). Ligand binding induces the formation of the NLRP3 inflammasome by recruiting ASC and caspase-1. The proteolytic activity of caspase-1 leads to the production and secretion of active IL-1$\beta$ and IL-18. The transcription of the cytokine precursors requires an initial signal delivered for instance by TLR signaling. *Reproduced from Elinav et al.*[36].

system that will help to limit and clear the infection. A schematic representation of the downstream signaling cascades of Nod1 and Nod2 is presented in Figure I.4.

The spectrum of PAMPs recognized by Nod2 was recently extended when the receptor was found to activate signaling in response to viral single-stranded RNA (ssRNA). Interestingly, the recognition of ssRNA did lead to expression of type I interferons, which is not observed when stimulating Nod2 with MDP. The signaling pathway was further found to be independent of RIP2, but required the proteins

MAVS and the transcription factor IRF3[68]. Similarly, Nod1 was found to initiate the production of interferon-$\beta$ during *H. pylori* infection. In contrast to Nod2, the signaling was dependent on RIP2 and additionally required TRAF3, IRF7 and ISGF3[69,70]. Taken together, this indicates that Nod1/2 might have functions beyond the recognition of peptidoglycan and that the receptors can induce a ligand-specific response.

Several publications have also provided insight into the downregulation of Nod1 and Nod2 signaling. For example, the protein A20 has been shown to interfere with Nod1/2-mediated NF-$\kappa$B activation by de-ubiquitination of RIP2[71]. Moreover, a short isoform of Nod2 was found to act as a negative regulator for Nod2 signaling[72]. Finally, Erbin, caspase-12 and MEKK4 were shown to act as negative regulators by directly interacting with Nod2 or by disrupting the interaction between Nod2 and RIP2[73–75]. More research is required to fully understand the mechanisms that negatively regulate Nod1/2 signaling.

Recently, Nod1 and Nod2 have also been associated with the induction of autophagy in response to *S. typhimurium* and *S. flexneri* infection. The receptors were shown to recruit Atg16L to entry sites, thereby promoting the formation of autophagosomes[77,78]. Strikingly, mutations in Nod2 and Atg16L that had previously been associated with Crohn's disease, a chronic inflammatory disorder of the intestine, were demonstrated to impair Nod2 induced autophagy[78]. At the same time, Nod1 was proven to enhance systemic innate immunity through the recognition of peptidoglycan, which is constantly released by the microbiota of the gut. It is speculated that the constant detection of peptidoglycan by Nod1 primes neutrophils and facilitates a rapid innate immune response in case of an infection[79]. Furthermore, derivatives of MDP and iE-DAP are known to act as adjuvants for antigen-specific IgG production, which is attributed in part to a costimulatory effect in monocytes and dendritic cells[80–82]. This convincingly points out that Nod1/2 are also involved in the initiation of the adaptive immune response[48,83]. Noteworthy, Nod1 and Nod2 were both found to have additional functions independent of their role in inflammation signaling. Nod1 was reported to negatively control tumor growth in MCF-7 cells, while Nod2 promotes proliferation and survival of colonic epithelial cells[84,85].

In summary, Nod1 and Nod2 play a central role in the immune response during bacterial infections. The association of Nod1/2 mutations and deficiency with both, increased inflammation (e.g. in Crohn's disease) and reduced immune responses (e.g. infections in Nod1 deficient mice), further suggests that the receptors are key players in the delicate regulation of intestinal inflammation.

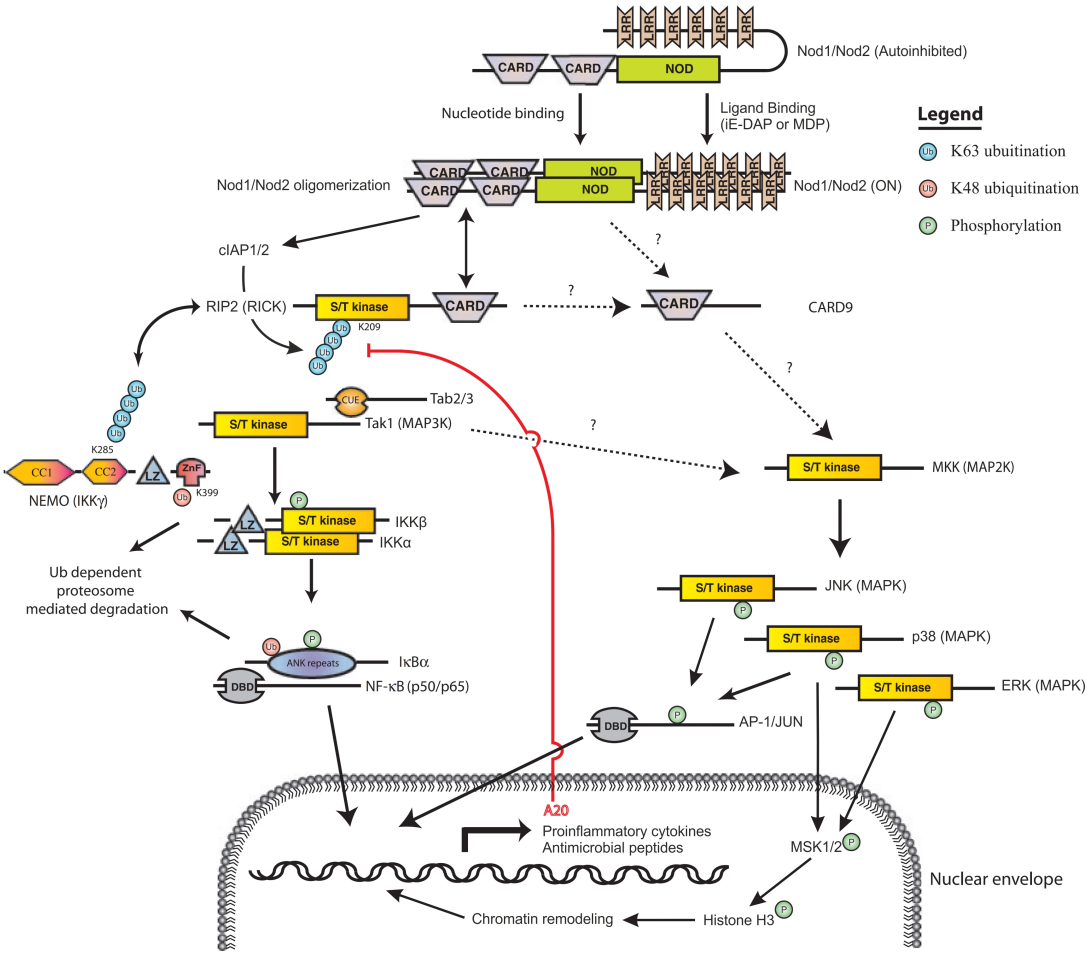


**Figure I.4 Signaling pathways activated upon stimulation of Nod1 and Nod2.** Recognition of peptidoglycan moieties containing iE-DAP or MDP leads to oligomerization of Nod1 and Nod2, respectively. The activated receptors recruit the serine/threonine kinase RIP2, which gets ubiquitinated by cIAP1 and cIAP2. This modification is required for the recruitment of the TAK1 complex consisting of TAK1, TAB1 and TAB2. RIP2 further recruits the IKK complex, consisting of NEMO, IKK$\alpha$ and IKK$\beta$ and promotes the ubiquitination of NEMO. Together with the kinase activity of TAK1, this leads to the activation of the IKK complex that phosphorylates I$\kappa$B$\alpha$. Phosphorylated I$\kappa$B$\alpha$ gets ubiquitinated and is targeted for proteasomal degradation, allowing the previously bound transcription factor NF-$\kappa$B to translocate to the nucleus. Additionally, stimulation of Nod1 and Nod2 leads to the activation of the MAP kinase signaling pathway. The precise mechanism of activation has not been described but is likely to involve TAK1, CARD9 and an unknown MAP2 kinase. Ultimately, the MAP kinases JNK, p38 and ERK get activated. JNK and p38 control the activity of the transcription factor AP-1 thereby contributing to expression of proinflammatory genes. p38 and ERK induce changes in the chromatin structure by phosphorylating histone H3 via MSK1 and MSK2. Several mechanisms have been described that negatively control the downstream signaling cascades of Nod1 and Nod2. For example, A20 downregulates signaling by de-ubiquitination of RIP2. *Adapted with modifications from Franchi et al.*[76].

### The inflammasomes

Several Nod-like receptors have been reported to form higher molecular structures upon stimulation by their corresponding ligands. Additional adaptor proteins as well as caspase-1 get recruited to these complexes. Based on the proinflammatory activity of caspase-1 and in analogy to the previously described apoptosome, these signaling platforms were termed "inflammasomes"[86]. Up to date, four inflammasomes have been described. The NLRP1 inflammasome consists of NLRP1, the adaptor protein ASC and caspase-1. In addition, caspase-5 is recruited. NLRP3 (also known as NALP3 or cryopyrin) forms the NLRP3 inflammasome together with ASC and caspase-1. However, recent evidence has assigned an important role to NLRC5 in the formation of the NLRP3 inflammasome[87]. The NLRC4 inflammasome consists of NLRC4 (also known as Ipaf), ASC and caspase-1, although the requirement for ASC is a matter of debate. Finally, the protein AIM2, which is not a member of the NLR protein family, was found to form an inflammasome in conjunction with ASC and caspase-1. The precise mechanism of inflammasome formation has not been described, but it is speculated that stimulation induces CARD-CARD and PYD-PYD domain interactions between the NLRs, ASC and caspase-1[36,37,76,88].

As for Nod1 and Nod2, the NLRs forming inflammasomes are believed to detect molecular PAMPs and DAMPs via their LRR domain. NLRP1 senses muramyl dipeptide from bacterial peptidoglycan as well as the anthrax lethal factor from *Bacillus anthracis* lethal toxin[89,90]. The NLRC4 inflammasome forms upon detection of flagellin and conserved rod components of type III secretion systems[91,92]. Recent evidence has indicated that the receptors detecting the stimuli might be NAIP proteins. In mice it was demonstrated that *Naip5* and *Naip2* directly interact with flagellin and T3SS rod components, respectively, thereby activating the NLRC4 inflammasome. Similarly, NAIP, the sole NAIP family member in humans, detects a T3SS rod component[93]. The NLRP3 inflammasome has been studied intensively and is thought to be a general sensor for DAMPs. It is formed in response to stimuli of bacterial or viral origin (e.g. pore-forming toxins), endogenous danger signals (e.g. extracellular ATP) and crystalline particles[37,94–96]. Although many stimuli have been described, the detailed mechanism of activation remains elusive. The wide range of molecules detected by NLRP3 has implicated that the receptor senses a common signal, which is induced by the various stimuli. In correspondence with this hypothesis, the production of reactive oxygen species (ROS) is a common feature to many NLRP3 stimuli[96]. On the other hand, there might be additional, yet unknown receptors involved in the activation of the NLRP3 inflammasome, as has recently been exemplified by Davis and colleagues[87]. Finally, the AIM2 inflammasome detects cytosolic double-stranded DNA (dsDNA), apparently independent of its origin. AIM2 does not belong to the family of NLRs, but still contains a PYD domain that allows for the recruitment of ASC. Instead of a LRR domain, the recognition of dsDNA is mediated by a so-called HIN200 domain[97,98].

Common to all inflammasomes is the recruitment of caspase-1 in its inactive form (also known as pro-caspase-1). The association of pro-caspase-1 with inflammasomes is likely to occur through CARD-CARD domain interactions and induces its activation through autoproteolytic cleavage. Activated caspase-1 is released from the inflammasome and forms oligomeric complexes. These complexes can convert the cytokine precursors pro-IL-1$\beta$ and pro-IL-18 into their active forms by proteolytic cleavage[37,86]. The availability of pro-IL-1$\beta$ is additionally controlled at the transcriptional level and requires the activation of NF-$\kappa$B, for example through TLR signaling. This assures that no excess of IL-1$\beta$ is released, which would be deleterious for the host. Secretion of mature IL-1$\beta$ and IL-18 contributes to the activation of the immune system. IL-1$\beta$ is known as a potent inducer of endothelial adhesion molecules and thus promotes the infiltration of the tissue by immune cells. Additionally, it is well known as an inducer of fever. Mature IL-18 activates NK cells and induces the production and secretion of interferon-$\gamma$[99].

All four inflammasomes are activated in response to bacterial infections. The NLRP1 inflammasome is associated with susceptibility to *Bacillus anthracis* in mice. Macrophages expressing a certain allele of *Nlrp1b* are sensitive to anthrax lethal toxin, resulting in caspase-1 dependent cell death[89]. Moreover, the NLRP1 inflammasome forms in response to MDP from bacterial peptidoglycan, suggesting that it might act as a general sensor for bacteria[100]. So far, this could only be confirmed in response to infection by *Bacillus anthracis*. Interestingly, the activation of the inflammasome requires the interaction of NLRP1 with Nod2[101]. The NLRC4 inflammasome is associated with the recognition of Gram-negative bacteria expressing a type III or type IV secretion system (T3SS/T4SS). In case of *Salmonella* and *Legionella*, NLRC4 activates caspase-1 in response to the bacterial protein flagellin[102,103]. As the activation of the NLRC4 inflammasome is dependent on functional secretion systems, it is currently hypothesized that flagellin monomers might get translocated into the cytosol by the T3SS or T4SS[103]. Although non-flagellated, the pathogen *Shigella* activates the NLRC4 inflammasome as well. Indeed, NLRC4 detects the basal rod proteins of T3SSs (MxiI in the case of *Shigella*) through a sequence motif that is found both in the T3SS rod proteins and flagellin[92]. The NLRP3 inflammasome is activated in response to pore-forming toxins that are produced by several pathogenic bacteria. For instance, *Listeria monocytogenes* and *Streptococcus pneumoniae* activate the NLRP3 inflammasome through Lysteriolysin O and Streptolysin O, respectively. This recognition seems to be important *in vivo*, as *Nlrp3*$^{-/-}$ mice show a delayed clearance of infection in both cases[94,104]. NLRP3 inflammasome activation has further been reported in response to *S. aureus* and *M. tuberculosis* infections[94,105]. Finally, the AIM2 inflammasome plays an important role in the detection of cytosolic bacteria, as well as DNA viruses. Activation of caspase-1 through the AIM2 inflammasome was detected upon vaccinia virus, *Francisella tularensis* and, partially, *L. monocytogenes* infection[106].

The central role of inflammasomes is emphasized by the fact that they have been

associated with several inflammatory disorders[107]. *Nlrp3*$^{-/-}$ mice were, for example, found to be more susceptible to dextran sodium sulfate induced colitis[108]. In humans, NLRP3 has a protective function against intestinal inflammation, as mutations that reduced the NLRP3 expression level were strongly associated with the risk of Crohn's disease[109]. The NLRP3 inflammasome plays a crucial role in gout and type II diabetes by contributing to constant secretion of IL-1$\beta$[95,110]. This finding had an astonishing impact on the clinics, as the administration of an IL-1 receptor antagonist (anakinra) significantly improved glycemia and $\beta$ cell secretory functions in type II diabetes patients[111]. Finally, variants of NLRP1 have been associated with the autoimmune diseases vitiligo (destruction of melanocytes in the skin) and Addison's disease (destruction of the adrenal cortex)[112,113].

## 2.2 Pathogen recognition and inflammation signaling during *S. flexneri* infection

Tissue-resident macrophages, which are associated to M cells, are the first cells to encounter invading *Shigella* in the submucosal space. The presence of *S. flexneri* activates TLR signaling in macrophages. TLR2 was reported to detect a 34 kD outer membrane protein of *Shigella* spp.. This leads to the activation of NF-$\kappa$B and MAP kinase p38 that promote cytokine and chemokine production[114]. The heterodimer TLR2/6 was further reported to detect a porin from *S. dysenteriae*. Again, ligand binding induces NF-$\kappa$B activation and promotes secretion of cytokines[115]. LPS from *Shigella* can also activate TLR4 signaling. Interestingly, LPS from *S. flexneri* leads to a lower activation of NF-$\kappa$B and reduced cytokine release when compared to LPS from non-pathogenic *E. coli*. This can be attributed to additional acetylation of lipid A in the case of *Shigella*[116].

Although macrophages can efficiently phagocytose *Shigella*, they fail to degrade the bacteria and instead undergo pyroptosis (see also section 4.1.2)[117,118]. The induction of pyroptosis in macrophages is independent of TLR signaling and instead requires the Nod-like receptor NLRC4 (also known as Ipaf). Miao and colleagues could show that NLRC4 does detect the protein MxiI, which is a basal body rod component of the T3SS. Recognition of MxiI leads to the assembly of the NLRC4 inflammasome, activation of caspase-1 and the massive release of IL-1$\beta$ and IL-18, a hallmark of pyroptosis[92,118].

The cytoplasm of enterocytes represents the main replicative niche for *Shigella*. The pathogen is able to trigger its uptake into enterocytes and escapes the phagocytic vacuole to reach the cytoplasm (refer to section 4.1.3 for more details). Although enterocytes are of non-myeloid origin, they represent an integral part of the innate immune system. They act as sentinels for intestinal infections and can activate the immune system by secreting cytokines. In case of *Shigella*, the presence of intracellular bacteria is sensed through the pathogen recognition receptor Nod1, which detects peptidoglycan moieties shed on the bacterial surface[43,44]. Ad-

**Table I.2 Cytokines and chemokines upregulated during *S. flexneri* infection.**

| Gene | Fold increase[a] |
|---|---|
| Interleukin-8 | 304.79 |
| CXCL1 | 133.74 |
| CCL20 | 38.67 |
| CXCL2 | 13.17 |
| TNF-*alpha* inducible protein A20 | 4.23 |
| CXCL3 | 3.12 |
| TNF-$\alpha$ | 3.06 |
| TNF-*alpha* inducible protein B94 | 1.66 |
| GM-CSF | 33.24/12.64 |
| IEX-1 | 1.88 |

[a] Comparing cells incubated with invasive *S. flexneri* (M90T) and uninfected cells. *Adapted with modifications from Pédron et al.*[119].

ditionally, GEF-H1 senses the presence of certain *Shigella* effector proteins that get injected into the cell by the type III secretion system (T3SS) of the bacterium (for more details on the T3SS and effector proteins refer to section 3.2). While the mechanism, by which GEF-H1 detects effector proteins, remains currently unknown, GEF-H1 was also reported to be involved in Nod1-mediated recognition of peptidoglycan[120].

Pathogen recognition by Nod1 induces the activation of the transcription factor NF-$\kappa$B and the MAP kinases JNK, p38 and ERK[43,121,122]. JNK and p38 regulate the activity of the transcription factor AP-1[27]. At the same time, p38 and ERK induce changes in the chromatin structure by phosphorylating histone H3 via the kinases MSK1 and MSK2. These rearrangements are believed to mark promoters of inflammatory genes for enhanced recruitment of transcription factors like NF-$\kappa$B[28]. Collectively, these signaling events initiate an inflammatory response. Transcriptome analysis of epithelial cells revealed that several genes encoding for cytokines and chemokines get transcribed upon *S. flexneri* infection (Table I.2). Remarkebly, the transcription of the chemokine IL-8 was upregulated more than 300-fold[119]. This was in line with the previous finding of IL-8 playing a central role during shigellosis by recruiting polymorphonuclear neutrophils to sites of infection[123]. Additionally, enterocytes also produce antimicrobial peptides like $\beta$-defensins in response to infection[124].

Notably, *S. flexneri* is downmodulating the inflammatory response in infected cells by injecting several effector proteins through its T3SS. For instance, the effector OspF interferes with IL-8 expression by dephosphorylation of p38 and ERK[125,126]. An overview of the different mechanisms applied by *Shigella* to control the host's inflammatory response is presented in section 4.2.2. The observation of a strong inflammatory response during *S. flexneri* infection – despite the immunosuppressive activity of effector proteins – represents a steady matter of debate in the field. It is hypothesized that the bacterial effector proteins only partially block inflammation signaling. Alternatively, the host cell might be able to evade or compensate the ef-

fect of effector proteins. Chapter II describes a novel mechanism, by which infected cells can propagate proinflammatory signals to uninfected neighboring cells. This cell-cell communication significantly amplifies the immune response and allows the host cell to circumvent the inhibitory effect of bacterial effectors.

# 3 *Shigella* – the causative agent of bacillary dysentery

The *Bacillus dysenterie*, later identified as *Shigella dysenteriae* 1, was discovered by Kiyoshi Shiga[127]. Shiga worked at the Institute for Infectious Diseases in Tokyo where he isolated the etiological agent of dysentery – a dreaded disease with periodical outbreaks in Japan during the late 19$^{th}$ century – from patients. He accurately described the bacillus as a gram-negative bacterium of which subcultures would cause diarrhea when fed to dogs. He first published his findings in 1897 and an article in German was published one year later[128,129]. In honor of his discovery, the genus was later named "Shigella"[127].

## 3.1 Shigellosis

More than 100 years after Shiga's discovery, the bacillary dysentery – also called shigellosis – caused by *Shigella* spp. still accounts for an estimated 5-15% of all diarrheal episodes worldwide. It's prevalent in developing countries and mainly affects children under the age of 5 years. Although the disease can be efficently treated with antibiotics and proper rehydration in most cases, 1.1 million fatal incidents per year are attributed to *Shigella* infections. The genus *Shigella* consists of 4 species: *S. dysenteriae*, *S. flexneri*, *S. boydii* and *S. sonnei*. *S. flexneri* and *S. sonnei* are endemic in several countries of Asia, Africa and South America and account for a majority of the infections. *S. dysenteriae* is responsible for epidemic outbreaks and displays the most severe course of disease with significantly increased mortality[130].

*Shigella* spp. are transmitted via the feco-oral route by ingestion of contaminated water or food. The pathogen proves to be highly contagious as small inocula of only 10-100 microorganisms can cause disease[131]. Infected patients suffer from abdominal cramps, bloody and mucous diarrhea, fever and dehydration. In most cases, proper rehydration will resolve the disease within a week. In young children and in severe cases, antibiotics should be administered in combination with a nutritional therapy to avoid malnutrition. As for many other pathogenic bacteria, *Shigella* has acquired resistance towards many antibiotics. Especially in endemic regions, strains have been described that are resistant towards antibiotics commonly used to treat the disease including ciprofloxacin, ceftriaxone and azithromycin[132].

The increasing number of antibiotic-resistant strains has emphasized the requirement for an efficient vaccine against *Shigella*. The major challenge in vaccine development for shigellosis is the diversity of the *Shigella* genus. The majority of incidents is caused by the three different species *S. flexneri*, *S. dysenteriae* and *S. sonnei*. While the latter two are represented by only one or a predominant serotype, 14 serotypes of *S. flexneri* are regularly isolated during disease. Kiyoshi

Shiga was actually the first who had tested a vaccine by injecting himself with a heat-killed whole-cell preparation[127]. Unfortunately, his approach showed little success, an outcome that was shared by many vaccine trials up to now. Current vaccine trials have mainly focused on polysaccharide and synthetic conjugates, as well as invasion complex-based and live attenuated preparations. Although significant advances have been made in the field of *Shigella* vaccines, it seems that a broad-spectrum vaccine that would protect from shigellosis in endemic areas around the world is not within reach in the near future[132,133].

## 3.2 Determinants of *Shigella* virulence

*Shigella* spp. are known to have evolved from non-pathogenic *E. coli* through the acquisition of a large virulence plasmid and several chromosomal pathogenicity islands (PAIs). The sequence of the chromosome as well as the virulence plasmid is available for several *Shigella* strains and has revealed that the divergence from *E. coli* K-12 is as little as 1.5%. In total, 5 PAIs have been identified on the *Shigella* chromosome that were acquired at different times during evolution. Only for some of the genes, located within pathogenicity islands, a virulence-associated function could be assigned. Table I.3 summarizes the known virulence factors, which are located within PAIs on the *Shigella* chromosome.

Besides the chromosomal virulence factors, invasive *Shigella* possess a virulence plasmid that is approximately 200 kb in size. pWR100, the virulence plasmid of *S. flexneri* strain M90T (serotype 5), is made up for one third by insertion sequence elements. Approximately 100 open reading frames were identified, most of which could be assigned to previously identified genes[134]. Of particular interest is the 31 kb gene cluster, which encodes the structural components of the Mxi-Spa type III secretion system (T3SS), translocator and effector proteins, as well as chaperones and regulatory proteins. As this part of the virulence plasmid is necessary and sufficient for *Shigella* invasion of cells, it is referred to as "entry region". An overview of the genetic organization within the "entry region" is presented in Figure I.5 (bottom).

The expression of the T3SS and its substrates is under tight control of a regulatory system that senses environmental stimuli. The major activating factor is a temperature shift to 37°C, which is indicative for uptake into the host organism[136]. Osmolarity, pH and iron concentration are additional factors that control virulence plasmid gene expression[135]. While the systems sensing the environmental cues are encoded on the chromosome, the main transcriptional activator, VirF, is encoded on the virulence plasmid itself. VirF expression is induced at 37°C and will activate VirB, a second essential regulator[136]. VirB controls the expression of the genes located in the "entry region" and a first set of T3SS substrates (also called "early effectors"), including the translocators IpaB and IpaC[137]. Within the entry region, a third transcriptional regulator, MxiE, is encoded. MxiE controls the expression

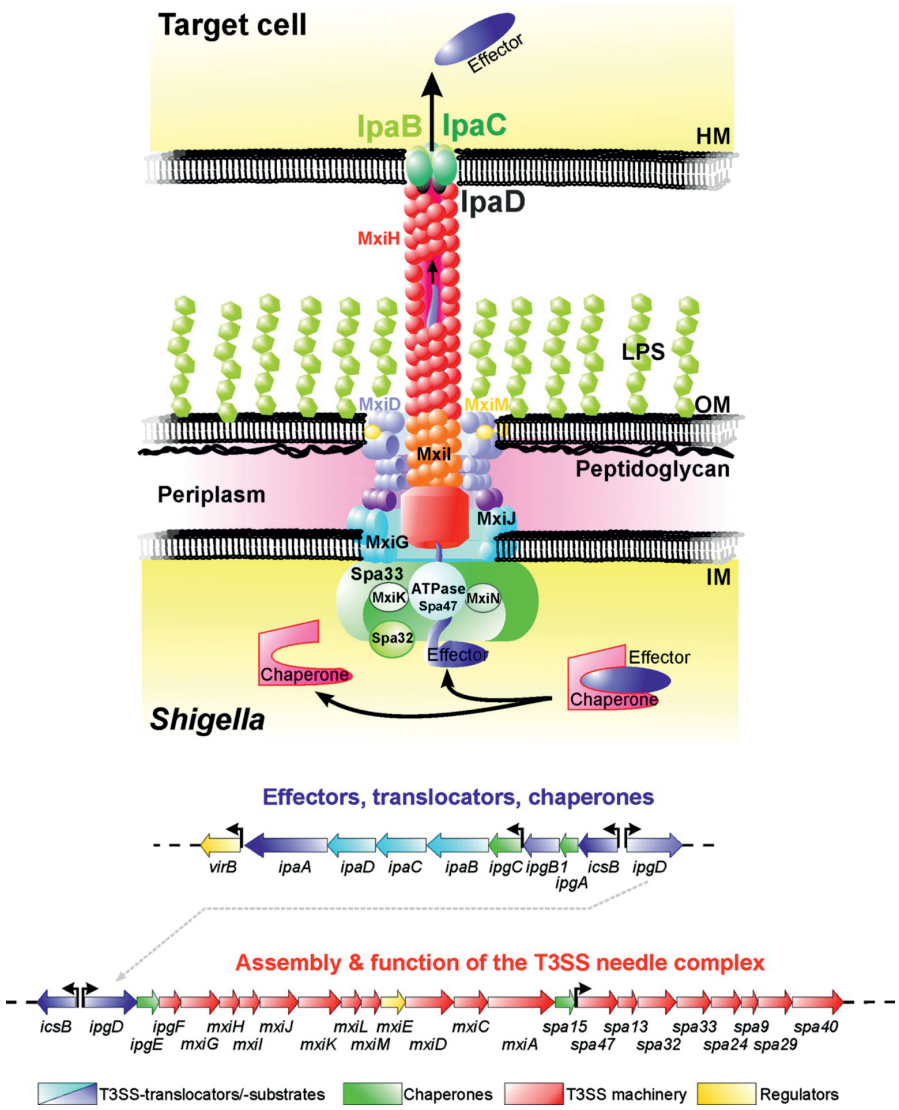


**Figure I.5 The Mxi-Spa type III secretion system and the "entry region" gene locus.** TOP: Schematic representation of the T3SS. The T3SS consists of a basal body that spans the inner membrane, the periplasm and the outer membrane. The basal body is formed by the oligomerization of MxiG, MxiJ, MxiD and MxiM. Spa33 forms the so-called C ring, which is located in the cytoplasm and associated to the basal body. The C ring serves as a platform for several proteins that energize secretion (ATPase Spa47), assemble the needle structure (MxiN, MxiK) and control needle length and substrate-specificity (Spa32). The needle extends from the basal body to the bacterial surface. At the tip of the needle IpaB and IpaC are exposed, which will insert into the membrane upon contact with the host cell allowing direct translocation of effector proteins.
BOTTOM: Genetic organization of the "entry region" located on the virulence plasmid pWR100. The genes of the "entry region" encode for the structural components of the Mxi-Spa type III secretion system (T3SS), translocator and effector proteins, as well as chaperones and regulatory proteins. Genes are colored according to their corresponding function. *Adapted with modifications from Schroeder and Hilbi*[135].

of a second set of T3SS substrates (known as "late effectors"). Although MxiE is expressed upon VirB activation, its target genes will only get transcribed once the

early effectors have been secreted. This is achieved by the early effector OspD1 and its chaperone Spa15 that bind MxiE and repress its transcriptional activity[137,138]. The regulatory network allows the bacterium to temporally control the expression and secretion of effector proteins. Thus, the bacterium is initially equipped with a T3SS and a first set of effectors that allow host cell invasion. Only upon successful invasion, the bacterium will express and secrete the late effectors.

The major part of the "entry region" consists of genes named membrane presentation of Ipa antigens (*mxi*) and surface presentation of Ipa antigens (*spa*). The proteins encoded by the *mxi-spa* locus are components of the T3SS, a molecular syringe-like structure that allows *Shigella* to translocate proteins into mammalian cells[139,140]. The Mxi-Spa T3SS consists of a basal body, which spans the bacterial inner membrane (IM), the periplasm and the outer membrane (OM). The basal body is formed by oligomerization of 4 proteins (MxiG, MxiJ, MxiD and MxiM) that anchor the complex in the IM and OM[141–143]. Associated with the IM ring of the basal body is Spa33, which forms the so-called C ring[144]. The C ring serves as a platform for several proteins that energize secretion (ATPase Spa47), assemble the needle structure (MxiN, MxiK) and control needle length and substrate-specificity (Spa32)[145–148]. The needle structure itself is build by the subunits MxiI and MxiH. The needle is 45-60 nm in length and contains a central channel having a diameter of 2-3 nm[143]. Secretion of proteins through the narrow needle structure requires the partial unfolding of the secreted proteins, which is mediated by proteins associated to the C ring and energized by Spa47[149]. The translocator proteins IpaB, IpaC and IpaD are exported to the tip of the needle. IpaD is believed to serve as a "plug" only allowing secretion of IpaB and IpaC upon detection of a secretion signal (e.g. host cell contact). Together, IpaB and IpaC form the translocator pore, which is inserted into the host cell membrane in an IpgD-dependent manner[139,150,151]. Upon successful insertion, the T3SS system is able to secrete effector proteins directly into the host cell. A schematic representation of the T3SS is presented in Figure I.5 (top).

In total, the virulence plasmid encodes approximately 25 T3SS substrates[134]. Additionally, there are up to seven genes located on the chromosome that encode effectors of the IpaH family[152]. Some of the T3SS effectors, especially the hydrophobic translocators IpaB and IpaC, require chaperones to prevent aggregation or premature activation in the bacterial cytoplasm. Four chaperones (IpgA, IpgC, IpgE and Spa15) are encoded within the "entry region"[153]. Some effector proteins might further have the capacity of self-chaperoning, as was reported for IpaD[154]. For some effectors, the biochemical activity, as well as their role during infection has been described in detail (e.g. OspF). For others, little is known about their activity upon secretion by the T3SS[155,156]. Table I.4 lists some T3SS effectors, their function during *Shigella* infection and known homologues in other pathogenic bacteria. A detailed description of the functions of the various effectors during the course of a *Shigella* infection is presented in section 4.1 and 4.2.

**Table I.3 Virulence factors encoded by chromosomal *Shigella* pathogenicity islands.**

| PAI | Gene(s) | Virulence function(s) |
|---|---|---|
| SHI-1 | *sigA* | Intestinal fluid accumulation, cytopathic toxin |
| | *pic* | Mucus permeabilization, serum resistance, hemagglutination |
| | *set1A, set1B* | Intestinal fluid accumulation, development of watery diarrhea |
| SHI-2 | *iucA-iucD, iutA* | Iron acquisition |
| | *shiD* | Colicin I and colicin V immunity |
| | *shiA* | Downregulation of inflammation by suppression of T-cell signaling |
| SHI-3 | *iucA-iucD, iutA* | Iron acquisition (found only in *S. boydii*) |
| SHI-O | *gtrA, gtrB, gtrV* | Evasion of host immune response |
| SRL | *fecA-fecE, fecI, fecR* | Iron acquisition |
| | *tetA-tetD, tetR* | Tetracycline resistance |
| | *cat* | Chloramphenicol resistance |
| | *oxa-1* | Ampicillin resistance |
| | *aadA1* | Streptomycin resistance |

*Adapted with modifications from Schroeder and Hilbi*[135].

**Table I.4 Activities of *Shigella* type III secretion system (T3SS) effectors.**

| T3SS effector | Role in infection | Selected homologues |
|---|---|---|
| IpaA | Bacterial invasion | *Salmonella* spp. SipA (also called SspA) |
| IpaB | Macrophage apoptosis and cell cycle arrest | *Salmonella* spp. SipB (also called SspB) and *Yersinia* spp. YopB |
| IpaC | Bacterial invasion | *Salmonella* spp. SipC (also called SspC) |
| IpgB1 | Bacterial invasion | *Salmonella* spp. SifA and SifB; EHEC, EPEC and *C. rodentium* Map; and EHEC EspM1/2 |
| IpgB2 | Unknown | |
| IpgD | Bacterial invasion and host-cell survival | *Salmonella* spp. SopB (also called SigD) |
| VirA | Bacterial invasion and intracellular spreading | EHEC, EPEC and *C. rodentium* EspG and EPEC EspG2 (also called Orf3) |
| IcsB | Escape from autophagy | *Burkholderia* spp. BopA |
| OspC1 | Polymorphonuclear transepithelial migration | *Shigella* OspC2, OspC3 and OspC4 and *V. parahaemolyticus* OspC2 |
| OspE2 | Intercellular spreading | *Shigella* OspE1; *Salmonella* spp. EspO1STYM; and EHEC EspO1-1 and EspO1-2 |
| OspF | Suppression of innate immune responses | *Salmonella* spp. SpvC; *P. syringae* HopAI1; and *C. violaceum* VirA |
| OspG | Suppression of innate immune responses | *Y. enterocolitica* YE2447; *C. rodentium* NleH; and EHEC NleH1-1 and NleH1-2 |
| $IpaH_{9.8}$ | Suppression of innate immune responses | *Shigella* IpaH4.5; *Salmonella* spp. SspH1, SspH2 and SlrP; *Y. pestis* YP3416 and YP3418; *P. syringae* PSPTO1492 and PSPTO4093; and *Rhizobium* spp. Y4fR |
| $IpaH_{7.8}$ | Escape from endocytic vacuoles of phagocyte | |
| Chromosomal IpaHs | Suppression of innate immune responses | |

*Adapted with modifications from Ogawa et al.*[155].

# 4 Molecular mechanisms of *Shigella* pathogenesis

Upon ingestion, *Shigella* is passaged through the stomach and the small intestine in order to reach the large intestine where an infection is established. *Shigella* is not able to directly infect colonic enterocytes from the apical side[157]. To get access to the submucosal space, the bacteria need to cross the epithelial lining by transcytosis through microfold cells (M cells). Associated with M cells are resident macrophages and dendritic cells, which readily phagocytose the invading bacteria[158]. *Shigella* is able to lyse the phagocytic vacuole and escape into the cytoplasm of these cells[159]. Infected macrophages very rapidly undergo pyroptosis, thereby releasing IL-1$\beta$ and IL-18, which will attract polymorphonuclear neutrophils (PMNs) and induce immune activation via natural killer (NK) cells, respectively[117,118].

When released from macrophages, *Shigella* becomes able to colonize enterocytes through their basolateral pole. Upon contact with cell surface receptors, *Shigella* translocates several effector proteins into the host cell using its T3SS. A subset of these effectors (IpaA, IpaB, IpaC, IpaD, IpgB1, IpgB2, IpgD and VirA) are required to promote *Shigella* uptake into non-phagocytic cells[155,156]. The molecular mechanisms of the entry process have been studied intensively over the past two decades and significant insight has been gained on how the bacterial effectors shape the cytoskeletal machinery to allow for efficient invasion. Main targets for the effectors are the small guanosine triphosphatases (GTPases) Cdc42, Rac and Rho, which are central regulators of the actin cytoskeleton. The coordinated action of the bacterial effectors leads to the formation of filopodia and lamellipodia, which will engulf the invading pathogen[135,160]. In contrast to *Salmonella*, *Shigella* rapidly disrupts the surrounding membrane after internalization to get access to the cytoplasm of the host cell[159].

Within the cytosol, *Shigella* exerts directed actin polymerization that allows the bacteria to move intra- and intercellularly. The remarkable feature of actin-based motility is shared by other intracellular pathogens like *Listeria*, *Rickettsia* and the vaccinia virus[161]. Actin-based motility allows *Shigella* to rapidly disseminate throughout the epithelium, thereby extending the pool of available nutrients. Noteworthy, IcsA – the bacterial factor mediating directed actin polymerization – contains a recognition site for autophagy. To avoid the engulfment by autophagic vacuoles, the recognition site is masked by the T3SS substrate IcsB[162,163].

*Shigella* efficiently replicates within the cytoplasm with a generation time of less than 40 minutes. Transcriptional analyses have revealed an excellent adaptation of the pathogen to the intracellular environment. Still, little is known about the host-pathogen interactions required for efficient replication. Besides adaptation to the replicative niche, *Shigella* is known to promote survival of infected cells. The T3SS effectors IpgD and Spa15 induce survival signals and inhibit apoptosis, respectively.

A key feature in *Shigella* pathogenesis is the ability to modulate the host inflammatory response. Several effectors (OspB, OspC1, OspF, OspG, OspZ and proteins

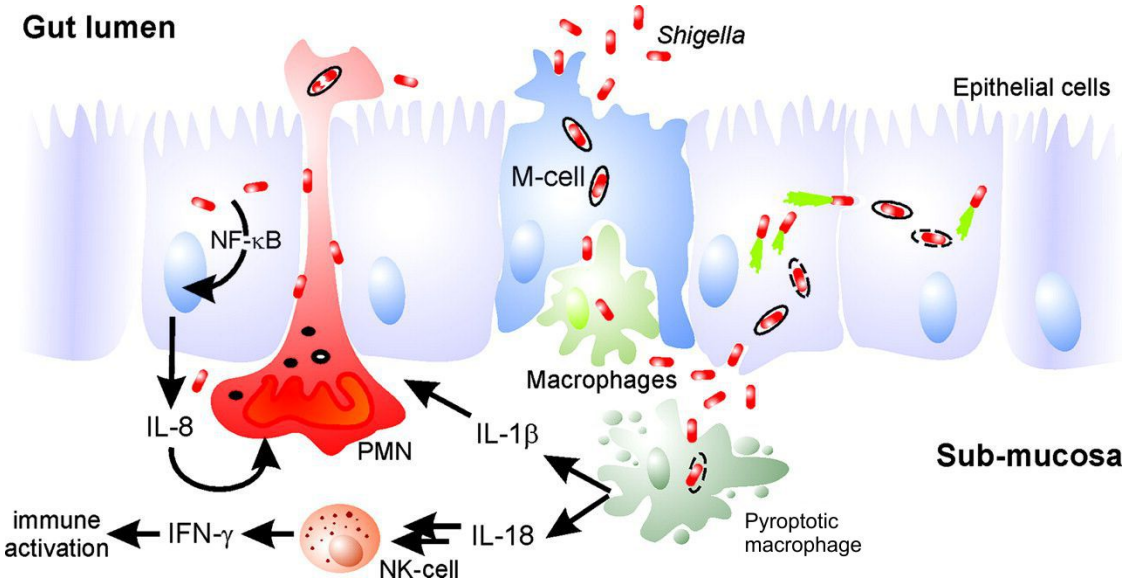


**Figure I.6 Schematic representation of *Shigella* pathogenesis.** *Shigella* crosses the colonic epithelium through M cells and gets phagocytosed by resident macrophages. Infected macrophages rapidly undergo pyronecrosis releasing IL-1$\beta$ and IL-18. Upon release from macrophages, *Shigella* infects enterocytes in a process resembling macropinocytosis. Within the host cell cytoplasm, *Shigella* replicates and disseminates to neighboring cells by actin-based motility. Intracellular bacteria are detected by pathogen recognition receptors leading to the secretion of IL-8. The release of proinflammatory cytokines from enterocytes and macrophages activates the immune system and attracts PMN cells to the site of infection. PMNs transmigrate across the epithelial layer thereby facilitating further invasion. Ultimately, PMNs phagocytose the invading bacteria, contributing to the clearance of the infection. *Adapted with modifications from Schroeder and Hilbi*[135].

from the IpaH family) are injected into the cytoplasm where they interact with components of the proinflammatory signaling cascade. Central targets are proteins of the MAPkinase and NF-$\kappa$B signaling pathways, resulting in a dampened inflammatory host response.

In the following sections, the different steps in *Shigella* pathogenesis will be presented in more detail with emphasis on invasion of enterocytes and downregulation of inflammatory signals. A schematic overview of *Shigella* infection is presented in Figure I.6.

## 4.1 Colonization of the gastrointestinal tract

Before reaching the colonic mucosa, where *Shigella* establishes an infection, the pathogen needs to sustain the acidic environment (pH = 1.5-3.5) of the stomach. *Shigella* has a survival rate of 50% when incubated at pH 2.5 for 2 hours[164]. This characteristic is shared with *E. coli*, while for example *S. typhimurium* is less resistant to acidification[165]. The acid resistance of *Shigella* is attributed to two

independent sytems. The glutamate-dependent acid resistance pathway stabilizes the intracellular pH by decarboxylation of glutamate and export of the product gamma-aminobutyric acid. Alternatively, the intracellular pH is maintained by the oxidative system, which is poorly understood but involves the alternative sigma factor RpoS[166]. The acid resistance of *Shigella* has been proposed as a major determinant for the low infective dose that is associated with shigellosis[131,164].

### 4.1.1 Crossing the epithelial layer by transcytosis

When reaching the colon, *Shigella* is not able to directly infect enterocytes from the apical side. The pathogen can barely interact with the apical surface of intestinal epithelial cells (IECs). *In vitro* infections using subconfluent Caco-2 cells revealed that invasion was almost exclusively limited to cells at the periphery of cell islets. Infected cells were shown to be stained with basolateral markers, suggesting that efficient invasion requires surface receptors that are only exposed at the basolateral surface of epithelial cells[157].

*In vivo* experiments using macaque monkeys revealed that sites of *Shigella* infection were located preferentially over lymphoid follicles[167]. Microfold cells (M cells) are associated with lymphoid tissues in the intestine. These specialized epithelial cells sample antigens, viruses, bacteria and even parasites from the gut lumen and present them to resident lymphocytes. This process is important for the homeostasis of the mucosal immune responses, but is at the same time exploited by different pathogens (e.g. *Salmonella* and *Yersinia*) to invade the host[168]. Wassef and colleagues proved that this is also true for *Shigella*. In the rabbit intestinal loop model, *Shigella* infected M cells and was transcytosed to the subepithelial space[169]. This process is actively controlled by *Shigella*, as the non-invasive strain, lacking the virulence plasmid, only poorly colonized M cells[158].

### 4.1.2 Evasion of killing by macrophages

After transcytosis through M cells, *Shigella* gets phagocytosed by tissue-resident macrophages and dendritic cells. To avoid phagosome-lysosome fusion, the phagosome is rapidly lysed in a IpaB/C-dependent way[159,170]. Within the cytoplasm, the bacteria can multiply, which kills the lymphocytes and results in a strong inflammatory response. Early publications have described the *Shigella*-induced cell death of macrophages as an apoptotic event that is mediated via the interaction of IpaB and caspase-1[171,172]. More recent publications have characterized the cell death as pyroptosis[117,118], a type of programmed cell death that is accompanied by nuclear condensation, membrane permeability and release of the cytokines IL-1$\beta$ and IL-18[173]. It was further shown that caspase-1 activation, which is necessary for pyroptosis, is mediated by the NOD-like receptor NLRC4 and its adaptor protein ASC[9]. Finally, Miao and colleagues found evidence that NLRC4 is recognizing the

basal body rod component of the T3SS of various pathogens. In case of *Shigella*, NLRC4 is binding to MxiI[92]. Noteworthy, pyroptosis was shown to be negatively regulated by autophagy[9]. It is tempting to speculate that *Shigella*'s ability to interfere with autophagy might further promote pyroptosis in infected macrophages.

At later time points and when infecting macrophages at higher multiplicity of infection (MOI), cell death takes another pathway resembling necrosis. NLRP3/ASC have been identified to mediate these signaling events in a caspase-1-independent way[118,174]. While it is currently not clear, which is the predominant pathway of macrophage cell death under physiological conditions, both lead to the massive release of cytokines IL-1$\beta$ and IL-18, major mediators of the inflammatory response observed during *Shigella* infections. IL-1$\beta$ promotes the infiltration of the infected tissue by PMNs. Additionally, PMNs transmigrate towards the gut lumen, thereby disrupting epithelial integrity. At initial stages, this can promote infection, as *Shigella* in the gut lumen get direct access to the basolateral pole of enterocytes[175]. At later stages, PMNs contribute to the clearance of infection by degrading *Shigella* virulence factors[176] and entrapping bacteria in NETs[177]. IL-18 activates NK cells, which in turn amplify the innate immune response by releasing INF-$\gamma$. INF-$\gamma$ is an important mediator for the clearance of a *Shigella* infection[178].

### 4.1.3 Invasion of epithelial cells

The following paragraphs introduce several molecular mechanisms that allow *Shigella* to trigger its uptake into non-phagocytic cells. These processes are controlled by several bacterial effectors, which are translocated by the T3SS. They target host cell systems including the actin cytoskeleton, focal adhesions and microtubules. The coordinated action of the bacterial effectors ultimately results in the uptake of the bacterium into the cell. A schematic overview of the most important molecular interactions during the entry process is presented in Figure I.7.

Invasion of enterocytes from the basolateral side requires initial contact of *Shigella* with the host cell membrane. The establishment of the initial interaction is poorly understood. *Shigella* is known to inefficiently adhere to host cell surfaces, what can be attributed to the lack of an adhesin. Expression of an ectopic adhesin (e.g. AfaE from UPEC[179]) or centrifugation are therefore common techniques to boost cell adhesion in *in vitro* experiments. Recently, Romero and colleagues proposed the initial contact to be established by thin filopodial structures that extend a few microns above the cell surface and capture bacteria. Contact formation is dependent on the T3SS tip complex and leads to retraction of the extension, bringing the bacterium in contact with the cell body. The retraction of the filopodial extensions requires the activation of the MAPkinase ERK1/2. While this process was observed frequently when infecting HeLa cells, it was observed at a lower rate in polarized Caco-2 cells. In fact, the relevance of this process *in vivo* remains to be validated[180].

### *Shigella* interacts with CD44 and $\alpha5\beta1$ integrin receptors

When getting in contact with the cell surface, *Shigella* preferentially interacts with cholesterol-enriched microdomains within the membrane, known as lipid rafts. The translocator component IpaB and its *Salmonella* homologue SipB bind cholesterol with high affinity and can integrate into liposomes mimicking lipid raft composition even in the absence of proteins[181,182]. Depletion of cholesterol and sphingolipids, known components of lipid rafts, reduces *Shigella* invasion[183]. Besides different physical properties, lipid rafts are believed to be enriched in receptors. Among these, the hyaluronic acid receptor CD44 accumulates in lipid rafts in a cholesterol-dependent way, where it interacts with the underlying actin cytoskeleton[184]. CD44 has been shown to colocalize with F-actin in *Shigella* entry foci. IpaB directly binds to the extracellular part of CD44. While pretreatment of cells with a CD44 antibody reduces *Shigella* invasion by 70%, it does not block infection completely, suggesting that the receptor is not essential for a successful entry process[185]. Furthermore, the interaction between IpaB and CD44 is not sufficient for bacterial entry as *ipaC* or *ipaD* mutants are deficient for invasion[186]. It was suggested that CD44 might promote close association of the bacterium with the host cell thereby favoring insertion of the translocator pore (IpaB/C) into the membrane.

A second putative receptor for *Shigella* was described by Watarai and colleagues[187]. The tip complex proteins IpaB, IpaC and IpaD immunoprecipitate with $\alpha5$ and $\beta1$ integrins. The $\alpha5\beta1$ integrin receptor binds fibronectin, a major component of the extracellular matrix. Indeed, the binding of IpaB/C/D was outcompeted by superfibronectin, a multimeric form of fibronectin. Surprisingly, the interaction with $\alpha5\beta1$ integrin was only observed when the Ipa proteins were released from the bacterial surface[187]. This finding was supported by the observation that Ipa proteins are released from the bacteria upon contact with the host cell or with proteins from the extracellular matrix[188] and that IpaB and IpaC formed a soluble complex[189]. The release of Ipa proteins is required for efficient bacterial invasion. For instance a *spa32* mutant, in which the Ipa proteins still form the tip complex, but can no longer be released, was strongly impaired in invasion[188–190]. Taken together, these results indicate that the interaction with the integrin receptor is not required for docking to the cell surface, but instead promotes bacterial invasion by outside-in signaling. Yet, the exact role of integrins in *Shigella* infection has not been clarified.

### Activation of the small GTPases Cdc42 and Rac leads to the formation of filopodia and lamellipodia

Rho GTPases Rac, Cdc42 and Rho are central regulators of the eukaryotic cytoskeleton and are therefore involved in processes like cell migration, cell cycle and cell polarity. Guanine-nucleotide exchange factors (GEFs) and GTPase-activating

proteins (GAPs) control the activation status of small GTPases. The wide range of host cell processes that are controlled by small Rho GTPases makes these proteins, as well as their corresponding guanine-nucleotide exchange factors (GEFs) and GAPs, prime targets for virulence factors[191]. As cell invasion by *Shigella* is known to lead to massive rearrangements of the actin cytoskeleton[179], it is not surprising to find the small GTPases to be involved.

Ménard and colleagues have reported that latex beads being coated with the IpaB/C complex were internalized into cells[189]. Although the internalization was not very efficient, it was further shown that this process is sensitive to *C. difficile* toxin B, a known inhibitor of Rho family proteins. The involvement of Rho family GTPases was confirmed through expression of dominant negative forms of Rac1, Cdc42 and Rho. For all constructs, a reduction in infection rate was observed[192]. The dominant negative forms of Rac1 and Cdc42, but not Rho, further showed less actin polymerization and a reduced number of entry foci[193]. In addition, Rac1 and Cdc42 were demonstrated to localize to *Shigella* entry foci[192].

The bacterial effector mediating the activation of Rac1 and Cdc42 was proven to be the translocator protein IpaC. Expression or microinjection of IpaC leads to the formation of filopodial structures and promotes *Shigella* invasion[194]. While the activation of Rac1 primarily induces the formation of lamellipodia, Cdc42 promotes both filopodial and lamellipodial structures[194]. Lamellipodia are cell extensions resulting from a mesh-like arrangement of actin filaments at the plasma membrane. Formation of lamellipodia can be observed at the leading edge of migrating cells. Filopodial structures arise from bundled actin filaments, which can extend over several microns. Actin-binding proteins like fascin or T-plastin mediate the formation of actin bundles by cross-linking individual filaments. In a *Shigella* infection, T-plastin is involved as the expression of a dominant negative construct reduces infection rate significantly[195]. To summarize, these data indicate that *Shigella* is promoting its entry by inducing the formation of filopodia and lamellipodia, which is controlled by the small GTPases Cdc42 and Rac.

### Src is targeted by IpaC and plays a central role in foci formation

The tyrosine kinase Src was first discovered as a proto-oncogene in chicken, having high similarity to the *v-src* gene of the sarcoma virus. Src plays a role in development and cell division and has been associated with a number of human cancers. Dehio and colleagues found that Src, together with its substrate cortactin, is recruited to *Shigella* entry foci[196]. While cortactin colocalized with F-actin, Src was associated with membranes in the vicinity of the invading bacterium. Cortactin was further demonstrated to be tyrosine-phosphorylated upon *Shigella* infection. Overexpression of Src did increase the amount of tyrosine-phosphorylated cortactin, indicating that this process is mediated by Src[196]. Remarkably, overexpression of Src significantly increased the internalization of non-invasive *Shigella* by HeLa

cells. Similar results were found when stimulating cells with EGF and are likely attributed to the induction of membrane ruffles in either of the two conditions[196,197].

The importance of Src in the *Shigella* entry process is emphasized by a strong reduction in infection rate and foci formation when expressing a dominant-negative form of the kinase. At the same time, expression of a constitutively active form also decreased infection rate and shortened the lifetime of entry foci, indicating that the level of Src activation is fine-tuned by *Shigella* to allow for efficient entry[199]. The delicate behavior of Src is likely to arise from a negative feedback loop that is mediated by Rho. Activated Rho is required for Src recruitment to entry sites. At the same time, Src negatively regulates Rho activation through tyrosine-phosphorylation of the Rho GAP ARHGAP35[193]. The level of Src activation might therefore indirectly control the kinetics of Src recruitment to the plasma membrane and the rate of entry foci formation.

A recent publication by Mounier et al. has clarified the role of the translocator protein IpaC in activating Src[200]. The carboxyterminal domain of IpaC recruits and activates Src. This process is independent of other translocated effectors. In agreement with previous results, Src mediates tyrosine-phosphorylation of cortactin, which can be efficiently inhibited by the Src family inhibitor PP2. Translocation of the carboxyterminal domain alone – using the Iota toxin system – is sufficient to induce Src activation and the formation of microspikes in HeLa cells[200].

### Abl1/2 control membrane recruitment of cortactin and Rac via Crk

Similar to Src, the oncogenes Abelson tyrosine-protein kinases 1 and 2 (Abl1/2, also known as Abl/Arg) are activated and recruited to entry sites during *Shigella* invasion with similar kinetics as seen for Src activation[201]. Infection rate decreased by 80-90% when infecting *Abl1/2* knockout mouse embryonic fibroblasts (MEFs), as compared to wildtype MEFs. Furthermore, the Abl inhibitor STI-571 reduced infection rate up to 98% when used at micromolar concentrations[201]. This is of particular interest, as STI-571 – better known as Glivec® – is already successfully applied in the clinic treating chronic myelogenous leukemia and gastrointestinal stromal tumors[202].

The strong impact of Abl1/2 on *Shigella* infection is likely to be attributed to

**Figure I.7 *(following page)* Schematic representation of *Shigella* entry into epithelial cells.** *Shigella* triggers its uptake into non-phagocytic cells by injecting effector proteins (orange) through its type III secretion system (T3SS) into the cell cytoplasm where they interact with proteins of the host (green). Several systems of the host cell are targeted including the actin cytoskeleton, focal adhesions and microtubules. The coordinated action of the effectors will promote membrane protrusions engulfing the bacterium and ultimately result in its uptake into the cell. For more details, refer to the corresponding sections of the manuscript. The data presented here has also been covered by several reviews[135,155,160,198].

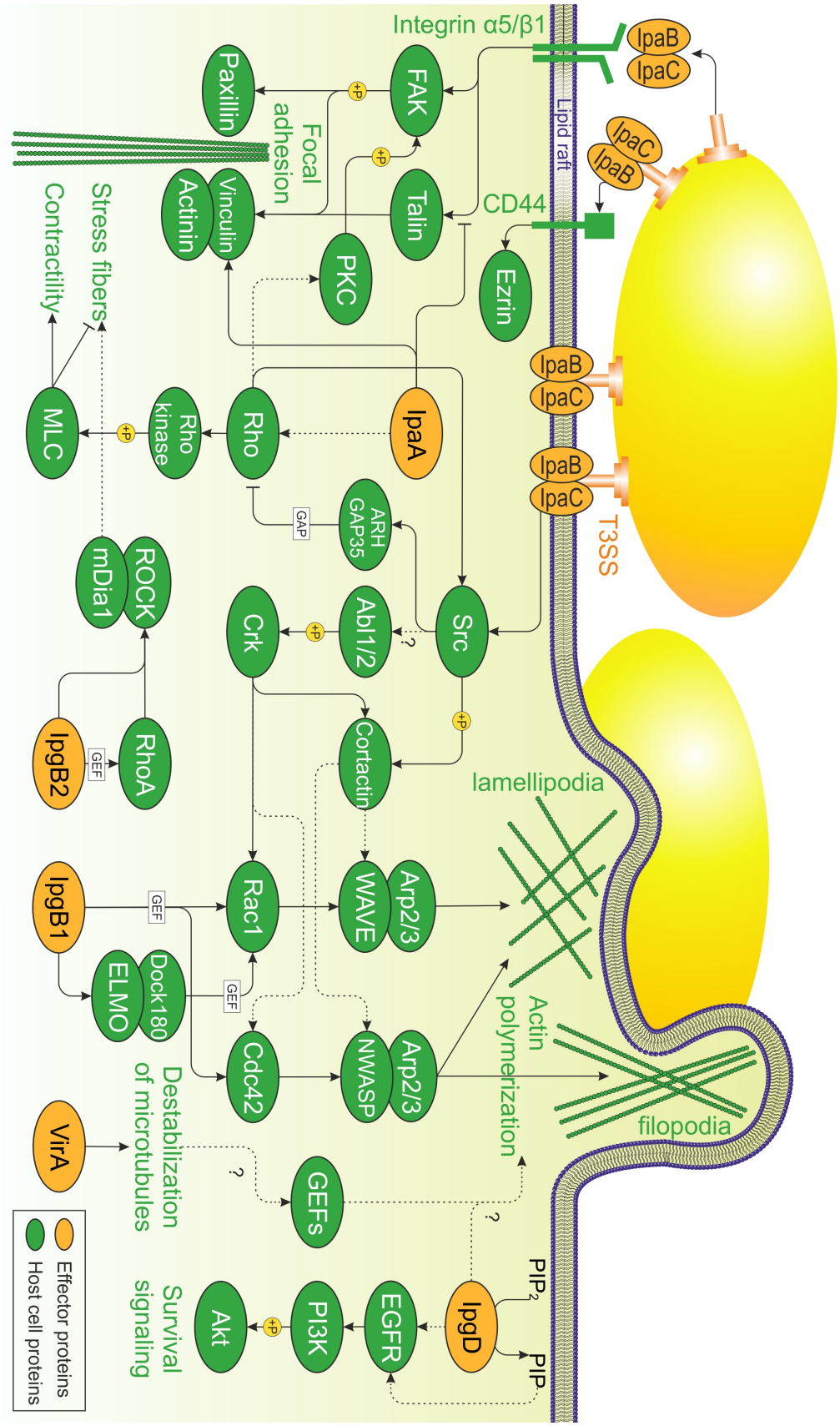
Integrin α5/β1
IpaB
IpaC
Lipid raft
Paxillin
FAK
Focal adhesion
Actinin
Vinculin
Talin
CD44
PKC
Ezrin
Stress fibers
Contractility
MLC
Rho kinase
Rho
IpaA
GAP
ARH GAP35
T3SS
mDia1
ROCK
Crk
Abl1/2
Src
IpgB2
GEF
RhoA
Cortactin
lamellipodia
IpgB1
Rac1
WAVE
Arp2/3
ELMO
Dock180
Cdc42
NWASP
Actin polymerization
filopodia
Destabilization of microtubules
VirA
GEFs
PIP2
PIP3
IpgD
EGFR
PI3K
Akt
Survival signaling
Effector proteins
Host cell proteins

its role in the activation of Rac and Cdc42. In *Abl1/2*$^{-/-}$ MEF, no activation of Rac or Cdc42 could be observed upon *Shigella* infection[201]. A recent study found that knockdown of Unc119, an adaptor protein inhibiting Abl1/2 kinase activity, promoted *Shigella* invasion in the mouse pulmonary infection model[203], thereby providing further evidence for the importance of Abl1/2 during *Shigella* invasion. Finally, Abl together with Src play a central role in *H. pylori* infections[204].

Burton and colleagues reported that tyrosine-phosphorylation of the adaptor protein Crk by Abl1/2 is an essential step in *Shigella* invasion[201]. The phosphorylation of Crk had previously been described to lead to membrane localization of the protein[205]. Indeed, Crk is recruited to entry foci and colocalized with cortactin and F-actin during *Shigella* invasion. Crk directly interacts with cortactin, which is strongly increased by Src-mediated phosphorylation of cortactin. Together, Crk and cortactin contribute to the formation of actin foci in a process dependent on the Arp2/3 binding domain of cortactin[206]. Crk has as well been reported to activate Rac by recruiting it to the plasma membrane[205]. It seems likely that the inability of *Abl1/2* knockout MEFs to recruit and activate Rac and Cdc42 can partially be attributed to mislocalization of Crk.

In conclusion, Abl1/2 kinases are essential to localize cortactin and possibly Rac to bacterial entry sites via phosphorylation of Crk. The recruitment of cortactin is significantly enhanced by Src-dependent tyrosine-phosphorylation. Cortactin in concert with Rac/WAVE leads to actin polymerization through the Arp2/3 complex promoting the formation of a permissive entry structure.

### IpgB1 and IpgB2 are bacterial GEF mimics

IpgB1 and IpgB2 show 17% amino acid sequence identity and are both secreted into host cells via the T3SS. While an *ipgB1* mutant displays a significant decrease in invasiveness, the *ipgB2* mutant has no phenotype in cell invasion assays and the Sereny test[207,208]. The *ipgB1/2* double mutant displays a pronounced defect in invasion and attenuated virluence in the Sereny test, as well as in the mouse pulmonary infection model, thereby indicating that the two effectors cooperate to facilitate invasion[208]. IpgB1 furthermore induces membrane ruffles when expressed in HeLa cells. The ruffle formation is sensitive to Rac1 or Cdc42 inhibition but is independent of Src and Abl1/2[207,209].

Initial reports have indicated that IpgB1/2 might mimic activated G proteins. IpgB1 is believed to mimic the activated form of RhoG, which results in the recruitment of ELMO and Dock180 to entry sites[209]. As Dock180 is a specific GEF for Rac1[210], it is hypothesized that IpgB1 activates Rac1 via ELMO/Dock180. IpgB2 was first reported to act as a mimic of activated RhoA, thereby interacting with Rock and mDia1 to induce actin stress fibers[211]. However, more recent publications have revealed that IpgB1/2 act as mimics of GEFs. IpgB1 has GEF activity for

Rac1 and to a lesser extent for Cdc42[212]. IpgB2 shows GEF activity for RhoA and with lower affinity for Rac1 and Cdc42. This was confirmed as the structure of the IpgB2/RhoA complex could be solved and the model agreed with the GEF activity of IpgB2[212,213].

Effectors harboring GEF activity for Rho family proteins have emerged as a common concept for controlling cytoskeletal rearrangements by bacterial pathogens[214]. Bacterial effectors that have been described as GEF mimics, including IpgB1 and IpgB2, all share a WxxxE sequence motif, which is essential for GEF activity[211]. Among these, one can find Map, EspM and EspT from EPEC and EHEC, BepF from *Bartonella henselae* and *Salmonella* effectors SopE, SifA and SifB.[211,215,216]. Structural analysis of the interaction between Map and Cdc42 has provided further evidence on how the effectors interact with Rho proteins. Besides two well conserved domains mediating GEF activity, there are two domains that define the specificity for a certain Rho protein. Changing several residues in the recognition site of Rho proteins can therefore alter substrate specificity of bacterial effectors (e.g. changing 4 amino acids in Rac1 makes it a substrate for Map)[212].

In summary, IpgB1 is interacting with ELMO and Dock180 and exhibits GEF activity mainly towards Rac1. In concert with the GEF activity of Dock180, IpgB1 might therefore be the main activator for Rac1, leading to membrane ruffles during *Shigella* invasion. IpgB2 binds Rock and mDia1, two proteins known to interact with RhoA, and exhibits GEF activity towards RhoA. RhoA in turn controls the formation of actin stress fibers and, via PKC, focal adhesion structures. As an *ipgB2* mutant shows no major phenotype in invasion assays, one can speculate that the effector might play a role at later stages of infection. In fact, IpgB2 is involved in NF-$\kappa$B activation[120]. Further work is required to delineate the precise function of IpgB2 during *Shigella* infection.

### Focal adhesions are involved in *Shigella* cell invasion

Besides the small GTPases Cdc42 and Rac, Rho plays an important role during *Shigella* invasion. Inhibition of Rho activity by the exotoxin C3 of *Clostridium botulinum* reduced infection rate by almost 90% and significantly less actin polamerization was observed. All three isoforms (RhoA, RhoB and RhoC) localize to entry foci, although at discrete locations within the entry structure[217,218]. Active RhoA was shown to activate and recruit PKC to the site of entry. Inhibitors of PKC (e.g. calphostin C) interfere with efficient cell invasion. PKC is known to be involved in the regulation of focal adhesion by phosphorylating focal adhesion kinase (FAK)[218].

The involvement of focal adhesion in *Shigella* infections is supported by the fact that the addition of Ipa invasins (IpaB/C/D) to the culture medium leads to actin rearrangements and accumulation of FAK, paxillin, vinculin and talin. Besides

that, FAK and paxillin get tyrosine phosphorylated[218]. As it is known that IpaB and IpaC form a soluble complex that interacts with $\alpha5\beta1$ integrins[187,189], it seems likely that the accumulation of proteins involved in focal adhesion is mediated by outside-in signaling through $\alpha5\beta1$ integrins. However, the exact mechanism of this signaling cascade has not been described. Additionally, Skoudy et al. found ezrin, a protein that links actin filaments to the plasma membrane, to play a role in *Shigella* invasion. Expression of a dominant-negative form of ezrin significantly reduced infection rate[219]. This is of particular interest, as ezrin associates with CD44[220], the hyaluronic acid receptor targeted by IpaB[185]. Besides outside-in signaling through integrins, IpaB might therefore promote cytoskeletal rearrangements by interacting with CD44 and ezrin.

Tran van Nhieu and colleagues discovered another pathway through which *Shigella* can control focal adhesions[221]. The effector IpaA binds vinculin, a protein involved in anchoring actin filaments to the membrane. An *ipaA* mutant displayed a 10-fold decrease in infection rate. However, infection was not entirely blocked and could still occur in a delayed fashion independent of vinculin. The mutant also induced an equal amount of actin polymerization when compared to the wildtype, with the only difference that the F-actin was not as closely associated with the invading bacterium. The importance of vinculin is emphasized by the fact that the invasion efficiency positively correlates with the amount of ectopically expressed vinculin in vinculin-deficient cells. IpaA also recruits vinculin and its interaction partner $\alpha$-actinin to *Shigella* entry sites[221]. Noteworthy, the interaction of IpaA and vinculin is another example for molecular mimicry. Two groups independently discovered that IpaA mimics talin-vinculin binding and activation[222,223].

More recent studies define IpaA functions more precisely, pointing out that IpaA is controlling F-actin dynamics and disrupting focal adhesions as well as stress fibers. The interaction of IpaA and vinculin stabilizes the interaction of vinculin with barbed ends of actin filaments, thereby controlling polymerization and depolymerization [224,225]. IpaA furthermore disrupts stress fibres. At first, it was assumed that this was a result of actin depolymerization through interaction with vinculin[224]. However, a later study showed that it was independent of vinculin but required the activation of Rho[226]. In fact, IpaA activates Rho, which leads to an increased phosphorylation of myosin light chain (MLC) mediated through Rho kinase. The phosphorylation of MLC results in a loss of stress fibers and increased contractility. Only recently, a similar pathway was described for *Salmonella* invasion involving myosin II[227]. And myosin VII plays a role in *L. monocytogenes* infections[228]. Furthermore, IpaA reduces the binding of vinculin and talin to the cytoplasmic domain of $\beta1$ integrins, which leads to a disruption of focal adhesions.

To sum up, the regulation of focal adhesion plays an important role in *Shigella* invasion. Initial results suggested that the formation of focal adhesion structures at entry sites promotes invasion. This is supported by the fact that proteins from focal adhesions are recruited to sites of entry via outside-in signaling through in-

tegrins, which is mediated by the IpaB/C complex[187,189]. Moreover, inhibition of PKC reduces invasion[218]. And ezrin, which interacts with CD44 and promotes membrane anchoring of actin filaments, is involved in *Shigella* invasion[219]. Contradictory, the effector IpaA promotes disruption of actin stress fibers and focal adhesions[226]. While these effects seem to be antagonistic at the first glance, it is worthwhile to note that focal adhesions in cells – in the absence of any perturbation – are turned over by an endocytic process[229]. One might hypothesize that *Shigella* first triggers assembly of a focal adhesion structure through outside-in signaling involving integrins and CD44 and subsequently disrupts this structure by injecting IpaA, thereby promoting endocytic processes. While there is no *in vivo* data available for *Shigella* that could support such a mechanism, a recent study has proposed a similar mechanism for *L. monocytogenes*, where InlB promotes junctional endocytosis through interaction with the receptor c-Met[230].

### IpgD and VirA accomplish dual functions during *Shigella* invasion

The enzymatic activity of IpgD has been defined very precisely as phosphatidylinositol (PtdIns) phosphatase that can convert PtdIns$_{4,5}$-bisphosphate ($PIP_2$) into PtdIns$_5$-phosphate (PIP)[231]. $PIP_2$ regulates membrane-cytoskeleton adhesion[232] and binds several actin-interacting proteins like vinculin, WASP and ezrin[233]. The depletion of $PIP_2$ from the membrane through IpgD leads to a lower adhesion energy between membrane and cytoskeleton which is believed to promote dissociation of F-actin from membranes. In fact, the overexpression of IpgD in HeLa cells gives rise to membrane blebbing and cell rounding. This effect on actin filaments seems to enhance the effect of Cdc42 and Rac on cytoskeletal rearrangements. An *ipgD* mutant induces much smaller entry foci having a cup-like structure[231]. A recent publication has confirmed the effect of IpgD on the cytoskeletal organization by showing that the effector inhibits migration of T lymphocytes[234]. Besides its effect on the actin cytoskeleton, IpgD promotes cell survival through activation of PI3K and Akt[235]. A precise description of the mechanism can be found in section 4.2.1.

VirA is another effector secreted into host cells by *Shigella*. Infections using a *virA* mutant have revealed a defect in intercellular spread of *Shigella*[236,237]. Additionally, Uchiya and colleagues have reported a strong defect in cell invasion[236]. This observation could not be reproduced by Demers et al., although they had noticed attenuated virulence in the Sereny test. Furthermore, infections with the *virA* mutant using the rabbit ileal loop model did not show any major phenotypes[237], indicating that VirA might only possess an accessory role in cell invasion.

More recent publications describe that VirA interacts with tubulins *in vitro* and destabilizes microtubules *in vivo*[238]. It was initially speculated that VirA might directly cleave $\alpha$-tubulin as it shares similarities with cysteine proteases[239]. However, structural data for VirA revealed a unique fold that did not resemble any known cysteine proteases, but shared homology with the EspG virulence factor of

pathogenic *E. coli*[240,241]. VirA might therefore destabilize microtubules by interacting with host proteins controlling microtubule dynamics. VirA further promotes Rac1 activation leading to membrane ruffles through an unknown mechanism[238]. It was suggested that microtubule disassembly might promote Rac1 activity by releasing microtubule-associated GEFs (e.g. GEF-H1)[242].

In summary, VirA destabilizes microtubules, which is considered to be important for efficient intracellular motility and cell-to-cell spread[239]. Additionally, VirA promotes Rac1 activity that might enhance cell invasion[238]. It is noteworthy that two recent publications have described the VirA homologue EspG to act as a scaffolding protein for PAK and Arf6, thereby altering membrane trafficking. However, no destabilizing effect on microtubules could be found[243,244]. Whether VirA works similarly or has diverging activities from EspG remains to be validated.

### 4.1.4 Intercellular motility and intracellular growth

Upon successful uptake into host cells, *Shigella* is surrounded by a lipid bilayer termed the phagosome. In contrast to *S. typhimurium*, which modifies the membrane compartment into a so-called *Salmonella*-containing vacuole (SCV) permissive for replication, *Shigella* lyses the phagosome and escapes into the cytoplasm in less than 15 minutes. Membrane lysis is dependent on the T3SS and the translocators IpaB, IpaC and IpaD[159,179,245]. Although all three proteins are required, IpaC is the biochemical mediator of phagosome lysis[246]. Remarkably, IpaC is also capable of lysing the SCV when expressed in *Salmonella*[247].

Within the host cell cytoplasm, *Shigella* is able to move by actin-based motility. This special feature is shared by other pathogens including *Listeria monocytogenes*, *Rickettsia rickettsii*, *Mycobacterium marinum*, *Burkholderia pseudomallei* and the vaccinia virus[161]. The driving force for the movement is directed actin polymerization at one pole of the bacterium. The mediator for actin polymerization is the *Shigella* IcsA protein[248,249]. Its polar localization is controlled by the serine protease SopA (IcsP) and the apyrase PhoN2[250,251]. IcsA directly interacts with the host protein N-WASP, which will in turn recruit the Arp2/3 complex. The recruited host cell factors mediate actin nucleation and directed elongation of the actin tail, propelling *Shigella* through the cytoplasm[252].

Besides intracellular movement, actin-based motility allows *Shigella* to move from cell to cell. Intercellular spread is achieved by forming protrusions at tight junctions connecting adjacent enterocytes. These protrusions can be endocytosed by the targeted cell in a process that requires the host factor myosin light-chain kinase[253]. After successful intercellular movement, *Shigella* lyses the surrounding double membrane in a process that requires again the IpaB/C/D invasins and is believed to be identical to the lysis of the phagosome[245,254]. Efficient intra- and intercellular movement was reported to be dependent on the *Shigella* virulence factor VirA. It was suggested that VirA destabilizes microtubules, which might otherwise hinder

movement within the cytoplasm[239]. A recent publication has demonstrated that the host cell can interfere with actin-based motility. Bacteria producing actin comet tails got associated with septins, proteins involved in cell devision. In fact, some bacteria got entrapped in a cage-like structure formed by septins, which prevented intercellular spread[255].

An important feature of *Shigella* in order to survive and multiply within the host cell cytoplasm is the evasion of autophagy. Autophagy is a mechanism of eukaryotic cells, which is able to degrade host cell components, including entire organelles, by surrounding them in double-membrane-bound compartments that get targeted for lysosomal degradation[256]. Besides the function of cell maintenance, autophagy plays pivotal roles in the host innate immune system[257]. For instance, proteins from the autophagic machinery associate with intracellular bacteria eventually leading to their degradation. Furthermore, autophagy acts downstream of pathogen-recognition receptors (PRRs) like Nod1[77]. Ogawa and colleagues were the first to describe that intracellular *Shigella* get targeted for autophagy when the T3SS effector IcsB is absent. IcsB prevents autophagy by masking the surface-exposed virulence factor VirG that mediates actin-based motility. In the absence of IcsB, VirG is recognized by the autophagy protein Atg5, which recruits the autophagic machinery[163,258]. A recent report additionally implicated the PRRs Nod1 and Nod2 to promote autophagy of *Shigella* by interacting with the autophagy regulator Atg16L1 and recruiting it to bacterial entry sites[77,78]. Moreover, the entrapment of *Shigella* in septin-cages is more efficient when autophagic markers like Atg5 are present[255].

The cytoplasm of enterocytes represents the main replicative niche for *Shigella* where it multiplies with a generation time of less than 40 minutes. Lucchini and colleagues revealed that after successful cell invasion almost 25% of the *Shigella* genes are significantly up- or downregulated[259]. This indicates that survival and replication within enterocytes requires a high degree of adaptation to the intracellular environment. At the same time, little is known about critical factors for intracellular survival and replication. The study from Lucchini argued that access to iron, magnesium and phosphate might be a limiting factor. TonB, a membrane protein providing energy for iron uptake systems, is required for intracellular growth of *Shigella dysenteriae*. However, a *tonB* mutant is not affected in iron uptake, suggesting that TonB might be crucial for the uptake of a nutrient other than iron[260]. Mutants, which cannot synthesize guanine, thymine and p-aminobenzoic acid were shown to be defective in intracellular replication. Additionally, mutants auxotrophic for diaminopimelate can not survive in the cytoplasm[261–263]. The carbon sources for intracellular *Shigella* are not known, but it was shown that *uhpT*, which encodes for a hexose phosphate transporter, is highly upregulated upon successful infection. Nevertheless, a *uhpT* mutant is able to grow intracellulary indicating that *Shigella* is accessing alternative carbon sources[264]. A very recent study has indicated that *Shigella* can sustain oxidative stress, which is regulated by the transcriptional activators *oxyR*, *soxR* and *soxS*. While resistance to oxidative

stress is important at different stages of a *Shigella* infection, it proves to play a role in intracellular growth as mutants show a slight decrease in plaque formation[265]. Finally, efficient intracellular growth also requires the host cell to remain permissive for intracellular growth. Different ways of how *Shigella* controls the fate of the host cell are discussed in the following section.

## 4.2 Modulation of host cell signaling

As presented in the previous section, *Shigella* very efficiently subverts the cytoskeletal machinery to promote its uptake into non-phagocytic cells. These processes are mediated by a set of effector proteins that get secreted into the host cell cytoplasm via the T3SS. Besides the effectors that manipulate signaling cascades controlling cytoskeletal rearrangements, there are further effector proteins injected, which control post-invasion aspects during a *Shigella* infection. First of all, the intracellular bacteria promote the survival of the host cell in order to protect the replicative niche. Secondly, *Shigella* slows down self-renewal mechanisms of the intestinal epithelium that would otherwise result in a rapid clearance of the infection. And finally, several effectors target proinflammatory signaling cascades resulting in a modulated immune response that is more permissive for bacterial survival and replication.

### 4.2.1 *Shigella* promotes host cell survival

The first effector that was described to promote the survival of infected epithelial cells was IpgD. Pendaries and colleagues found that cells overexpressing IpgD are protected from apoptosis induced by staurosporin[235]. The inhibition of apoptosis is dependent on the phosphoinositide phosphatase activity of IpgD resulting in the production of phosphatidylinositol-5-phosphate (PIP)[231]. Furthermore, IpgD induces the phosphorylation of Akt and its substrates GSK3 and FKHR. The phosphorylation of Akt in turn requires a class IA PI3K. Noteably, the activation of Akt is dependent on tyrosine-phosphorylation, as treatment with the tyrosine-inhibitor herbimycin A blocks Akt phosphorylation[235]. This observation was recently confirmed when the EGF receptor (EGFR), a receptor tyrosine-kinase, was demonstrated to be required for activation of Akt[266]. Furthermore, the EGFR is recruited to entry foci in an IpgD-dependent manner. It seems likely that production of PIP by IpgD targets EGFR to the membrane, where it tyrosine-phosphorylates PI3K and leads to survival signaling via Akt.

Moreover, PIP, together with EGFR, gets enriched in endosomes where it interferes with trafficking of early endosomes to lysosomes. This impairs EGFR degradation in lysosomes and represents an essential mechanism prolonging the survival signaling via PI3K/Akt[266]. In addition, the perturbation of membrane trafficking might explain the entry phenotype observed in an *ipgD* mutant infection[231]. Localization

of Cdc42, the small GTPase essential for *Shigella* entry, is dependent on membrane traffic in the context of cell migration and polarity[267,268]. It is tempting to hypothesize that the capability of IpgD to alter membrane trafficking by producing PIP promotes localization of Cdc42 (and possibly other G proteins) to the plasma membrane. Although this hypothesis seems plausible, there is currently no experimental data available supporting this conclusion.

A second effector known to promote host cell survival is Spa15. This protein has already been described as a chaperone for several effectors[269]. Faherty et al. unveiled that Spa15 is secreted by the T3SS and that a *spa15* mutant is not able to protect infected cells from staurosporin-induced cell death to the same extent as the wild type. In fact, cells infected with the *spa15* mutant display activated caspase-3, while no activation is found in wild type infections[270]. This indicates that Spa15 is able to interfere with apoptosis upstream of caspase-3.

Intestinal epithelial cells are subject to rapid turnover and exfoliation, which represents an innate defense mechanism[271]. Nevertheless, many intestinal pathogens are able to efficiently colonize these cells. *Shigella* overcomes this defense mechanism by secreting the effector OspE. OspE consists of the proteins OspE1 and OspE2 and is highly conserved among pathogenic *E. coli* and *Salmonella* strains. OspE interacts with integrin-linked kinase within focal adhesions of HeLa cells, thereby facilitating the formation of focal adhesions and suppressing their turnover. This, in turn, promotes the attachment of infected cells to the extracellular matrix through integrins. The importance of OspE was demonstrated *in vivo* where an *ospE* mutant displayed reduced inflammation and colonization in the guinea pig infection model[272].

In the intestine, self-renewal is mediated by progenitor cells, which provide new epithelial cells through cell division and are located at the base of crypts. Iwai and colleagues revealed that *Shigella* interferes with this process by inducing a cell cycle arrest[273]. The inhibition of cell cycle progression is mediated by the translocator IpaB, which targets Mad2L2, a protein involved in metaphase-to-anaphase transition. It was proposed that *Shigella* infects progenitor cells directly or through intercellular motility. Upon infection, *Shigella* blocks cell cycle progression and therefore self-renewal of the epithelial tissue. While most of these effects are difficult to directly demonstrate *in vivo*, an *ipaB* mutant unable to bind Mad2L2 was shown to reduce colonization in the rabbit intestinal loop model[273].

In summary, *Shigella* is promoting cell survival and inhibiting apoptosis in infected epithelial cells. Additionally, it modulates self-renewal and exfoliation at the level of the infected epithelium by strengthening cell attachment and inducing cell cycle arrest in progenitor cells. Presumably, these processes protect the replicative niche and allow for a prolonged infection of the host. It is though important to note that *Shigella* induces cell death in epithelial cells at later stages of infection[274,275]. This implies that during the early phase of infection, survival signals are dominating, while at later stages, when the bacterial load is increasing and conditions might

become less favorable, cell death pathways are activated.

### 4.2.2 Modulation of proinflammatory signaling cascades

Besides the protection of the replicative niche by promoting host cell survival, the control of the inflammatory response is a key factor for a successful infection. The presence of intracellular pathogens is sensed by the cytoplasmic pathogen recognition receptor Nod1. Nod1 is activated upon binding of peptidoglycan moieties that are shed from the bacterial surface[44]. In turn, Nod1 oligomerizes and activates the NF-$\kappa$B and MAPkinase signaling cascades, which promote the expression of proinflammatory genes[276]. Among these genes are several cytokines (e.g. IL-8) that get secreted and promote the attraction of immune cells to the site of infection[123]. Furthermore, the enterocytes express antimicrobial peptides (e.g. $\beta$-defensins) that can contribute to the clearance of the pathogen[124].

*Shigella* has brought forth several effector proteins that get injected into the host cell cytoplasm through the T3SS where they manipulate proinflammatory signaling cascades[155,277]. OspG, for instance, inhibits NF-$\kappa$B activation by preventing the degradation of I$\kappa$B, the negative regulator of NF-$\kappa$B. OspG specifically targets UbcH5, a ubiquitin-conjugating enzyme, thereby interfering with the ubiquitination of I$\kappa$B. Consequently, I$\kappa$B fails to be degraded and NF-$\kappa$B is retained in the cytoplasm[278]. The effector OspZ, when ectopically expressed in HeLa cells, prevents NF-$\kappa$B nuclear translocation in response to TNF$\alpha$ or IL-1$\beta$ stimulation. Similar to OspG, I$\kappa$B is no longer degraded when OspZ is present, but the mechanism of inhibition remains currently unknown[279]. Finally, IpaH$_{9.8}$ was found to act as a ubiquitin ligase targeting NEMO for proteasomal degradation. NEMO is part of the IKK complex that phosphorylates I$\kappa$B as a prerequisite for subsequent ubiquitination. Accordingly, the IpaH$_{9.8}$-induced degradation of NEMO leads to a reduction in NF-$\kappa$B activation[280]. Noteworthy, IpaH$_{9.8}$ exerts a second function upon translocation to the nucleus. Nuclear IpaH$_{9.8}$ interacts with the splicing factor U2AF[35], thereby reducing the mRNA level for several cytokines including IL-8 and IL-1$\beta$[281]. In addition, IpaH proteins constitute an entire family of T3SS effectors, which are all presumed to be ubiquitin ligases[282]. It is therefore highly probable that *Shigella* modifies additional host proteins by ubiquitination[283].


**Figure I.8 Phosphothreonine lyase reaction catalyzed by *Shigella* effector OspF.** The *Shigella* effector OspF irreversibly dephosphorylates p38 and ERK by its phosphothreonine lyase activity. *Reproduced from Li et al.*[126].

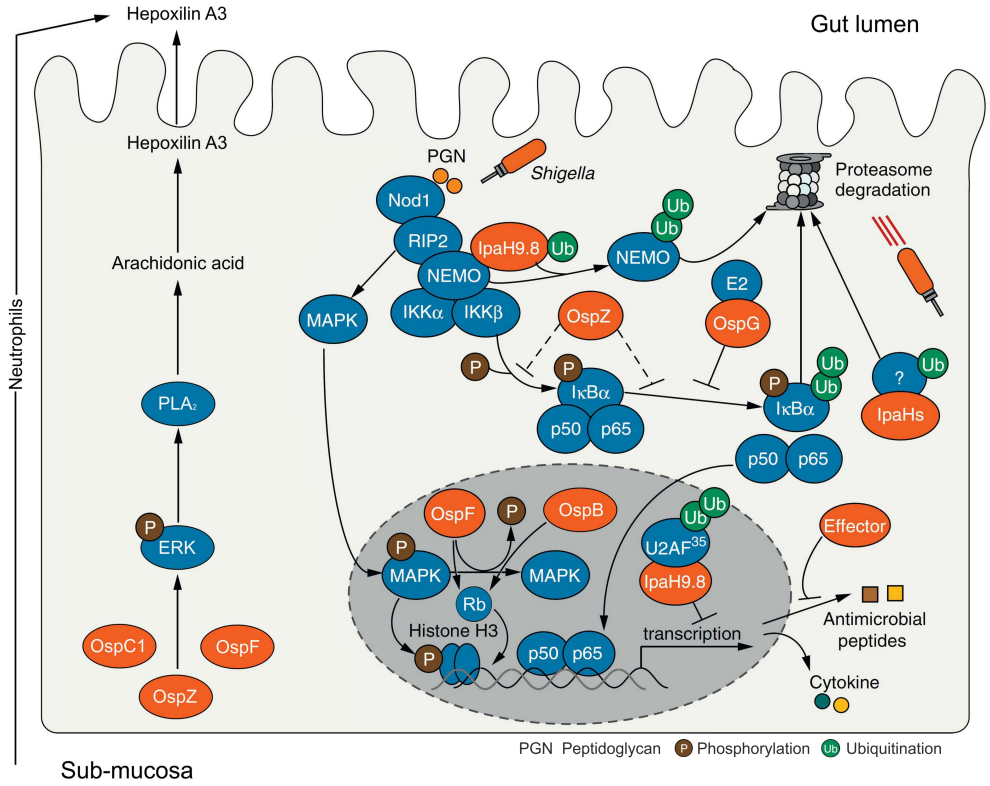


**Figure I.9 *Shigella* modulates the host immune response.** Intracellular *Shigella* secrete several effector proteins via the T3SS into the cytoplasm of the host cell. These effectors interfere with the NF-$\kappa$B and MAPkinase signaling cascades, downregulate the production of cytokines and antimicrobial peptides and promote transepithelial migration of neutrophils. For more details, refer to the corresponding sections of the manuscript. *Adapted with modifications from Ashida et al.*[277].

The *Shigella* effector OspF is well known to interfere with the MAPkinase signaling pathway. The effector exhibits phosphothreonine lyase activity towards p38 and ERK, which is – in contrast to dephosphorylation – an irreversible modification (Figure I.8)[125,126]. The inhibition of p38 and ERK, in turn, reduces the phosphorylation of histone H3, which is required for chromatin modifications that allow transcriptional activation of NF-$\kappa$B-regulated genes. The activity of OspF therefore leads to a downregulation of proinflammatory genes like IL-8[28,125]. OspF was further shown to interact, together with the effector OspB, with the retinoblastoma protein, another regulator of chromatin. Again, this leads to a downregulation of the proinflammatory response[284].

The effectors OspC1, OspZ and OspF are involved in the regulation of PMN transepithelial migration. During *Shigella* infection, PMNs are recruited to the site of infection where they transmigrate across the epithelial layer. The migration in between enterocytes can promote infection, as it disrupts tight junctions giving bacteria in the gut lumen direct access to the basolateral pole of IECs. OspC1,

OspZ and OspF phosphorylate ERK in the cytoplasm, which leads to the activation of phospholipase A2 ($PLA_2$). $PLA_2$ produces arachidonic acid that gets converted to Hepoxilin A3 via the 12/15-lipoxygenases pathway. Hepoxilin A3 is secreted into the gut lumen where it acts as potent chemoattractant for PMNs[285–288].

The importance of antimicrobial peptides (AMPs) for controlling a *Shigella* invasion has been demonstrated in the newborn mouse model and in rabbits[124,289]. Yet again, *Shigella* has evolved mechanisms to evade the action of these antimicrobial agents. Islam et al. have reported that LL-37 and $\beta$-defensin-1, two human AMPs, are downregulated early during *Shigella* infection[290]. Another study found that an entire set of AMPs get suppressed at the transcriptional level[291]. How *Shigella* interferes with the production of AMPs remains currently unknown. Islam and colleagues proposed that bacterial DNA plays a role, while Sperandio et al. reported the suppressing effect to be dependent on *Shigella*'s transcriptional regulator MxiE, suggesting the involvement of effector proteins[290,291]. Noteworthy, a recent report has pointed out that AMPs might not always be beneficial for the host, as the release of AMPs from neutrophils promoted *Shigella* adhesion and invasion of epithelial cells[292].

In conclusion, *Shigella* has brought forth several T3SS effectors that can control various aspects of the innate immune response by modulating signaling cascades within infected cells. While some effectors dampen an inflammatory response (e.g. OspG, $IpaH_{9.8}$), others can promote attraction and transmigration of neutrophils (e.g. OspC1, OspZ). This exemplifies that *Shigella* is not completely blocking the inflammatory response, but rather shapes it to allow an efficient colonization and a prolonged infection. A schematic overview of the effectors that modulate the innate immune system is presented in Figure I.9.

## 4.3 *Shigella flexneri* as a versatile model system for host-pathogen interactions

*Shigella flexneri* is an attractive model organism to study various aspects of host pathogen interactions. First of all, the pathogen interacts both with cells from the immune system and non-myeloid cells. *In vitro* infection models have been established that enable the study of macrophage killing and invasion of epithelial cells at the molecular level. Secondly, the pathogen harbors a T3SS, which is also found in other enteroinvasive pathogens. Intensive research on *Shigella*'s T3SS has significantly contributed to the current knowledge about the structure of this remarkable injection machinery. Of equal interest are the T3SS effector proteins, which are injected into host cells and control various cellular functions like cytoskeletal rearrangements, cell survival and inflammation signaling. Remarkably, effector proteins can also be used as molecular tools to dissect host signaling networks. A publication from our group has exemplified this on the basis of the *Shigella* effector OspF (see Chapter V)[293]. A more complete picture of the impact of effector proteins can

be obtained by comparing the phosphoproteome of cells infected with *Shigella* wild type or effector deletion mutants (Ch. Schmutz, unpublished results). Finally, the *in vitro* infection models are well suited to study cell invasion and inflammation signaling using high-throughput image-based RNAi screens (see Chapter III)[294].

A major restriction, however, is the lack of a suitable animal model for *Shigella* infection. A similar pathology to the disease in humans could only be observed when infecting primates. Vaccine trials, for instance, have been successfully conducted in macaque monkeys[295]. Some aspects of *Shigella* pathogenicity can be studied in the rabbit ileal loop model[296]. *Shigella* virulence is often assessed by infections of the corneal epithelium in guinea pigs (also known as Sereny test)[297]. Although highly desirable, mice have proven to be refractive to *Shigella* infections once they are older than five days[298]. Nevertheless, intragastric infection of newborn mice, as well as intranasal infections are two model systems, which have been established for *Shigella* infections in mice[299,300]. Additionally, Zhang and colleagues have demonstrated the infection of human intestinal xenografts, which are transplanted into SCID mice[301]. Recently, intrarectal infection of guinea pigs has been introduced as a new promising animal model for shigellosis and was already successfully applied in vaccine trials[272,302,303].

# 5 Aim of the thesis

A hallmark of shigellosis is an acute mucosal inflammation, which is accompanied by the massive production and secretion of cytokines. On the other hand, *Shigella* is known to downregulate inflammation signaling, as several T3SS effectors interfere with the expression of cytokines in infected epithelial cells. One might speculate that this discrepancy results from an incomplete inhibition of inflammation signaling in infected cells. Alternatively, host mechanisms might compensate for the immunosuppressive activity of *Shigella* effectors.

The main objective of my thesis was to investigate inflammation signaling during *Shigella* infection in epithelial cells. In particular, we focused on the proposed mechanisms explaining the massive cytokine secretion despite the presence of immunosuppressive effectors. In order to study the immune response of epithelial cells in response to *Shigella*, we applied an *in vitro* infection model using HeLa cells. By means of immunofluorescence microscopy and automated image analysis, the activation of proinflammatory signaling cascades at the single-cell level was quantified. Furthermore, the production of cytokines was measured both with immunofluorescence and enzyme-linked immunosorbent assay (ELISA). In addition, we compared inflammation signaling during infection with *Shigella* wild type or effector deletion strains.

In a second project, we aimed at systematically identifying proteins that mediate inflammation signaling during *Shigella* infection. We adapted the *in vitro* infection assay to allow for the application of high-throughput screening techniques. Using RNA interference, two independent human kinome libraries and a genome-wide library were screened. By means of automated microscopy and image analysis, we quantified the production of the cytokine IL-8, as well as *Shigella* cell invasion and intracellular growth.

In the course of this thesis, the results found for inflammation signaling in epithelial cells during *Shigella* infection are presented and a novel host mechanism amplifying cytokine production is proposed (Chapter II). In a second part, a high-content image-based siRNA screen for *in vitro Shigella* infections is introduced and preliminary results from screening the human kinome are summarized (Chapter III).

# Chapter II

# Cell-Cell Propagation of NF-$\kappa$B Transcription Factor and MAP Kinase Activation Amplifies Innate Immunity against Bacterial Infection

This chapter has been published as:
**Kasper CA**, Sorg I, Schmutz C, Tschon T, Wischnewski H, Kim ML, Arrieumerlou C. Cell-cell Propagation of NF-$\kappa$B Transcription Factor and MAP Kinase Activation Amplifies Innate Immunity against Bacterial Infection. *Immunity*, 33(5):804-16, 2010.

# 1 Summary

The enteroinvasive bacterium *Shigella flexneri* downregulates inflammation by injecting a set of effector proteins into the cytoplasm of infected epithelial cells. Yet, massive production and secretion of cytokines, especially IL-8, is a hallmark of *Shigella* infections. In our studies, we found a mechanism of cell-cell communication that allows the infected cell to circumvent the action of effector proteins by propagating inflammatory signals to uninfected bystander cells. These cells contribute to a massive amplification of the immune response by expressing and secreting proinflammatory cytokines.

By monitoring proinflammatory signals at the single-cell level, we found that the activation of the transcription factor NF-$\kappa$B is rapidly propagated to neighboring cells within the first 15 minutes after infection. The MAP kinases JNK, ERK and p38 were also found to be activated in cells adjacent to infected cells. While infected cells did not produce cytokines, uninfected bystander cells were found to efficiently express IL-8, TNF$\alpha$ and GM-CSF. Cytokine production in bystander cells was also observed during *Listeria monocytogenes* and *Salmonella typhimurium* infections and could be reproduced in various cell lines including HeLa, Caco-2 and HUVEC cells. Additionally, microinjection of peptidoglycan moieties was sufficient to trigger the response. The cell-cell communication was found to be independent of paracrine secretion, but instead was sensitive to gap junction inhibitors. Furthermore, overexpression of connexin 43, the protein forming gap junctions, massively increased the number of bystander cells producing IL-8. Taken together, we have identified a host mechanism that allows infected cells to propagate proinflammatory signals to uninfected bystander cells thereby amplifying the immune response during bacterial infections.

# 2 Statement of contribution

I conducted most of the experiments mentioned in the paper. Additionally, I performed all quantifications that were based on image analysis. Additional experiments were contributed by Isabel Sorg (microinjection, Fig. 5 and S5), Christoph Schmutz (IL-8 upon infection with *S. flexneri* $\Delta$*ospF*, Fig. 4E/F; validation of Cx43 knockdown, Fig. S7F), Therese Tschon (in situ hybridization, Fig. 4B; infections in *Tnfr*$^{-/-}$ MEF, Fig. 6A and S6A/B; TNF$\alpha$ and GM-CSF in bystander cells, Fig. S4E-G), Man Lyang Kim (ELISA for IL-8 secretion, Fig. 4A) and Cécile Arrieumerlou (Infections under flow conditions, Fig. 6D and S6D; Infections in HUVEC cells, Fig. S1A and S4D). The manuscript was written by Cécile Arrieumerlou and myself.

Immunity
Article

# Cell-Cell Propagation of NF-κB Transcription Factor and MAP Kinase Activation Amplifies Innate Immunity against Bacterial Infection

Christoph Alexander Kasper,[1] Isabel Sorg,[1] Christoph Schmutz,[1] Therese Tschon,[1] Harry Wischnewski,[1] Man Lyang Kim,[1] and Cécile Arrieumerlou[1,*]
[1]Biozentrum, University of Basel, Klingelbergstrasse 50-70, CH-4056, Basel, Switzerland
*Correspondence: cecile.arrieumerlou@unibas.ch
DOI 10.1016/j.immuni.2010.10.015

## SUMMARY

**The enteroinvasive bacterium *Shigella flexneri* uses multiple secreted effector proteins to downregulate interleukin-8 (IL-8) expression in infected epithelial cells. Yet, massive IL-8 secretion is observed in Shigellosis. Here we report a host mechanism of cell-cell communication that circumvents the effector proteins and strongly amplifies IL-8 expression during bacterial infection. By monitoring proinflammatory signals at the single-cell level, we found that the activation of the transcription factor NF-κB and the MAP kinases JNK, ERK, and p38 rapidly propagated from infected to uninfected adjacent cells, leading to IL-8 production by uninfected bystander cells. Bystander IL-8 production was also observed during *Listeria monocytogenes* and *Salmonella typhimurium* infection. This response could be triggered by recognition of peptidoglycan and is mediated by gap junctions. Thus, we have identified a mechanism of cell-cell communication that amplifies innate immunity against bacterial infection by rapidly spreading proinflammatory signals via gap junctions to yet uninfected cells.**

## INTRODUCTION

The ability of a host organism to mount an innate immune response after pathogen infection is critical for survival. The epithelial cells, which represent the first physical barrier to invasive pathogens, play a critical role in this process. They act as sentinels of the immune system and largely contribute to the secretion of factors that orchestrate inflammation in infected tissues. Infection by *Shigella* bacteria is a well-suited model to analyze the complex host-pathogen interactions that shape the immune response of intestinal epithelial cells (IECs) to invasive bacteria (Phalipon and Sansonetti, 2007). *Shigella* are Gram-negative foodborne bacteria that invade the colonic and rectal epithelium of humans, causing an acute mucosal inflammation called Shigellosis, responsible for 1.1 million deaths annually (Schroeder and Hilbi, 2008).

*Shigella flexneri,* the etiological agent of the most endemic form of Shigellosis, translocates across the intestinal epithelial barrier by transcytosis through M cells. In the submucosal area, *S. flexneri* makes use of a type III secretion (T3S) apparatus to trigger apoptosis in macrophages and to actively invade IECs via their basolateral surface. The T3S apparatus is a syringe-like nanomachine enabling the translocation of bacterial effector proteins (Cornelis, 2006) that subvert various host cellular pathways in order to promote bacterial entry, modulate cell cycle, and dampen inflammation signaling (Iwai et al., 2007; Parsot, 2009; Phalipon and Sansonetti, 2007). Once internalized, *S. flexneri* multiplies in the cytoplasm and uses actin-based motility to spread to adjacent IECs. During infection, massive mucosal inflammation is observed in the intestine of infected patients (Islam et al., 1997). IECs are critical in this process. They sense pathogenic invasion and respond by inducing a transcriptional program whose major function is to stimulate innate immune defense mechanisms. *Shigella* recognition by IECs occurs essentially intracellularly via the pattern recognition receptor Nod1 that recognizes the core dipeptide structure, γ-D-glutamyl-meso-diaminopimelic acid (Girardin et al., 2003), found in the peptidoglycan of all Gram-negative and certain Gram-positive bacteria (Kufer et al., 2006). Upon ligand recognition, Nod1 homodimerizes and recruits the kinase RIPK2 (Strober et al., 2006). This leads to the sequential recruitment and activation of the TAK1-TAB1-TAB2 and IKKα-IKKβ-IKKγ complexes and the phosphorylation of inhibitor of NF-κB alpha (IκBα). Once phosphorylated, IκBα undergoes polyubiquitination and proteasomal degradation. NF-κB, released from IκBα, translocates to the nucleus and upregulates expression of proinflammatory genes. TAK1 activation also leads to activation of the MAP kinases c-Jun-N-terminal kinase (JNK) and p38 (Lee et al., 2000; Ninomiya-Tsuji et al., 1999; Wang et al., 2001). The MAP kinase ERK is also activated during *S. flexneri* infection of IECs (Köhler et al., 2002). NF-κB, JNK, ERK, and p38 contribute collectively to the initiation of a proinflammatory program. JNK and p38 regulate the activity of the transcription factor AP-1 (Holtmann et al., 1999). p38 and ERK control the access of chromatin to transcription factors via phosphorylation of histone H3 by the kinases MSK1 and MSK2 (Saccani et al., 2002). Among the genes upregulated during infection of IECs, the chemokine interleukin-8 (IL-8) plays a central role (Sansonetti et al., 1999) by attracting polymorphonuclear cells (PMNs) from the peripheral circulation to the infected area to limit the spread of *S. flexneri* invasion.

Immunity
Propagation of Inflammatory Signals in Infection

*S. flexneri* uses multiple strategies to downregulate inflammation. For example, T3 secreted effector proteins OspG and OspF attenuate IL-8 expression by preventing IκBα degradation and dephosphorylating nuclear p38 and ERK, respectively (Arbibe et al., 2007; Kim et al., 2005; Li et al., 2007).

Despite the immunosuppressive activity of multiple bacterial effector proteins, massive IL-8 expression is observed in IECs during Shigellosis, suggesting that the secreted molecules may partially block IL-8 expression or that a host mechanism compensates for their effect. Here, we report the discovery of a host cell-cell communication mechanism that circumvents the bacterial effector proteins and amplifies IL-8 expression. By monitoring proinflammatory signals at the single-cell level, we found that, within minutes of infection, the activation of NF-κB and the MAP kinases JNK, ERK, and p38, propagates from infected to uninfected bystander cells. These cells, in which signaling is not altered by bacterial effector proteins, represent the main source of IL-8 secretion during *S. flexneri* infection. Bystander IL-8 expression can be triggered by recognition of peptidoglycan via Nod1 and is mediated by gap junctions. Thus, we have identified a gap junction-mediated cell-cell communication mechanism that strongly amplifies innate immunity during bacterial infection by rapidly spreading proinflammatory signals to yet-uninfected cells.

## RESULTS

### NF-κB Is Activated in Bystander Cells of *S. flexneri* Infection

To better characterize the molecular mechanisms that control inflammation during bacterial infection, we analyzed NF-κB activation at the single-cell level during *S. flexneri* infection of epithelial cells. The nuclear translocation of the NF-κB p65 subunit, which follows IKK-mediated IκBα degradation, was used as readout for NF-κB activation and was visualized by immunofluorescence microscopy. HeLa cells were infected with noninvasive BS176 or wild-type invasive M90T *S. flexneri* strains at low and high multiplicity of infection (MOI). As expected, extracellular bacteria failed to activate NF-κB in HeLa cells as shown by the fact that p65 remained exclusively cytosolic after infection with BS176 *S. flexneri* (Figure 1A, top left). In contrast, cells infected with M90T at MOI 20 showed massive nuclear localization of p65, reflecting the detection of intracellular bacteria and activation of NF-κB (Figure 1A, top right). Surprisingly, when cells were challenged with M90T at low MOI, a strong p65 nuclear translocation was also observed in some cells that were not infected (Figure 1A, bottom left). Single-cell measurements of *S. flexneri* invasion and p65 nuclear/cytoplasmic ratio (NF-κB activation ratio) confirmed that, at low MOI, more cells were NF-κB activated than infected (Figure 1A, bottom right). False color representations of the NF-κB activation ratio clearly showed that uninfected NF-κB-activated cells were not randomly distributed in the field of view but located in close proximity with infected cells forming NF-κB activation foci around them (Figure 1B). A similar pattern of NF-κB activation was observed during *S. flexneri* infection of the colonic epithelial cell line Caco-2, the lung epithelial cell line A549, and the human umbilical vein endothelial cells (HUVECs) derived from umbilical cord (Figure S1 available online), suggesting that bystander activation of NF-κB represents a broad response to *S. flexneri* infection.

During infection, *S. flexneri* uses actin-based motility to spread to adjacent IECs. To control that bystander NF-κB activation was not due to bacterial intercellular motility, we examined NF-κB activation in cells infected with the nonmotile *virG* deletion mutant (Δ*virG*) (Makino et al., 1986). As expected, Δ*virG* bacteria efficiently invaded HeLa cells (Figure 1C, right). However, unlike wild-type (Figure 1C, left), they failed to form actin comet tails and accumulated overtime in the perinuclear region (Figure 1C, right). Interestingly, infection with the Δ*virG* mutant induced p65 nuclear translocation in infected and in bystander cells (Figure 1D) similarly to infection with wild-type *S. flexneri* (Figure 1A), suggesting that bystander NF-κB activation was not caused by intercellular motility, but reflected instead a novel host response to bacterial infection. Because the intracellular microcolonies formed by the Δ*virG* mutant were easily detected by automated image analysis, this mutant was used hereafter in our studies.

In order to further characterize bystander NF-κB activation, we analyzed its kinetic during *S. flexneri* infection in HeLa cells. Representative examples of bystander activation at different time points were chosen for illustration (Figure 1E). Within 15 min of infection, NF-κB was almost exclusively activated in infected cells. Then, at 30 min and up to 120 min, NF-κB activation was observed in infected and bystander cells, suggesting that the signals underlying bystander NF-κB activation were generated very early during infection (within 30 min) and propagated from infected to bystander cells. Considering that each infected cell was surrounded by approximately 2–6 NF-κB-activated cells, our results demonstrate that this mechanism of cell-cell communication strongly amplifies the total NF-κB response to *S. flexneri* infection.

### JNK and ERK Are Also Activated in Bystander Cells of *S. flexneri* Infection

The activation of the JNK signaling pathway is required to mount an inflammatory response, and in particular, to induce IL-8 expression. We therefore tested, whether in addition to NF-κB, the JNK pathway was also activated in bystander cells of *S. flexneri* infection in HeLa and Caco-2 cells. JNK activation was analyzed by immunofluorescence microscopy via a phospho-specific antibody that detects p46 and p54 JNKs phosphorylated at residues threonine 183 and tyrosine 185 (p-JNK). Cytosolic p65 localization and basal p-JNK staining indicated that both pathways were inactive in control cells (Figure 2A). As expected, a clear nuclear translocation of p65 and a significant increase of p-JNK were observed in *S. flexneri*-infected cells. Interestingly, bystander cells of infection also showed an increase of p-JNK, indicating that the JNK pathway was turned on in these cells as well (Figure 2A and Figure S2A). This observation was confirmed by measuring with automated image processing the degree of nuclear p-JNK in control, infected, and bystander cell populations (Figure 2B, see Supplemental Experimental Procedures).

In addition to JNK, the activation of ERK was analyzed by immunofluorescence microscopy by means of an antibody that recognizes p22 and p44 ERKs phosphorylated at residues threonine 202 and tyrosine 204 (p-ERK). Representative images of NF-κB and p-ERK at different time points were chosen for

Immunity
Propagation of Inflammatory Signals in Infection

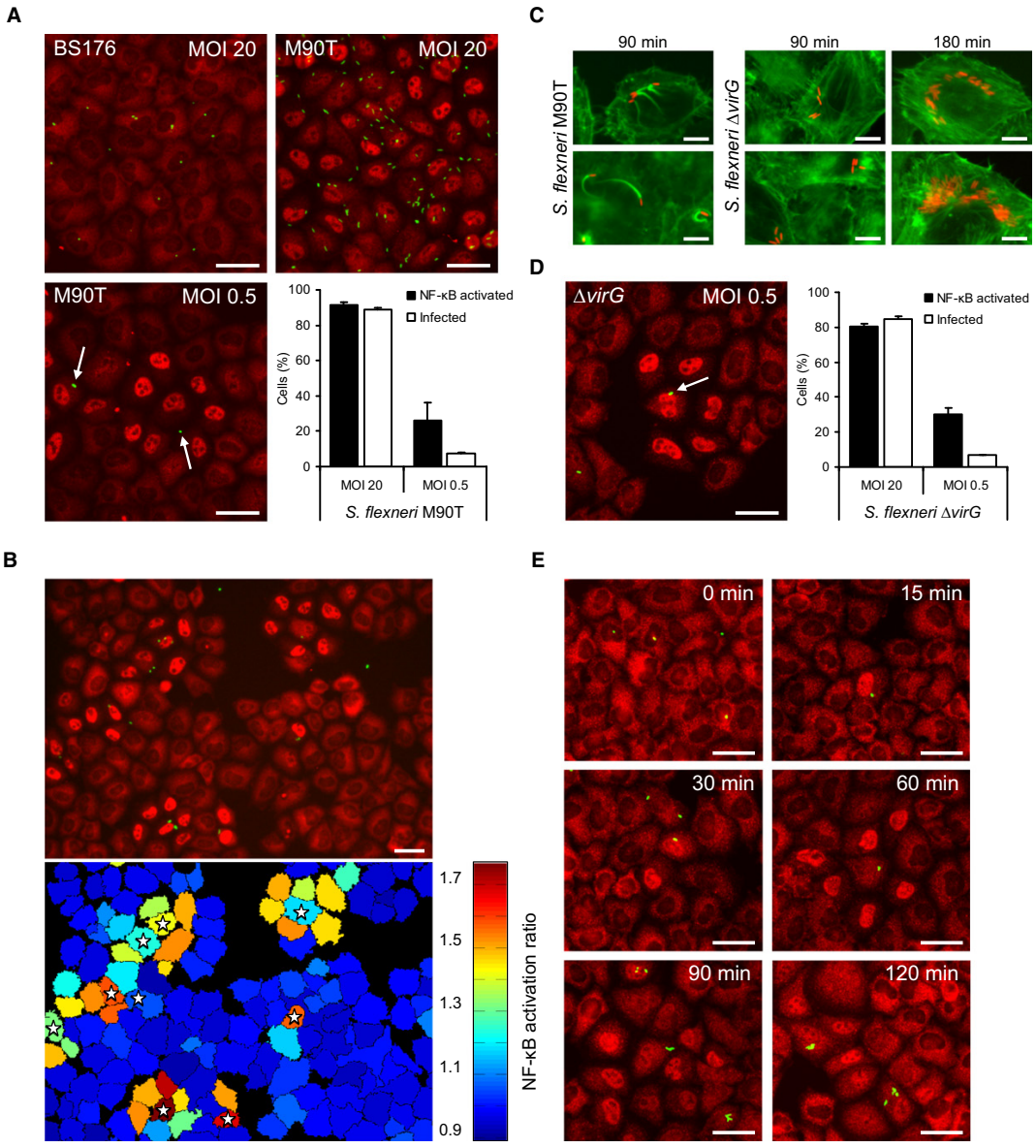


**Figure 1. NF-κB Is Activated in Bystander Cells of *S. flexneri* Infection**

(A) Nuclear localization of NF-κB p65 during *S. flexneri* infection. HeLa cells were infected for 1 hr with BS176 (MOI = 20, top left) and M90T (MOI = 20, top right; MOI = 0.5, bottom left), stained with a p65 antibody, and visualized by fluorescence microscopy (p65 in red, *S. flexneri* in green). Arrows indicate *S. flexneri*. Percent of NF-κB activated and infected cells at high and low MOI (bottom right, means ± SD of triplicate wells, graph representative of two independent experiments). Scale bars represent 40 μm.

(B) False color representation of NF-κB activation ratio during *S. flexneri* M90T infection of HeLa cells. Stars indicate infected cells. Scale bar represents 40 μm.

(C) Actin-based motility of *S. flexneri* M90T (left) and Δ*virG* mutant (right). After infection, cells were stained for F-actin with phalloidin (F-actin in green, *S. flexneri* in red). Scale bars represent 10 μm.

(D) Bystander NF-κB activation during infection with *S. flexneri* Δ*virG* (left). p65 in red, *S. flexneri* in green. Arrow indicates *S. flexneri*. Percent of NF-κB activated and infected cells at high and low MOI (right, means ± SD of triplicate wells, graph representative of two independent experiments). Scale bar represents 40 μm.

(E) Time course of p65 translocation during infection with *S. flexneri* Δ*virG*. Representative images were selected for illustration. Scale bars represent 40 μm.

Immunity
Propagation of Inflammatory Signals in Infection

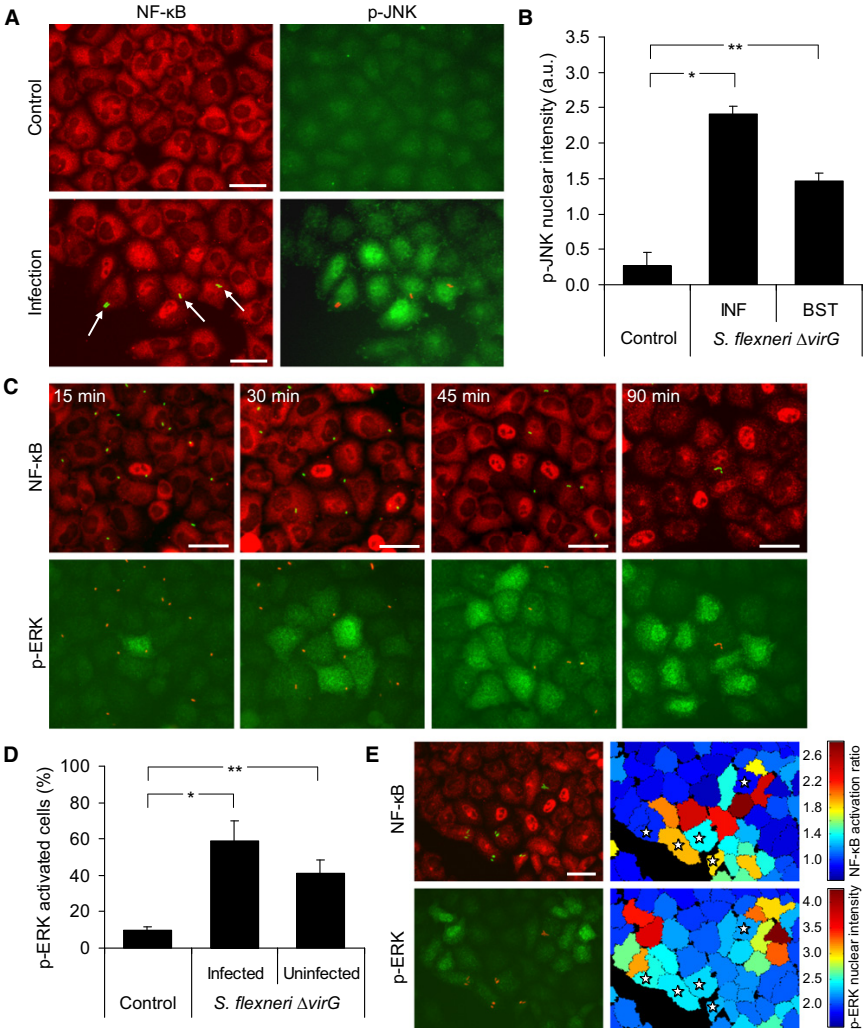


**Figure 2. JNK and ERK Are Activated in Bystander Cells of *S. flexneri* Infection**

(A) Analysis of JNK and NF-κB activation by immunofluorescence microscopy. HeLa cells were left untreated or infected with *S. flexneri* Δ*virG* at MOI = 0.5 for 90 min and costained with p65 and p-JNK antibodies. Arrows indicate *S. flexneri*. Scale bars represent 40 μm.

(B) Quantification of nuclear p-JNK intensity in control, infected (INF), and bystander (BST) cell populations by automated image processing (a.u., arbitrary units, means ± SD of triplicate wells, graph representative of five independent experiments, *p = 7.2E-5, **p = 7.6E-4).

(C) Time course of ERK and NF-κB activation during infection with *S. flexneri.* HeLa cells were infected with *S. flexneri* Δ*virG* at MOI = 0.5 for indicated time periods and costained with p65 and p-ERK antibodies. Scale bars represent 40 μm.

(D) Percent of ERK-activated cells during *S. flexneri* infection. Cells were infected for 1 hr at MOI = 5. Quantification was performed by automated image processing as described in Supplemental Experimental Procedures (means ± SD of triplicate wells, graph representative of three independent experiments, *p = 1.9E-3, **p = 4.7E-3).

(E) False color representations of NF-κB activation ratio and nuclear p-ERK 1 hr after infection with *S. flexneri* Δ*virG*. Stars indicate infected cells. Scale bar represents 40 μm.

illustration (Figure 2C). Within 15 min of infection, ERK activation was observed in only a fraction of infected cells. At 30 min and up to 90 min, ERK was also activated in bystander cells of infection (Figures 2C and 2D and Figure S2B). NF-κB and ERK activation did not strictly correlate at the single-cell level. Indeed, after 45 min of infection, ERK activation was no longer visible in a fraction of infected or proximal bystander cells, suggesting that this pathway was only transiently induced. Furthermore, ERK activation was observed in cells located outside the NF-κB activation foci, suggesting that ERK activation preceded NF-κB activation (Figures 2C and 2E). Altogether, these results suggested that besides the activation of NF-κB, the activation of JNK and ERK also propagates from infected to bystander cells during *S. flexneri* infection of HeLa and Caco-2 cells.

Immunity
Propagation of Inflammatory Signals in Infection

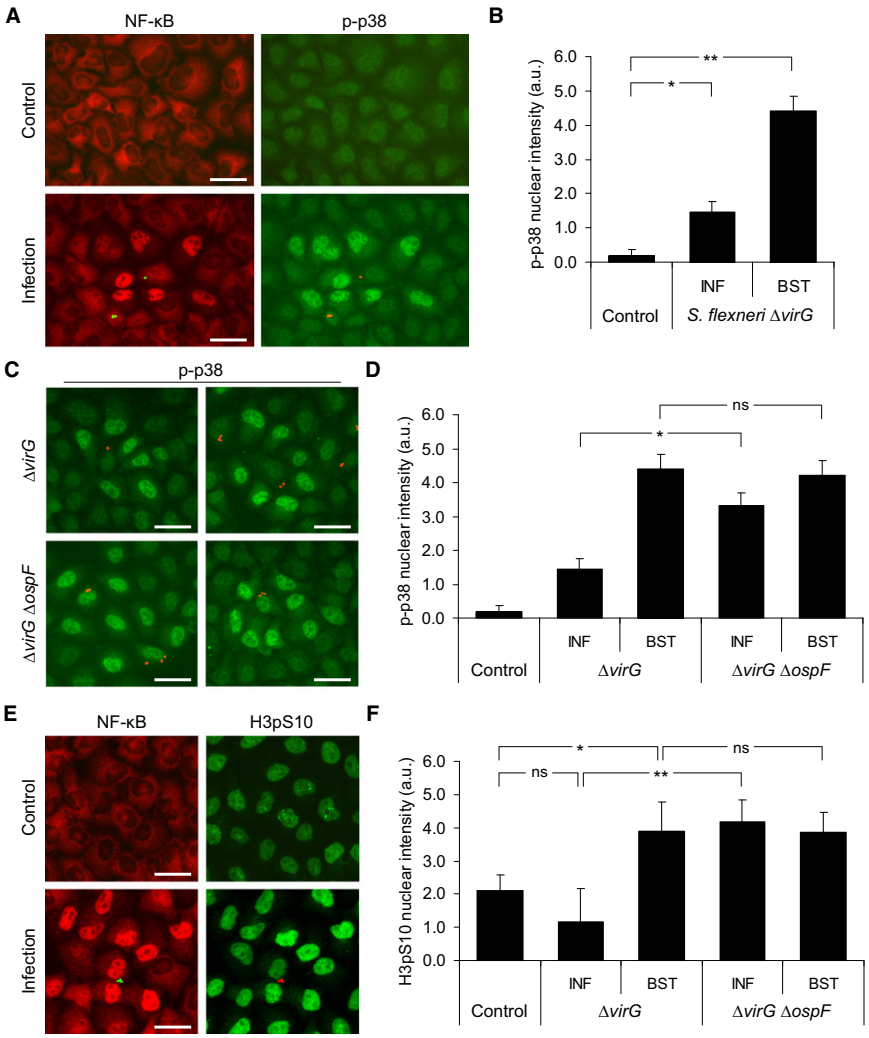


**Figure 3. p38 Activation and Histone H3 Phosphorylation Occur Mainly in Bystander Cells**

(A) Analysis of p38 and NF-κB activation by immunofluorescence microscopy. HeLa cells were left untreated or infected with *S. flexneri* Δ*virG* at MOI = 0.5 for 90 min and costained with p65 and p-p38 antibodies. Scale bars represent 40 μm.

(B) Quantification of nuclear p-p38 intensity in control, infected (INF), and bystander (BST) cell populations (a.u., arbitrary units, means ± SD of triplicate wells, graph representative of five independent experiments, *p = 4.1E-3, **p = 1.0E-4).

(C) Phosphorylation of p38 in cells infected with Δ*virG* or Δ*virG* Δ*ospF S. flexneri* visualized by immunofluorescence microscopy. Scale bars represent 40 μm.

(D) Quantification of nuclear p-p38 intensity by automated image processing in control, infected, and bystander cell populations during infection with Δ*virG* or Δ*virG* Δ*ospF S. flexneri* (means ± SD of triplicate wells, graph representative of five independent experiments, *p = 4.2E-3).

(E) Analysis of histone H3 phosphorylation by immunofluorescence microscopy. HeLa cells were left untreated or infected with *S. flexneri* Δ*virG* at MOI = 0.5 for 90 min and costained with p65 and H3pS10 antibodies. Scale bars represent 40 μm.

(F) Quantification of nuclear H3pS10 intensity in control, infected, and bystander cell populations (means ± SD of triplicate wells, graph representative of five independent experiments, *p = 4.9E-2, **p = 1.1E-3).

## p38 Activation and Histone H3 Phosphorylation Mainly Occur in Bystander Cells of Infection

Because p38 activation is also critical for IL-8 expression, we examined whether p38 was activated in bystander cells of *S. flexneri* infection in HeLa and Caco-2 cells. p38 activation was analyzed by immunofluorescence microscopy by means of an antibody that detects p38 phosphorylated at residues threonine 180 and tyrosine 182 (p-p38). As reported previously (Arbibe et al., 2007), a very modest increase of p38 activation was observed in infected cells (Figures 3A and 3B and Figure S3). In contrast, a strong increase was found in bystander cells of infection indicating that, in addition to NF-κB, JNK, and ERK, p38 was also activated in these cells (Figures 3A and 3B and Figure S3). Signal transduction in infected cells is altered by multiple

Immunity
Propagation of Inflammatory Signals in Infection

effectors that translocate into the host cytoplasm via the T3S apparatus. In particular, p38 is dephosphorylated in the nucleus of infected cells by the phosphothreonine-lyase activity of OspF (Li et al., 2007). Given that bystander cells showed massive p38 activation, we hypothesized that the activation of p38 in bystander cells was not affected by OspF. To test this assumption, HeLa cells were infected with Δ*virG* and Δ*virG* Δ*ospF S. flexneri* mutants. As previously reported (Arbibe et al., 2007), p38 activation was restored in cells infected with Δ*ospF* bacteria, confirming the role of OspF in p38 dephosphorylation (Figures 3C and 3D). In contrast, the amount of p38 activation in bystander cells remained unchanged (Figure 3D), indicating that OspF failed to impair the ability of the host to spread p38 activation to neighboring cells. Taken together, our data showed that the mechanism of bystander p38 activation circumvents the suppressive activity of OspF in infected cells and amplifies p38 activation during *S. flexneri* infection.

In addition to its role in AP-1 phosphorylation, p38 controls IL-8 expression by regulating chromatin accessibility to transcription factors such as NF-κB via the phosphorylation of histone H3 by MSK1 and MSK2 (Saccani et al., 2002). To assess whether bystander p38 activation led to histone H3 phosphorylation in bystander cells, phosphorylation at serine 10 (H3pS10) was analyzed by immunofluorescence microscopy via a phospho-specific antibody. To minimize H3pS10 staining from mitotic cells, HeLa cells were arrested in S phase by a double-thymidine block. Consistent with the pattern of p38 activation during *S. flexneri* infection, H3pS10 was higher in bystander than infected cells (Figures 3E and 3F). Furthermore, the deletion of *ospF* restored H3pS10 in infected cells but had no effect in bystander cells (Figure 3F). Collectively, these results demonstrate that p38 activation and the subsequent phosphorylation of histone H3, which are both impaired in infected cells because of the activity of OspF, are fully operating in bystander cells of *S. flexneri* infection.

### Cell-Cell Propagation of Proinflammatory Signals Amplifies Cytokine Expression

The NF-κB, JNK, ERK, and p38 signaling pathways were turned on in bystander cells of *S. flexneri* infection. Given that these pathways control the expression of proinflammatory genes including IL-8, we tested whether bystander cells of *S. flexneri* infection secreted IL-8. IL-8 secretion was first measured by an enzyme-linked immunosorbent assay (ELISA) in the supernatant of HeLa cells infected by *S. flexneri* at different MOIs. We observed that the amount of secreted IL-8 decreased as the MOI was raised (Figure 4A). Because low and high MOIs corresponded to low and high infected to bystander cell ratios, respectively (Figure S4A), this result suggested that IL-8 was most probably secreted by bystander cells of infection. This hypothesis was tested by in situ mRNA hybridization to visualize at the single-cell level the amount of IL-8 mRNA produced during *S. flexneri* infection. As shown in Figure 4B, IL-8 mRNAs were almost exclusively present in bystander cells of infection. To confirm that bystander cells were the main IL-8-producing cells during *S. flexneri* infection, we performed an intracellular IL-8 immunofluorescence microscopy assay in cells treated with monensin, a protein transport inhibitor that blocks secretion and enables intracellular IL-8 accumulation in the Golgi apparatus (Mollenhauer et al., 1990). In line with the ELISA and the mRNA data, almost no IL-8 was visible in infected cells, but massive intracellular IL-8 accumulation was found in bystander cells (Figures 4C and 4D). An average of 2.8 ± 1.6, 4.2 ± 2.5, 6.5 ± 4.7, and 29.3 ± 13.5 bystander IL-8-producing cells per infected one was measured in HeLa, Caco-2, A549, and HUVEC cells, respectively (Figures S4B–S4D). Interestingly, tumor necrosis factor α (TNF-α) and granulocyte macrophage colony-stimulating factor (GM-CSF), two other inflammatory cytokines upregulated during *S. flexneri* infection of epithelial cells (Pédron et al., 2003), were also found in bystander cells (Figures S4E–S4G), suggesting that the mechanism of bystander activation contributes to different facets of inflammation during infection.

Strong cytokine expression in bystander cells indicated that cell-cell communication was not affected by *S. flexneri* effector proteins. This was tested by investigating the effect of OspF on IL-8 expression in infected and bystander cell populations. As previously reported (Arbibe et al., 2007), an increase of IL-8 production was observed in cells infected with Δ*ospF S. flexneri* (Figure 4E). In contrast, the number of bystander cells producing IL-8 was independent of OspF (Figure 4F) indicating that, in line with our p38 activation and H3pS10 results, OspF failed to affect IL-8 expression in bystander cells.

To further characterize the mechanism of bystander activation, we tested whether it also occurred after infection with *Listeria monocytogenes* or *Salmonella typhimurium*, two enteroinvasive bacteria that induce IL-8 expression during invasion of IECs (Eckmann et al., 1993). Consistent with data on *S. flexneri* infection, IL-8 accumulation was also observed in bystander cells of *L. monocytogenes* and *S. typhimurium* infection (Figure 4G) but at a lower frequency. In conditions where bystander IL-8 expression was observed for nearly 100% of *S. flexneri*-infected cells, it occurred for approximately 40% and 70% of *Listeria*- and *Salmonella*-infected cells, respectively. In contrast to *S. flexneri* infection, IL-8 accumulation was also detected in a fraction of cells infected with *L. monocytogenes* or *S. typhimurium* (approximately 20% and 40%, respectively), indicating that these bacteria do not manipulate their host to the same extent as *S. flexneri,* for which low levels of IL-8 were detected in less than 5% of infected cells (Figure 4E). Altogether these results show that cell-cell communication between infected and uninfected bystander cells leads to the potentiation of inflammatory cytokine expression during bacterial infection. They also establish that this is a general host response to invasive bacteria that occurs with an amplitude and a frequency that vary between cell types and pathogens.

### Nod1-Mediated Peptidoglycan Sensing Is Sufficient to Induce Bystander IL-8 Expression

During *S. flexneri* infection, the presence of intracellular bacteria is sensed through peptidoglycan recognition by the intracellular receptor Nod1 (Girardin et al., 2003). To determine whether pathogen sensing via Nod1 was sufficient to induce bystander IL-8 production, we monitored IL-8 accumulation after microinjection of the synthetic Nod1 ligand L-Ala-D-γ-Glu-meso-diaminopimelic acid (TriDAP) into the cytoplasm of A549 cells. An Alexa 488-labeled IgG antibody (IgG A488) was used as fluorescent marker to identify microinjected cells. In response to IgG A488 microinjection, no IL-8 was detected (Figure 5A, left, and

Immunity
Propagation of Inflammatory Signals in Infection

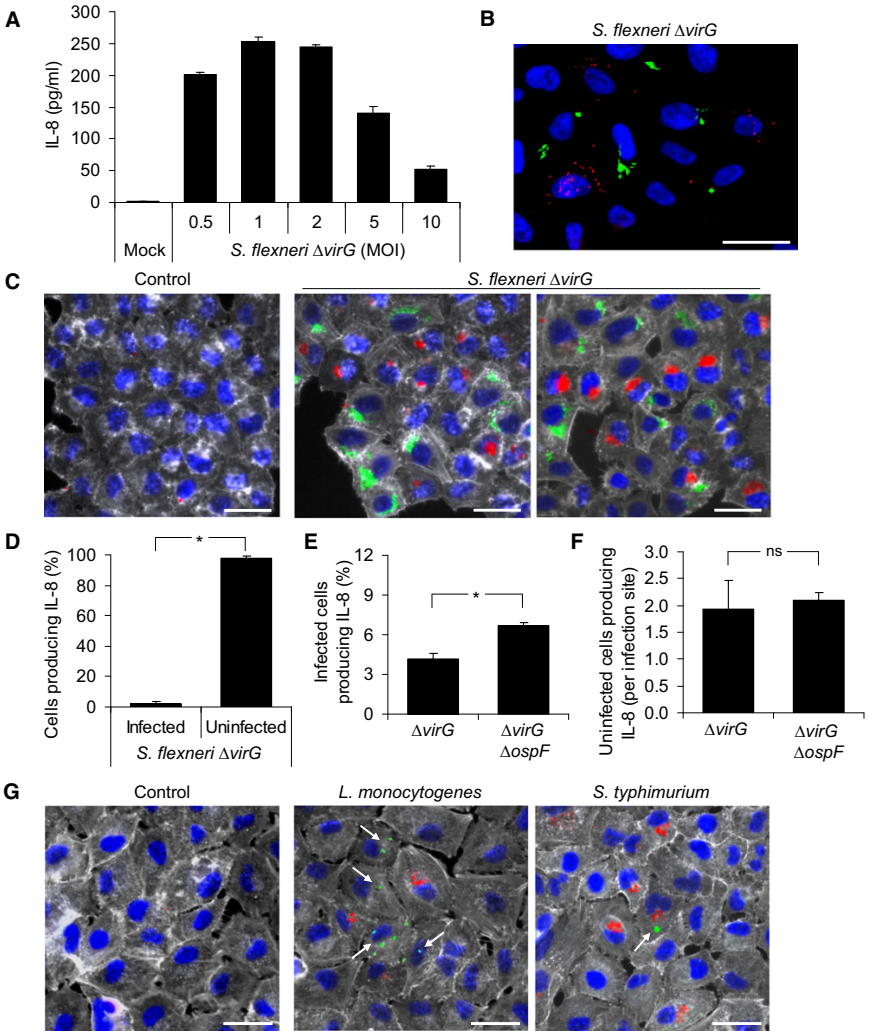


**Figure 4. IL-8 Production by Bystander Cells Is a General Response to Bacterial Infection**

(A) Measurements of IL-8 secretion by ELISA 6 hr after infection (means ± SD of triplicate wells, graph representative of two independent experiments).

(B) Visualization of IL-8 mRNA 2 hr after infection by in situ hybridization (IL-8 mRNAs in red, *S. flexneri* in green, Hoechst in blue, MOI = 2). Scale bar represents 40 μm.

(C) IL-8 accumulation in bystander cells of infection. IL-8 staining of monensin-treated HeLa cells 3 hr after infection (IL-8 in red, *S. flexneri* in green, Hoechst in blue, F-actin in gray, MOI = 2). Scale bars represent 40 μm.

(D) Percent of infected and uninfected cells among all IL-8-producing cells (MOI = 1). Quantification was performed by automated image processing based on the use of threshold intensity values for bacterial and IL-8 detection (means ± SD of triplicate wells, graph representative of three independent experiments, *p = 3.9E-16).

(E) Percent of infected cells producing IL-8 during infection with Δ*virG* and Δ*virG* Δ*ospF S. flexneri* (MOI = 5). Quantification was performed as described in (D) (means ± SD of triplicate wells, graph representative of two independent experiments, *p = 4.5E-4).

(F) Number of uninfected cells producing IL-8 per site of infection during infection with Δ*virG* and Δ*virG* Δ*ospF S. flexneri* (MOI = 1). Quantification was performed as described in (D) (means ± SD of triplicate wells, graph representative of two independent experiments).

(G) IL-8 production (in red) in bystander cells during *L. monocytogenes* (MOI = 0.25, green) and *S. typhimurium* (MOI = 0.5, green) infection of A549 cells. F-actin in gray, arrows indicate bacteria. Scale bars represent 40 μm.

Figure 5B). In contrast, when TriDAP was combined with IgG A488, both microinjected and bystander cells showed massive intracellular IL-8 accumulation (Figure 5A, right, and Figure 5B). To verify that IL-8 production was not caused by extracellular TriDAP leaking during microinjection, the concentration of TriDAP used in the microcapillary was uniformly applied to the extracellular medium. In contrast to TNF-α, extracellular TriDAP failed to induce IL-8 expression (Figure 5C and Figure S5).

Immunity
Propagation of Inflammatory Signals in Infection

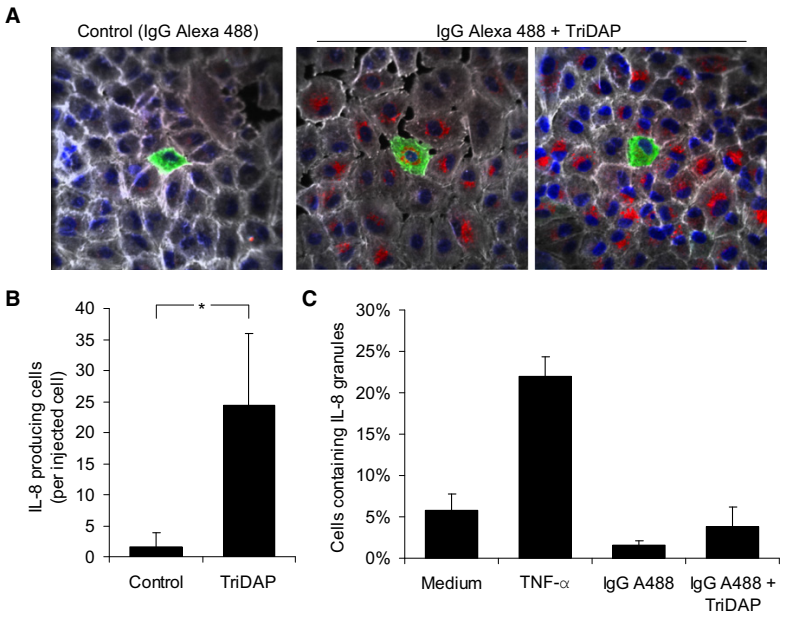


**Figure 5. Intracellular Recognition of a Nod1 Ligand Is Sufficient to Induce IL-8 Expression in Bystander Cells**

(A) IL-8 accumulation in bystanders of microinjected A549 cells. After injection of IgG Alexa 488 alone (left) or combined with TriDAP (right), cells were stained for IL-8, F-actin, and DNA (IgG A488 in green, IL-8 in red, F-actin in gray, Hoechst in blue).

(B) Number of IL-8-producing cells per injected cell. Quantification was performed by counting all IL-8-expressing cells located in contact with microinjected cells or other bystander cells (control, n = 20; TriDAP, n = 21; *p = 1.0E-9).

(C) Percent of cells containing IL-8 after extracellular treatment with TNF-α, IgG A488 alone, or combined with TriDAP. Cells were stained for IL-8 and DNA and analyzed by automated image processing (means ± SD of triplicate wells, graph representative of two independent experiments).

Together, these results suggested that Nod1-mediated recognition of intracellular TriDAP was necessary and sufficient to induce IL-8 expression by bystander cells of microinjection. Because Nod1-mediated recognition of peptidoglycan also takes place in *S. flexneri*-infected cells, this result suggested that pathogen sensing may be sufficient to trigger IL-8 expression in bystander cells of *S. flexneri* infection.

## Bystander Activation Is Not Mediated by Paracrine Signaling but Requires Cell-Cell Contact

Reports indicating that TNF-α is upregulated during *S. flexneri* infection and that NF-κB, p38, ERK, and JNK are activated by TNF-α suggested that this cytokine may induce bystander activation via paracrine signaling (Dong et al., 2002; Pédron et al., 2003). This hypothesis was tested by examining bystander activation in tumor necrosis factor receptor 1 (TNFR1)-deficient mouse embryonic fibroblasts (*Tnfr1*$^{-/-}$ MEFs). Because mice are deficient for the *IL8* gene, the chemokine macrophage inflammatory protein-2 (MIP-2) was chosen as readout of inflammation. Whereas *Tnfr1*$^{-/-}$ cells did not respond to TNF-α stimulation, massive MIP-2 expression was observed in bystander cells of *S. flexneri* infection (Figure 6A; Figures S6A and S6B), indicating that TNF-α was not the mediator of bystander activation. To investigate the role of protein secretion more broadly, we tested whether this process was impaired when protein secretion was abolished by the protein transport inhibitor brefeldin A (BFA). For conditions of drug treatment that blocked phorbol 12-myristate 13-acetate (PMA)-induced IL-8 secretion (Figure S6C), BFA had no effect on bystander activation during *S. flexneri* infection of Caco-2 cells (Figures 6B and 6C), suggesting that cell-cell propagation of proinflammatory signals was not mediated by secreted proteins.

To further explore the hypothesis of paracrine signaling, experiments of *S. flexneri* infection were performed in a flow chamber where fresh medium was perfused to wash away any potential secreted factors. A flow rate corresponding to the replacement of the entire volume of the chamber every second was used. IL-8 accumulation was still visible in bystander cells of infection located along an axis perpendicular or opposite to the direction of the flow (Figure S6D). Quantification of IL-8 (Figure 6D) showed no effect of perfusion, indicating that bystander activation was very improbably mediated by a long-ranged diffusing soluble factor.

To characterize the mechanism of bystander activation, we investigated whether it was cell-cell contact dependent. Infection was performed at subconfluent cell density to evaluate IL-8 expression in Caco-2 cells that had no physical interactions with infected cells. Inspection of images and manual quantification indicated that IL-8 was exclusively found in cells having direct or indirect contacts with infected cells and defined as class 1 (Figures 6E and 6F). Class 2 cells present in the vicinity of the infected cell (Experimental Procedures) but, separated by a gap, did not exhibit markedly more IL-8 than class 3 cells distant from any infection foci (Figure 6F). Collectively, these results demonstrated that the expression of IL-8 in bystander cells depends on cell-cell contact and is most probably not mediated by paracrine signaling.

## Cell-Cell Propagation of Inflammatory Signals Is Mediated by Connexin Gap Junctions

An alternative hypothesis to paracrine signaling is direct communication via gap junction channels formed by connexin proteins. This hypothesis was directly tested by evaluating the effect of the gap junction blocker 18β-glycyrrhetinic acid (18β-GA) on IL-8 expression in bystander cells during *S. flexneri* infection of Caco-2 cells. In conditions of drug treatment that blocked Lucifer Yellow transfer through gap junctions of adjacent Caco-2 cells (Figure S7A), IL-8 expression in bystander

Immunity
Propagation of Inflammatory Signals in Infection

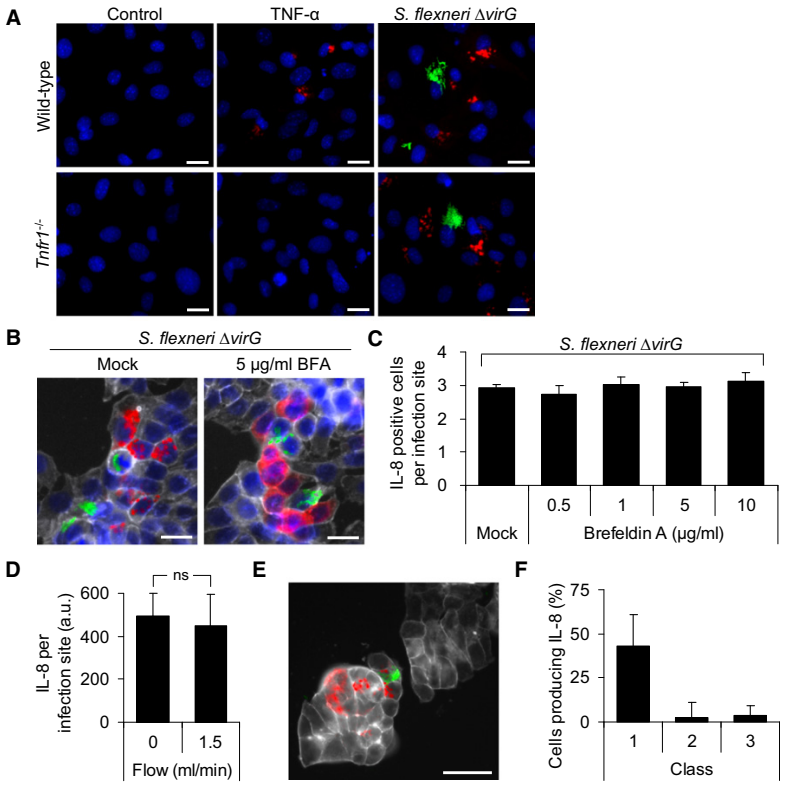


**Figure 6. Bystander Activation Is Not Mediated by Paracrine Signaling but Is Cell-Cell Contact Dependent**

(A) MIP-2 expression in wild-type and *Tnfr1*$^{-/-}$ MEF cells after TNF-α stimulation or *S. flexneri* infection visualized by fluorescence microscopy. After infection, cells were stained for MIP-2 and DNA with a MIP-2 antibody and Hoechst, respectively (MIP-2 in red, *S. flexneri* in green, Hoechst in blue). Scale bars represent 20 μm.

(B) Bystander IL-8 expression in Caco-2 cells pretreated with BFA and infected with *S. flexneri*. After infection (*S. flexneri* in green), cells were stained for IL-8, DNA, and F-actin with an IL-8 antibody (in red), Hoechst (in blue), and phalloidin (in gray), respectively. Scale bars represent 20 μm.

(C) Quantification of bystander IL-8 expression upon BFA treatment by automated image analysis (means ± SD of triplicate wells, graph representative of two independent experiments).

(D) Quantification of bystander IL-8 expression under flow conditions. IL-8 was quantified by measuring for each infected cell the area of IL-8 staining (a.u., arbitrary units, means ± SD, n = 10, graph representative of two independent experiments).

(E) Cell-cell contact analysis of bystander IL-8 expression. Caco-2 cells, seeded at subconfluent density and infected with *S. flexneri* (in green), were stained for IL-8 (in red) and F-actin (in gray). Scale bar represents 50 μm.

(F) Fractions of IL-8-producing cells in class 1, 2, 3 cell populations as defined in Experimental Procedures (means ± SD, n > 38, graph representative of two independent experiments).

cells of infection was strongly reduced (Figures 7A and 7B). In contrast, TNF-α-induced IL-8 secretion, used as control, was not affected (Figures S7B and S7C). A similar result was obtained with the gap junction inhibitor carbenoxolone (Figures S7D and S7E). Furthermore, treatment with glycyrrhizic acid, a compound structurally related to 18β-GA but which fails to block gap junction communication at concentrations below 100 μM (Davidson et al., 1986), had no effect on *S. flexneri*-induced IL-8 expression by bystander cells (Figure 7B). Taken together, these results suggested that IL-8 expression by bystander cells of infection was mediated by communication through gap junctions.

Because gap junction inhibitors have unspecific effects, we further validated this finding by testing whether the propagation of inflammatory signals was connexin dependent. In A431 cells that are poorly coupled via gap junctions and express connexin43 (Cx43) below the level of detection with antibodies (Troyanovsky et al., 1994), very limited activation of NF-κB, JNK, p38, and ERK and residual IL-8 expression were found in bystander cells of *S. flexneri* infection (Figure 7C, left, and Figure 7D, top). In contrast, in Cx43-overexpressing A431 cells (A431-Cx43) that are effectively coupled via gap junctions (Neijssen et al., 2005), large foci of NF-κB, JNK, p38, and ERK activation and IL-8 expression were found around infected cells (Figure 7C, right, and Figure 7D, bottom). Quantification of IL-8 expression in consecutive A431 or A431-Cx43 bystander cells by automated image processing, as described in Supplemental Experimental Procedures, confirmed that the propagation of IL-8 expression was Cx43 dependent (Figures 7D and 7E). As expected, bystander IL-8 expression was strongly reduced when A431-Cx43 cells were depleted of Cx43 by RNA interference (Figure 7F and Figure S7F) or treated with 18β-GA (Figure 7G and Figure S7G).

In contrast to typical hemichannel-based signaling, communication via gap junction channels requires connexin proteins in both donor and recipient cells. To confirm that this condition was fulfilled for bystander activation, the propagation of inflammatory signals from *S. flexneri*-infected A431-Cx43 cells to either A431-Cx43 or A431 bystander cells was analyzed in experiments where A431-Cx43 and A431 cells were mixed prior seeding. Cx43, used to discriminate A431 and A431-Cx43 cells, as well as IL-8 were detected by immunofluorescence. Whereas IL-8 expression robustly spread within consecutive A431-Cx43 cells, the propagation from infected A431-Cx43 to adjacent A431 cells was very limited (Figure S7H). This observation, quantified by automated image processing (Figure 7H and Figure S7I), indicated that Cx43 proteins were also required in uninfected bystander cells to efficiently potentiate inflammation. Taken together, these data convincingly showed that the propagation of inflammation during bacterial infection of epithelial cells depends on connexin gap junctions.

Immunity
Propagation of Inflammatory Signals in Infection

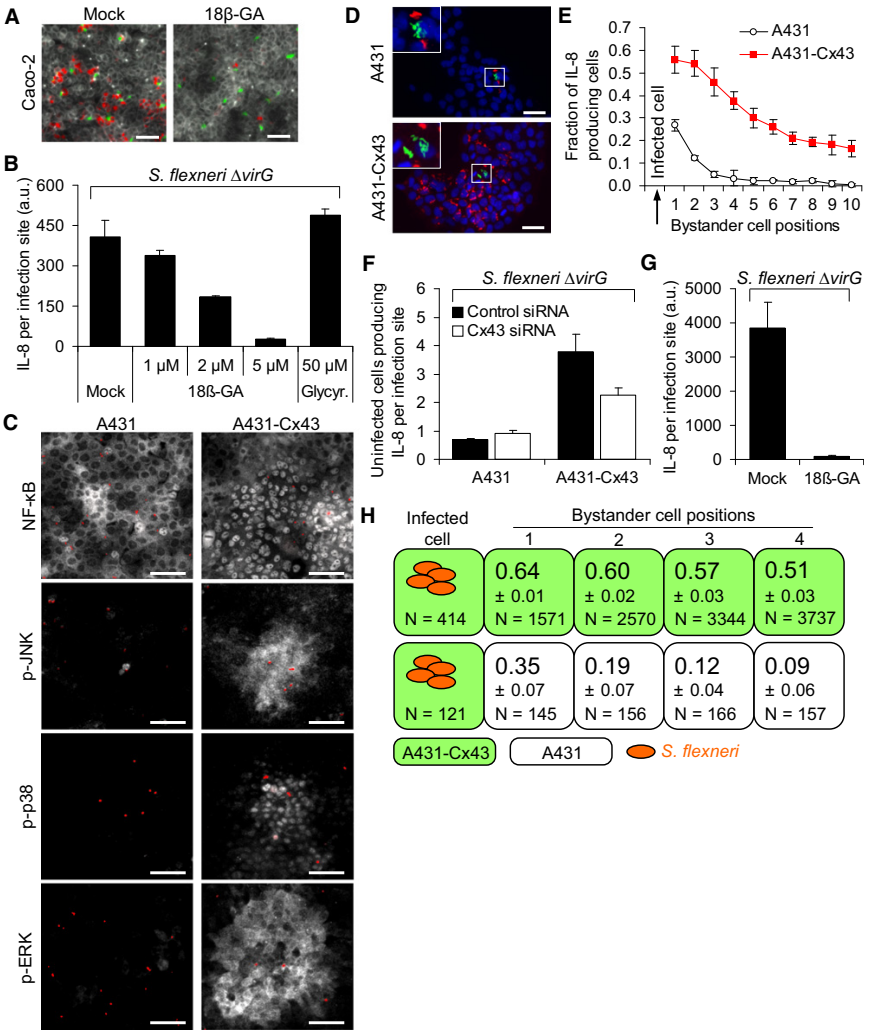


**Figure 7. Propagation of Inflammation Is Mediated by Gap Junctions**

(A) Effect of 18β-GA on IL-8 expression during infection of Caco-2 cells. Cells were pretreated with 18β-GA, infected with Δ*virG S. flexneri*, and stained for IL-8 and F-actin with an IL-8 antibody and phalloidin, respectively (IL-8 in red, *S. flexneri* in green, F-actin in gray). Scale bars represent 50 μm.

(B) Quantification of IL-8 accumulation per site of infection in cells left untreated or pretreated with 18β-GA or glycyrrhizine. Quantification was performed by automated image processing as described in Supplemental Experimental Procedures (means ± SD of triplicate wells, graph representative of two independent experiments).

(C) Cell-cell propagation of proinflammatory signals in A431 and A431-Cx43 cells visualized by immunofluorescence. NF-κB p65, p-JNK, p-p38, and p-ERK immunofluorescence staining in A431 cells (left) and A431-Cx43 cells (right) after *S. flexneri* infection (NF-κB p65, p-JNK, p-p38, and p-ERK in gray, *S. flexneri* in red). Scale bars represent 40 μm.

(D) Propagation of IL-8 expression during *S. flexneri* infection of A431 and A431-Cx43 cells visualized by immunofluorescence. After infection, cells were stained for IL-8 and DNA with an IL-8 antibody and Hoechst, respectively (IL-8 in red, *S. flexneri* in green, Hoechst in blue). Inserts show the infection foci (magnification: ×2.5). Scale bars represent 40 μm.

(E) Spatial propagation of IL-8 expression in consecutive A431 or A431-Cx43 bystander cells during *S. flexneri* infection (means ± SD of six wells; graph representative of two independent experiments). Quantification was performed as described in Supplemental Experimental Procedures.

(F) Quantification of bystander IL-8 expression after siRNA-mediated Cx43 depletion. IL-8 was analyzed by immunofluorescence in A431 and A431-Cx43 cells transfected with control or Cx43 siRNAs and infected with *S. flexneri* and quantified by automated image analysis (means ± SD of triplicate wells, graph representative of two independent experiments, p = 3.9E-06).

(G) Quantification of bystander IL-8 expression in A431-Cx43 cells pretreated with 18β-GA and infected with *S. flexneri* (means ± SD of triplicate wells, graph representative of three independent experiments).

(H) Spatial propagation of IL-8 expression from *S. flexneri*-infected A431-Cx43 cells into either A431-Cx43 or A431 adjacent cells. Each number corresponds to the fraction of IL-8-producing cells for a given bystander cell position. Quantification was performed by automated image processing and is described in Supplemental Experimental Procedures (means ± SD of triplicate wells, graph representative of two independent experiments, p < 7.5E-04 at any given position).

Immunity
Propagation of Inflammatory Signals in Infection

## DISCUSSION

In the present study, we provide evidence that during *S. flexneri* infection, the activation of the proinflammatory pathways NF-κB, JNK, ERK, and p38 propagates from infected to uninfected adjacent cells leading to IL-8 expression in bystander cells of infection. This mechanism, mediated by gap junction communication between infected and uninfected cells, circumvents the immunosuppressive activity of bacterial effectors and massively amplifies inflammation during bacterial infection.

Nod1 contributes to the detection of intracellular *S. flexneri* via the recognition of peptidoglycan-derived peptides (Girardin et al., 2003). In infected IECs, Nod1 ligation leads to NF-κB activation and upregulation of proinflammatory genes. By using an in vitro single-cell assay of *S. flexneri* infection, we found that NF-κB activation was not restricted to infected cells. Indeed, by performing infections at low MOIs, we observed within minutes of infection the propagation of NF-κB activation from infected to uninfected bystander cells. This cell-cell communication mechanism resulted in massive amplification of the total NF-κB response to *S. flexneri* infection. Because NF-κB controls the expression of proinflammatory genes, this result suggested that the mechanism of bystander activation may amplify the inflammatory response of an infected epithelial cell layer. This hypothesis was supported by the observation that JNK, ERK, and p38, three kinases involved in the control of inflammation, were also activated in bystander cells of *S. flexneri* infection. Noticeably, p38 activation was markedly higher in bystander than infected cells, suggesting that the effector OspF, which dephosphorylates p38 in the nucleus of infected cells via its phosphothreonine-lyase activity, did not affect p38 bystander activation. This hypothesis was validated by the observation that the deletion of *ospF* enhanced p38 activation in infected but not in bystander cells. Infection at low MOI reflects the early phase of Shigellosis, when the number of bacteria that have reached the basolateral surface of the IECs is limited. By rapidly propagating NF-κB and MAP kinase activation to uninfected cells, the mechanism of bystander activation may enable the host to fully activate these signaling pathways before their manipulation by future internalized bacteria, for instance via the effectors OspG and OspF (Arbibe et al., 2007; Kim et al., 2005).

The concept of bystander responses has been previously described in the context of ionizing radiation where nonirradiated cells receive signals from neighboring or distant irradiated ones (Hamada et al., 2007), in wound healing (Yang et al., 2004), or more recently after double-stranded DNA recognition (Patel et al., 2009). In all cases, the activation of signaling pathways emanates from cells exposed to local stress and propagates into the adjacent healthy tissue to amplify and orchestrate a multicellular response to an aggression. Here, we provide evidence for a similar mechanism in innate immunity against pathogenic bacteria.

By attracting neutrophils to the infected area, IL-8 has a central function in innate immunity against pathogens and in Shigellosis, in particular. It has been proposed that IL-8 is secreted by *S. flexneri*-infected cells after recognition of intracellular peptidoglycan-derived peptides via Nod1 (Girardin et al., 2003). Yet, the immunosuppressive activity of several effectors that alters signaling in infected cells challenges the ability of these cells to secrete large amounts of IL-8 as observed in Shigellosis. To directly address this question, we analyzed IL-8 expression during *S. flexneri* infection at the mRNA and protein level by in situ hybridization and intracellular immunofluorescence microscopy, respectively, two methods that combine single-cell resolution and spatial information at the site of infection. Here, we showed that the propagation of NF-κB, JNK, ERK, and p38 activation leads to IL-8 expression in bystander cells of infection. This mechanism efficiently amplifies the total IL-8 response of the infected cell monolayer by increasing the number of IL-8-producing cells per site of infection. Furthermore, our results clearly demonstrated that infected cells were inefficient at producing IL-8, confirming the immunosuppressive activities of secreted effectors on IL-8 expression. In line with the effect of OspF on p38 and histone H3 phosphorylation, IL-8 production was increased in cells infected with a Δ*ospF* mutant. However, the deletion of *ospF* had only a limited effect on IL-8 expression, suggesting that the complete block observed in infected cells is mediated by multiple effectors. Additional effectors such as OspG, OspB, and $IpaH_{9.8}$ may also contribute to block IL-8 expression in infected cells (Kim et al., 2005; Okuda et al., 2005; Zurawski et al., 2009). Interestingly, we showed that OspF did not affect IL-8 expression in bystander cells, indicating that through cell-cell communication, the host appears to circumvent the activity of OspF in infected cells and amplifies the global IL-8 response to *S. flexneri* infection. In the rabbit intestinal loop model of Shigellosis, IL-8 expression was found in epithelial cells located beyond the zones of bacterial invasion, providing evidence for the physiological relevance of bystander IL-8 expression in vivo (Sansonetti et al., 1999).

IL-8 expression was also found in bystander cells of *S. typhimurium* and *L. monocytogenes* infection, showing that the potentiation of innate immunity by cell-cell communication corresponded to a broad host response to bacterial infection. However, the contribution of this mechanism to inflammation can vary for different pathogens. It depends on its frequency of occurrence but also on the ability of bacteria to alter signaling in infected cells. For *S. flexneri* that very efficiently blocks signaling in infected cells, bystander activation clearly constitutes the key pathway of IL-8 expression.

We addressed the role of peptidoglycan recognition in the mechanism of cell-cell communication leading to IL-8 expression in bystander cells and its underlying molecular basis. Interestingly, we found that the microinjection of the Nod1 ligand TriDAP was sufficient to induce IL-8 expression in bystander cells of microinjection, suggesting that the recognition of Nod1 ligands in infected cells may be sufficient to generate the underlying signals that mediate IL-8 expression in bystander cells of *S. flexneri* infection. Cell-cell communication can be mediated by different mechanisms: paracrine signaling, direct diffusion of small molecules through gap junctions, or membrane protein interactions. In Caco-2 cells, bystander IL-8 expression was not inhibited by BFA treatment or by perfusion, indicating that this process was most probably not mediated by paracrine signaling. Furthermore, it was cell-cell contact dependent, and therefore compatible with gap junction-mediated communication that enables direct diffusion of small molecules between adjacent

Immunity
Propagation of Inflammatory Signals in Infection

cells. This hypothesis was confirmed by showing that the mechanism of bystander IL-8 expression was blocked by gap junction inhibitors, limited in cells that are poorly coupled via gap junctions, and massively amplified by the overexpression of the gap junction protein Cx43. Finally, as required for the formation of connexins gap junction channels between adjacent cells, we showed that the presence of connexin proteins was necessary in both infected and bystander cells to efficiently propagate inflammation during bacterial infection.

Further studies are required to identify the small molecules (i.e., <2 kDa) diffusing from infected to bystander cells that control NF-κB, JNK, ERK, and p38 activation and lead to IL-8 expression during *S. flexneri* infection. Among potential candidates, the roles of known second messengers, which are involved in proinflammatory gene expression, including calcium, IP3, and cAMP, should be examined. An alternative hypothesis is the direct diffusion of small peptidoglycan-derived peptides through gap junctions.

In summary, we show that during *S. flexneri* infection, the activation of the proinflammatory pathways NF-κB, JNK, ERK, and p38 propagates from infected to uninfected adjacent cells leading to IL-8 expression in bystander cells of infection. This mechanism enables the host to circumvent the immunosuppressive activity of bacterial effectors and to massively amplify inflammation during bacterial infection. Moreover, by showing that this process is gap junction mediated, we provide evidence for a direct connection between gap junction communication and amplification of innate immunity during bacterial infection.

## EXPERIMENTAL PROCEDURES

### Cell Culture

HeLa, A549, Caco-2, A431, and MEF cells were cultured in Dulbecco's modified Eagle's medium (DMEM) supplemented with 10% FCS and 2 mM L-Glutamine. HUVECs were generously provided by C. Dehio (Biozentrum, University of Basel, Switzerland) and cultivated as previously described (Dehio et al., 1997).

### Bacterial Strains

The *S. flexneri* strains M90T wild-type, its noninvasive derivative BS176, and the *icsA (virG)* deletion mutant were generously provided by P. Sansonetti (Bernardini et al., 1989). The Δ*virG* Δ*ospF* deletion mutant was generated as described in Supplemental Experimental Procedures (Table S1). The *Salmonella typhimurium* LT2 strain was provided by U. Jenal (Biozentrum, University of Basel, Switzerland) and the stably expressing GFP *Listeria monocytogenes* A21/B5 strain by M. Loessner (ETH Zurich, Switzerland).

### Infection Assays

*S. flexneri, S. typhimurium*, and *L. monocytognes* were used in exponential growth phase. *S. flexneri* and *S. typhimurium* were coated with poly-L-lysine prior to infection. Cells seeded in 96-well plates were infected at indicated MOIs in DMEM supplemented with 10 mM HEPES and 2 mM L-glutamine. After adding bacteria, plates were centrifuged for 5 min and placed at 37°C for indicated time periods. Extracellular bacteria were killed by gentamicin (100 μg $ml^{-1}$). Infection assays were stopped by 4% PFA fixation.

### Immunofluorescence and IL-8 Measurements

Immunofluorescence and IL-8 measurements were performed as described in Supplemental Experimental Procedures.

### Automated Microscopy and Image Analysis

Images were automatically acquired with an ImageXpress Micro (Molecular devices, Sunnyvale, USA). Image analysis was performed via CellProfiler (Carpenter et al., 2006) and MATLAB (The MathWorks, Inc, Natick, USA) as described in Supplemental Experimental Procedures.

### Microinjection and Flow Chamber Experiments

Microinjection and flow chamber experiments are described in Supplemental Experimental Procedures.

### Analysis of Cell-Cell Contact

Infection was performed at subconfluent cell density. Cellular contacts and IL-8 were visualized by phalloidin and IL-8 staining, respectively. For each site of infection, the distance between the infected cell and the most distant bystander cell producing IL-8 was used as the radius of the "circle of bystander activation" centered on the infected cell. Within this circle, cells contacting directly the infected cell or indirectly by interacting with other bystander cells were classified as class 1. Cells making no direct or indirect contact with infected cells were defined as class 2. Cells located outside the circle and distant from any sites of infection were defined as class 3.

### Statistical Analysis

Data are expressed as mean ± standard deviation of triplicate samples. p values were calculated with a two-tailed two-sample equal variance t test.

## SUPPLEMENTAL INFORMATION

Supplemental Information includes Supplemental Experimental Procedures, seven figures, and one table and can be found with this article online at doi:10.1016/j.immuni.2010.10.015.

## ACKNOWLEDGMENTS

We thank J. Neefjes (NKI, Amsterdam, Netherlands) and M. Kelliher (Massachusetts Medical School, Worcester, USA) for the generous gift of A431-Cx43 cells and *Tnfr1*$^{-/-}$ MEFs, respectively. We also thank G. Cornelis, U. Jenal, and C. Dehio for comments on the manuscript and M. Podvinec for help with research IT. This work was funded by the Swiss National Science Foundation (grant 3100A0-113561 to C.A.) and the InfectX project from SystemsX.ch. C.A.K. was supported by the Werner-Siemens Foundation.

Received: May 10, 2010
Revised: August 25, 2010
Accepted: September 17, 2010
Published online: November 18, 2010

## REFERENCES

Arbibe, L., Kim, D.W., Batsche, E., Pedron, T., Mateescu, B., Muchardt, C., Parsot, C., and Sansonetti, P.J. (2007). An injected bacterial effector targets chromatin access for transcription factor NF-kappaB to alter transcription of host genes involved in immune responses. Nat. Immunol. *8*, 47–56.

Bernardini, M.L., Mounier, J., d'Hauteville, H., Coquis-Rondon, M., and Sansonetti, P.J. (1989). Identification of icsA, a plasmid locus of Shigella flexneri that governs bacterial intra- and intercellular spread through interaction with F-actin. Proc. Natl. Acad. Sci. USA *86*, 3867–3871.

Carpenter, A.E., Jones, T.R., Lamprecht, M.R., Clarke, C., Kang, I.H., Friman, O., Guertin, D.A., Chang, J.H., Lindquist, R.A., Moffat, J., et al. (2006). CellProfiler: Image analysis software for identifying and quantifying cell phenotypes. Genome Biol. *7*, R100.

Cornelis, G.R. (2006). The type III secretion injectisome. Nat. Rev. Microbiol. *4*, 811–825.

Davidson, J.S., Baumgarten, I.M., and Harley, E.H. (1986). Reversible inhibition of intercellular junctional communication by glycyrrhetinic acid. Biochem. Biophys. Res. Commun. *134*, 29–36.

Dehio, C., Meyer, M., Berger, J., Schwarz, H., and Lanz, C. (1997). Interaction of *Bartonella henselae* with endothelial cells results in bacterial aggregation on the cell surface and the subsequent engulfment and internalisation of the bacterial aggregate by a unique structure, the invasome. J. Cell Sci. *110*, 2141–2154.

Immunity
Propagation of Inflammatory Signals in Infection

Dong, C., Davis, R.J., and Flavell, R.A. (2002). MAP kinases in the immune response. Annu. Rev. Immunol. *20*, 55–72.

Eckmann, L., Kagnoff, M.F., and Fierer, J. (1993). Epithelial cells secrete the chemokine interleukin-8 in response to bacterial entry. Infect. Immun. *61*, 4569–4574.

Girardin, S.E., Boneca, I.G., Carneiro, L.A., Antignac, A., Jéhanno, M., Viala, J., Tedin, K., Taha, M.K., Labigne, A., Zähringer, U., et al. (2003). Nod1 detects a unique muropeptide from gram-negative bacterial peptidoglycan. Science *300*, 1584–1587.

Hamada, N., Matsumoto, H., Hara, T., and Kobayashi, Y. (2007). Intercellular and intracellular signaling pathways mediating ionizing radiation-induced bystander effects. J. Radiat. Res. (Tokyo) *48*, 87–95.

Holtmann, H., Winzen, R., Holland, P., Eickemeier, S., Hoffmann, E., Wallach, D., Malinin, N.L., Cooper, J.A., Resch, K., and Kracht, M. (1999). Induction of interleukin-8 synthesis integrates effects on transcription and mRNA degradation from at least three different cytokine- or stress-activated signal transduction pathways. Mol. Cell. Biol. *19*, 6742–6753.

Islam, D., Veress, B., Bardhan, P.K., Lindberg, A.A., and Christensson, B. (1997). In situ characterization of inflammatory responses in the rectal mucosae of patients with shigellosis. Infect. Immun. *65*, 739–749.

Iwai, H., Kim, M., Yoshikawa, Y., Ashida, H., Ogawa, M., Fujita, Y., Muller, D., Kirikae, T., Jackson, P.K., Kotani, S., and Sasakawa, C. (2007). A bacterial effector targets Mad2L2, an APC inhibitor, to modulate host cell cycling. Cell *130*, 611–623.

Kim, D.W., Lenzen, G., Page, A.L., Legrain, P., Sansonetti, P.J., and Parsot, C. (2005). The *Shigella flexneri* effector OspG interferes with innate immune responses by targeting ubiquitin-conjugating enzymes. Proc. Natl. Acad. Sci. USA *102*, 14046–14051.

Köhler, H., Rodrigues, S.P., and McCormick, B.A. (2002). *Shigella flexneri* interactions with the basolateral membrane domain of polarized model intestinal epithelium: Role of lipopolysaccharide in cell invasion and in activation of the mitogen-activated protein kinase ERK. Infect. Immun. *70*, 1150–1158.

Kufer, T.A., Banks, D.J., and Philpott, D.J. (2006). Innate immune sensing of microbes by Nod proteins. Ann. N Y Acad. Sci. *1072*, 19–27.

Lee, J., Mira-Arbibe, L., and Ulevitch, R.J. (2000). TAK1 regulates multiple protein kinase cascades activated by bacterial lipopolysaccharide. J. Leukoc. Biol. *68*, 909–915.

Li, H., Xu, H., Zhou, Y., Zhang, J., Long, C., Li, S., Chen, S., Zhou, J.M., and Shao, F. (2007). The phosphothreonine lyase activity of a bacterial type III effector family. Science *315*, 1000–1003.

Makino, S., Sasakawa, C., Kamata, K., Kurata, T., and Yoshikawa, M. (1986). A genetic determinant required for continuous reinfection of adjacent cells on large plasmid in *S. flexneri* 2a. Cell *46*, 551–555.

Mollenhauer, H.H., Morré, D.J., and Rowe, L.D. (1990). Alteration of intracellular traffic by monensin; Mechanism, specificity and relationship to toxicity. Biochim. Biophys. Acta *1031*, 225–246.

Neijssen, J., Herberts, C., Drijfhout, J.W., Reits, E., Janssen, L., and Neefjes, J. (2005). Cross-presentation by intercellular peptide transfer through gap junctions. Nature *434*, 83–88.

Ninomiya-Tsuji, J., Kishimoto, K., Hiyama, A., Inoue, J., Cao, Z., and Matsumoto, K. (1999). The kinase TAK1 can activate the NIK-I kappaB as well as the MAP kinase cascade in the IL-1 signalling pathway. Nature *398*, 252–256.

Okuda, J., Toyotome, T., Kataoka, N., Ohno, M., Abe, H., Shimura, Y., Seyedarabi, A., Pickersgill, R., and Sasakawa, C. (2005). *Shigella* effector IpaH9.8 binds to a splicing factor U2AF(35) to modulate host immune responses. Biochem. Biophys. Res. Commun. *333*, 531–539.

Parsot, C. (2009). *Shigella* type III secretion effectors: How, where, when, for what purposes? Curr. Opin. Microbiol. *12*, 110–116.

Patel, S.J., King, K.R., Casali, M., and Yarmush, M.L. (2009). DNA-triggered innate immune responses are propagated by gap junction communication. Proc. Natl. Acad. Sci. USA *106*, 12867–12872.

Pédron, T., Thibault, C., and Sansonetti, P.J. (2003). The invasive phenotype of *Shigella flexneri* directs a distinct gene expression pattern in the human intestinal epithelial cell line Caco-2. J. Biol. Chem. *278*, 33878–33886.

Phalipon, A., and Sansonetti, P.J. (2007). *Shigella's* ways of manipulating the host intestinal innate and adaptive immune system: A tool box for survival? Immunol. Cell Biol. *85*, 119–129.

Saccani, S., Pantano, S., and Natoli, G. (2002). p38-dependent marking of inflammatory genes for increased NF-kappa B recruitment. Nat. Immunol. *3*, 69–75.

Sansonetti, P.J., Arondel, J., Huerre, M., Harada, A., and Matsushima, K. (1999). Interleukin-8 controls bacterial transepithelial translocation at the cost of epithelial destruction in experimental shigellosis. Infect. Immun. *67*, 1471–1480.

Schroeder, G.N., and Hilbi, H. (2008). Molecular pathogenesis of *Shigella* spp.: Controlling host cell signaling, invasion, and death by type III secretion. Clin. Microbiol. Rev. *21*, 134–156.

Strober, W., Murray, P.J., Kitani, A., and Watanabe, T. (2006). Signalling pathways and molecular interactions of NOD1 and NOD2. Nat. Rev. Immunol. *6*, 9–20.

Troyanovsky, S.M., Troyanovsky, R.B., Eshkind, L.G., Krutovskikh, V.A., Leube, R.E., and Franke, W.W. (1994). Identification of the plakoglobin-binding domain in desmoglein and its role in plaque assembly and intermediate filament anchorage. J. Cell Biol. *127*, 151–160.

Wang, C., Deng, L., Hong, M., Akkaraju, G.R., Inoue, J., and Chen, Z.J. (2001). TAK1 is a ubiquitin-dependent kinase of MKK and IKK. Nature *412*, 346–351.

Yang, L., Cranson, D., and Trinkaus-Randall, V. (2004). Cellular injury induces activation of MAPK via P2Y receptors. J. Cell. Biochem. *91*, 938–950.

Zurawski, D.V., Mumy, K.L., Faherty, C.S., McCormick, B.A., and Maurelli, A.T. (2009). *Shigella flexneri* type III secretion system effectors OspB and OspF target the nucleus to downregulate the host inflammatory response via interactions with retinoblastoma protein. Mol. Microbiol. *71*, 350–368.

# SUPPLEMENTAL DATA

## SUPPLEMENTAL FIGURES AND LEGENDS

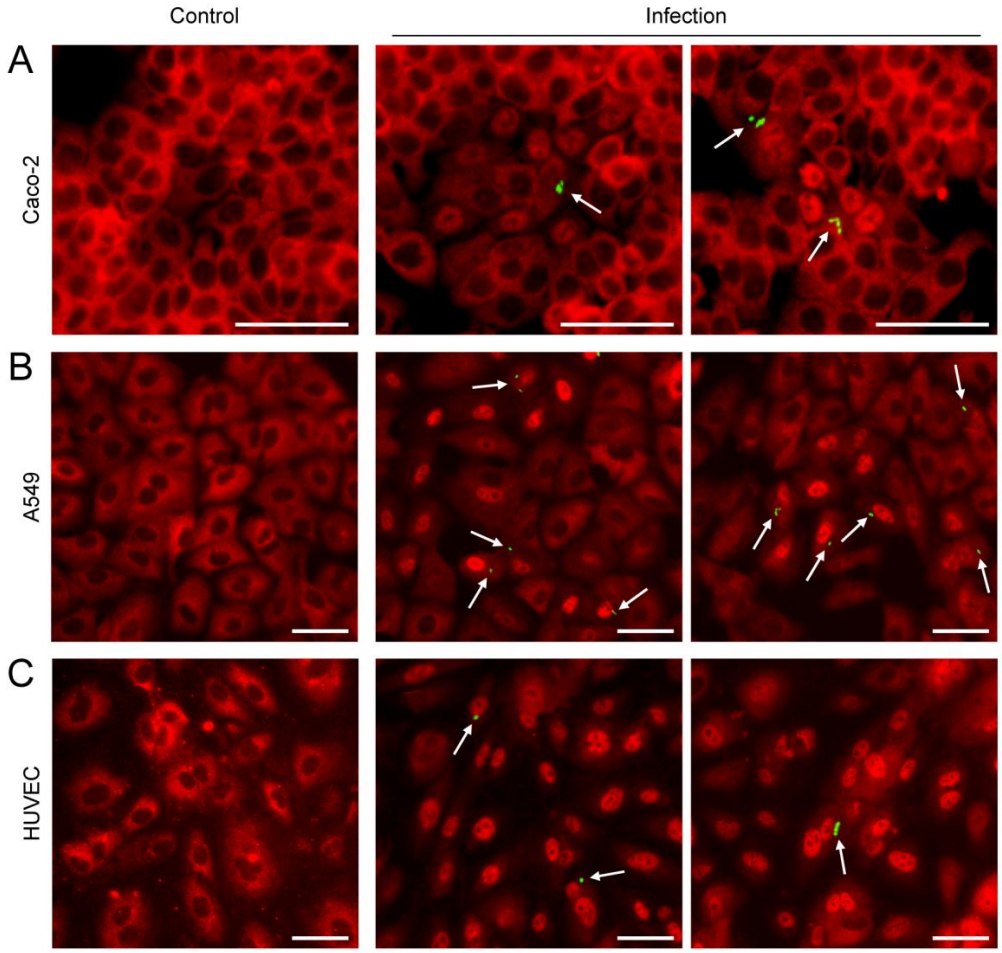


**Figure S1, relates to Figure 1. NF-κB is activated in bystander cells during *S. flexneri* infection of Caco-2, A549 and HUVEC cells.**

(A) Caco-2 cells

(B) A549 cells

(C) HUVEC cells

White arrows indicate bacteria. Bars, 50μm.

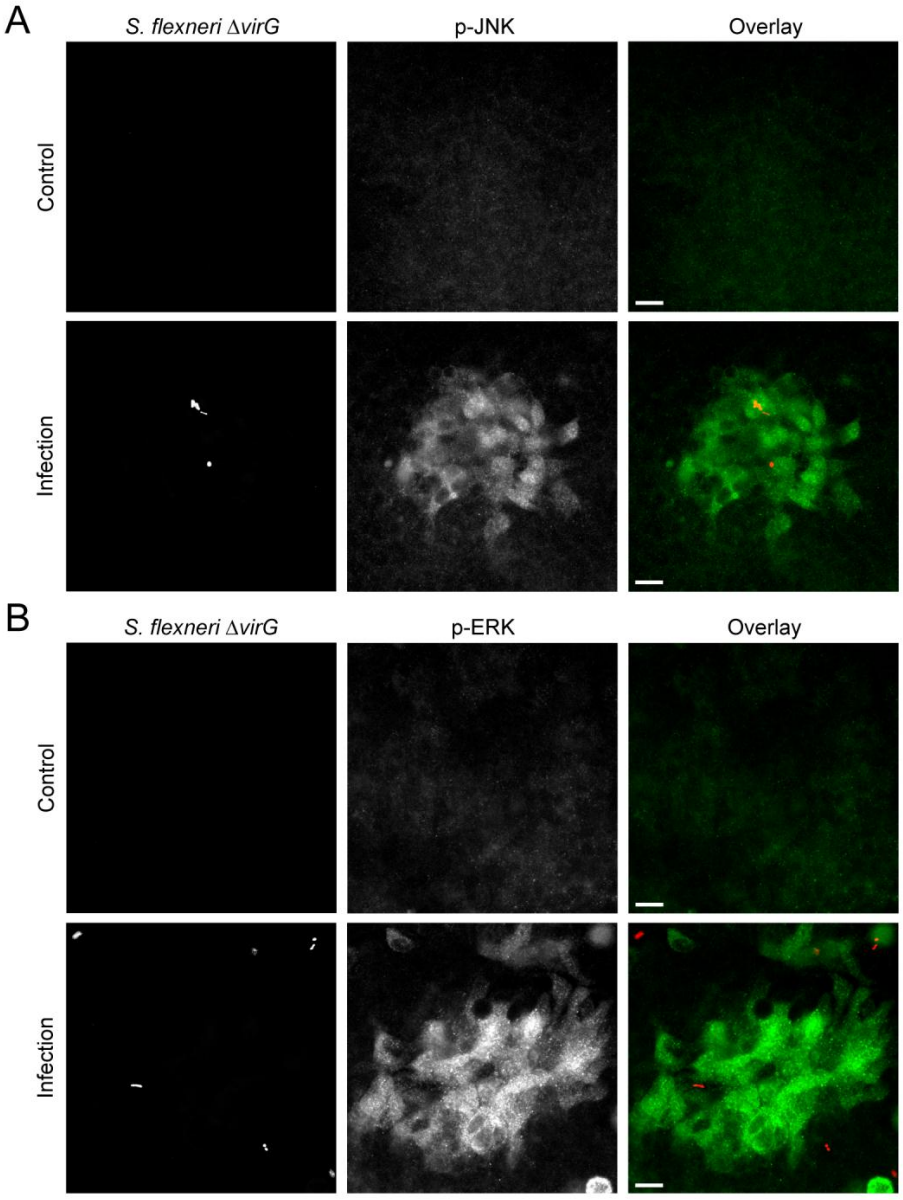


**Figure S2, relates to Figure 2. JNK and ERK are activated in bystander cells of *S. flexneri* infection in Caco-2 cells**

(A) JNK is activated in infected and bystander cells of *S. flexneri* infection in Caco-2 cells. Control or Δ*virG* infected cells (MOI=2, 90 minute infection) were stained for p-JNK (overlay: *S. flexneri* in red, p-JNK in green). Bars, 20 μm.

(B) ERK is mostly activated in bystander cells of *S. flexneri* infection in Caco-2 cells. Control or Δ*virG* infected cells (MOI=2, 90 minute infection) were stained for p-ERK (overlay: *S. flexneri* in red, p-ERK in green). Bars, 20 μm.

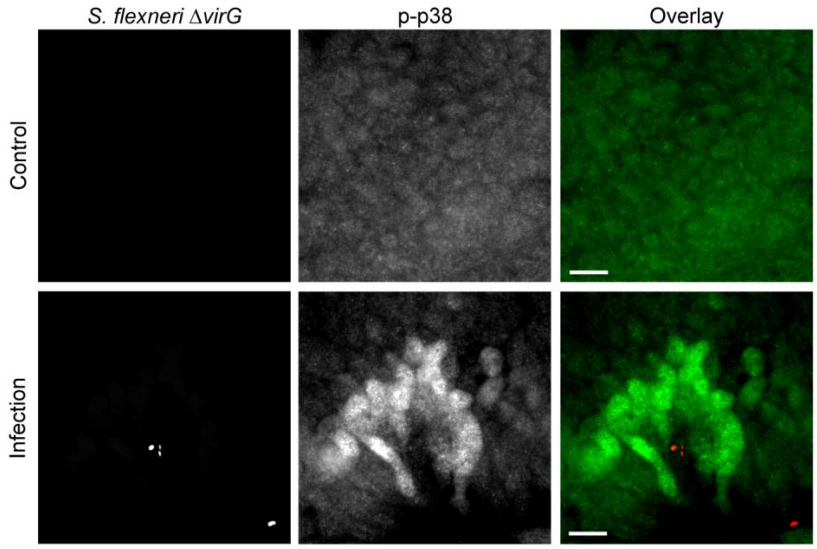


**Figure S3, relates to Figure 3. p38 is activated in bystander cells of *S. flexneri* infection in Caco-2 cells**

p38 is activated in bystander cells of *S. flexneri* infection in Caco-2 cells. Control or Δ*virG* infected cells (MOI=2, 90 minute infection) were stained for p-p38 (overlay: *S. flexneri* in red, p-p38 in green). Bars, 20 μm.

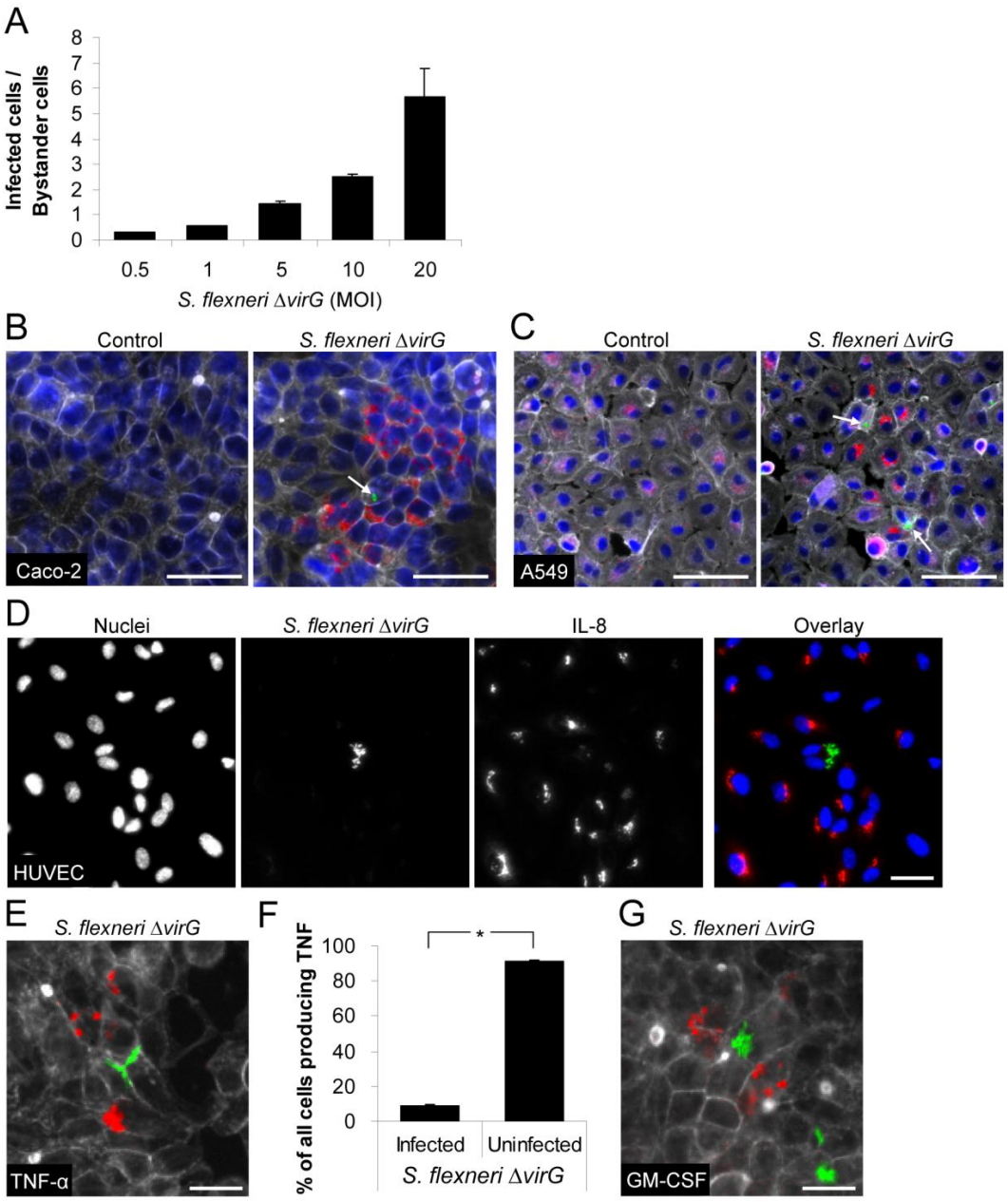


**Figure S4, relates to Figure 4. Proinflammatory cytokines are expressed in bystander cells of *S. flexneri* infection.**

(A) Infected to bystander cell ratios at different MOIs. HeLa cells were infected with the Δ*virG* mutant at indicated MOIs. The ratio between infected and bystander cells was determined by automated image processing. Results represent the mean +/- SD of triplicate wells. The graph shows a representative of 2 independent experiments.

(B) IL-8 production in bystander cells during *S. flexneri* infection of Caco-2 cells. Arrow indicates the infected cell (IL-8 in red, *S. flexneri* in green, Hoechst in blue, F-actin in grey). Bar, 40 μm.

(C) IL-8 production in bystander cells during *S. flexneri* infection of A549 cells Arrows indicate infected cells (IL-8 in red, *S. flexneri* in green, Hoechst in blue, F-actin in grey). Bar, 40 μm.

(D) HUVEC cells were infected for 3 hours with *S. flexneri* Δ*virG*. Bar, 50 μm.

(E) TNF-α accumulation in bystander cells of *S. flexneri* infection in Caco-2 cells. TNF-α staining of monensin-treated Caco-2 cells during infection (TNF-α in red, *S. flexneri* in green, F-actin in grey). Bar, 20 μm.

(F) Quantification of TNF-α expression during *S. flexneri* infection of Caco-2 cells. The vast majority of cells producing TNF-α are uninfected cells. In conditions were 2% of cells were infected, around 1% of all cells exhibited TNF-α expression. Results represent the mean +/- SD of triplicate wells. The graph shows a representative of 2 independent experiments, *p = 2.16E-06.

(G) GM-CSF accumulation in bystander cells of *S. flexneri* infection in Caco-2 cells. GM-CSF staining of monensin-treated Caco-2 cells during infection (GM-CSF in red, *S. flexneri* in green, F-actin in grey). Bar, 20 μm.

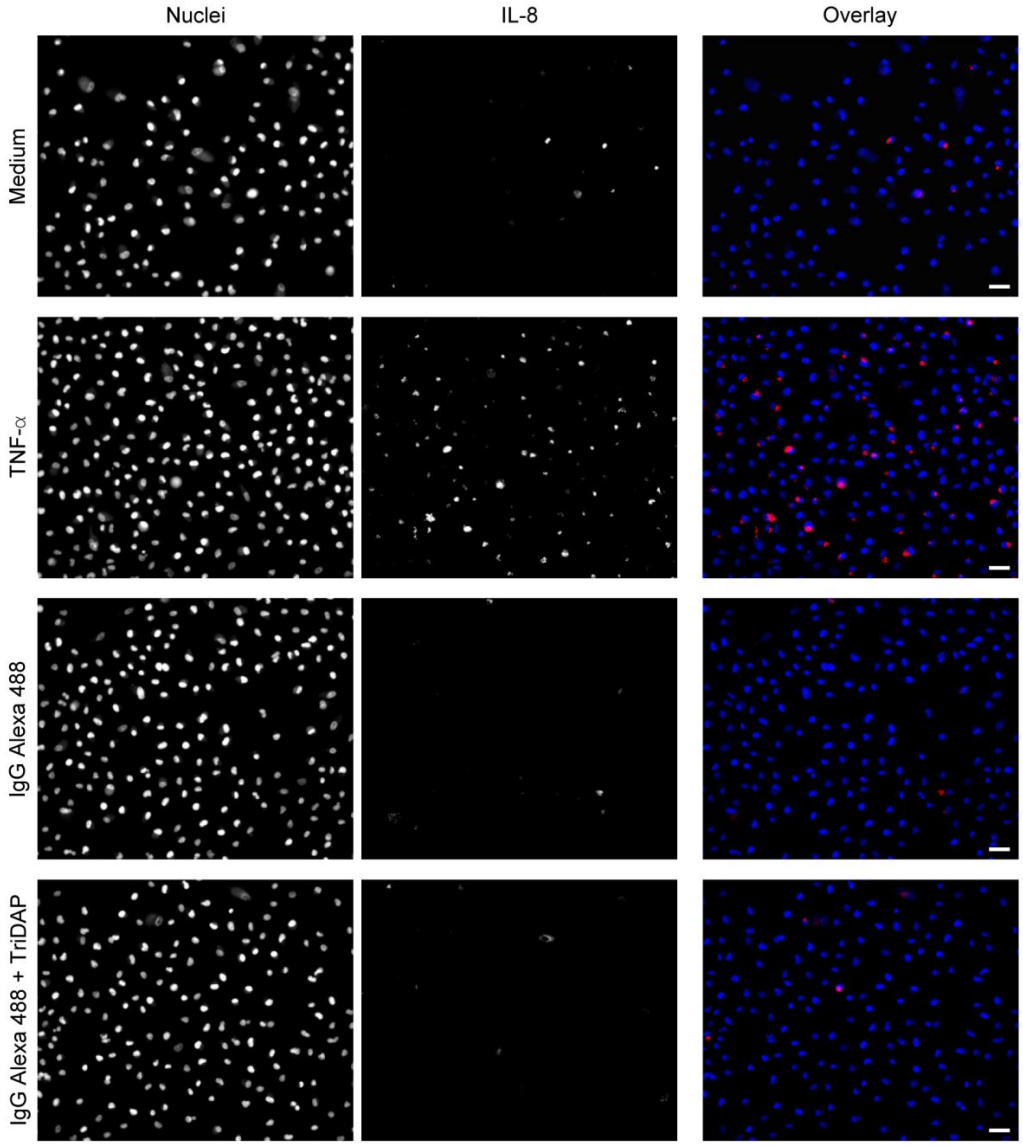


**Figure S5, relates to Figure 5. Extracellular treatment with TriDAP failed to induce IL-8 expression.**

IL-8 staining in A549 cells left untreated or treated extracellularly with TNF-α, IgG Alexa 488 alone or combined with TriDAP.

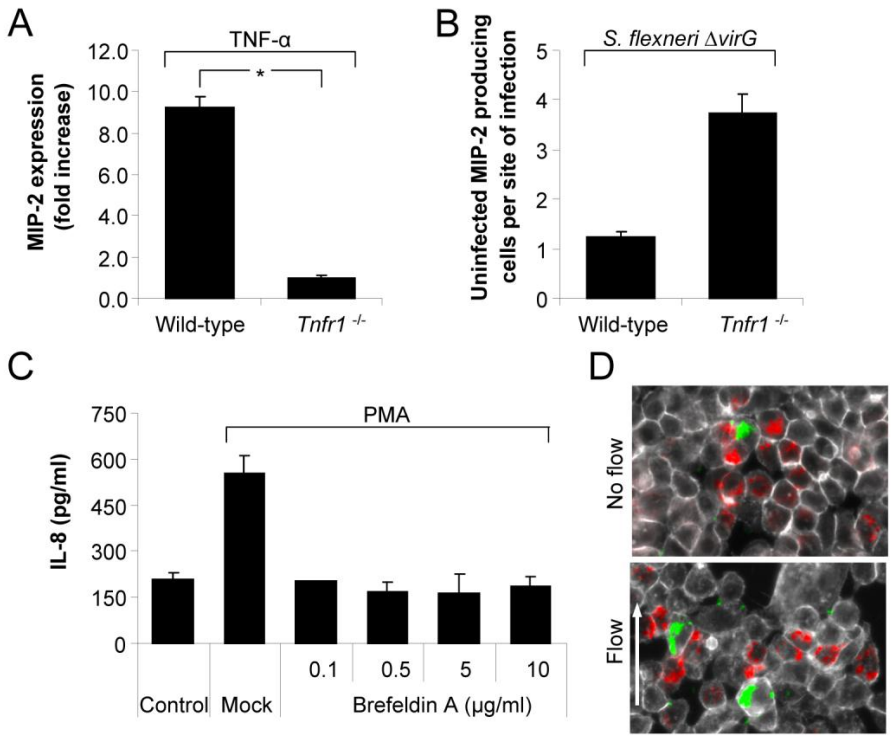


**Figure S6, relates to Figure 6. *S. flexneri*-induced bystander IL-8 expression is not mediated by paracrine signaling but is cell-cell contact dependent.**

(A) *Tnfr1*$^{-/-}$ MEF cells are TNF-α-irresponsive. MIP-2 expression was not induced in response to TNF-α stimulation in *Tnfr1*$^{-/-}$ MEF cells (mean +/- SD of triplicate wells, graph representative of 3 independent experiments, *p = 2.0E-03).

(B) Massive bystander MIP-2 expression was found during *S. flexneri* infection of *Tnfr1*$^{-/-}$ MEF cells (mean +/- SD of triplicate wells, graph representative of 3 independent experiments).

(C) BFA blocks PMA-induced IL-8 secretion. Effect of BFA pretreatment on IL-8 secretion measured by ELISA in the supernatant of resting or PMA-stimulated Caco-2 cells (mean +/- SD of triplicate wells, graph representative of 2 independent experiments).

(D) IL-8 expression in bystander cells of infection is not abolished under flow conditions. The direction of the flow is given by the white arrow (IL-8 in red, *S. flexneri* in green, F-actin in grey).

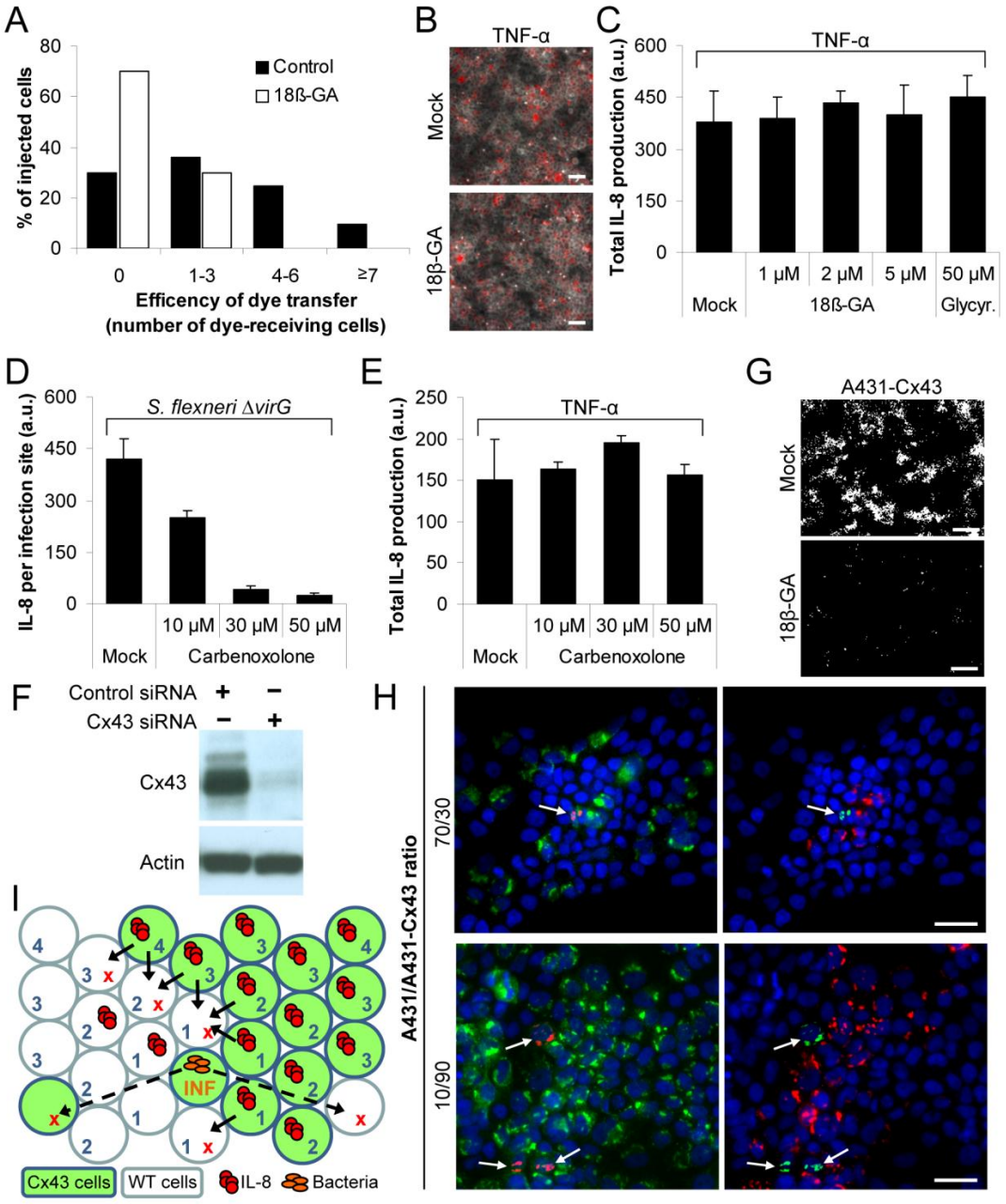


**Figure S7, relates to Figure 7. *S. flexneri*-induced bystander IL-8 expression is mediated by gap junctions.**

(A) Caco-2 cells have functional gap junctions that are sensitive to 18β-GA. Lucifer Yellow transfer from microinjected to neighboring cells in absence or in presence of 18β-GA (Control: n=334, 18β-GA: n=207).

(B) TNF-α-induced IL-8 accumulation is not affected by 18β-GA (5 μM) in Caco-2 cells. Bars, 50 μm.

(C) Effect of 18β-GA and glycyrrhizic acid on TNF-α-induced IL-8 accumulation quantified by automated image analysis (a.u., arbitrary unit; mean +/- SD of triplicate wells, graph representative of 2 independent experiments).

(D) Quantification of intracellular IL-8 accumulation per site of *S. flexneri* infection in cells left untreated or pretreated with carbenoxolone (mean +/- SD of triplicate wells, graph representative of 2 independent experiments).

(E) Quantification of total IL-8 production in cells left untreated or pretreated with carbenoxolone following TNF-α stimulation (mean +/- SD of triplicate wells, graph representative of 2 independent experiments).

(F) siRNA-mediated depletion of Cx43 in A431-Cx43 cells. Cells were transfected with control or Cx43 siRNAs. Cx43 expression was analyzed 72 hours after transfection by a Cx43 immunoblot (top panel). Equal loading was verified with an actin immunoblot (bottom panel).

(G) *S. flexneri*-induced bystander IL-8 expression is inhibited by 18β-GA (5 μM) in A431-Cx43 cells. Bars, 300 μm.

(H) Images illustrating the spatial propagation of IL-8 expression from *S. flexneri* infected A431-Cx43 cells into either A431-Cx43 or A431 adjacent cells. Left panels: Cx43 in green, *S. flexneri* in red, Hoechst in blue. Right panels: IL-8 in red, *S. flexneri* in green, Hoechst in blue. Arrows indicate infected cells. Bars, 40 μm.

(I) Sketch representing the analysis algorithm used to quantify the propagation from *S. flexneri* infected A431-Cx43 cells into either A431-Cx43 or A431 adjacent cells. Numbers represent the position of the cell in the "path" from the infected cell. Cells at position 1-4 were exclusively considered for analysis. Cells containing an "X" were excluded from analysis. Black arrows indicate A431 cells in contact with A431-Cx43 producing IL-8. Dashed black arrows indicate invalid paths.

## SUPPLEMENTAL TABLES

| Mutant | Forward | Reverse |
|---|---|---|
| Δ*ospF* | ATTCTATTATATAGATAAAATATCT CCTGCAAAAGATACGGGTATTTT TGTGTAGGCTGGAGCTGCTTCG | TCAAAAGTTCGATGTTCCACCACAT CGACCGTAGAAGAGATGAGATAGTA CATATGAATATCCTCCTTAG |

**Table S1. Oligonucleotide primers used to generate the Δ*ospF* mutant.**

The underlined sequences represent the priming sites used to amplify the *cat* resistance cassette from pKD3.

## SUPPLEMENTAL EXPERIMENTAL PROCEDURES

### Bacterial strains

All *Shigella* and *Salmonella* strains were transformed with the pMW211 plasmid to express the DsRed protein under control of a constitutive promoter. The pMW211 plasmid was a generous gift from Dr. D. Bumann (Biozentrum, University of Basel, Switzerland).

The Δ*virG* Δ*ospF* deletion mutant was generated from the Δ*virG* mutant by allelic exchange using a modification of the lambda red-mediated gene deletion (Datsenko and Wanner, 2000). The genes for lambda red recombination were expressed from the pKM208 plasmid (Murphy and Campellone, 2003). The chloramphenicol

resistance cassette (*cat*) of the pKD3 plasmid was amplified using the primers listed in Table S1. After *Dpn*I digestion, the PCR product was electroporated into the *virG* mutant. Recombinants were selected on TSB plates containing 5 or 10 µg $ml^{-1}$ chloramphenicol. The *cat* cassette was removed by transformation of pCP20 and incubation at 30°C on TSB plates containing 100 µg $ml^{-1}$ ampicillin. Single colonies were screened by PCR.

**Double-thymidine block**

HeLa cells were seeded in a 96-well plate at 2750 cells per well. The next day, 2 mM thymidine was added. After 19 hours, cells were washed and incubated with fresh growth medium for 9 hours. Thymidine was, then, added again for a period of 16 to 18 hours. Cells were washed and infection performed as described above.

**Immunofluorescence**

After fixation, cells were permeabilized in 0.3-0.5% Triton X-100 for 10 minutes, incubated in PBS supplemented with 5% goat serum for 2 hours and then, overnight at 4°C, with different combinations of primary antibodies. NF-κB p65 localization was visualized by using a mouse monoclonal anti-p65 antibody (Santa Cruz Biotechnology, Santa Cruz, USA). The phosphorylated forms of p38, JNK and ERK were stained with a rabbit monoclonal anti-phospho(T180/Y182)-p38, a rabbit polyclonal anti-phospho(T183/Y185)-SAPK/JNK and a rabbit monoclonal anti-phospho(T202/Y204)-p44/p42 antibody (Cell signaling technology, Beverly, USA), respectively. The phosphorylated form of histone H3 was detected with a rabbit polyclonal anti-phospho(S10)-Histone H3 (Upstate signaling solution, Billerica, USA). Intracellular TNF-α and GM-CSF were stained with a purified mouse anti-human TNF-α and a purified rat anti-human GM-CSF antibody, respectively (BD

Pharmingen, San Jose, USA). Cells were then stained with Cy5-, Alexa 647- or FITC-conjugated secondary antibodies accordingly (Invitrogen, Carlsbad, USA). DNA and F-actin were stained with Hoechst and FITC-phalloidin, respectively.

**IL-8 and MIP-2 measurements**

IL-8 secretion was measured by ELISA in the supernatant of HeLa cells infected with *S. flexneri* for 6 hours. The cell-free supernatant from triplicate wells was analyzed for its IL-8 content using the commercial ELISA kit (BD Pharmingen, San Jose, USA). *In situ* hybridization of *IL-8* mRNA was performed with the QuantiGene ViewRNA Plate-Based Assay kit (Panomics, Fremont, USA) 2 hours after infection. Alternatively, the production of IL-8 and MIP-2 was measured by immunofluorescence using an anti human IL-8 antibody (BD Pharmingen, San Jose, USA) and an anti mouse MIP-2 antibody (BD Pharmingen, San Jose, USA) 3 hours after infection. Monensin (50 μM) was used in the infection assay to trap IL-8 and MIP-2 in intracellular compartments.

**Drug treatments**

When specified, cells were pretreated 30-60 minutes before infection with drugs at concentration indicated on the figures. Brefeldin A, 18β-glycyrrhetinic acid, glycyrrhizine and carbenoxolone were from Sigma-Aldrich (Saint Louis, USA).

**siRNA transfection and western blot analysis**

A431-Cx43 cells were transfected with ON-TARGETplus SMARTpool siRNAs targeting Cx43 or ON-TARGETplus siCONTROL (Dharmacon, Dallas, USA). 72 hours after transfection, cells were lysed in Phosphosafe Extraction Buffer (Novagen, Darmstadt, Germany) supplemented with 1x protease inhibitor cocktail (Calbiochem, Darmstadt, Germany). Protein concentration was measured using the bicinchoninic

acid (BCA) kit (Pierce, Rockford, USA). Equal amounts of proteins were resolved by SDS-PAGE and transferred to Hybond C-Extra membrane (Amersham Bioscience, Pittsburgh, USA) for immunoblotting with a rabbit anti-Cx43 antibody or an anti actin antibody (Invitrogen, Carlsbad, USA). Primary antibody was detected using horseradish peroxidase-conjugated anti-rabbit and visualized with the ECL system (Pierce).

**Image acquisition and analysis**

At each site, images were acquired at 360 nm, 480 nm, 594 nm and 640 nm to visualize Hoechst, FITC-phalloidin or FITC-conjugated secondary antibodies, DsRed expressing *S. flexneri* and Cy5- or Alexa 647-conjugated secondary antibodies, respectively. For image analysis, the Hoechst staining was used as a mask to automatically identify cell nuclei. Cellular area was defined by extension of the nuclear mask. Subtraction of the nuclear area from the cellular area was used to define the cytoplasm.

For each cell, the ratio of p65 intensity in the nucleus and in the cytoplasm, defined as the NF-κB activation ratio, was calculated. In order to automatically quantify the fraction of NF-κB activated cells, a threshold of activation (T) was automatically calculated as such that 90% of control cells remained below this value. In parallel, the presence of bacteria within the area of each cell was also quantified. *S. flexneri* bacteria express DsRed at high levels and are therefore very effectively detected by automated image analysis. For automated detection, the "Robust Background Adaptive" algorithm described by Carpenter et al. was used (Carpenter et al., 2006). Briefly, the "Robust Background" method trims the brightest and dimmest 5% of pixel intensities off first, in a way that the remaining pixels represent a gaussian of intensity values that are mostly background pixels. It then calculates the mean and standard

deviation of the remaining pixels and calculates the threshold as the mean + 2 times the standard deviation. As this is a dynamic method, the threshold value was calculated for each image. Performance of bacterial detection was checked by visual inspection of several images prior to automated processing. In control images (no infection), the algorithm generally classified less then 1% of cells as infected.

Based on these measurements, cells containing bacteria and showing a NF-κB activation ratio > T were defined as infected cells. Cells, which did not contain bacteria, but had a ratio > T were classified as bystanders. The nuclear mask was used to measure activation of MAP kinases or histone H3 for infected and bystander cell populations. To automatically quantify the fraction of ERK activated cells, a threshold based on p-ERK nuclear intensity was defined as described above. For Caco-2 cells, the intracellular accumulation of IL-8 was quantified by measuring the area of IL-8 granules in uninfected cells using threshold intensity and size exclusion values. In the experiment performed to test the effect of BFA, we used a lower threshold intensity value for IL-8 detection combined to a higher threshold value for size exclusion.

**Microinjection**

For microinjection, A549 cells were seeded subconfluently in 35 mm µ-dishes (Ibidi, Munich, Germany). Cells were microinjected with L-Ala-D-γ-Glu-meso-diaminopimelic acid (TriDAP; 2 µg $ml^{-1}$ in PBS from AnaSpec, San Jose, USA) using Eppendorf Femtotips II capillaries and an Eppendorf FemtoJet with an injection pressure (pi) of 80 hPa. For identification of injected cells, the goat anti-rabbit-IgG-Alexa 488 antibody (0.5 mg $ml^{-1}$) was co-injected with TriDAP. Control cells were injected with the IgG-Alexa 488 antibody alone. After microinjection, growth medium containing 50 µM monensin was added. After 3 hours, cells were fixed, stained for IL-8, and

analyzed with a Revolution XD spinning disk confocal microscope (Andor technology, Belfast, Ireland). For dye transfer experiments, Caco-2 cells were microinjected with a solution containing LY and the anti-rabbit-IgG-Alexa 594 antibody. LY transfer to neighboring cells was analyzed 10-15 minutes after microinjection.

**Flow chamber experiments**

Caco-2 cells were seeded in a flow chamber (Ibidi, Munich, Germany) and used at confluency. For infection, bacteria were added to cells and the chamber centrifuged at 37°C for 10 minutes. A constant perfusion of pre-warmed assay medium was then immediately started at a flow rate of 1.5 ml $min^{-1}$. After 1 hour, this solution was replaced by a solution containing 50 µM monensin and 100 µg $ml^{-1}$ gentamicin. After 2 more hours, cells were fixed and stained for IL-8.

**Quantification of the propagation of IL-8 expression during *S. flexneri* infection of A431 and A431-Cx43 cells**

Quantification of the propagation of IL-8 across infection foci was performed by automated image analysis as follows. The "MeasureObjectNeighbors" analysis module of CellProfiler was used to classify cells into different subgroups based on their position relative to the infected cell: uninfected cells in direct contact with the infected cell belong to the subgroup "Position 1" (P1), uninfected cells in contact with P1 cells belong to P2, outer uninfected cells in contact with P2 cells belong to P3 et cetera. For each subgroup, the fraction of IL-8 positive cells was measured and compared between the two cell lines.

**Quantification of the propagation of IL-8 expression in mixed A431 and A431-Cx43 cell populations**

In order to test whether Cx43 expression was required in bystander cells, the propagation from *S. flexneri* infected A431-Cx43 cells to either A431-Cx43 or A431 cells, was analyzed. Cells were mixed prior seeding in the A431/A431-Cx43 ratios (70/30) and (10/90) and infected with *S. flexneri* at MOI 0.5 the next day. One hour after adding bacteria, cells were treated with monensin to trap IL-8 intracellularly. Following infection, cells were stained by immunofluorescence for IL-8 and Cx43, used here to identify A431 and A431-Cx43 cells (Cx43 negative: A431 cells, Cx43 positive: A431-Cx43 cells). Cells surrounding *S. flexneri* infected A431-Cx43 cells were exclusively considered. For all these bystander cells, the position relative to the infected cell (positions 1 to 4 were only considered for analysis), as well as the identification of their neighbors, were defined by the "MeasureObjectNeighbors" analysis module of CellProfiler. In addition, the intensity of Cx43 and IL-8 was quantified for all cells. The propagation from infected A431-Cx43 to bystander A431-Cx43 cells (A431/A431-Cx43 ratio 10/90) was quantified by measuring IL-8 expression in A431-Cx43 cells that were in direct contact with infected cells (position 1) or were connected to infected cells via other A431-Cx43 cells (positions 2,3,4 of the "A431-Cx43 path"). Alternatively, the propagation from infected A431-Cx43 to A431 cells (A431/A431-Cx43 ratio 70/30) was quantified by measuring IL-8 expression in A431 cells having direct contact with infected A431-Cx43 cells (position 1) or in adjacent A431 cells connected to infected cells exclusively via A431 cells (positions 2,3,4 of the "A431 path"). A431 cells in contact with uninfected A431-Cx43 producing IL-8 cells were excluded from our analysis. A sketch illustrating the algorithm used for analysis is illustrated in Figure S7H.

**SUPPLEMENTAL REFERENCES**

Carpenter, A.E., Jones, T.R., Lamprecht, M.R., Clarke, C., Kang, I.H., Friman, O., Guertin, D.A., Chang, J.H., Lindquist, R.A., Moffat, J.*, et al.* (2006). CellProfiler: image analysis software for identifying and quantifying cell phenotypes. Genome Biol *7*, R100.

Datsenko, K.A., and Wanner, B.L. (2000). One-step inactivation of chromosomal genes in Escherichia coli K-12 using PCR products. Proc Natl Acad Sci U S A *97*, 6640-6645.

Murphy, K.C., and Campellone, K.G. (2003). Lambda Red-mediated recombinogenic engineering of enterohemorrhagic and enteropathogenic E. coli. BMC Mol Biol *4*, 11.

# Chapter III

# Probing *Shigella* cell invasion, intracellular growth and propagation of inflammatory signals by high-content image-based RNAi screens

# 1 Summary

The foodborne enteroinvasive bacterium *Shigella flexneri* infects the colonic epithelium in humans causing an acute mucosal inflammation, also known as shigellosis. In the submucosa, the pathogen actively invades intestinal epithelial cells (IECs) by a so-called "trigger mechanism". *S. flexneri* makes use of a type III secretion system (T3SS), a syringe-like nanomachine, to inject several effector proteins into host cells. By targeting factors of the cytoskeletal machinery, these effectors induce the formation of filapodial and lamellipodial extensions that engulf the invading bacterium. Upon successful invasion, *Shigella* rapidly lyses the surrounding vacuole and replicates within the cytoplasm of infected cells. Infected IECs sense the presence of intracellular bacteria and activate proinflammatory signaling cascades in order to mount an innate immune response. Although several T3SS effectors downregulate inflammation signaling in infected cells, massive production and secretion of cytokines are observed during shigellosis. In fact, epithelial cells were found to propagate proinflammatory signals to uninfected bystander cells, thereby evading the immunosuppressive activity of effectors and strongly amplifying the production of cytokines.

In this chapter, the implementation of a high-content RNAi screen to study aspects of *Shigella* infection is reported. Using automated microscopy and image analysis, cell invasion, intracellular growth and production of cytokines in bystander cells during *S. flexneri* infection were quantified. To validate the assay, control knockdowns of genes previously described in the context of *Shigella* infection were performed. Furthermore, the reproducibility of the different readouts was quantified. Finally, results from screens performed on two kinome libraries from different suppliers were compared.

# 2 Statement of contribution

All experiments mentioned in this chapter were performed by myself. Additionally, I have optimized and validated the experimental protocols used for the screens according to the standards defined by the InfectX research consortium. Preparation and spotting of siRNA kinome libraries was performed by Simone Muntwiler and Simone Eicher (group of Ch. Dehio, Biozentrum, University of Basel). Image analysis procedures were established by Mario Emmenlauer (group of Ch. Dehio, Biozentrum, University of Basel) and myself. Eva Pujadas, Vincent Rouilly and Michael Podvinec (Research IT, Biozentrum, University of Basel) have developed the image analysis environment iBRAIN2. Data aggregation and feature Z scoring was implemented by Pauli Rämö (group of Ch. Dehio, Biozentrum, University of Basel). The data management software openBIS was developed by the group of Bernd Rinn (CISD, ETH Zurich).

# 3 Introduction

The enteroinvasive pathogen *S. flexneri* infects the colonic epithelium of humans upon ingestion of contaminated water or food. The Gram-negative pathogen causes an acute inflammation of the mucosa, called shigellosis, responsible for 1.1 million deaths every year[130]. In the submucosa, *S. flexneri* infects intestinal epithelial cells (IECs) by a so-called "trigger mechanism". Upon successful invasion, *Shigella* starts to replicate and can spread throughout the tissue by actin-based motility[135]. Intracellular bacteria are sensed by the pathogen recognition receptor Nod1 that initiates an inflammatory response[44].

When reaching the gut, *S. flexneri* crosses the intestinal epithelium by transcytosis through M cells and evades the killing by macrophages[117,159]. Released into the submucosal space, *S. flexneri* interacts with receptors CD44 and $\alpha5\beta1$ integrin on the cell surface of intestinal epithelial cells (IECs)[185,187]. To invade IEC, the pathogen makes use of a type III secretion system (T3SS), a syringe-like nanomachine, which allows the translocation of effector proteins into the host cell cytoplasm. A subset of these effectors induces membrane ruffles by targeting the host's cytoskeletal machinery. In the vicinity of entry foci, an increase in polymerized actin forming filopodial and lamellipodial extensions is observed[179]. This process is controlled by the small GTPases Rac1 and Cdc42[192,193]. The tyrosine kinases Src and Abl1/2 are involved in the activation and membrane recruitment of the small GTPases[196,201]. Src, in turn, is localized to entry sites by interaction with the bacterial translocator protein IpaC[200]. The activation of Rac1 and of Cdc42 is further promoted by the *Shigella* effector IpgB1[209,212]. Additionally, proteins of focal adhesions are associated with *S. flexneri* cell invasion. The small GTPase Rho is recruited to sites of entry where it controls actin stress fibers and contributes to phosphorylation of the focal adhesion kinase (FAK) by PKC[217,218,226]. The activation of FAK is enhanced by the bacterial translocator proteins IpaB/C, possibly through outside-in signaling by the $\alpha5\beta1$ integrin receptor[189]. FAK controls focal adhesion formation through phosphorylation of paxillin and vinculin[218]. On the other hand, the effector IpaA was reported to disrupt focal adhesions and stress fibers by interacting with vinculin and Rho[221,224,226]. Moreover, the effector VirG promotes cell invasion by destabilization of microtubules[236,238]. The concerted action of *S. flexneri* effectors thus promotes the internalization of the bacteria in a process involving cytoskeletal rearrangements, focal adhesions and microtubule destabilization.

Upon successful cell invasion, *Shigella* rapidly lyses the surrounding vacuole and is released into the cytoplasm of IECs, which represents the main replicative niche for the pathogen. Efficient replication (i.e. generation time less than 40 minutes) requires a high degree of adaptation, which is highlighted by the fact that almost 25% of the genes are significantly up- or downregulated in intracellular bacteria[259]. Nevertheless, little is known about critical factors for successful survival and replication in infected cells. The access to carbon sources and nutrients (e.g. iron, magnesium and phosphate) has been suggested as important determinant for growth[259,264].

Furthermore, the pathogen needs to sustain oxidative stress[265] and avoid killing by autophagy[163]. Finally, *S. flexneri* injects effector proteins IpgD and Spa15 to promote host cell survival[235,266,270].

Infected IECs are able to sense intracellular *S. flexneri* through the pathogen recognition receptor Nod1, which detects peptidoglycan moieties released from the bacterial surface[44]. Upon ligand binding, Nod1 triggers downstream signaling cascades leading to the activation of NF-$\kappa$B and the MAP kinases JNK and p38[43,121]. The MAP kinase ERK is also activated in infected cells[122]. Collectively, these signals promote the transcription of proinflammatory genes that will initiate an innate immune response. Among these genes, the cytokine IL-8 was shown to be strongly upregulated[119]. IL-8 plays a central role in the immune response to *Shigella* invasion by recruiting polymorphonuclear cells (PMNs) to the site of infection[123]. Remarkably, *S. flexneri* translocates several effector proteins to downmodulate inflammation. The effector OspG, for instance, interferes with NF-$\kappa$B activation, while OspF dephosphorylates the MAP kinases p38 and ERK[125,126,278]. An explanation for these conflicting observations was recently provided, when infected cells were shown to propagate inflammatory signals to their uninfected bystander cells[304]. While infected cells were not able to express cytokines, this capacity was restored in activated bystander cells. Moreover, it was shown that this cell-cell communication is mediated by gap junctions, although the precise molecular mechanism remains currently unknown[304].

In this chapter, the implementation of a high-content RNAi screen to study aspects of *Shigella* virulence is introduced. Using automated microscopy and image analysis, cell invasion, intracellular growth and production of cytokines in bystander cells during *S. flexneri* infection were quantified. To validate the assay, control knockdowns of genes previously described in the context of *Shigella* invasion and bystander activation were performed. Furthermore, reproducibility of the assay and the different readouts were investigated. Finally, results from screens performed on two kinome libraries from different suppliers were compared.

The high-content RNAi screen on *Shigella* cell invasion is part of the InfectX project*, which compares results on pathogen entry from standardized RNAi screens covering five bacterial (*Bartonella*, *Brucella*, *Listeria*, *Salmonella* and *Shigella*) and four viral (adenovirus, rhinovirus, rotavirus and vaccinia) pathogens.

*The InfectX project is funded by the Swiss Initiative in Systems Biology. More information about InfectX is available on the project homepage:
http://www.systemsx.ch/projects/systemsxch-projects/research-technology-and-development-projects-rtd/infectx/

# 4 Results

## 4.1 Implementation and optimization of an *in vitro* infection assay for RNAi screens

To identify new proteins involved in *S. flexneri* cell invasion and intracellular growth, as well as bystander IL-8 production, the *in vitro* infection assay previously described by Kasper et al.[304] was adapted to be adequate for high-throughput screening. The assay was upscaled from 96-well plates to 384-well plates. All liquid handling steps, including siRNA transfection, cell seeding, infection, addition of drugs, fixation and immunofluorescence staining, were automated using liquid dispensers and pipetting robots.

To comply with the standards defined by the InfectX consortium, we used HeLa CCL-2 cells instead of HeLa Kyoto $\alpha$. Infections were performed using the non-motile *S. flexneri* M90T $\Delta virG$ strain, which forms microcolonies when replicating within cells and is therefore advantageous for image analysis[304]. To discriminate between intra- and extracellular bacteria, *S. flexneri* $\Delta virG$ was transformed with a plasmid coding for the fluorophore DsRed under control of the *uhpT* promoter. The *uhpT* gene is part of an operon coding for a hexose phosphate transport system, which is highly conserved among *E. coli*, *S. typhimurium* and *S. flexneri*[305,306]. The expression of UhpT is strongly upregulated in response to the presence of glucose-6-phosphate[259,264] and therefore serves as an excellent sensor for intracellular *Shigella*. Infections with *S. flexneri* carrying the plasmid reveal an increase in fluorescence about two hours post infection and a strong signal is recorded after 3-3.5 hours of infection (data not shown).

To promote adhesion to the cell surface, plates were centrifuged after adding the bacteria. Extracellular bacteria were killed by adding gentamicin 30 minutes post infection. At the same time, secretion was blocked by adding monensin[307]. This allows to intracellularly trap cytokines, which would otherwise get secreted. After a total infection time of 3.5 hours, cells were fixed and stained for DNA, F-actin and the cytokine IL-8 using appropriate dyes and antibodies. By means of automated microscopy, images from all wells were acquired and stored for subsequent image analysis. A detailed description of the experimental procedures can be found in section 5 of this chapter and an overview of the workflow is presented in Figure III.1.

The different steps of the experimental workflow were optimized for quality, use of reagents and reproducibility. Conditions for siRNA transfection were tested by members of the InfectX consortium and subsequently standardized for all screens. Reproducibility of the infection rate was significantly increased by using frozen aliquots of bacterial culture for inoculation of day cultures, instead of inoculating with colonies from agar plates. Infections on test plates revealed that an estimated multiplicity of infection (MOI) of 15 results in a reproducible infection rate of 40%

(data not shown). However, quantification of the infection rate on test plates revealed the presence of plate effects. Displaying the infection rate as heat map with respect to the position on the plate showed lower values for the left edge of the plate, which gradually increased towards the right edge of the plate (Figure III.2). One possible explanation for the presence of the gradient would be temperature differences introduced during centrifugation. This was confirmed as the gradient changed its orientation when plates were rotated by 180° prior to centrifugation. While the differences in infection rate measured between the left and right edge were initially up to 50%, the effect could be reduced to below 10% by shortening the duration of centrifugation and by thoroughly equilibrating temperature in the centrifuge before every run. Additionally, remaining temperature differences are equilibrated more rapidly by incubating the assay plates on metal blocks that remain in the incubator. Figure III.2 presents the gradient in infection rate measured by averaging all plates obtained from screening the Dharmacon kinome library (left) and the Ambion kinome library (right).

## 4.2 Quantification of infection rate, intracellular growth and bystander IL-8 production by automated image analysis

In order to identify the genes that alter the infection rate, intracellular growth or bystander IL-8 production when depleted by RNAi, an automatic quantification of the acquired images was established. For that purpose, the open source software CellProfiler[308] was used and extended by custom modules implemented in MATLAB. The image analysis pipeline segments cell nuclei, the cell body, bacterial microcolonies and IL-8 granules using object detection algorithms. For every segmented object, features including intensities, area or shape can be extracted. Bacterial microcolonies and IL-8 granules are additionally assigned to the cell that contains them. Certain readouts (e.g. cell number) represent basic features, which are determined during the image analysis procedure. However, most of the readouts are only calculated after the image analysis, as they result from the combination of several features. The infection rate is calculated by summing all cells containing at least one bacterial object and by dividing by the total number of cells. The score for intracellular replication of *S. flexneri* (referred to as intracellular growth) is quantified by averaging the area occupied by bacterial microcolonies in infected cells. Bystander IL-8 production is measured by calculating the fraction of uninfected cells that contain IL-8 objects. To record the spread of proinflammatory signals, the fraction was calculated depending on the distance to infected cells (direct contact with infected cell, connected to infected cell by one uninfected cell,...). In this chapter, only cells directly neighboring infected cells are used to calculate the fraction of IL-8 producing cells (referred to as bystander IL-8 production).

To validate knockdown efficiency and quantification of the main readouts, control small interfering RNAs (siRNAs) were included into the screens. Non-targeting

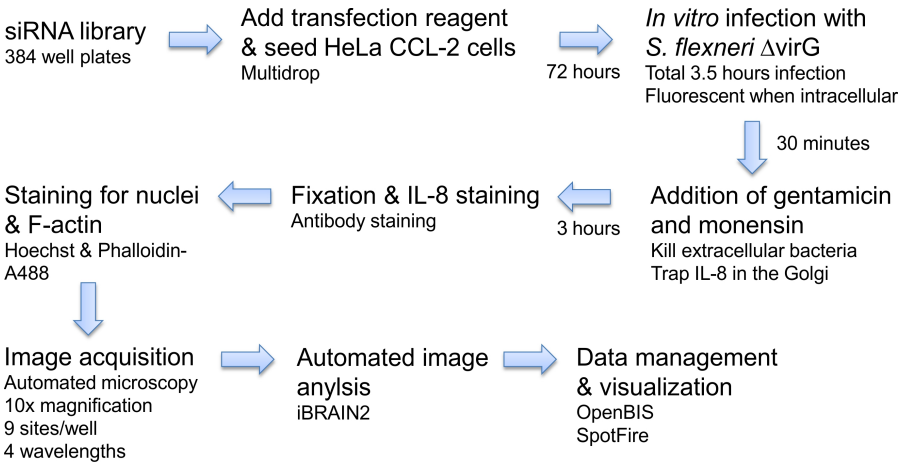


**Figure III.1 Assay setup for the high-content image-based RNAi screen.** The siRNA library from the supplier is diluted to the appropriate concentration and spotted into 384-well plates. Transfection reagent is aliquoted into each well using an automated dispenser. HeLa CCL-2 cells are seeded and incubated for 72 hours allowing the knockdown of the target gene. Cells are then infected with a non-motile strain of *S. flexneri* M90T carrying a plasmid coding for the fluorophore DsRed, which only gets expressed once the bacterium is intracellular. Plates are briefly centrifuged and subsequently incubated at 37°C. 30 minutes post infection, extracellular bacteria are killed by adding gentamicin. Furthermore, secretion is blocked by adding monensin allowing to trap IL-8 produced during infection. After a total infection time of 3.5 hours, cells are fixed and stained for DNA, F-actin and IL-8. An automated microscope acquires images for all wells at 4 different wavelengths. Afterwards, images are analyzed by specialized software and data is stored for browsing and visualization. Detailed protocols of the screening assay are presented in section 5 of this chapter.

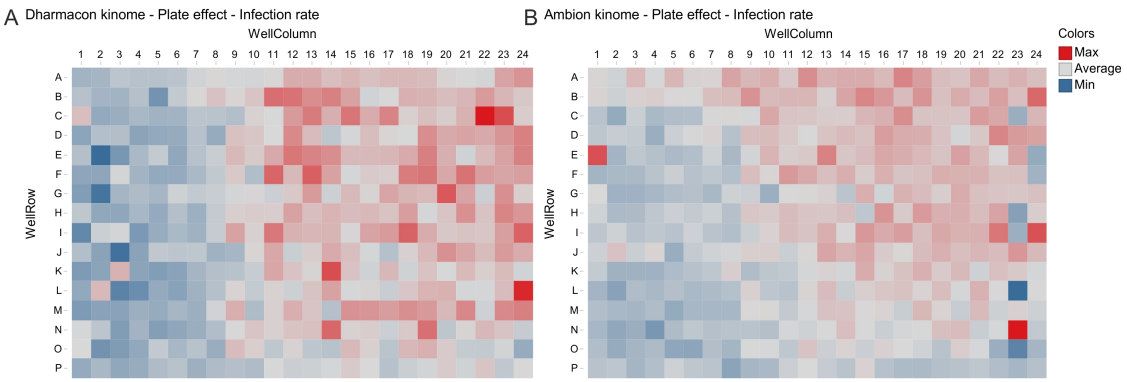


**Figure III.2 The infection rate is subject to plate effects.** (A) Results from the Dharmacon kinome library. The infection rate determined by automated image analysis was averaged over all plates from 4 independent replicates (12 plates in total). The resulting average infection rate is represented as a heat map with respect to the localization on the 384-well plate. (B) Results from the Ambion kinome library. The infection rate determined by automated image analysis was averaged over all plates from 2 independent replicates (12 plates in total). The resulting average infection rate is represented as a heat map with respect to the localization on the 384-well plate.

siRNAs and siRNAs targeting GFP were used as negative controls. Additionally, some wells did not receive any siRNA (mock treated wells). The transfection efficiency was validated by using siRNA against KIF11, which is known to result in cell death when depleted from cells[309]. Figure III.3 (panels A and C) illustrates the impact of a KIF11 knockdown on cell number. The negative control siRNAs only mildly affect cell number (except for the Ambion EGFP siRNA). Mock treated wells have consistently higher cell numbers. Noteworthy, several kinases included in the kinome libraries (Figure III.3, panel A and C, siRNA) lead to a similar decrease in cell number as a KIF11 knockdown. The strong reduction in cell number by KIF11 knockdown was stably reproduced in all assays, arguing for an efficient and reproducible transfection efficiency.

To validate the assay with a functional readout, siRNAs against genes, which have previously been associated with *Shigella* cell invasion, were included. As general control for all InfectX screens, siRNA against ARPC3, a subunit of the Arp2/3 complex, and CDC42, a small GTPase important for the control of cytoskeletal rearrangements, were chosen. In the Dharmacon kinome screen, we additionally included siRNAs against the catalytic subunit of phosphatidylinositol 4-kinase (PIK4CA) and ADP-ribosylation factor 1 (ARF1), for which we had previously observed a reduction in *Shigella* cell invasion (S. Weichsel, unpublished results). Figure III.3 (panels B and D) illustrates the effect of the different control siRNAs on infection rate quantified by automated image analysis. For siRNA from both suppliers, the ARPC3 knockdown results in a reduced infection rate. Similarly, CDC42 knockdown significantly decreases invasion. However, only two siRNA sequences from Ambion show a reduction, while the third one has the opposite effect. The reduction of invasion previously observed for an ARF1 knockdown could not be reproduced in this assay. PIK4CA knockdown even resulted in a moderate increase in infection rate. Eventually, these deviating observations result from the modified experimental conditions (e.g. different cell line and transfection reagent). Generally, the impact of positive controls on infection rate was not as strong as expected. To further investigate this finding, knockdown efficiency of the positive controls should be validated by western blotting. Noteworthy, the CDC42 knockdown as well significantly reduces microcolony size (Figure III.3 panel F, CDC42), which might indicate that the invasion process is delayed rather than inhibited. In fact, several siRNAs from the kinome libraries show much more pronounced changes in infection rate (Figure III.3, panel B and D, siRNA), indicating that the assay is capable of detecting knockdowns affecting *Shigella* cell invasion.

Knockdowns for MAP3K7 (TAK1), CHUK (IKK$\alpha$) and NOD1 were chosen as positive controls for bystander IL-8 production, as these proteins are involved in the signaling cascade downstream of Nod1-mediated pathogen recognition[76]. Depletion of MAP3K7 consistently reduced bystander IL-8 production (Figure III.3, panel E). Knockdown of CHUK did only result in a small decrease, while Nod1 knockdown even moderately increased bystander IL-8 production (Figure III.3, panel E). To pursue this observation, knockdown efficiency of the positive controls should be

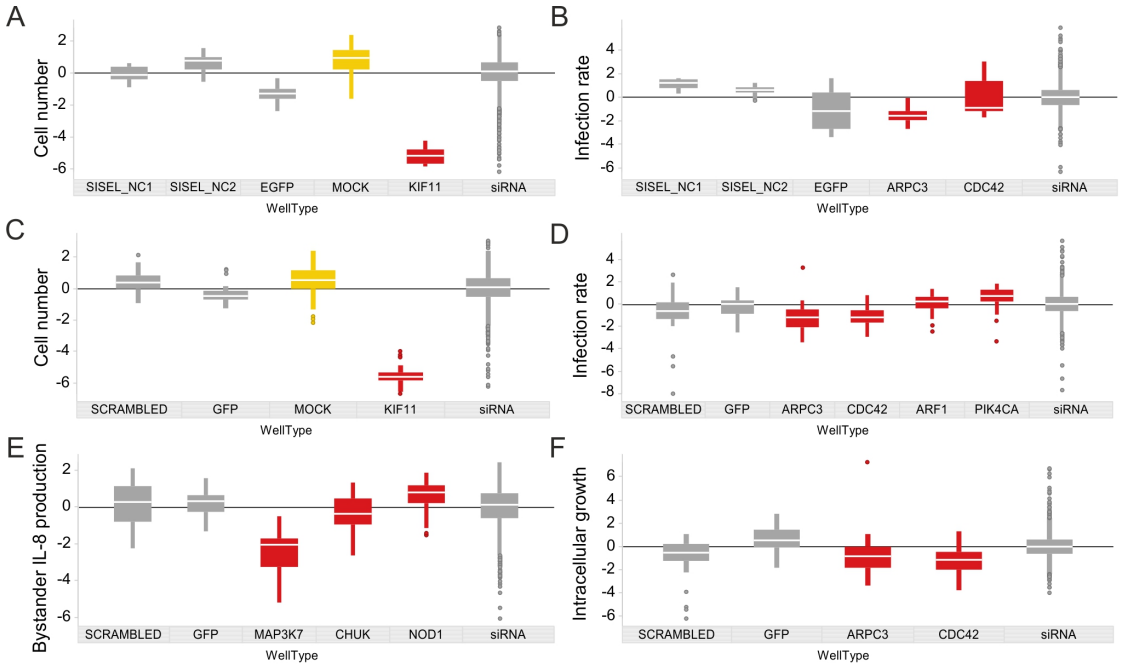


**Figure III.3 Effect of the different control siRNAs on the main readouts.** (A) Quantification of cell number using siRNA from Ambion. The effect of negative control siRNAs (SISEL NC1, SISEL NC2 and EGFP; grey) and the positive control KIF11 (red) on cell number are represented. As reference, results from mock treated cells (MOCK; yellow) and from the Ambion kinome library (siRNA; grey) are indicated. (B) Quantification of infection rate using siRNA from Ambion. The effect of negative control siRNAs (SISEL NC1, SISEL NC2 and EGFP; grey) and positive controls (ARPC3, CDC42; red) on infection rate are represented. As reference, results from the Ambion kinome library (siRNA; grey) are indicated. (C) Quantification of cell number using the siRNA from Dharmacon. The effect of negative control siRNAs (SCRAMBLED, GFP; grey) and positive control KIF11 (red) on cell number is represented. As reference, results from mock treated cells (MOCK; yellow) and from the Dharmacon kinome library (siRNA; grey) are illustrated. (D) Quantification of infection rate using siRNA from Dharmacon. The effect of negative control siRNAs (SCRAMBLED, GFP; grey) and positive controls (ARPC3, CDC42, ARF1, PIK4CA; red) on infection rate is represented. As reference, results from the Dharmacon kinome library (siRNA; grey) are depicted. (E) Quantification of bystander activation using siRNA from Dharmacon. The effect of negative control siRNAs (SCRAMBLED, GFP; grey) and positive controls (MAP3K7, CHUK, NOD1; red) on bystander activation is represented. As reference, results from the Dharmacon kinome library (siRNA; grey) are indicated. (F) Quantification of intracellular growth using siRNA from Dharmacon. The effect of negative control siRNAs (SCRAMBLED, GFP; grey) and positive controls (ARPC3, CDC42; red) on intracellular growth is represented. As reference, results from the Dharmacon kinome library (siRNA; grey) are indicated.

validated by western blotting. Noteworthy, transfection of siRNA against RELA (NF-$\kappa$B p65 subunit), which is included in the kinome library from Dharmacon, reduced bystander IL-8 production to the same extent as a MAP3K7 knockdown (data not shown).

Since literature does not provide target genes that could serve as positive control for intracellular growth, a direct validation of this measurement was not possible. On the other hand, knockdowns that partially reduce infection rate are likely to affect the microcolony size by delaying the entry process. Figure III.3 (panel F) reveals that this is indeed the case for the ARPC3 and CDC42 knockdowns. The correlation between infection rate and intracellular growth is a general observation, which is confirmed when analyzing the entire kinome data set (Figure III.4, panel E). While the effect of ARPC3 and CDC42 knockdown on intracellular growth might serve as an indirect validation of the measurement, it also points out the challenging discrimination between hits affecting cell invasion and intracellular growth.

A stable reproducibility of the main readouts between biological replicates is a central prerequisite for assays intended for usage in high-throughput screens. The kinome libraries were screened in duplicate (Ambion) and quadruplicate (Dharmacon) and all experiments were performed independently from each other. Therefore, the obtained datasets are ideal to verify the reproducibility of the main readouts. Table III.1 presents the correlation coefficients obtained for the two libraries. The correlation coefficients obtained for the Dharmacon library are generally lower than for the Ambion library, which might partially reflect that these experiments were performed over a longer time span. Among the major readouts, intracellular growth has the lowest reproducibility for both libraries. It seems possible that the quantification of bacterial replication by measuring microcolony size has the lowest accuracy. Therefore, alternative features (e.g. integrated intensity of the microcolony) should be considered for quantification of intracellular growth. In general, a correlation coefficient higher than 0.5 is adequate, but optimizations in the feature extraction and readout calculation (e.g. object classification) should allow to further improve the reproducibility.

**Table III.1 Correlation coefficients for the main readouts comparing replicates from the kinome library.**

| Readout | Dharmacon kinome[a] | Ambion kinome |
|---|---|---|
| Cell number | 0.67±0.07 | 0.79 |
| Infection rate | 0.50±0.03 | 0.78 |
| Intracellular growth | 0.50±0.03 | 0.54 |
| Bystander IL-8 production | 0.51±0.13 | 0.84 |

[a] Average of the 6 individual correlation coefficients.

## 4.3 Correlations between readouts introduce a bias in the generation of hit lists

A general procedure after feature extraction is the generation of hit lists by sorting the genes according to a certain readout. While this approach is feasible for basic features (e.g. cell number), it is problematic if the readout of interest correlates with additional features. In the case of the kinome screen, the infection rate negatively correlates with cell number (Figure III.4, panel A). Extracting top hits by sorting according to the infection rate, would enrich genes that positively or negatively affect cell number upon knockdown. Differences in cell number is a common phenomenon of RNAi experiments and therefore needs to be considered when generating hit lists. For the kinome data, the correlation between infection rate and cell number can be approximated with a linear regression curve (Figure III.4, panel A). Defining the corrected infection score as distance from the original infection rate to the regression curve represents a simple way to account for the bias introduced by variations in cell number.

Figure III.4 illustrates correlations for the main readouts of the *Shigella* infection assay. For instance, bystander activation strongly correlates with cell number (Figure III.4, panel B). This outcome is expected, regarding the fact that the propagation of inflammatory signals is cell-cell contact dependent[304]. Interestingly, no obvious correlation between bystander activation and infection rate can be detected (Figure III.4, panel C), indicating that the range of infection rate observed during the experiment (i.e. 20-70%) does not significantly alter the capacity for bystander activation.

The quantification of intracellular growth by microcolony size reveals correlations with cell number, infection rate and cell size (Figure III.4, panels D-F). The correlation with infection rate as well as cell size could be approximated by a linear regression curve. On the other hand, the correlation between colony size and cell number displays a non-linear behavior. A strong dependency is only observed at low cell numbers. A second order polynomial regression curve is proposed as a possible approximation of the correlation (Figure III.4, panel D). The correlation of colony size with several other features might partly explain the lower reproducibility observed for the readout of intracellular growth.

The correlations illustrated in Figure III.4 only represent a subset of possible dependencies. Nevertheless, they indicate that hit list generation based on single features can be misleading. Therefore, a thorough validation and correction of the readouts used to generate hit lists is required.

## 4.4 Comparison of results obtained by screening different kinome libraries

The validation of potential hits represents the main goal of screening the kinome with libraries from two different suppliers. It is therefore of interest to compare the two datasets. However, the comparison is complicated, as the Dharmacon library contains pooled siRNAs resulting in a single value per gene, while the Ambion library generates three values for a single gene as consequence of three individual siRNAs. As already mentioned for positive control CDC42, the three sequences targeting the same gene do not necessarily generate the same effect. Therefore, gene-wise comparison of the two libraries, using the average of the three individual sequences, results in a scarce correlation, even when comparing reproducible features like cell number. Validation is therefore only reasonable when comparing results for single genes and without averaging the values obtained from individual sequences.

As stated in the previous section, the ranking or comparison of single features is problematic because correlations with additional features can bias the outcome. Hence, Figure III.5 includes features, which can bias the readout of interest, into the visualization. The results obtained from screening the two kinome libraries for a selection of genes are compared. Data resulting from screening the Dharmacon library are indicated in blue and the outcome from the individual Ambion siRNAs are depicted in red.

The comparison of cell counts (Figure III.5, panel A) illustrates the different outcomes that can be obtained from the two libraries. For instance, the knockdown of PLK1 leads to a massive reduction in cell number for all data points acquired. Knockdown of WEE1 or AURKB results in a loss of cells when using the siRNA pool from Dharmacon, but only two out of three sequences from Ambion confirm this observation. Finally, the effect observed with one library might not be confirmed by the other, or possibly even opposite effects are measured.

Figure III.5, panel B compares the effect on the infection rate obtained for selected genes. As infection rate negatively correlates with cell number (Figure III.4, panel A), the marker size is used to visualize the corresponding cell count for every data point. Therefore, large and small markers representing siRNAs that affect cell number should be handled with caution. For example, the reduction in infection rate observed for a TGFBR2 or PRKR knockdown might possibly be an indirect result of the increased cell number. On the other hand, RPS6KA3, FRAP1 (mTOR) and TGFBR1 represent promising candidates that should be further validated in follow-up experiments.

Selected genes affecting bystander IL-8 production are presented in Figure III.5, panel C. The marker size represents the cell count measured for the corresponding data point, as bystander activation correlates with cell number. This indicates that the increase in bystander IL-8 production observed for SLK knockdowns possibly

represents an indirect result of increased cell number. TRIB3 and MASTL, on the other hand, exemplify genes that are worth to be further investigated.

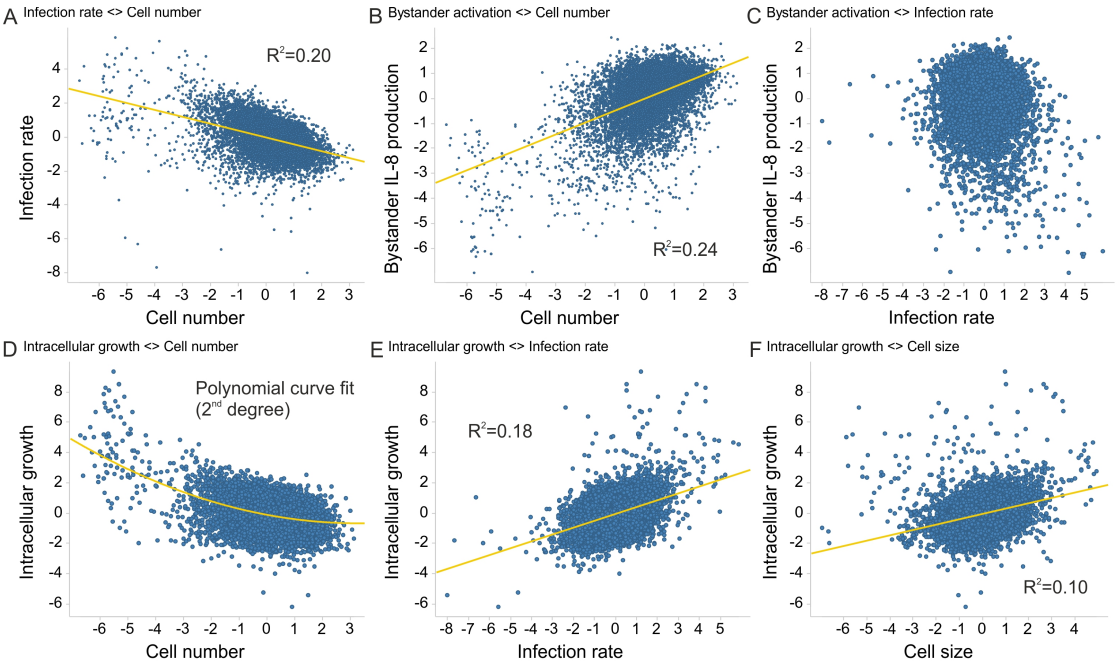


**Figure III.4 Correlation between selected readouts.** Data used for these plots is aggregated from both kinome screens. (A) Correlation between infection rate and cell number. The infection rate negatively correlates with the cell number. A linear fit is indicated in yellow. (B) Correlation between bystander activation and cell number. Bystander activation positively correlates with cell number. A linear fit is indicated in yellow. (C) Correlation between bystander activation and infection rate. No correlation between the two features is observed. (D) Correlation between intracellular growth and cell number. The majority of the population (population mean ± 3) shows little correlation with cell number. At low cell numbers intracellular growth is increased. A 2$^{nd}$ order polynomial fit is indicated in yellow. (E) Correlation between intracellular growth and infection rate. Intracellular growth positively correlates with infection rate. A linear fit is indicated in yellow. (F) Correlation between intracellular growth and cell size. Intracellular growth positively correlated with cell size. A linear fit is indicated in yellow. For all linear fits the corresponding $R^2$ value is indicated.

**Figure III.5 *(following page)* Comparison of selected genes from the Dharmacon and Ambion library.** (A-D) Blue markers represent the results obtained from screening the Dharmacon kinome library in quadruplicate. Red markers represent the results obtained from screening the Ambion library in duplicate. Each data point corresponds to the siRNA pool (Dharmacon) or to an individual siRNA sequence (Ambion) of one replicate. (A) Effect of selected knockdowns on cell number. (B) Effect of selected knockdowns on infection rate. The measured cell number for every data point is visualized by the marker size. Large and small markers indicate increased cell number and reduced cell number, respectively. (C) Effect of selected knockdowns on bystander activation. The measured cell number for every data point is visualized by the marker size. Large and small markers indicate increased cell number and reduced cell number, respectively. (D) Effect of selected knockdowns on intracellular growth. The measured infection rate of every data point is visualized by the marker size. Large and small markers indicate increased infection rate and reduced infection rate, respectively.

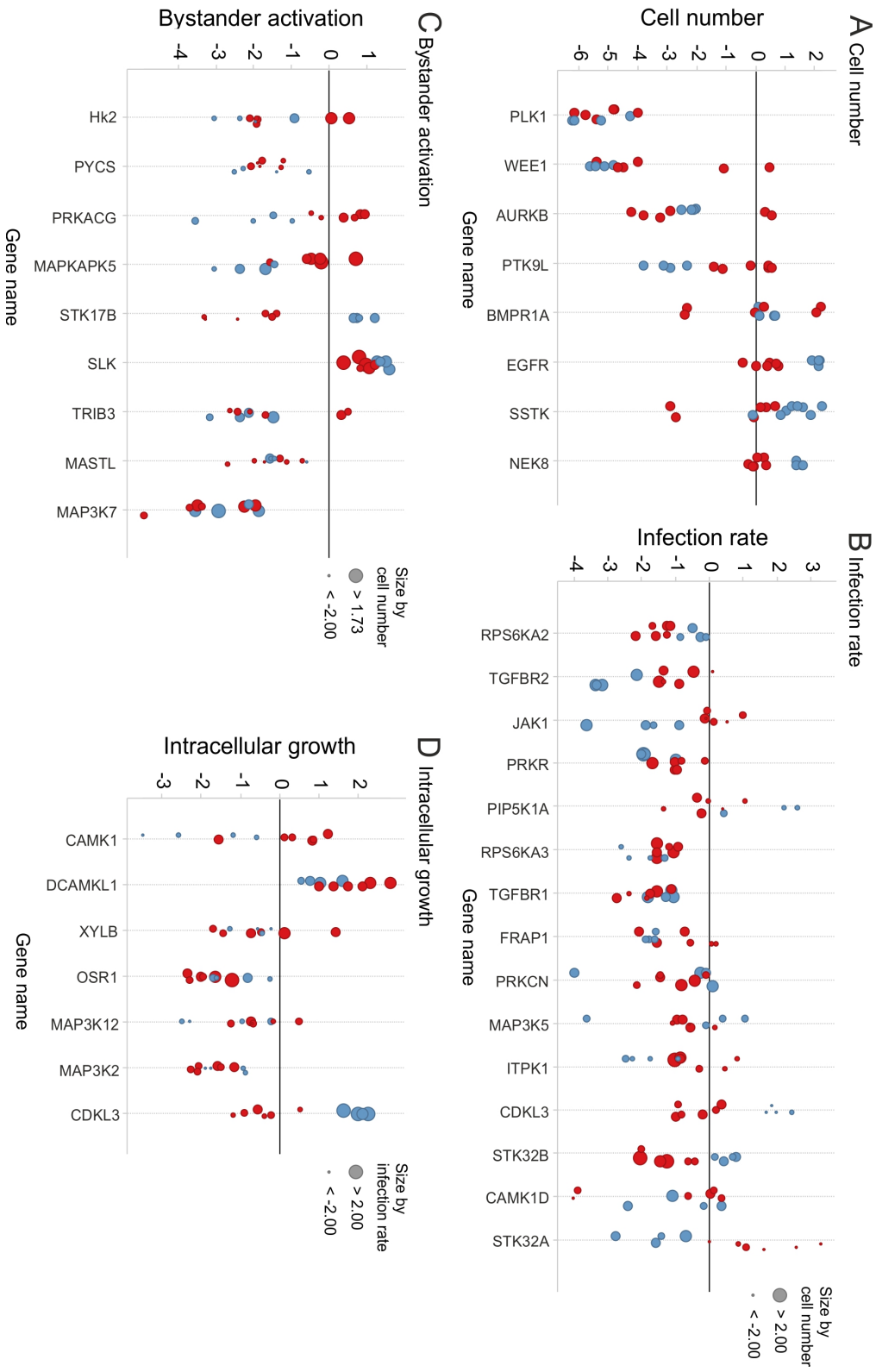
A Cell number
Cell number
Gene name
PLK1
WEE1
AURKB
PTK9L
BMPR1A
EGFR
SSTK
NEK8
B Infection rate
Infection rate
Gene name
RPS6KA2
TGFBR2
JAK1
PRKR
PIP5K1A
RPS6KA3
TGFBR1
FRAP1
PRKCN
MAP3K5
ITPK1
CDKL3
STK32B
CAMK1D
STK32A
Size by cell number
> 2.00
< -2.00
C Bystander activation
Bystander activation
Gene name
Hk2
PYCS
PRKACG
MAPKAPK5
STK17B
SLK
TRIB3
MASTL
MAP3K7
Size by cell number
> 1.73
< -2.00
D Intracellular growth
Intracellular growth
Gene name
CAMK1
DCAMKL1
XYLB
OSR1
MAP3K12
MAP3K2
CDKL3
Size by infection rate
> 2.00
< -2.00

Figure III.5, panel D summarizes the results obtained on intracellular growth for selected genes. As mentioned in the previous section, microcolony size is correlating with additional features among which the infection rate had the strongest influence. Consequently, the size of the marker is representative of the infection rate determined for the corresponding data point. Knockdowns for DCAMKL1, OSR1 and MAP3K2 are confirmed by both libraries and are potential candidates for additional experiments.

# 5 Experimental Procedures

### Cell Culture

HeLa CCL-2 ATCC cells were maintained at 37° and 5% $CO_2$ in Dulbecco's modified Eagle's medium (DMEM; Sigma-Aldrich) supplemented with 10% heat-killed FCS and 2mM L-Glutamine (Invitrogen). For all HTS protocols, cells were used at passages seven to nine.

### siRNA and transfection

RNA interference directed against cellular kinases was achieved using siRNA pools of four sequences (ON-TARGET*plus*® SMARTpool® siRNA Library - Human Protein Kinase, Dharmacon) or three individual sequences per gene (Silencer® Select Human Kinase siRNA Library, Ambion). Kinome screens were performed at least in duplicate for each library. All experiments were conducted in a 384-well plate format. In addition to assay plates, control plates were included when screening the library from Dharmacon. These plates contained control siRNAs for transfection efficiency and cell toxicity, as well as, control siRNAs for *Shigella* invasion and IL-8 production. Assay plates included controls for transfection efficiency, cell toxicity and *Shigella* invasion.

For each plate, 25$\mu$l of RNAiMAX (Invitrogen) in DMEM (0.1$\mu$l/24.9$\mu$l) mixture was added to each well of the assay plates containing 1.6 picomoles siRNA diluted in siRNA buffer (Thermo Scientific). Assay plates were then incubated at room temperature for 1 hour. Following the incubation, 600 HeLa CCL-2 cells were added per well in a volume of 50$\mu$l DMEM/16%FCS, resulting in a final FCS concentration of 10%. Afterwards, plates were incubated at 37°C and 5% $CO_2$ for 72 hours prior to infection.

### Bacterial strains

The non-motile *S. flexneri* strain M90T $\Delta virG$ was generously provided by P. Sansonetti[248]. The strain was transfected with the plasmid pCK100, which expresses DsRed under the control of the native promoter of the *S. flexneri* gene *uhpT*. Briefly, the 251bp promoter region upstream of *uhpT* was amplified by PCR (Primers: GAGAGAGAATGCAGTGCTCGATACCTGGCACT, GCTCTAGAGGGTTACTCCTGAAATGAATACCT) and ligated into pMW211 plasmid using BsmI and XbaI. The pMW211 plasmid was a generous gift from Dr. D. Bumann (Biozentrum, University of Basel, Switzerland). Bacteria were grown in tryptic soy broth (TSB; Fluka) containing 100 $\mu$g/ml ampicillin (Invitrogen). Aliquots of bac-

terial culture in TSB/7%DMSO were stored at -80°C and subcultured in 2ml TSB on the day of use.

### Infection assay

*S. flexneri* M90T Δ*virG* pCK100 were harvested in exponential growth phase and coated with 0.005‰poly-L-lysine (Sigma-Aldrich). Afterwards, bacteria were washed with PBS and resuspended in assay medium (DMEM, 2mM L-Glutamine, 10mM HEPES). 20$\mu$l of bacterial suspension was added to each well with a final multiplicity of infection (MOI) of 15. Plates were then centrifuged for 1 minute at 37°C and 13'000 rpm and incubated at 37°C and 5%$CO_2$ on aluminium plates. After 30 minutes of infection, 75$\mu$l were aspirated from each well and monensin and gentamicin were added to a final concentration of 66.7$\mu$M and 66.7 $\mu$g/ml, respectively. After a total infection time of 3.5 hours, cells were fixed in 4% PFA for 10 minutes. Liquid handling was performed using the Multidrop 384 (Thermo Scientific) for dispension steps and the ELx50 Microplate Strip Washer (BioTek) for aspiration steps.

### Immunofluorescence

Cells were washed with PBS using the Power Washer 384 (Tecan). Subsequently, cells were incubated with a mouse anti-human IL-8 antibody (1:300; BD Biosciences) in staining solution (0.2% saponin in PBS) for 2 hours at room temperature. After washing the cells with PBS, Hoechst (1:2000; Invitrogen), DY-495-Phalloidin (1:250; Dyomics) and Alexa Fluor 647-coupled goat anti-mouse IgG (1:400; Invitrogen) were added and incubated for 1 hour at room temperature. After two washes with PBS, plates were sealed prior to imaging on automated microscopes. The staining procedure was performed using the Biomek NXP Laboratory Automation Workstation (Beckman Coulter).

### Automated microscopy and image processing

Images were automatically acquired with an ImageXpress Micro (Molecular Devices). Per well, 4 wavelengths (360nm, 480nm, 594nm and 640nm) at 9 different sites were imaged with a CFI Super Fluor 10x objective (Nikon). Image processing and analysis was supported by the workflow processing manager iBRAIN2, which was developed by Research IT (Biozentrum, University of Basel; Podvinec et al., manuscript in preparation). iBRAIN2 computes image quality control, shading correction, image analysis and result summaries by parallel processing on a Linux Beowulf-Cluster.

### Image analysis

Image analysis was performed with the open source software CellProfiler[308] that was extended by custom modules implemented in MATLAB (Mathworks) by M. Emmenlauer (Biozentrum, University of Basel). Briefly, the analysis pipeline identifies cell nuclei, the cell body, bacterial microcolonies and IL-8 granules within the corresponding images using object detection algorithms[308]. Additionally, the region around the nucleus is defined as an additional object (perinucleus). Features including intensity, texture, area and shape are extracted for every object. Detected bacterial microcolonies and IL-8 granules are assigned to the cell that contains them based on the cell segmentation. Subsequently, per well averages are calculated for the infection rate, the average bacterial area per infected cell (intracellular growth) and the fraction of uninfected cells producing IL-8 among cells directly neighboring infected cells (bystander IL-8 production).

### Data management, normalization and visualization

All data generated during image acquisition, image processing and image analysis were stored in the data management system openBIS, which was developed by the group of Dr. B. Rinn (CISD, ETH Zurich)[310]. All features obtained from image analysis were normalized by subtracting the plate mean and dividing by the standard deviation of the plate (Z score). For the calculation of the plate mean and standard deviation only wells containing siRNA were considered. Z scoring and result summaries were implemented by P. Rämö (Biozentrum, University of Basel). Data was visualized using the program Spotfire (TIBCO software Inc.). If not stated differently, all feature measurements represent Z scored values.

# 6 Discussion and Outlook

In this chapter, the implementation of an *S. flexneri in vitro* infection assay suited for image-based RNAi screens was described. The assay allows quantifying infection rate, bacterial intracellular replication and bystander IL-8 production by means of automated microscopy and image analysis. The experimental workflow was validated by performing siRNA knockdowns against genes known to affect cell number, *Shigella* cell invasion or bystander activation. Based on the results obtained from these control knockdowns, it was concluded that the assay is able to detect phenotypes for cell invasion, bystander activation and probably intracellular growth.

The reproducibility of the assay and of the major readouts was quantified by comparing biological replicates obtained from screening two kinome libraries from different suppliers. In general, correlations among replicates were in the range of 0.5-0.8 depending on the library and the selected readout. The lowest correlation was calculated for the quantification of intracellular growth, which is mainly based on the microcolony size. Alternative features for quantifying intracellular growth should therefore be considered. A more precise quantification is expected when measuring integrated intensities of all microcolonies within a cell. The integrated intensity should reflect the number of bacteria contained within each colony. Currently, additional scripts are implemented to calculate these values.

Sources of noise are the so-called plate effects, which were observed when quantifying the infection rate. Temperature differences introduced during centrifugation of the plates led to a gradual increase in infection rate from the left to the right edge of each plate. The differences were reduced by adapting experimental procedures, nonetheless the gradient is still present. Remarkably, the observed pattern is similar on every plate. Fitting a polynomial curve to the smoothened pattern might allow to computationally correct for the temperature-induced plate effect.

Scatter plots of different features reveal correlation between certain readouts (e.g. infection rate and cell number). This correlation can strongly bias the results when only considering a single readout. Often, these correlations follow a linear behavior. Fitting the data with a linear regression curve might therefore allow to normalize the readout. Scripts, which can correct for these effects, are currently under development. Furthermore, Snijder et al.[311] have reported that the local population context of every cell can affect the measured readouts. Indeed, our preliminary results indicate that *Shigella* preferentially infects cells at the edges of cell layers. Therefore, population-context correction has to be included in the future image analysis workflow.

Additionally, a program allowing cell classification based on supervised machine learning (called CellClassifier) is currently being established[312]. The classifier enables to train models, which can discriminate between different classes of cells (e.g. infected and uninfected cells or IL-8 positive or negative cells). Furthermore, the

program automatically calculates combinations of several models. This will, for instance, allow to quantify the number of infected cells producing IL-8. The results obtained from cell classification are expected to be more precise than the readouts calculated from individual features.

After successfully screening the kinome libraries, the infection assay was performed in duplicate on a genome-wide library (Dharmacon, pooled siRNA). Experiments and image acquisition have been completed and the data from image analysis should soon be available. Expectedly, that the genome-wide screen will bring forth new candidate proteins involved in *Shigella* cell invasion, intracellular growth and bystander IL-8 production. Promising genes will be validated in a secondary screen using individual siRNAs from Ambion.

In conclusion, the implementation of an image-based high-throughput screen allowing the quantification of *S. flexneri* cell invasion and intracellular growth, as well as bystander IL-8 production has been presented. The assay was validated by performing control knockdowns and by quantifying reproducibility using two kinome libraries. Preliminary results have indicated a few promising candidates for the different readouts. However, the data generated so far requires visual validation and normalization of plate effects and feature correlations.

# Chapter IV

# Discussion and Outlook

# 1 Discussion

The ability of a host organism to mount an immune response during infection is critical for survival. Epithelial cells represent a first line of defense by forming an impermeable cell layer that prevents microbial access to the underlying tissue. Besides this function, epithelial cells serve as important sentinels for microbial infections. By expressing pathogen recognition receptors (PRRs), epithelial cells can recognize bacterial products and respond by secreting proinflammatory cytokines. These cytokines induce an inflammatory response by attracting phagocytic cells to the site of infection.

A massive inflammatory response is, for instance, observed during infection with the enteroinvasive bacterium *Shigella flexneri*. The Gram-negative pathogen infects the colonic epithelium in humans and replicates within intestinal epithelial cells. The presence of intracellular *Shigella* is sensed by the PRR Nod1[44], which contributes to the activation of proinflammatory signaling cascades. In our study, we used an *in vitro* model for *Shigella* infection and visualized the activation of proinflammatory signals at the single-cell level. Infections at low MOI revealed that the activation of the transcription factor NF-$\kappa$B was not restricted to infected cells, but could as well be observed in uninfected neighboring cells. Using phospho-specific antibodies we could additionally show that the MAP kinases JNK, ERK and p38 get activated in uninfected cells adjacent to infected cells. Our results indicate that infected cells, within minutes after infection, propagate proinflammatory signals to uninfected bystander cells.

The concept of bystander cell activation has previously been described in other contexts. For instance in wound healing, $Ca^{2+}$ and ATP get released and activate distant cells, thereby promoting cell migration towards the injured tissue[313,314]. In radiotherapy of tumors, bystander effects represent a major problem, as irradiated cells secrete cytokines and propagate signals through gap junctions that induce DNA damage in non-irradiated cells[315]. Moreover, Patel and colleagues recently reported the expression of interferon-$\beta$ and TNF$\alpha$ in bystander cells upon recognition of double-stranded DNA[316]. All these cases have in common that a local aggression induces cell-cell communication, which amplifies the host response. Our findings provide evidence that a similar mechanism is observed during bacterial infection.

Remarkably, we found that the activation of the MAP kinase p38 is enhanced in bystander cells. This is in line with a previous report that *Shigella* efficiently dephosphorylates p38 via the phosphothreonine-lyase activity of the effector protein OspF[125]. In fact, p38 phosphorylation in infected cells was restored upon infection with an *ospF* deletion strain in our study. This was confirmed by demonstrating that histone H3, a downstream target of p38, is predominantly phosphorylated in bystander cells during *S. flexneri* wild type infection. Again, histone H3 phosphorylation could be restored in infected cells when infecting with the $\Delta$*ospF* strain.

Noteworthy, no differences in the level of p38 and histone H3 phosphorylation in bystander cells could be observed when comparing *S. flexneri* wild type and $\Delta ospF$ infections. This finding indicates that bystander activation might represent a mechanism to evade the immunosuppressive activity of bacterial effectors.

Histone H3 controls accessibility to transcription factor binding sites of proinflammatory genes by modulating chromatin structure[28]. To assess the expression level of proinflammatory genes, we focused on the cytokine IL-8, which is strongly upregulated during *S. flexneri* infection[119]. By means of immunofluorescence, we found that the major source of IL-8 production are uninfected bystander cells. Infected cells, on the other hand, were inefficiently producing IL-8, which was confirmed for the expression of TNF$\alpha$ and GM-CSF, two other cytokines upregulated during *S. flexneri* infection[119]. IL-8 expression in infected cells increased upon infection with the *S. flexneri* $\Delta ospF$ strain, suggesting that OspF downregulates the expression of cytokines. However, the gain in IL-8 production was very limited, indicating that additional effectors such OspG, OspB or $IpaH_{9.8}$ might contribute to the immunosuppressive activity of *Shigella*. Propagation of proinflammatory signals from infected to uninfected cells thus allows the host to circumvent the immunosuppressive activity of bacterial effectors and to massively amplify the total amount of cytokines produced.

Intracellular *Shigella* are recognized by Nod1, which detects peptidoglycan fragments [44]. To address the role of peptidoglycan recognition in bystander activation, we microinjected $\gamma$-D-glutamyl-meso-diaminopimelic acid (iE-DAP), a Nod1 ligand, into single cells. Surprisingly, we found the injection of iE-DAP to efficiently induce IL-8 expression in bystander cells of microinjected cells. This demonstrates that Nod1-mediated recognition of peptidoglycan moieties is sufficient to activate the signaling cascade underlying bystander activation. We have further investigated the role of Nod1 in bystander activation by performing infections in cells depleted for Nod1 by RNAi. In preliminary experiments, only a slight reduction in the number of bystander cells was observed, when Nod1 was depleted (unpublished results). Although these experiments require validation, it seems likely that Nod1 is sufficient, yet not necessary, for inducing bystander activation. This outcome indicates that additional PRRs, such as Nod2 or other Nod-like receptors, might contribute to the activation of bystander cells.

In this work, the molecular mechanism that underlies bystander activation was addressed as well. Cell-cell communication is a concept abundantly found in nature and can essentially be mediated by three different mechanisms: paracrine signaling, direct diffusion of small molecules through gap junctions or membrane protein interactions. Bystander IL-8 production was not affected when we interfered with paracrine secretion by brefeldin A treatment or perfusion, pointing out that bystander activation was not mediated by secretion of signaling molecules. Instead, bystander activation was strictly dependent on cell-cell contact. The hypothesis of signaling through gap junctions was therefore tested by treating cells with gap

junction inhibitors. Treatment with 18$\beta$-glycyrrhetinic acid and carbenoxolone, two different gap junction inhibitors, resulted in a dose-dependent inhibition of bystander IL-8 production. Additionally, cells poorly coupled by gap junctions displayed a limited number of IL-8-producing bystander cells, which could be significantly increased when overexpressing Connexin43 (Cx43) in these cells. Finally, the expression of Cx43 was required in both infected and bystander cells to allow an efficient propagation of inflammatory signals.

Gap junctions consist of two hemichannels located in the membrane of neighboring cells. Hemichannels are formed by a hexamer of connexin proteins. Interaction between two hemichannels located in adjacent membranes results in a continuous channel connecting the cytoplasm of two cells. Gap junctions therefore allow direct intercellular diffusion of small molecules (i.e. <1-2 kDa), including ions, second messengers, nucleotides, amino acids and metabolites[317]. Consequently, the mediator of the cell-cell communication underlying bystander activation is expected to be found among these molecules. Calcium, for instance, has already been associated with *Shigella* infections. Tran Van Nhieu and colleagues reported transient peaks in intracellular calcium concentrations during cell invasion[318]. To visualize changes in intracellular calcium concentrations, we performed live cell microscopy of *S. flexneri* infection in A549 cells loaded with the calcium dye Fluo-4. In fact, transient peaks in calcium concentrations that coincided with invasion events could be observed. Moreover, the increase in calcium concentration propagated from the infected cells to adjacent cells (unpublished results). However, treating cells with the intracellular calcium chelator BAPTA-AM did not interfere with NF-$\kappa$B activation in bystander cells, indicating that calcium is not mediating the propagation of NF-$\kappa$B activation. Nevertheless, calcium might potentially induce other pathways in bystander cells. For instance the activation of ERK, which followed a transient kinetic and preceded the activation of NF-$\kappa$B, JNK and p38. Further studies are required to understand the nature of these calcium waves – i.e. direct $Ca^{2+}$ diffusion, diffusion of $IP_3$ or release of ATP – and their potential role in bystander activation.

Besides calcium, other second messengers could diffuse through gap junctions. A screen for small metabolites and nucleotides using high resolution mass spectrometry [319] has revealed an increase in cAMP and cGMP concentrations early during *S. flexneri* infection (T. Tschon, unpublished results). cAMP might be produced in infected cells by adenylate cyclases and control NF-$\kappa$B and MAP kinase signaling in bystander cells through the activation of PKA[320,321]. Alternatively, cGMP, produced by guanylate cyclases in infected cells, may contribute to signaling in bystander cells by activating PKG. Finally, peptidoglycan fragments (e.g. iE-DAP) shed on the bacterial surface are small enough to passage through gap junctions. One might speculate that these moieties could activate Nod1 signaling in bystander cells. Further experiments are required to evaluate the different hypotheses.

Of equal interest to the nature of the diffusing mediator is the mechanism, by

which the signal is propagated. Several models come in to question, which all have in common that the mediator is initially produced or released in the infected cell and diffuses to neighboring cells through gap junctions. In the simplest scenario, the infected cell is the sole source for the mediator and the signal is propagated by passive diffusion. This would result in a concentration gradient in the vicinity of infected cells. Assuming an activation threshold (i.e. minimal mediator concentration) for signaling in bystander cells, the signal propagation would be self-limiting. The condition of infected cells representing the sole source for the mediator is met if the molecule would originate from bacterial peptidoglycan. Alternatively, the signal propagation could be amplified by the production of additional mediator molecules in bystander cells. This positive feedback mechanism would allow a more rapid signal propagation and increased spread. On the other hand, amplification of the mediator results in a signal propagation that is no longer self-limiting. This implies the existence of additional control mechanisms that negatively regulate bystander activation, as excessive inflammation is detrimental for the host. Several parameters could assure a negative regulation, including rapid turnover of the mediator or modification of gap junction permeability. Noteworthy, the second messengers calcium, cAMP and cGMP, as well as the MAP kinase ERK are all able to regulate gap junctional permeability through the phosphorylation of connexin proteins[317,322–326]. Furthermore, it seems plausible that more than one signal might be propagated from infected to bystander cells. One mediator might contribute to the activation of proinflammatory signals, while a second signal limits the inflammation to a confined area around the infected cell. Hitherto, no experimental data is available to identify the mechanism that is underlying bystander activation.

Cell-cell communication through gap junctions represents a reoccurring principle in many biological processes like cell growth, differentiation, migration and electric coupling[327]. Consequently, gap junction deficiencies are associated with several diseases including cataracts, hereditary deafness, neuropathies and cancer[327]. In addition, it has become increasingly clear that gap junctions are involved in processes of the immune system. Neijssen and colleagues, for instance, have demonstrated that small peptides can be transferred to neighboring cells through gap junctions. This is of particular interest in the context of antigen presentation during viral infections, as it allows infected cells to transfer viral peptides to specialized antigen-presenting cells[328,329]. Furthermore, gap junctional communication between dendritic cells is required for their activation[330]. The secretion of the chemokine CXCL12 by human bone marrow stromal cells was recently shown to be controlled by calcium transmission through gap junctions and by the activation of PKA[331]. Moreover, gap junctions were proven to play a crucial role in drug-induced liver injury (DILI), an inflammatory response to certain therapeutic compounds that can cause hepatic failure. Inhibition of gap junctional communication in mice limited DILI and prevented hepatic failure[332]. The importance of gap junctions during inflammation is further highlighted by the fact that many microbial pathogens target gap junctions by modulating connexin expression or phosphorylation[333,334]. In fact, *Shigella*

opens connexin hemichannels allowing release of ATP into the extracellular space. This process enhances *Shigella* invasion and intercellular spread[318]. It is worth to note that ATP release is not involved in bystander activation, as neither treatment with apyrase or suramin, nor addition of extracellular ATP did affect the number of bystander cells (unpublished results).

To validate whether bystander activation is a specific response to *S. flexneri* infection or represents a more general mechanism, we performed infections with *S. typhimurium* and *L. monocytogenes*, two enteroinvasive pathogens that are known to induce IL-8 expression during infection of epithelial cells[335]. Indeed, IL-8 production in bystander cells during infections with these bacteria could be observed, although the frequency was lower when compared to *S. flexneri* infections. Differences between the pathogens might explain this finding. Intracellular *S. typhimurium*, for example, reside within a membrane-enclosed compartment, which might interfere with efficient pathogen recognition. *L. monocytogenes*, on the other hand, is a Gram-positive bacterium that might activate different pathogen recognition receptors than Gram-negative bacteria. A recent study by Dolowschiak at al., has pointed out that cell-cell communication observed during *Listeria* infection of murine intestinal epithelial cells is independent of gap junctions, but is instead mediated by the production of reactive oxygen intermediates (ROIs)[336]. In their work, it was proposed that intracellular *Listeria* get detected by Nod-like receptors (i.e. *Nod2* and *Nlrc4*), which contribute to the production of ROIs by activating the NADPH oxidase *Nox4*. The release of ROIs by infected cells induces the expression of *Cxcl-2* (the mouse homolog of human IL-8) and *Cxcl-5* in uninfected bystander cells, through an unknown mechanism[336]. The differences observed for *S. flexneri* and *L. monocytogenes* infections could indicate that different pathogens induce alternative pathways to promote bystander activation. In addition, the two studies were performed in distinct cell types (human A549 versus murine m-$IC_{cl2}$ cells). Parallel infections with *S. flexneri* and *L. monocytogenes*, using the same cell type, are required to properly determine the signaling pathways controlling inflammation during invasion.

In summary, we have identified a mechanism of cell-cell communication that allows infected cells to propagate proinflammatory signals to uninfected neighboring cells. These bystander cells contribute to a substantial amplification of the immune response during bacterial infections by producing cytokines like IL-8. In addition, bystander activation assures an inflammatory response in the presence of immunosuppressive effector proteins in infected cells. Infections at low MOI might reflect the early onset of shigellosis, when only a limited number of bacteria have reached the basolateral surface of enterocytes. Indeed, experiments using the rabbit intestinal loop model of shigellosis, revealed IL-8 production beyond sites of infection, providing evidence for the physiological relevance of bystander IL-8 production *in vivo*[123].

# 2 Outlook

Future work will focus on the characterization of the molecular mechanism underlying bystander activation. In this context, the identification of the small molecule(s) diffusing through gap junctions is of particular interest. Potential candidates, including second messengers and peptidoglycan moieties, should be addressed. The involvement of cAMP and cGMP, for example, could be validated by measuring their concentrations during *Shigella* infection. As bystander NF-$\kappa$B activation can be observed as early as 15 minutes post infection, an increase in concentration would be expected within minutes after invasion. In addition, adenylate or guanylate cyclases, as well as PKA and PKG could be targeted using RNAi or pharmacological tools. To further investigate the role of calcium in bystander activation, phosphorylation of MAP kinases p38, JNK and ERK, as well as IL-8 expression should be measured in cells pretreated with the intracellular calcium chelator BAPTA-AM. Increased calcium concentrations can also result from signaling by the second messenger inositol-trisphosphate ($IP_3$). $IP_3$ is able to diffuse through gap junctions and could induce calcium release from the ER in bystander cells by binding to the $IP_3$ receptor[337]. To validate an involvement of $IP_3$, calcium responses, bystander NF-$\kappa$B and MAP kinase activation should be monitored, while treating cells with an inhibitor for phospholipase C[338].

As an alternative to second messengers, peptidoglycan moieties could be diffusing through gap junctions and activate Nod1 signaling in bystander cells. Fluorescently labeled molecules of the Nod1 ligand iE-DAP could be microinjected into cells and their diffusion monitored over time. If iE-DAP does indeed diffuse to neighboring cells, the activation of NF-$\kappa$B in these cells should be visualized. However, it is questionable whether this experiment is representative for the physiological condition, as microinjection is likely to inject an excess of iE-DAP into cells. Therefore, it might be more promising to test the requirement for the receptor Nod1 in bystander cells. If iE-DAP diffuses through gap junctions, Nod1 is expected to be indispensable for the initiation of proinflammatory signaling in bystander cells. Knockdown of Nod1 or overexpression of a dominant negative form of the receptor (lacking the CARD domain) specifically in bystander cells and monitoring IL-8 expression should verify this hypothesis.

A more systematic approach to identify the small molecule(s) mediating bystander activation makes use of high resolution mass spectrometry as described by Kiefer et al.[319]. This technique allows to measure the concentration of metabolites in the femtomole range. The emphasis will be placed on metabolites and nucleotides that get produced within minutes after *Shigella* infection. Promising candidates could be tested in the *in vitro* infection model using RNAi or pharmacological tools and measuring bystander IL-8 production.

Besides the nature of the diffusing signal, further studies should focus on the proteins and signaling pathways involved in the cell-cell communication. The image-

based genome-wide RNAi screen described in Chapter III is expected to identify new proteins involved in bystander activation. In addition, the phosphoproteome of *Shigella* infected cells might identify signaling pathways required for bystander activation. Comparing the phosphoproteome of cells infected at low MOI in the presence or absence of gap junction inhibitors might reveal proteins that get specifically phosphorylated in bystander cells. A similar dataset could be obtained by isolating infected and uninfected cell populations using a fluorescence-activated cell sorter prior to mass spectrometric analysis. Promising candidates should be validated by siRNA knockdown either in infected or bystander cells. Preliminary results from experiments with mixed wild type and knockdown cell populations have revealed that depletion of TAK1 and the NF-$\kappa$B subunit p65 in infected cells does not interfere with bystander IL-8 production (T. Tschon, unpublished results). This finding indicates that the signaling cascade mediating bystander activation is triggered upstream of TAK1. Future experiments with mixed cell populations will therefore focus on proteins upstream of TAK1, including Nod1/2, RIP2 and cIAP1/2.

Monitoring the propagation of proinflammatory signals using live cell microscopy would allow to quantify the kinetics and dynamics of bystander activation. Live *S. flexneri* infections were already performed with a cell line expressing endogenous levels of ERK-YFP[339]. Preliminary results revealed the propagation of ERK activation to direct neighbors of infected cells. Stable overexpression of Connexin43 in these cells might increase the spread of ERK activation and allow the quantification of bystander activation kinetics. Live cell experiments with cells stably expressing the NF-$\kappa$B subunit p65 tagged to GFP represent another option[340]. The precise quantification of bystander activation kinetics may allow to determine the underlying mechanism of signal propagation. As already mentioned in the previous section, the signal could be propagated by passive diffusion of a mediator exclusively produced in infected cells. Alternatively, the signal could be amplified by the production of the mediator molecule in bystander cells, which would imply an additional control mechanism that spatially limits the inflammation signaling. Finally, it seems plausible that more than one signaling molecule is propagated from infected to bystander cells. For the diffusion of small molecules through gap junctions within a monolayer of cells, several mathematical models have been deduced and extended[341–343]. Making use of these mathematical models, one could predict the propagation of signaling molecules for the proposed mechanisms and validate the results by comparison with the experimental data obtained from live cell microscopy. This would be of particular interest upon perturbation of the system, for example by treating cells with gap junction inhibitors.

Future work should also address the differences in bystander activation reported for *L. monocytogenes*, *S. typhimurium* and *S. flexneri* infections[304,336]. Parallel infections using both human and murine epithelial cells lines, might reveal whether alternative routes for bystander activation exist in response to different pathogens. In this context, the two proposed mechanisms, production of ROIs and signal-

ing through gap junctions, should be addressed by treating cells with respective inhibitors or by siRNA knockdowns. The reduced frequency of bystander activation observed in *S. typhimurium* infections could be investigated by using a strain expressing the *Shigella* translocator protein IpaC, which lyses the *Salmonella*-containing vacuole after infection[247]. Moreover, it might be interesting to test pathogens that invade epithelial cells without inducing a pronounced inflammatory response (e.g. *Salmonella typhi* or *Chlamydia* spp.). Possibly, these bacteria have evolved virulence factors to downregulate bystander activation[344].

Besides the initiation and amplification of the inflammatory response, bystander activation possibly provides protection to further bacterial invasion. Interferon-$\alpha$, for instance, was reported to provide a protective function against *S. flexneri* infection by inhibiting a Src-mediated pathway required for efficient *Shigella* invasion[199]. This hypothesis could be validated by performing primary and secondary infections with differently labeled bacteria. In the case of a protective function conferred by bystander activation, a reduced secondary infection rate in the vicinity of primary infected cells is expected. Another physiologically relevant function of bystander activation could be the enhancement of transepithelial migration by PMNs. Transepithelial migration is promoted by the apical secretion of the chemoattractant hepoxilin A3 by epithelial cells[288,345]. Upon infection, the production of hepoxilin A3 is upregulated by the activation of phospholipase A2 ($PLA_2$), which is controlled by the MAP kinases ERK and p38[285,288,345]. As ERK and p38 are phosphorylated in bystander cells, the contribution of these cells to the secretion of hepoxilin A3 and transepithelial migration will be investigated. In the *in vitro* infection model, the activation of $PLA_2$ can be visualized by immunofluorescence using a phospho-specific antibody and the involvement of ERK and p38 in the phosphorylation of $PLA_2$ could be validated by treating cells with respective inhibitors. The contribution of bystander cells to transepithelial migration should be tested by infecting polarized cell layers. Caco-2 and T84 cells are cultivated on filters to form a tight epithelial layer that can be infected from the basolateral side[288]. Quantification of transepithelial migration by neutrophils in the presence or absence of gap junction inhibitors might reveal whether bystander cells contribute to this process. In addition, apically secreted hepoxilin A3 could be quantified using HPLC and MS/MS as described by Mrsny et al.[345].

The finding of Sansonetti and colleagues who showed that IL-8 expression is found in epithelial cells beyond sites of infection[123], represents a first line of evidence for the *in vivo* relevance of bystander activation. Further work using animal models is required to assess the contribution of bystander activation to immune responses. *In vivo* infections with *S. flexneri* might be performed using the newborn mouse model[299], monitoring the production of *Cxcl2* (the homolog of human IL-8) in tissue sections. Furthermore, intranasal infections in mice, which lead to a massive inflammation of the lung epithelium, could serve as a suitable model system[300]. Alternatively, the production of IL-8 may be monitored in tissue sections of guinea pigs infected intragastrically with *S. flexneri*[302]. One could also make use of the estab-

lished *in vivo* infection models for *L. monocytogenes* and *S. typhimurium* in mice. The relevance of bystander activation in the immune response against bacterial infections should further be validated by administering gap junction inhibitors or other drugs blocking bystander activation *in vitro*. The genome-wide RNAi screen is expected to provide a better understanding of the molecular mechanism underlying bystander activation. With this knowledge, the contribution of bystander activation to the innate immune response could be addressed more specifically by using selected knockout mice. It is important to note that the verification of bystander activation *in vivo* is technically demanding. Additional components of the innate immune system, which can be excluded or controlled *in vitro*, will contribute to the response observed during infections in animals. The production of cytokines in uninfected cells could, for instance, result from paracrine signaling or by activation of TLRs. It will be important to verify the contribution of additional pathways by using appropriate knockout mice. TLR signaling, for instance, might be excluded by using *MyD88*$^{-/-}$ mice.

# Chapter V

# Appendix

---

The following article has been published as:
Reiterer V, Grossniklaus L, Tschon T, **Kasper CA**, Sorg I, Arrieumerlou C. *Shigella flexneri* type III secreted effector OspF reveals new crosstalks of proinflammatory signaling pathways during bacterial infection. *Cellular Signaling*, 23(7):1188-96, 2011.

# 1 Summary

*Shigella flexneri* injects several effector proteins into the cytoplasm of infected cells to downregulate the inflammatory response. One of theses effectors, OspF, has been described to harbor phosphothreonine lyase activity that irreversibly dephosphorylates the MAP kinases p38 and ERK. In our study we found that OspF also regulated the activation of the transcription factor NF-$\kappa$B and the MAP kinase JNK. In contrast to p38 phosphorylation, which is strongly reduced during *S. flexneri* infection, NF-$\kappa$B and JNK activation was potentiated. This unexpected effect of OspF was further shown to be dependent of the phosphothreonine activity on p38. Knockdown experiments revealed that OspF disrupts a negative feedback loop between p38 and the MAP3 kinase TAK1. Activation of p38 was found to lead to the phosphorylation of TAB1, which in turn negatively regulated TAK1 activity. Interestingly, the potentiated activation of JNK did not enhance signaling by c-Jun, a known target of JNK, as OspF interfered with c-Jun expression at the transcriptional level. Thus, our data reveal that OspF controls the activation of NF-$\kappa$B, JNK and c-Jun. Additionally, we demonstrate the existence of a negative feedback loop between p38 and TAK1 during *S. flexneri* infection. Finally, this study validates the use of effector proteins as molecular tools to probe signaling networks during bacterial infection.

# 2 Statement of contribution

I have performed initial experiments that had revealed differences in JNK phosphorylation when infecting cells with wild type or $\delta$*ospF S. flexneri* (illustrated in Figure 1). Additionally, I have performed the image analysis for NF-$\kappa$B activation during infection with wild type or $\Delta$*ospF S. flexneri* (Figure 2B). The other experiments were perfomed by Veronika Reiterer and Lars Grossniklaus. The paper was written by Cécile Arrieumerlou and Veronika Reiterer.

Cellular Signalling 23 (2011) 1188–1196

Contents lists available at ScienceDirect

Cellular Signalling

journal homepage: www.elsevier.com/locate/cellsig

# *Shigella flexneri* type III secreted effector OspF reveals new crosstalks of proinflammatory signaling pathways during bacterial infection

Veronika Reiterer, Lars Grossniklaus, Therese Tschon, Christoph Alexander Kasper, Isabel Sorg, Cécile Arrieumerlou *

*Biozentrum, University of Basel, Klingelbergstrasse 50/70, 4056 Basel, Switzerland*

ARTICLE INFO

*Article history:*
Received 18 February 2011
Accepted 7 March 2011
Available online 11 March 2011

*Keywords:*
OspF
Signaling
Crosstalks
NF-κB
MAPK
*Shigella flexneri*

ABSTRACT

*Shigella flexneri* type III secreted effector OspF harbors a phosphothreonine lyase activity that irreversibly dephosphorylates MAP kinases (MAPKs) p38 and ERK in infected epithelial cells and thereby, dampens innate immunity. Whereas this activity has been well characterized, the impact of OspF on other host signaling pathways that control inflammation was unknown. Here we report that OspF potentiates the activation of the MAPK JNK and the transcription factor NF-κB during *S. flexneri* infection. This unexpected effect of OspF was dependent on the phosphothreonine lyase activity of OspF on p38, and resulted from the disruption of a negative feedback loop regulation between p38 and TGF-beta activated kinase 1 (TAK1), mediated via the phosphorylation of TAK1-binding protein 1. Interestingly, potentiated JNK activation was not associated with enhanced c-Jun signaling as OspF also inhibits c-Jun expression at the transcriptional level. Altogether, our data reveal the impact of OspF on the activation of NF-κB, JNK and c-Jun, and demonstrate the existence of a negative feedback loop regulation between p38 and TAK1 during *S. flexneri* infection. Furthermore, this study validates the use of bacterial effectors as molecular tools to identify the crosstalks that connect important host signaling pathways induced upon bacterial infection.



## 1. Introduction

During bacterial infection, the ability of a host organism to mount an innate immune response is critical to limit bacterial colonization. Such a response is initiated by the recognition of bacterial components including lipopolysaccharide (LPS), peptidoglycan and nucleic acids by the Toll-like receptors (TLRs) and Nod-like receptors, which in turn activate downstream proinflammatory cascades that orchestrate innate immunity [1–3]. Despite a large spectrum of innate defense mechanisms, many pathogens can effectively colonize their host. Successful infection often results from evolutionary selected strategies that circumvent or manipulate the host response to infection [4]. A widespread stratagem developed by pathogenic bacteria consists of injecting effector proteins into the cytoplasm or the nucleus of a target cell to inhibit or usurp specific cellular processes or signaling pathways [5]. This strategy is successfully exploited by the bacterium *Shigella flexneri* to invade and colonize the intestinal epithelium of humans, causing an acute mucosal inflammation called shigellosis or bacillary dysentery [6]. Once in contact with the basolateral surface of epithelial cells, these bacteria inject, by means of a type III secretion (T3S) apparatus, a set of effector proteins that promote their internalization. In addition, *S. flexneri* interferes with multiple host signaling pathways to dampen the inflammatory response of infected epithelial cells [7]. This response is initiated by initial sensing of bacterial invasion via a pool of membrane-localized Nod1 proteins, recruited at the site of bacterial entry and remaining on cell membrane fragments after rupture of the internalization vacuole [8,9]. This early recognition is potentiated by Nod1-mediated sensing of peptidoglycan-derived peptides released by bacteria multiplying in the cytoplasm of infected epithelial cells [10]. Peptidoglycan recognition is generally followed by the homo-dimerization of Nod1, the recruitment and polyubiquitination of the kinase RICK/RIPK2 and the sequential activation of TGF-β-activated kinase-1 (TAK1), a member of the mitogen-activated protein (MAP) kinases kinase kinase (MAP3K) family [11]. TAK1 forms with the proteins TAK1-binding protein 1 (TAB1), TAB2 and/or TAB3 a complex that controls the activation of downstream key signaling pathways that lead to activation of the transcription factors nuclear factor-kappa B (NF-κB) and activator protein-1 (AP-1) and induce proinflammatory gene expression [12,13]. Once activated, TAK1 phosphorylates inhibitor of NF-κB (IκB) kinase-β (IKKβ) at key serine residues in the activation loop, resulting in its activation and leading to the phosphorylation and degradation of IκB and the nuclear translocation of NF-κB [14] . It has been recently reported that both IKKα and IKKγ/NEMO also contribute to NF-κB activation during *S. flexneri* infection [15]. In addition, TAK1 phosphorylates members of

* Corresponding author at: Focal Area Infection Biology, Biozentrum, University of Basel, Klingelbergstrasse 50/70, CH-4056 Basel, Switzerland. Tel.: +41 61 267 21 20; fax: +41 61 267 21 18.
*E-mail address:* cecile.arrieumerlou@unibas.ch (C. Arrieumerlou).

0898-6568/$ – see front matter © 2011 Elsevier Inc. All rights reserved.
doi:10.1016/j.cellsig.2011.03.006

the MAP kinase kinase (MAP2K) family, which in turn phosphorylate and activate the MAP kinases Jun N-terminal kinase (JNK) and p38 [12].

Interestingly, *S. flexneri* has developed a set of T3S effectors that interfere with inflammation signaling and downregulate the expression of the inflammatory chemokine interleukin-8 (IL-8) IL-8, which recruits polymorphonuclear cells to the site of infection [7]. Among these effectors, OspF harbors a phosphothreonine lyase activity, which leads to the irreversible dephosphorylation of p38 and ERK in the nucleus of infected cells [16,17]. The elimination of a phosphate by OspF suppresses MAPK activity by changing the conformation of the activation loop. It has been reported that a defect in MAPK activation is associated with inhibition of histone H3 phosphorylation and gene-specific repression of a subset of NF-κB regulated genes, including *IL-8* [16]. A recent study from our laboratory, monitoring IL-8 expression at the single-cell level, confirms the role of OspF on IL-8 expression in infected cells and shows that, uninfected bystander epithelial cells constitute the main source of IL-8 secretion during *S. flexneri* infection [18].

Whereas the phosphothreonine lyase activity of OspF on MAPKs has been well characterized [16,17], the impact of OspF on other host signaling pathways remains unknown. Here we report that, in addition to the dephosphorylation of p38 and ERK, OspF potentiates the activation of the JNK and NF-κB pathways triggered by *S. flexneri* infection. This unexpected effect of OspF was dependent on p38 and resulted from the disruption of a negative feedback loop regulation between p38 and TAK1 mediated via the phosphorylation of TAB1. Interestingly, potentiated JNK activation was not associated with enhanced c-Jun signaling as OspF also inhibits c-Jun expression at the transcriptional level. Altogether, our data reveal the broad impact of OspF on the activation of NF-κB, JNK and c-Jun and the crosstalks that connect these signaling pathways during bacterial infection.

## 2. Materials and methods

### 2.1. Cell lines and reagents

Mouse embryonic fibroblasts (MEFs) from wild-type and p38α knockout mice were kindly provided by Prof. A.R. Nebreda (CNIO, Madrid, Spain). MEFs and HeLa Kyoto cells [19] were cultured in DMEM, supplemented with 10% FCS, antibiotics and L-glutamine. Antibodies against TAK1, MAPK p38, the phosphorylated form of MAPK p38, JNK, TAK1 and c-Jun were obtained from Cell Signaling Technology. Total c-Jun antibody was obtained from BD Transduction Laboratories. Antibodies against IκBα, NF-κB p65 and Lamin B were purchased from Santa Cruz. Antibodies against TAB1 and phosphorylated TAB1 were obtained from the laboratory of Prof. Philip Cohen (Dundee University, Dundee, Scotland, UK). Antibody against actin was purchased from Milipore. TNFα was from R&D systems.

### 2.2. Bacterial strains

The *icsA* (*virG*) deletion mutant (Δ*virG*) generated in the M90T *S. flexneri 2a* strain was generously provided by Prof. P. Sansonetti (Institut Pasteur, Paris, France). The Δ*virG* Δ*ospF* mutant was generated as previously described [15]. All *S. flexneri* strains were transformed with the pMW211 plasmid to express the DsRed protein under control of a constitutive promoter. The pMW211 plasmid was a generous gift from Prof. D. Bumann (Biozentrum, University of Basel, Switzerland).

### 2.3. Plasmids and transfection

*OspF* was amplified using the following oligos: *ospF*-1 sense (5′-actgggatccatgcccataaaaagccctgtc) and *ospF*-2 antisense (5′-actggaattcctactctatcatcaaacgataaaa) from *S. flexneri* MT90 using Vent-DNA-polymerase (New England Biolabs). The resulting PCR fragment was cloned into the BamHI/EcoRI sites of the pCMV-Tag3B vector (Stratagene) called pIS11 (pCMV-Tag3B::ospF). For cDNA transfection, HeLa cells were seeded in a 6-well plate at a density of 400,000 cells/well. The next day, cells were transfected with 2 ug of plasmid using FugeneHD™ (Roche) according to the manufacturer's instructions.

### 2.4. siRNA transfection

Transfection of siRNAs was carried out using Lipofectamine 2000 (Invitrogen). HeLa cells, seeded in a 6-well plate (100,000 cells/well), were reversely transfected with 10 nM siRNA according to the manufacturer's instructions. Cells were used 72 h after transfection.

### 2.5. Cell lysis and immunoblotting

Cells were washed twice in ice cold PBS, lysed in PhosphoSafe™ extraction reagent (Novagen), incubated on ice for 20 min and subsequently centrifuged at 4 °C for 20 min at 16,000 *g*. BCA Protein Assay kit (Pierce) was used to determine protein concentration. 10–15 ug of protein was subjected to SDS-polyacrylamide gels and electroblotted onto nitrocellulose membranes. Immunoblotting was performed using primary antibodies diluted in phosphate buffered saline 0.1% tween containing 5% bovine serum albumin or 5% nonfat dry milk. HRP-conjugated secondary antibodies were purchased from GE Healthcare or Cell signaling technology or Thermo Scientific. The blots were developed with an enhanced chemiluminescence method (ECL, Pierce).

### 2.6. Infection assay

*S. flexneri* strains were grown in tryptic soy broth (TSB) to exponential log phase at 37 °C and coated with poly-L-lysine before infection. 30 min before infection, complete growth medium was replaced by DMEM supplemented with 10 mM Hepes and 2 mM L-glutamine (assay medium). Bacteria were added to cells in 96-well or 6-well plates at the indicated multiplicity of infection (MOI). Infection was initiated by centrifuging the plates for 5 min and placing them at 37 °C for the indicated time periods. Extracellular bacteria were killed by adding gentamycin (50 μg/ml) 30 min after infection.

### 2.7. Immunofluorescence

Cells were fixed in 4% paraformaldehyde in PBS. For p-JNK staining, cells were permeabilized in 0.3% Triton X-100 in PBS and subsequently blocked using 5% goat serum in PBS. Cells were incubated with p-JNK antibody in 10% goat serum in PBS overnight. For NF-κB and phospho-p38 staining, cells were permeabilized and blocked in 0.3% Triton X-100 5% goat serum in PBS for one hour. Subsequently, cells were incubated with the appropriate primary antibody in 0.3% Triton X-100 5% goat serum in PBS overnight followed, by incubation with Alexa 647- or Alexa 488-conjugated secondary antibodies. In addition, cells were stained with Hoechst to visualize nuclei.

### 2.8. Automated microscopy and image analysis

Images were automatically acquired with an ImageXpress Micro (Molecular devices, Sunnyvale, USA). At each site, images at 360 nm, 480 nm, 594 nm and 640 nm were acquired to visualize Hoechst, DsRed expressing *S. flexneri* and Alexa 647- or Alexa 488-conjugated secondary antibodies. Image analysis was performed with CellProfiler [20]. The activation of NF-κB was determined by calculating the nuclear/cytosolic intensity ratio of the NF-κB p65 staining as previously described [18].

### 2.9. Subcellular fractionation

Preparation of nuclear proteins was adapted from Mattioli et al. [21]. Briefly, cells were lysed in buffer A (10 mM HEPES/KOH, pH 7.9,

10 mM KCl, 0.1 mM EDTA, 1 mM DTT, and 0.5 mM PMSF). After incubation at 4 °C for 20 min, Triton X-100 (final concentration: 0.25%) was added to the lysates. The samples were then centrifuged for 30 s at 16,000 g and the pellets dissolved in 40 μl of buffer C (20 mM HEPES/KOH, pH 7.9, 0.4 M NaCl, 1 mM EDTA, 1 mM DTT, 0.5 mM PMSF). Samples were incubated on ice for 15 min and frequently vortexed. Subsequently, samples were centrifuged for 20 min at 16,000 *g*. Supernatants were transferred into fresh tubes. Protein concentration was determined by BCA Protein Assay kit. Equal amounts of protein were subjected to SDS page.

### 2.10. Quantitative real-time PCR

The level of c-*Jun* mRNA was measured by quantitative real-time PCR (qRT-PCR) as follows. Total RNA was isolated from cells infected with Δ*virG* and Δ*virG* Δ*ospF S. flexneri* for 1 h using the RNeasy Mini Kit (Qiagen). Total RNA was reverse transcribed using oligo$(dT)_{15}$ primer (Promega) with Superscript III reverse transcriptase (Invitrogen). qRT-PCR was performed on StepOne Real time PCR system (Applied Biosystems) using the SYBR green PCR Master Mix (Applied Biosystems). GAPDH was used as an internal control to normalize mRNA expression. Each sample was analyzed in triplicate. The primer sequences used are as follows. c-*Jun*-forward: 5′-AGGAGGAGCCTCAGACAGTG; c-*Jun*-reverse: 5′-AGCTTCCTTTTTCGGCACTT; *GAPDH*-forward: 5′-GAAGGTGAAGGTCGGAGTC; *GAPDH*-reverse: 5′-GAAGATGGTGATGGGAT TTC.

### 2.11. Statistical analysis

Data presented in the manuscript are representative of at least three independent experiments. Data are expressed as mean ± standard deviation of triplicate samples or as indicated in the figure legends. p values were calculated with a two-tailed two-sample equal variance *t*-test.

## 3. Results

### 3.1. OspF dephosphorylates p38 and potentiates the activation of JNK

The activation of the JNK signaling pathway is critical to mount an inflammation response against *S. flexneri* infection [22]. Therefore, in order to characterize the impact of OspF on inflammation signaling, we examined whether OspF affected the activation of JNK during infection. The effect of OspF on the activation of p38 was analyzed in parallel for comparison. To avoid secondary invasion resulting from intercellular bacterial motility that would complicate the analysis of time course experiments, the non-motile *virG* deletion mutant (Δ*virG*) [23] was used as the reference background strain in the entire study. The activation of p38 and JNK was analyzed by western immunoblotting at different time-points after infection of HeLa epithelial cells with *S. flexneri* Δ*virG* or with a *virG ospF* double deletion mutant (Δ*virG* Δ*ospF*). Phospho-specific antibodies that detect p38 phosphorylated at residues threonine 180 and tyrosine 182 (p-p38) and p46 and p54 JNKs phosphorylated at residues threonine 183 and tyrosine 185 (p-JNKs) of the activation loop were used. As previously described [16,17], no detectable phosphorylation of p38 was found in cells infected with Δ*virG S. flexneri* (Fig. 1A, upper panel) whereas massive p-p38 was found during infection with Δ*virG* Δ*ospF* (Fig. 1A, lower panel), confirming the role of OspF in the dephosphorylation of p38 during *S. flexneri* infection. Surprisingly, in contrast to p38, the phosphorylation of both p46 and p54 JNKs was more prolonged in cells infected with Δ*virG* bacteria compared to Δ*virG* Δ*ospF* infected cells (Fig. 1B and C), showing for the first time, that OspF positively regulated JNK signaling during infection. This result was unexpected given that the phosphothreonine lyase activity of OspF was reported to also dephosphorylate JNK in a cell transfection assay [17]. The effects of OspF on p38 and JNK activation were confirmed by immunofluorescence microscopy experiments using the phospho-specific antibodies described above. Whereas almost no p-p38 staining was found in cells infected with dsRed-expressing *S. flexneri* Δ*virG* (Fig. 1D, middle panel), high nuclear p-JNK intensity was still detected 90 min after infection (Fig. 1E, middle panel). In contrast, p38 phosphorylation was found in cells infected with Δ*virG* Δ*ospF* (Fig. 1D, right panel), but these cells exhibited a weak p-JNK staining (Fig. 1E, right panel), indicating that OspF induced a sustained activation of JNK during infection. Taken together, these data confirm the inhibitory effect of OspF on p38 and show that OspF enhances JNK activation during *S. flexneri* infection of epithelial cells.

### 3.2. OspF enhances the activation of NF-κB induced by S. flexneri infection and TNF-α stimulation

In addition to JNK and p38, the activation of the transcription factor NF-κB is critical during *S. flexneri* infection to induce the expression of various proinflammatory genes and to promote host cell survival [24]. The NF-κB pathway is turned on downstream of peptidoglycan recognition via Nod1 and the subsequent activation of TAK1 and the IKK complex. To investigate the effect of OspF on NF-κB during infection, we examined the impact of this effector on the translocation of the NF-κB subunit p65, resulting from the phosphorylation and degradation of IκB proteins initiated by the IKK complex [15]. The localization of p65 was first addressed by immunofluorescence microscopy with a p65 antibody. In uninfected cells, p65 was found in the cytoplasm (Fig. 2A, left panel), indicating that NF-κB was inactive. As expected, cells infected with *S. flexneri* Δ*virG* for 90 min exhibited a strong nuclear translocation of p65 (Fig. 2A, middle panel). Interestingly, the nuclear localization of p65 in cells infected with Δ*virG* Δ*ospF* bacteria was more modest (Fig. 2A, right panel). Quantification of p65 nuclear translocation at different time-points, by calculation of the nuclear/cytoplasmic p65 intensity ratio with automated image processing, indicated that, whereas initial p65 translocation was similar in Δ*virG* and Δ*virG* Δ*ospF* infected cells, a more transient nuclear localization was observed after Δ*virG* Δ*ospF* infection (Fig. 2B). A similar result was obtained when monitoring the nuclear localization of p65 by western blot analysis in nuclear extracts of infected cells (Fig. 2C), showing that, in contrast to its inhibitory activity on p38, OspF enhances NF-κB activation following *S. flexneri* infection. During bacterial challenge, epithelial cells are exposed to microbial products including peptidoglycan and LPS but also to proinflammatory cytokines, such as tumor necrosis factor alpha (TNF-α), that also induce NF-κB activation. To better characterize the mode of action of OspF on NF-κB activation, we tested whether OspF also potentiated the activation of NF-κB triggered by TNF-α. For this purpose, HeLa cells were transiently transfected with an empty vector or a plasmid encoding OspF, and stimulated with TNF-α. To verify the activity of ectopic OspF expression on cell signaling, we first examined its effect on the phosphorylation of p38 induced by TNF-α stimulation (Fig. 2D, upper panel). Whereas p-p38 was detected in TNF-α-stimulated cells transfected with the empty vector, almost no phosphorylation was detected in cells expressing OspF, confirming that this effector inhibited TNF-α-induced p38 activation. We then tested the activity of OspF on TNF-α-induced NF-κB activation by monitoring the degradation of IκBα after stimulation. We found that OspF effectively potentiated the degradation of IκBα after TNF-α stimulation (Fig. 2D, lower panel), indicating that the expression of OspF was sufficient to enhance NF-κB signaling in cells. Taken together, these data show that OspF potentiates the activation of JNK and NF-κB, and that this effector has thus a broad impact on inflammation signaling during bacterial infection.

### 3.3. OspF potentiates the activation of JNK by a p38-dependent mechanism

OspF harbors a phosphothreonine lyase activity that removes the phosphate group of threonine residues present in the activation loop

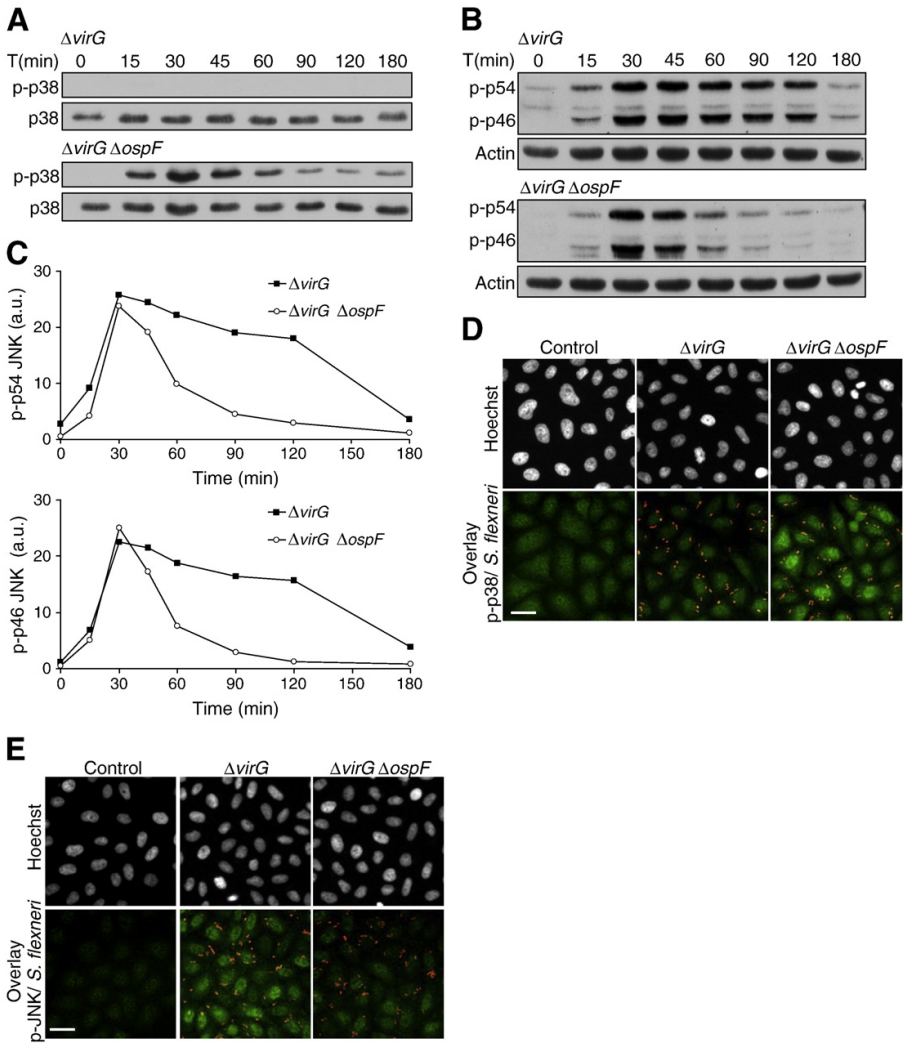


**Fig. 1.** OspF dephosphorylates p38 and potentiates JNK activation. (A) OspF dephosphorylates p38 in infected cells. Whole cell lysates from HeLa cells, infected at MOI = 40 with *S. flexneri* Δ*virG* or Δ*virG* Δ*ospF* for indicated time periods, were analyzed by western immunoblotting using a phospho-specific antibody that detects p38 phosphorylated at threonine 180 and tyrosine 182 residues (p-p38). Total p38 was used as loading control. (B) OspF prolongs the activation of JNK during infection. Lysates from HeLa cells infected at MOI = 40 with *S. flexneri* Δ*virG* or Δ*virG* Δ*ospF* for indicated time periods were analyzed by western immunoblotting using a phospho-specific antibody that detects p46 and p54 JNKs phosphorylated at residues threonine 183 and tyrosine 185 (p-p46 and p-p54 JNKs). Actin was used as loading control. (C) Densitometric quantification of phosphorylated p46 (lower panel) and p54 (upper panel) JNKs at different time-points of Δ*virG* or Δ*virG* Δ*ospF* infection based on western blot analysis shown in (B); graph representative of 3 independent experiments. (D) Analysis of p38 phosphorylation by immunofluorescence microscopy. HeLa cells were mock treated (control) or infected with *S. flexneri* Δ*virG* or Δ*virG* Δ*ospF* at MOI = 30 for 60 min. After fixation, cells were stained for p-p38 and DNA (Hoechst). In overlay images, p-p38 is in green, *S. flexneri* in red. (E) Analysis of JNK phosphorylation by immunofluorescence microscopy. HeLa cells were mock treated (control) or infected with Δ*virG* or Δ*virG* Δ*ospF S. flexneri* at MOI = 30 for 90 min. After fixation, cells were stained for p-JNK and DNA (Hoechst). In the overlay images, p-JNK is in green, *S. flexneri* in red; scale bars, 20 μm.

of MAPKs [17]. As p38 is an important target of OspF, we tested whether the potentiation of JNK activation by OspF was dependent on p38. To test this hypothesis, we investigated by western blot analysis the phosphorylation of JNKs during infection of mouse embryonic fibroblasts wild-type (wt MEFs) or deficient for p38α ($p38^{-/-}$ MEFs) previously described by Ambrosino et al. [25]. In line with the data obtained in HeLa cells, the phosphorylation of p46 and p54 JNKs was more sustained after Δ*virG* than Δ*virG* Δ*ospF* infection in wt MEFs (Fig. 3, left panels), indicating that the positive regulation of JNK by OspF was not restricted to HeLa cells but corresponded to a general regulation mechanism. In contrast, the profile of JNK activation was similar after Δ*virG* and Δ*virG* Δ*ospF* infection in $p38^{-/-}$ MEFs, showing that OspF had no effect on JNK in absence of p38 (Fig. 3, right panels) and therefore, that OspF regulated the activation of JNK via a p38-dependent mechanism. Whereas wt MEFs infected with Δ*virG* Δ*ospF* bacteria showed a transient JNK activation (Fig. 3, bottom left panel), sustained activation was found in wt MEFs infected with Δ*virG* (Fig. 3, top left panel) and in $p38^{-/-}$ MEFs infected with Δ*virG* (Fig. 3, top right panel) or Δ*virG* Δ*ospF* bacteria (Fig. 3, bottom right panel). As these conditions corresponded to high and low/no p38

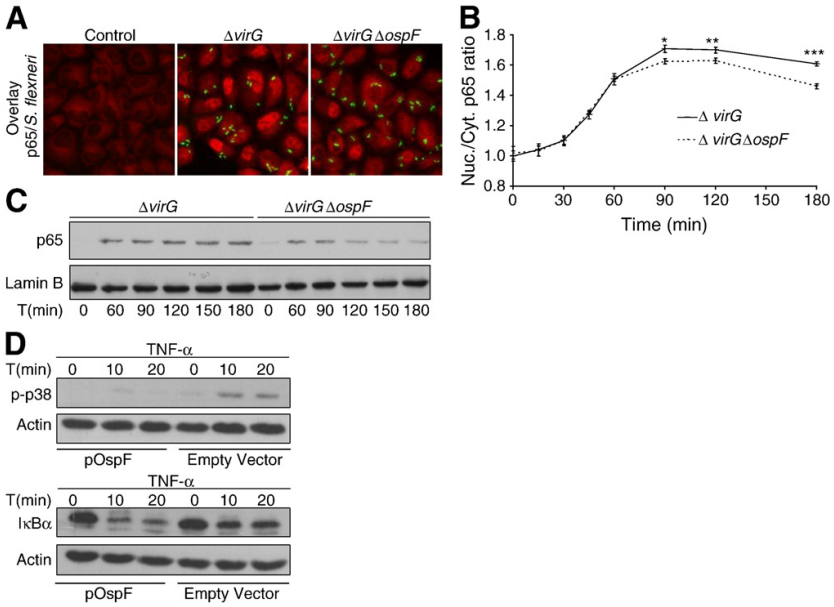


**Fig. 2.** OspF potentiates the activation of NF-κB after *S. flexneri* infection or TNF-α stimulation. (A) Localization of NF-κB p65 in response to *S. flexneri* infection. HeLa cells were mock treated (control) or infected at MOI = 40 with Δ*virG* or Δ*virG* Δ*ospF S. flexneri* for 90 min. After fixation, cells were stained with a p65 antibody. In overlay images, p65 is in red, *S. flexneri* in green; scale bar, 20 μm. (B) Quantification of the nuclear translocation of p65 by automated image analysis at different time-points of infection. The nuclear/cytoplasmic p65 intensity ratio was calculated as described in Materials and methods. The data shown are mean values +/− SD of 4 wells per condition; graph representative of 3 independent experiments; *p = 8.73E−03, **p = 9.60E−03, ***p = 6.31E−05. (C) NF-κB p65 nuclear localization analyzed by western immunoblotting after cell fractionation. Nuclear extracts from HeLa cells infected at MOI = 40 with Δ*virG* or Δ*virG* Δ*ospF S. flexneri* for indicated time periods were analyzed by western immunoblotting using a p65 antibody. The nuclear protein Lamin B was used as loading control. (D) Effects of OspF on the activation of p38 and NF-κB upon TNF-α stimulation. Lysates from HeLa cells, transiently transfected with an empty vector or OspF containing plasmid (pOspF) and stimulated with TNF-α for indicated time periods, were analyzed by western immunoblotting. The activation of p38 and NF-κB was analyzed by detecting p-p38 (upper panel) and IκBα (lower panel), respectively. Actin was used as loading control.

activation respectively, these data suggested that activated p38 inhibited JNK and therefore, that OspF potentiated JNK signaling through its inhibitory effect on p38. Taken together, these data demonstrate that OspF upregulates the activation of JNK via a p38-dependent mechanism, suggesting that OspF affects JNK signaling indirectly via its phosphothreonine lyase activity on p38. In addition, these results also provide evidence for a new crosstalk between the p38 and JNK pathways during *S. flexneri* infection.

### *3.4. OspF potentiates the activation of JNK and NF-κB by disrupting a p38/TAK1 negative feedback loop regulation*

In order to determine how OspF potentiated the activation of NF-κB and JNK while dephosphorylating p38, we examined the upstream mechanisms controlling these pathways during infection. It has been proposed that the activation of NF-κB, p38, and JNK occurs downstream of TAK1 activation following peptidoglycan recognition via

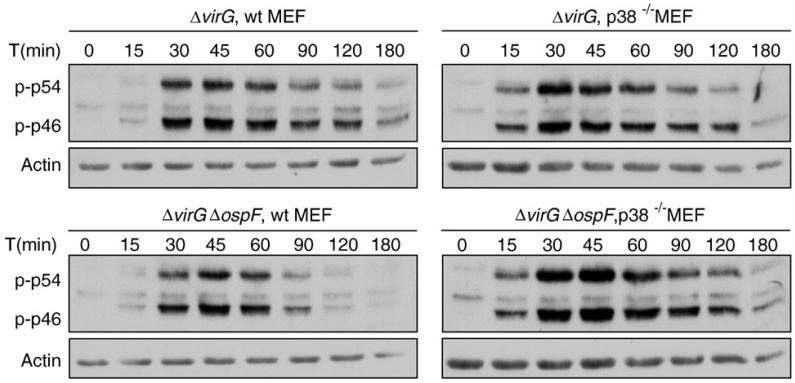


**Fig. 3.** OspF potentiates the activation of JNK via a p38-dependent mechanism. Whole cell lysates from wt MEFs (left panels) and p38$^{-/-}$ MEFs (right panels) infected at MOI = 40 with *S. flexneri* Δ*virG* (upper panels) or Δ*virG* Δ*ospF* (lower panels) for indicated time periods were analyzed by western immunoblotting using a phospho-specific antibody that detects p46 and p54 JNKs phosphorylated at residues threonine 183 and tyrosine 185 (p-p54 and p-p46 JNKs). Actin was used as loading control.

Nod1 [26]. As peptidoglycan recognition is the main pathway leading to inflammation signaling during *S. flexneri* infection [10], it was expected that TAK1 controls the downstream activation of p38, JNK and NF-κB during infection. This assumption was directly tested by monitoring the activation of p38, JNK and NF-κB in HeLa cells depleted of TAK1 by RNA interference (RNAi). The activation of p38 and JNK was examined by western blot analysis using the phospho-specific antibodies described above. The activation of NF-κB was analyzed by measuring the degradation of IκBα. To prevent the dephosphorylation of p38 by OspF, the effect of TAK1 knockdown on the activation of p38 was examined in cells infected with Δ*virG* Δ*ospF* bacteria. For the analysis of JNK and NF-κB activation, cells were infected with *S. flexneri* Δ*virG*. Knocking down TAK1 reduced the activation of p38 (Fig. 4A) and JNK (Fig. 4B), as well as the degradation of IκBα (Fig. 4B) induced by infection, confirming that p38, JNK and NF-κB were activated downstream of TAK1 during *S. flexneri* infection.

As NF-κB and JNK are activated downstream of TAK1 and are both positively regulated by OspF, we tested whether OspF directly potentiated TAK1 activation during *S. flexneri* infection. HeLa cells were infected with Δ*virG* or Δ*virG* Δ*ospF* bacteria and the activation of TAK1 was analyzed by western immunoblotting using a phospho-specific antibody that detects TAK1 phosphorylated in its activation loop at threonine 187 [27]. As expected, TAK1 phosphorylation was induced during Δ*virG* infection (Fig. 4C). Interestingly, a more modest phosphorylation was found in cells infected with Δ*virG* Δ*ospF* (Fig. 4C), showing that OspF potentiated TAK1 activation during infection. Because cells infected with *S. flexneri* Δ*virG* Δ*ospF* exhibited a high degree of p38 activation (Fig. 1A), we tested whether the low level of TAK1 activation observed in these cells was caused by p38. We addressed this question by monitoring the phosphorylation of TAK1 in HeLa cells depleted of p38 by RNAi after Δ*virG* Δ*ospF S. flexneri* infection. Knocking down p38 increased TAK1 phosphorylation (Fig. 4D), showing that p38 negatively regulates TAK1 during *S. flexneri* infection. As OspF blocks p38 activation, these results suggested that OspF potentiated TAK1 indirectly via its phosphothreonine lyase activity on p38.

Based on the observation that TAK1 functions upstream of p38 activation during infection and the data showing that, TAK1 activation was negatively regulated by a p38-dependent mechanism, we

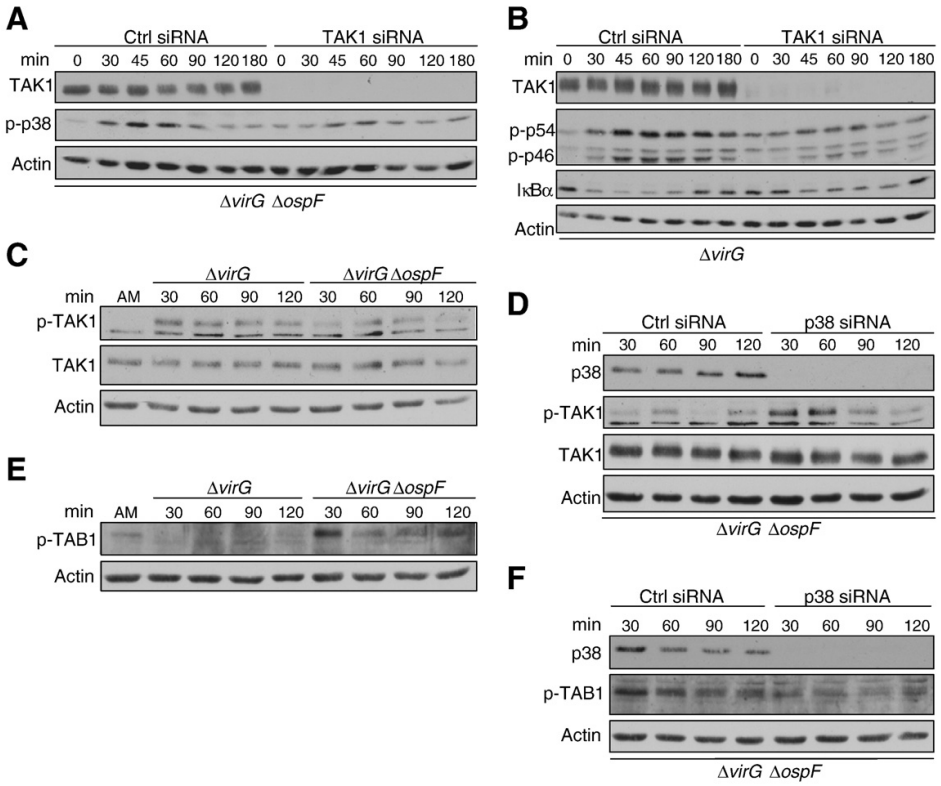


**Fig. 4.** OspF potentiates the activation of JNK and NF-κB by blocking the p38/TAK1 negative feedback loop. (A) Effect of TAK1 knockdown on *S. flexneri* infection-induced p38 activation. HeLa cells, transfected with control or TAK1 siRNAs, were infected at MOI = 40 with Δ*virG* Δ*ospF S. flexneri* for indicated time periods. Whole cell lysates were analyzed by western immunoblotting for p-p38. Actin was used as loading control. (B) Effect of TAK1 knockdown on *S. flexneri* infection-induced JNK activation and IκBα degradation. HeLa cells, transfected with control or TAK1 siRNAs, were infected at MOI = 40 with Δ*virG S. flexneri* for indicated time periods. Whole cell lysates were analyzed by western immunoblotting using indicated antibodies. Actin was used as loading control. (C) Effect of OspF on TAK1 activation during *S. flexneri* infection. Whole cell lysates from HeLa cells, infected at MOI = 40 with *S. flexneri* Δ*virG* or Δ*virG* Δ*ospF* for indicated time periods, were analyzed by western immunoblotting using a phospho-specific antibody that detects TAK1 phosphorylated at threonine 187 (p-TAK1). Cells treated with assay medium (AM) were used as control. Total TAK1 and actin were used as loading control. (D) Effect of p38 knockdown on the activation of TAK1 induced by Δ*virG* Δ*ospF* infection. Whole cell lysates from HeLa cells, infected at MOI = 40 with *S. flexneri* Δ*virG* Δ*ospF* for indicated time periods, were analyzed by western immunoblotting using a p-TAK1 antibody. (E) Effect of OspF on TAB1 activation during *S. flexneri* infection. Whole cell lysates from HeLa cells, infected at MOI = 40 with *S. flexneri* Δ*virG* or Δ*virG* Δ*ospF* for indicated time periods, were analyzed by western immunoblotting using a phospho-specific antibody that detects TAB1 phosphorylated at serine 423 (p-TAB1). Cells treated with assay medium (AM) were used as control. Actin was used as loading control. (F) Effect of p38 knockdown on the activation of TAB1 induced by Δ*virG* Δ*ospF* infection. Whole cell lysates from HeLa cells, infected at MOI = 40 with *S. flexneri* Δ*virG* Δ*ospF* for indicated time periods, were analyzed by western immunoblotting with a p-TAB1 antibody. Actin was used as loading control.

hypothesized that p38 negatively regulated TAK1 activation via a negative feedback loop. A similar negative feedback regulation between p38 and TAK1 was previously reported [28]. The authors showed that p38 suppresses the activity of TAK1 by phosphorylating TAB1 at serine 423. To test whether this feedback mechanism was effective during *S. flexneri* infection and could explain the activity of OspF on TAK1 activation, we compared the phosphorylation of TAB1 in HeLa cells infected with Δ*virG* or Δ*virG* Δ*ospF S. flexneri* by western immunoblotting using a phospho-specific antibody that detects TAB1 phosphorylated at serine 423 (p-TAB1). Residual p-TAB1 was found in untreated cells whereas almost no signal was detected after infection with Δ*virG* bacteria (Fig. 4E). In contrast, higher phosphorylation was induced by Δ*virG* Δ*ospF* infection (Fig. 4E), showing that OspF blocks the phosphorylation of TAB1 during infection and suggesting that OspF potentiates TAK1 activation by preventing the phosphorylation of TAB1 by p38. This hypothesis was directly tested by examining whether the phosphorylation of TAB1 found in Δ*virG* Δ*ospF* infected cells was reduced after p38 knockdown. A reduction of p-TAB1 was found in p38-depleted cells compared to control cells (Fig. 4F). This result indicated that the high level of p-TAB1 found in Δ*virG* Δ*ospF* infected cells was dependent on p38 and therefore, that OspF prevented the phosphorylation of TAB1 via its phosphothreonine lyase activity on p38 activation. Taken together, these data show that OspF potentiates the activation of TAK1 and the downstream activation of NF-κB and JNK, by disrupting the negative feedback loop between p38 and TAK1, which is mediated via the phosphorylation of TAB1.

### 3.5. OspF blocks c-Jun expression at the transcriptional level

As OspF strongly potentiated JNK activation during *S. flexneri* infection, we investigated the impact of this effector on the phosphorylation of c-Jun, a pivotal JNK substrate involved in various JNK-dependent biological processes including inflammatory responses, apoptosis, survival and cell cycle. c-Jun is a member of the AP-1 family of transcription factors and is phosphorylated on serine 63 and serine 73 within its N-terminal region by JNKs. The phosphorylation of c-Jun was analyzed by western immunoblotting using a phospho-specific antibody that detects c-Jun phosphorylated at serine 63. Surprisingly, the amount of phosphorylated c-Jun was lower in cells infected with Δ*virG S. flexneri* compared to cells infected with Δ*virG* Δ*ospF* bacteria (Fig. 5A). A reduced level of total c-Jun was also found after Δ*virG* infection compared to Δ*virG* Δ*ospF* (Fig. 5A), showing that OspF negatively regulates c-Jun signaling during *S. flexneri* infection. c-Jun expression is regulated at the transcriptional and posttranscriptional level. For the latter, the phosphorylation of c-Jun by JNK at serine 63 stabilizes c-Jun proteins by inhibiting ubiquitin-dependent degradation [29]. The effect of OspF on c-Jun expression may therefore be explained by an inhibition of c-*Jun* transcription or a defect in the stability of c-Jun proteins. In order to test whether OspF had an effect on the transcription of c-*Jun*, the level of c-*Jun* mRNA was analyzed by quantitative real-time PCR in control uninfected, Δ*virG* and Δ*virG* Δ*ospF* infected cells. An increase of c-*Jun* mRNA was found after one hour of infection (Fig. 5B), confirming that c-*Jun* is an early gene induced upon *S. flexneri* infection in epithelial cells. Interestingly, the level of mRNAs was more strongly induced after Δ*virG* Δ*ospF* than Δ*virG* infection, indicating that OspF prevented the transcription of c-*Jun*. Taken together, these results show that, although OspF potentiates the activation of JNK, it negatively regulates c-Jun signaling by strongly inhibiting the transcription of c-*Jun*. As c-Jun is an important transcription factor for the regulation of proinflammatory genes such as *IL-8* [30], these data reveal a new mechanism by which OspF blocks inflammation signaling in *S. flexneri* infected cells.

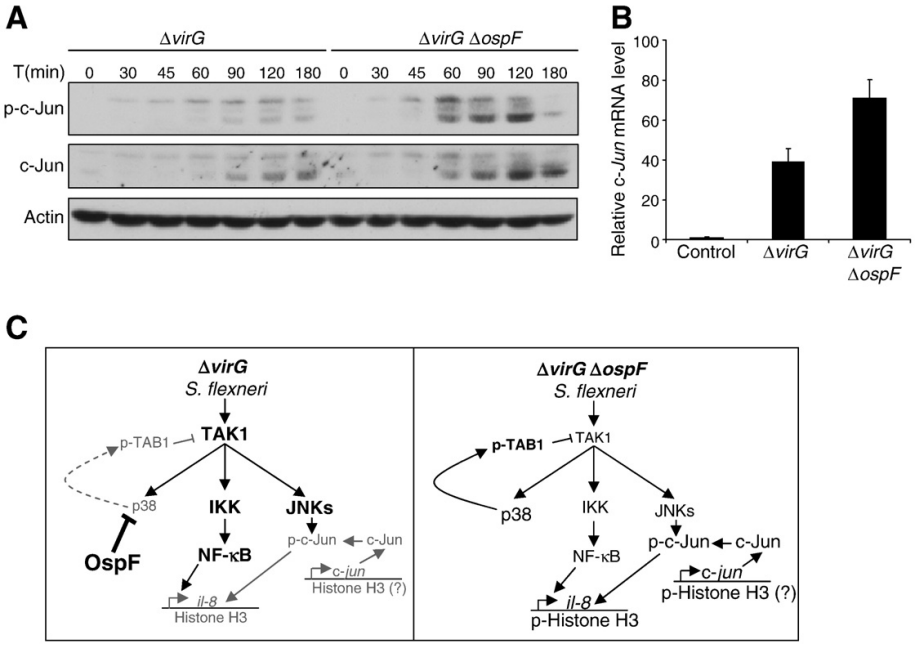


**Fig. 5.** OspF blocks the transcription of c-*Jun* during *S. flexneri* infection. (A) Effect of OspF on the phosphorylation and expression of c-Jun during *S. flexneri* infection. Whole cell lysates from HeLa cells, left untreated or infected at MOI = 40 with *S. flexneri* Δ*virG* or Δ*virG* Δ*ospF* for indicated time periods, were analyzed by western immunoblotting using a phospho-specific antibody that detects c-Jun phosphorylated at serine 63 (p-c-Jun) or a c-Jun antibody detecting total c-Jun. Actin was used as loading control. (B) Effect of OspF on the level of c-*Jun* mRNA during *S. flexneri* infection. Quantification of c-*Jun* mRNA was measured by quantitative real-time PCR after 1 h of infection with Δ*virG* or Δ*virG* Δ*ospF S. flexneri*. Uninfected cells were used as control. Values represent relative quantities (RQ) ± RQ max and RQ min of triplicate samples and indicate c-*Jun* mRNA expression relative to assay medium stimulated cells after normalization to *GAPDH* mRNA levels; graph representative of 3 independent experiments. (C) Model describing the impact of OspF on inflammation signaling during *S. flexneri* infection.

## 4. Discussion

Immune responses to bacterial infection are controlled by the complex molecular interactions that occur between the host signaling network and various bacterial products present at the surface of bacteria or released during infection. Structural components including LPS, peptidoglycan and lipoproteins as well as numerous bacterial proteins interact with specific receptors or signaling pathways and trigger or shape specific facets of host defense. In the case of *S. flexneri* infection, multiple T3S effectors interfere with the inflammatory response of infected epithelial cells, which is mainly triggered after recognition of peptidoglycan released by intracellular bacteria. Among these effectors, OspF is one the best characterized [17]. This effector protein harbors a phosphothreonine lyase activity that mediates irreversible dephosphorylation of MAP kinases and contributes to the repression of NF-κB-regulated genes by blocking the phosphorylation of histone H3 and thereby affecting chromatin access to transcription factors [16]. Here we broadly analyzed the impact of OspF on inflammation signaling, and in particular, examined whether OspF also affected the JNK and NF-κB pathways, which are also critical to mount an inflammation response during bacterial infection. Interestingly, we found that in addition to the inhibition of p38 and ERK activation, OspF potentiates the activation of JNK during infection. Indeed, both p46 and p54 JNKs were more strongly activated after infection with an OspF deletion mutant. Interestingly, our data showed that the initial peak of activation was not affected by OspF but instead that OspF was required to obtain a prolonged JNK activation. This result was unexpected as a phosphothreonine lyase activity of OspF towards JNK has been reported in vitro or in a cell transfection assay [17]. In addition to potentiating the activation of JNK, our data showed that OspF also enhanced the activation of NF-κB during *S. flexneri* infection or after stimulation with the proinflammatory cytokine TNF-α. These results were also surprising because several *S. flexneri* T3S effectors tend to block the activation of NF-κB during infection. For example, the protein OspG inhibits the activity of ubiquitinated E2s (Ub conjugating enzymes) that are essential for the ubiquitination of phospho-IκBα by E3 ubiquitin ligase $SCF^{\beta\text{-}TrCP}$, thereby preventing NF-κB activation [31]. The effector IpaH9.8 inhibits the NF-κB pathway by targeting the essential scaffolding protein of the IKK complex NEMO/IKKγ for proteasome-dependent degradation after polyubiquitination [32]. Finally, it has been recently reported that the effector OspZ, present as a full length protein in *S. flexneri 6* but not in *S. flexneri 2a*, also inhibits the activation of NF-κB during infection by a mechanism that remains unclear [33]. It is interesting to note that despite these effectors (at least OspG and IpaH9.8 in *S. flexneri 2a*), we found that the nuclear translocation of p65 during *S. flexneri* infection was still robust. This observation favors a model where the activation of NF-κB results from a fine balance between the inhibitory activities of OspG and IpaH9.8 and the positive regulation caused by OspF. As blocking NF-κB signaling seems to correspond to one of the strategies selected throughout evolution by *S. flexneri* to dampen inflammation in response to infection, we hypothesized that the positive effect of OspF reflected an indirect consequence of its phosphothreonine lyase activity on MAPKs.

We validated this assumption by demonstrating that the effect of OspF on JNK signaling was dependent on p38. Indeed, we found that OspF failed to affect the level of JNK activation in cells deficient for p38. Furthermore, we showed that high p38 activity during infection was associated with transient JNK activation whereas no/low activity, found in wt MEFs infected with Δ*virG* bacteria or in $p38^{-/-}$ MEFs, was associated with sustained JNK activation. These results indicated that p38 negatively regulates JNK, and that OspF affects JNK signaling indirectly via its phosphothreonine lyase activity on p38. In addition to unraveling a new activity of OspF on host signaling, these data also reveal a new crosstalk between p38 and JNK pathways during bacterial infection in epithelial cells. Crosstalks between signaling pathways are a common theme in cellular signaling. JNK and p38, which share common upstream regulators, are activated simultaneously in response to many stimuli, including cytokines, UV light or osmotic stress. Although they can synergize for the activation of AP-1 [34], they often have opposite effects. For example, JNK and p38 exert opposing effects on the development of myocyte hypertrophy [35] and in mouse models of liver cancer [36]. In addition to crosstalks taking place at the level of downstream targets, it has been reported that p38 can also negatively regulate JNK activity. The first evidence for this crosstalk was the observation that chemical inhibition of p38, with the commonly used p38 inhibitor SB203580, strongly increased the activation of JNK induced by interleukin-1 and sorbitol in epithelial cells, and by LPS in macrophages [28]. As SB203580 also inhibits RIPK2 [37], an upstream kinase essential for *S. flexneri*-induced inflammation signaling, this drug could not be used in our study. Instead, the crosstalk between p38 and JNK was unraveled by combining the use of OspF, which functions as an irreversible p38 inhibitor, and $p38^{-/-}$ MEFs or RNAi, which are needed to confirm that the effect of OspF results from its activity towards p38.

Because JNK and NF-κB were both potentiated by OspF, we tested whether this effect was mediated by an effect of OspF on the upstream common kinase TAK1. Following peptidoglycan recognition, the receptor Nod1 undergoes oligomerization and this mechanism leads to the subsequent recruitment of the kinase RIPK2 and the activation of TAK1. TAK1 functions as a MAP3K upstream of p38 and JNK, and phosphorylates IKKβ leading to NF-κB activation. We confirmed that TAK1 functions upstream of JNK, NF-κB and p38 activation during *S. flexneri* infection by showing that the activation of these pathways was impaired in TAK1-depleted cells. Furthermore, we found that OspF enhanced the activation of TAK1 during infection, suggesting that the potentiation of JNK and NF-κB pathways by OspF is mediated by its effect on TAK1. Finally, we showed that the reduction of TAK1 activation found in cells infected with Δ*virG* Δ*ospF* bacteria is dependent on the expression of p38, as high TAK1 phosphorylation was restored when p38 expression was reduced by RNAi. As TAK1 functions upstream of p38, JNK and NF-κB activation, and because the activation of TAK1 depends on p38 during infection, our data suggested that p38 negatively regulated TAK1 via a negative feedback loop. This hypothesis was further demonstrated by showing that p38 phosphorylates TAB1, a mechanism that inhibits the activation of TAK1 [28]. Therefore, we propose that OspF, via its phosphothreonine lyase activity which dephosphorylates p38, disrupts the negative feedback loop occurring between p38 and TAK1, resulting in enhanced TAK1 activation and sustained JNK and NF-κB activation. A model based on these data is illustrated in Fig. 5C.

JNK and NF-κB are two pathways important for the regulation of various cellular responses during infection, including inflammation, apoptosis and cell survival [24,38]. An increase in NF-κB activation by OspF could be associated with enhanced inflammation or a better host cell survival to infection. However, as OspF also impairs the accessibility of chromatin to transcription factors [16], the positive regulation of OspF on NF-κB activation may stay functionally silent. Sustained activation of JNK is usually associated with an increase of apoptosis [39], suggesting that OspF may indirectly affect the survival of infected cells. To test whether OspF affected the signaling pathways downstream of JNK, we examined its effect on c-Jun, which is involved in the regulation of many functions controlled by JNK. Interestingly, we found that although OspF potentiated the activation of JNK, it reduces the amount of phosphorylated c-Jun. This effect was most likely due to the fact that OspF affects the transcription of c-Jun and therefore, that less proteins are produced when OspF is secreted. Taken together, these data suggest that, in addition to the well characterized effect of OspF on IL-8 expression [16], OspF also impairs IL-8 expression by reducing the expression of c-*Jun*, an immediate-early gene whose product c-Jun functions as an essential transcription factor for IL-8 expression [30] (Fig. 5C). More work is needed to elucidate how OspF

blocks c-*Jun* transcription. We hypothesize that this may also be a consequence of reduced histone H3 phosphorylation, which is required for efficient c-Jun transcription [40,41] (Fig. 5C).

Because the host signaling pathways are highly interconnected, targeting a host protein has multiple consequences within the signaling network. As a general strategy, targeting the center of a negative feedback regulation in the host signaling network leads to the indirect regulation of multiple linked signaling pathways. When these indirect effects are beneficial or functionally silent, they may favor or not interfere with the evolutionary-driven selection process of the optimum host target. Conversely, when they turned out to be detrimental to the pathogen, they may contribute to counter-select a specific pathogenic strategy.

## 5. Conclusion

In conclusion, our data show that OspF has a complex impact on host signaling during infection. We found that, whereas OspF dephosphorylates p38, this effector potentiates the activation of JNK and NF-κB. This unexpected effect results from the disruption of a negative feedback loop between p38 and TAK1, which is mediated via the phosphorylation of TAB1 during infection. In addition, OspF inhibits c-Jun expression at the transcriptional level. Taken together, our data reveal new insights into the impact of OspF on host signaling during infection by *S. flexneri* and validate the use of bacterial effectors as molecular tools to identify the crosstalks that connect signaling pathways during bacterial infection.

## Acknowledgments

We thank Prof. A.R. Nebreda (CNIO, Madrid, Spain) for the generous gift of wt and $p38^{-/-}$ MEFs. We thank Dr. Hesso Farhan for comments on the manuscript. This work was funded by the Swiss National Science Foundation (grants 3100A0-113561 and 310030_1273361 to C.A.). C. Kasper was supported by the Werner-Siemens Foundation.

## References

[1] L.L. Bourhis, C. Werts, Microbes Infect. 9 (2007) 629–636.
[2] H. Kumar, T. Kawai, S. Akira, Biochem Biophys Res Commun. 388 (2009) 621–625.
[3] M. Kim, H. Ashida, M. Ogawa, Y. Yoshikawa, H. Mimuro, C. Sasakawa, Cell Host Microbe. 8 (2010) 20–35.
[4] L. Diacovich, J.P. Gorvel, Nat Rev Microbiol. 8 (2010) 117–128.
[5] J.E. Galan, Cell Host Microbe. 5 (2009) 571–579.
[6] G.N. Schroeder, H. Hilbi, Clin Microbiol Rev. 21 (2008) 134–156.
[7] H. Ashida, M. Ogawa, M. Kim, S. Suzuki, T. Sanada, C. Punginelli, H. Mimuro, C. Sasakawa, Curr Opin Microbiol (2010).
[8] T.A. Kufer, E. Kremmer, A.C. Adam, D.J. Philpott, P.J. Sansonetti, Cell Microbiol. 10 (2008) 477–486.
[9] F. Lafont, G. Tran Van Nhieu, K. Hanada, P. Sansonetti, F.G. van der Goot, Embo J. 21 (2002) 4449–4457.
[10] S.E. Girardin, I.G. Boneca, L.A. Carneiro, A. Antignac, M. Jehanno, J. Viala, K. Tedin, M.K. Taha, A. Labigne, U. Zahringer, A.J. Coyle, P.S. DiStefano, J. Bertin, P.J. Sansonetti, D.J. Philpott, Science. 300 (2003) 1584–1587.
[11] M. Hasegawa, Y. Fujimoto, P.C. Lucas, H. Nakano, K. Fukase, G. Nunez, N. Inohara, Embo J. 27 (2008) 373–383.
[12] J. Lee, L. Mira-Arbibe, R.J. Ulevitch, J Leukoc Biol. 68 (2000) 909–915.
[13] S. Sato, H. Sanjo, K. Takeda, J. Ninomiya-Tsuji, M. Yamamoto, T. Kawai, K. Matsumoto, O. Takeuchi, S. Akira, Nat Immunol. 6 (2005) 1087–1095.
[14] C. Wang, L. Deng, M. Hong, G.R. Akkaraju, J. Inoue, Z.J. Chen, Nature. 412 (2001) 346–351.
[15] M.L. Kim, H.G. Jeong, C.A. Kasper, C. Arrieumerlou, PLoS One 5 (2010) e15371.
[16] L. Arbibe, D.W. Kim, E. Batsche, T. Pedron, B. Mateescu, C. Muchardt, C. Parsot, P.J. Sansonetti, Nat Immunol. 8 (2007) 47–56.
[17] H. Li, H. Xu, Y. Zhou, J. Zhang, C. Long, S. Li, S. Chen, J.M. Zhou, F. Shao, Science. 315 (2007) 1000–1003.
[18] C.A. Kasper, I. Sorg, C. Schmutz, T. Tschon, H. Wischnewski, M.L. Kim, C. Arrieumerlou, Immunity. 33 (2010) 804–816.
[19] B. Neumann, M. Held, U. Liebel, H. Erfle, P. Rogers, R. Pepperkok, J. Ellenberg, Nat Meth. 3 (2006) 385–390.
[20] A.E. Carpenter, T.R. Jones, M.R. Lamprecht, C. Clarke, I.H. Kang, O. Friman, D.A. Guertin, J.H. Chang, R.A. Lindquist, J. Moffat, P. Golland, D.M. Sabatini, Genome Biol. 7 (2006) R100.
[21] I. Mattioli, A. Sebald, C. Bucher, R.P. Charles, H. Nakano, T. Doi, M. Kracht, M.L. Schmitz, J Immunol. 172 (2004) 6336–6344.
[22] S.E. Girardin, R. Tournebize, M. Mavris, A.L. Page, X. Li, G.R. Stark, J. Bertin, P.S. DiStefano, M. Yaniv, P.J. Sansonetti, D.J. Philpott, EMBO Rep. 2 (2001) 736–742.
[23] S. Makino, C. Sasakawa, K. Kamata, T. Kurata, M. Yoshikawa, Cell. 46 (1986) 551–555.
[24] L.A. Carneiro, L.H. Travassos, F. Soares, I. Tattoli, J.G. Magalhaes, M.T. Bozza, M.C. Plotkowski, P.J. Sansonetti, J.D. Molkentin, D.J. Philpott, S.E. Girardin, Cell Host Microbe. 5 (2009) 123–136.
[25] C. Ambrosino, G. Mace, S. Galban, C. Fritsch, K. Vintersten, E. Black, M. Gorospe, A.R. Nebreda, Mol Cell Biol. 23 (2003) 370–381.
[26] J. da Silva Correia, Y. Miranda, N. Leonard, J. Hsu, R.J. Ulevitch, Cell Death Differ. 14 (2007) 830–839.
[27] P. Singhirunnusorn, S. Suzuki, N. Kawasaki, I. Saiki, H. Sakurai, J Biol Chem. 280 (2005) 7359–7368.
[28] P.C. Cheung, D.G. Campbell, A.R. Nebreda, P. Cohen, Embo J. 22 (2003) 5793–5805.
[29] A.M. Musti, M. Treier, D. Bohmann, Science. 275 (1997) 400–402.
[30] K. Yasumoto, S. Okamoto, N. Mukaida, S. Murakami, M. Mai, K. Matsushima, J Biol Chem. 267 (1992) 22506–22511.
[31] D.W. Kim, G. Lenzen, A.L. Page, P. Legrain, P.J. Sansonetti, C. Parsot, Proc Natl Acad Sci U S A. 102 (2005) 14046–14051.
[32] H. Ashida, M. Kim, M. Schmidt-Supprian, A. Ma, M. Ogawa, C. Sasakawa, Nat Cell Biol 12 (2010) 66–73, sup pp 61–69.
[33] H.J. Newton, J.S. Pearson, L. Badea, M. Kelly, M. Lucas, G. Holloway, K.M. Wagstaff, M.A. Dunstone, J. Sloan, J.C. Whisstock, J.B. Kaper, R.M. Robins-Browne, D.A. Jans, G. Frankel, A.D. Phillips, B.S. Coulson, E.L. Hartland, PLoS Pathog 6 (2010) e1000898.
[34] C.A. Hazzalin, E. Cano, A. Cuenda, M.J. Barratt, P. Cohen, L.C. Mahadevan, Curr Biol. 6 (1996) 1028–1031.
[35] S. Nemoto, Z. Sheng, A. Lin, Mol Cell Biol. 18 (1998) 3518–3526.
[36] L. Hui, L. Bakiri, A. Mairhorfer, N. Schweifer, C. Haslinger, L. Kenner, V. Komnenovic, H. Scheuch, H. Beug, E.F. Wagner, Nat Genet. 39 (2007) 741–749.
[37] C. Nembrini, J. Kisielow, A.T. Shamshiev, L. Tortola, A.J. Coyle, M. Kopf, B.J. Marsland, J Biol Chem. 284 (2009) 19183–19188.
[38] C.S. Faherty, D.S. Merrell, C. Semino-Mora, A. Dubois, A.V. Ramaswamy, A.T. Maurelli, BMC Genomics 11 (2010) 272.
[39] J.J. Ventura, A. Hubner, C. Zhang, R.A. Flavell, K.M. Shokat, R.J. Davis, Mol Cell. 21 (2006) 701–710.
[40] P. Cheung, C.D. Allis, P. Sassone-Corsi, Cell. 103 (2000) 263–271.
[41] A.L. Clayton, S. Rose, M.J. Barratt, L.C. Mahadevan, Embo J. 19 (2000) 3714–3726.

# Abbreviations

| | |
|---|---|
| **Abl** | v-abl Abelson murine leukemia viral oncogene homolog |
| **AD** | acid transactivation domain |
| **Afa** | afimbrial adhesin |
| **AIM** | absent in melanoma |
| **Akt** | v-akt murine thymoma viral oncogene homolog |
| **AMP** | antimicrobial peptide |
| **AP-1** | activator protein 1 |
| **APC** | antigen-presenting cell |
| **ASC** | apoptosis-associated speck-like protein containing a CARD |
| **Atg** | autophagy related homolog |
| **BIR** | baculoviral inhibitory repeat |
| **cAMP** | cyclic adenosine monophosphate |
| **CARD** | caspase recruitment domain |
| **CCL** | chemokine (C-C motif) ligand |
| **Cdc** | cell division cycle |
| **cGMP** | cyclic guanosine monophosphate |
| **CHUK** | conserved helix-loop-helix ubiquitous kinase |
| **cIAP** | inhibitor of apoptosis protein homolog C |
| **CIITA** | MHC class II transactivator |
| **CLR** | C-type lectin receptor |
| **Crk** | v-crk sarcoma virus CT10 oncogene homolog |
| **Cx43** | Connexin43 |
| **CXCL** | chemokine (C-X-C motif) ligand |

| | |
|---|---|
| **DAMP** | danger-associated molecular pattern |
| **DC** | dendritic cell |
| **DILI** | drug-induced liver injury |
| **dsDNA** | double-stranded DNA |
| **EGF** | epidermal growth factor |
| **EGFP** | enhanced green fluorescent protein |
| **EGFR** | EGF receptor |
| **ER** | endoplasmatic reticulum |
| **ERK** | extracellular signal-regulated kinase |
| **Esp** | *E. coli* secreted protein |
| **F-actin** | filamentous actin |
| **FAK** | focal adhesion kinase |
| **FIIND** | function-to-find domain |
| **FKHR** | forkhead in rhabdomyosarcoma |
| **GAP** | GTPase-activating protein |
| **GEF** | guanine-nucleotide exchange factor |
| **GFP** | green fluorescent protein |
| **GSK3** | glycogen synthase kinase 3 |
| **GTPase** | guanosine triphosphatase |
| **HIN200** | hematopoietic expression, IFN-inducible, nuclear localization and length of 200 amino acids |
| **HPLC** | high-performance liquid chromatography |
| **IAP** | inhibitor of apoptosis protein |
| **Ics** | intracellular spread |
| **IEC** | intestinal epithelial cell |
| **iE-DAP** | $\gamma$-D-glutamyl-meso-diaminopimelic acid |
| **I$\kappa$B$\alpha$** | Inhibitor of NF-$\kappa$B $\alpha$ |
| **IKK** | inhibitor of $\kappa$ light polypeptide gene enhancer in B-cells kinase |
| **IL** | interleukin |
| **IL-8** | interleukin-8 |

| | |
|---|---|
| **INF** | interferon |
| **Inl** | internalin |
| **$IP_3$** | inositol-trisphosphate |
| **Ipa** | invasion plasmid antigens |
| **Ipg** | invasion plasmid gene |
| **IRAK** | IL-1 receptor-associated kinase |
| **IRF** | interferon regulatory factor |
| **ISGF** | interferon-stimulated gene factor |
| **JNK** | JUN N-terminal kinase |
| **LPS** | lipopolysaccharide |
| **LRR** | leucine-rich repeat |
| **M cells** | microfold cells |
| **Mad2L2** | mitotic arrest deficient 2-like protein 2 |
| **MAP2 kinase** | mitogen-activated protein kinase kinase |
| **MAP3 kinase** | mitogen-activated protein kinase kinase kinase |
| **MAP kinase** | mitogen-activated protein kinase |
| **MAVS** | mitochondrial antiviral signaling protein |
| **MD-2** | myeloid differentiation protein-2 |
| **MDP** | muramyl dipeptide |
| **MEFs** | mouse embryonic fibroblasts |
| **MEKK** | MAP/ERK kinase kinase |
| **Met** | met proto-oncogene |
| **MLC** | myosin light chain |
| **MOI** | multiplicity of infection |
| **MS/MS** | tandem mass spectrometry |
| **MSK** | mitogen- and stress-activated kinase |
| **MurNAc** | N-acetyl muramic acid |
| **Mxi** | membrane expression of Ipa |
| **MyD88** | myeloid differentiation primary response gene (88) |

| | |
|---|---|
| **NACHT** | domain present in NAIP, CIITA, HET-E and TP-1 |
| **NAD** | NACHT-associated domain |
| **NAIP** | neuronal apoptosis inhibitor protein |
| **NBD** | nucleotide-binding domain |
| **NEMO** | NF-$\kappa$B essential modulator |
| **NETs** | neutrophil extracellular traps |
| **NF-$\kappa$B** | nuclear factor of $\kappa$ light polypeptide gene enhancer in B-cells |
| **NK** | natural killer |
| **NLR** | Nod-like receptor |
| **NLRA** | acidic domain containing NLR |
| **NLRB** | BIR domain containing NLR |
| **NLRC** | CARD domain containing NLR |
| **NLRP** | pyrin domain containing NLR |
| **NLRX** | no strong N-terminal homology NLR |
| **Nod** | nucleotide-oligomerization domain |
| **N-WASP** | neural Wiskott-Aldrich syndrome protein |
| **Osp** | outer *Shigella* proteins |
| **PAMP** | pathogen-associated molecular pattern |
| **PGRP** | peptidoglycan recognition protein |
| **PI3K** | phosphoinositide-3-kinase |
| **PIP** | phosphatidylinositol-5-phosphate |
| **$PIP_2$** | phosphatidylinositol-4,5-bisphosphate |
| **PKA** | protein kinase A |
| **PKC** | protein kinase C |
| **PKG** | protein kinase G |
| **$PLA_2$** | phospholipase A2 |
| **PMN** | polymorphonuclear neutrophil |
| **PRR** | pathogen recognition receptor |
| **PtdIns** | phosphatidylinositol |

| | |
|---|---|
| **PYD** | pyrin domain |
| **Rac** | ras-related C3 botulinum toxin substrate |
| **Rho** | ras homolog |
| **RIP2** | receptor-interacting protein 2 |
| **RLR** | RIG-I-like receptor |
| **RNAi** | RNA interference |
| **ROI** | reactive oxygen intermediate |
| **ROS** | reactive oxygen species |
| **RpoS** | RNA polymerase sigma factor S, sigma 38 |
| **SCID** | severe combined immunodeficient |
| **SCV** | *Salmonella*-containing vacuole |
| **Sip** | *Salmonella* invasion protein |
| **siRNA** | small interfering RNA |
| **Spa** | surface presentation of antigen |
| **Src** | v-src sarcoma viral oncogene homolog |
| **ssRNA** | single-stranded RNA |
| **T3SS** | type III secretion system |
| **T4SS** | type IV secretion system |
| **TAB** | TAK1-binding protein |
| **TAK1** | Transforming growth factor-activated protein kinase 1 |
| **TBK1** | TANK-binding kinase 1 |
| **TIR** | Toll-IL-1 receptor |
| **TIRAP** | TIR domain containing adaptor protein |
| **TLR** | Toll-like receptor |
| **TNF** | tumor necrosis factor |
| **TRAF** | TNF receptor-associated factor |
| **TRAM** | TIR domain-containing adapter molecule |
| **TRIF** | TIR domain containing adaptor inducing interferon-$\beta$ |
| **U2AF** | U2 small nuclear RNA auxiliary factor |

| | |
|---|---|
| **UbcH5** | ubiquitin-conjugating enzyme E2 D1 |
| **UPEC** | uropathogenic *E. coli* |
| **Vir** | virulence |
| **WASP** | Wiskott-Aldrich syndrome protein |
| **YFP** | yellow fluorescent protein |

# References


[1] Jabes D. The antibiotic R&D pipeline: an update. *Current Opinion in Microbiology*, 14(5):564–569, 2011.

[2] Fischbach M. A. and Walsh C. T. Antibiotics for Emerging Pathogens. *Science*, 325(5944):1089–1093, 2009.

[3] Gudmundsson G. H., Bergman P., Andersson J., Raqib R. and Agerberth B. Battle and balance at mucosal surfaces – The story of Shigella and antimicrobial peptides. *Biochemical and Biophysical Research Communications*, 396(1):116–119, 2010.

[4] Kumar H., Kawai T. and Akira S. Pathogen Recognition by the Innate Immune System. *International Reviews of Immunology*, 30(1):16–34, 2011.

[5] Kawai T. and Akira S. Toll-like Receptors and Their Crosstalk with Other Innate Receptors in Infection and Immunity. *Immunity*, 34(5):637–650, 2011.

[6] Medzhitov R. Recognition of microorganisms and activation of the immune response. *Nature*, 449(7164):819–26, 2007.

[7] Takeuchi O. and Akira S. Pattern recognition receptors and inflammation. *Cell*, 140(6):805–20, 2010.

[8] Iwasaki A. and Medzhitov R. Regulation of Adaptive Immunity by the Innate Immune System. *Science*, 327(5963):291–295, 2010.

[9] Suzuki T., Franchi L., Toma C., Ashida H., Ogawa M., Yoshikawa Y., Mimuro H., Inohara N., Sasakawa C. and Nuñez G. Differential Regulation of Caspase-1 Activation, Pyroptosis, and Autophagy via Ipaf and ASC in *Shigella*-Infected Macrophages. *PLoS Pathog*, 3(8):e111, 2007.

[10] Lemaitre B., Nicolas E., Michaut L., Reichhart J. and Hoffmann J. A. The Dorsoventral Regulatory Gene Cassette spätzle/Toll/cactus Controls the Potent Antifungal Response in Drosophila Adults. *Cell*, 86(6):973–983, 1996.

[11] Medzhitov R., Preston-Hurlburt P. and Janeway C. A. A human homologue of the Drosophila Toll protein signals activation of adaptive immunity. *Nature*, 388(6640):394–397, 1997.

[12] Botos I., Segal D. and Davies D. The Structural Biology of Toll-like Receptors. *Structure*, 19(4):447–459, 2011.

[13] O'Neill L. The Toll/interleukin-1 receptor domain: a molecular switch for inflammation and host defence. *Biochemical Society Transactions*, 28(5):557–563, 2000.

[14] Shimazu R., Akashi S., Ogata H., Nagai Y., Fukudome K., Miyake K. and Kimoto M. MD-2, a Molecule that Confers Lipopolysaccharide Responsiveness on Toll-like Receptor 4. *The Journal of Experimental Medicine*, 189(11):1777–1782, 1999.

[15] Brinkmann M. M., Spooner E., Hoebe K., Beutler B., Ploegh H. L. and Kim Y.-M. The interaction between the ER membrane protein UNC93B and TLR3, 7, and 9 is crucial for TLR signaling. *The Journal of Cell Biology*, 177(2):265–275, 2007.

[16] Kim Y.-M., Brinkmann M. M., Paquet M.-E. and Ploegh H. L. UNC93B1 delivers nucleotide-sensing toll-like receptors to endolysosomes. *Nature*, 452(7184):234–238, 2008.

[17] Ewald S. E., Engel A., Lee J., Wang M., Bogyo M. and Barton G. M. Nucleic acid recognition by Toll-like receptors is coupled to stepwise processing by cathepsins and asparagine endopeptidase. *The Journal of Experimental Medicine*, 208(4):643–651, 2011.

[18] O'Neill L. A. J. and Bowie A. G. The family of five: TIR-domain-containing adaptors in Toll-like receptor signalling. *Nat Rev Immunol*, 7(5):353–364, 2007.

[19] Akira S. and Takeda K. Toll-like receptor signalling. *Nat Rev Immunol*, 4(7):499–511, 2004.

[20] Kawai T. and Akira S. The role of pattern-recognition receptors in innate immunity: update on Toll-like receptors. *Nat Immunol*, 11(5):373–384, 2010.

[21] Lien E., Means T., Heine H., Yoshimura A., Kusumoto S., Fukase K., Fenton M., Oikawa M., Qureshi N., Monks B., Finberg R., Ingalls R. and Golenbock D. Toll-like receptor 4 imparts ligand-specific recognition of bacterial lipopolysaccharide. *Journal of Clincal Investigation*, 105(4):497–504, 2000.

[22] Zähringer U., Lindner B., Inamura S., Heine H. and Alexander C. TLR2 - promiscuous or specific? A critical re-evaluation of a receptor expressing apparent broad specificity. *Immunobiology*, 213(3-4):205–224, 2008.

[23] Hayashi F., Smith K. D., Ozinsky A., Hawn T. R., Yi E. C., Goodlett D. R., Eng J. K., Akira S., Underhill D. M. and Aderem A. The innate immune response to bacterial flagellin is mediated by Toll-like receptor 5. *Nature*, 410(6832):1099–1103, 2001.

[24] Mancuso G., Gambuzza M., Midiri A., Biondo C., Papasergi S., Akira S., Teti G. and Beninati C. Bacterial recognition by TLR7 in the lysosomes of conventional dendritic cells. *Nat Immunol*, 10(6):587–594, 2009.

[25] Bauer S., Kirschning C. J., Häcker H., Redecke V., Hausmann S., Akira S., Wagner H. and Lipford G. B. Human TLR9 confers responsiveness to bacterial DNA via species-specific CpG motif recognition. *Proceedings of the National Academy of Sciences*, 98(16):9237–9242, 2001.

[26] Zhang D., Zhang G., Hayden M. S., Greenblatt M. B., Bussey C., Flavell R. A. and Ghosh S. A Toll-like Receptor That Prevents Infection by Uropathogenic Bacteria. *Science*, 303(5663):1522–1526, 2004.

[27] Holtmann H., Winzen R., Holland P., Eickemeier S., Hoffmann E., Wallach D., Malinin N. L., Cooper J. A., Resch K. and Kracht M. Induction of interleukin-8 synthesis integrates effects on transcription and mRNA degradation from at least three different cytokine- or stress-activated signal transduction pathways. *Mol Cell Biol*, 19(10):6742–53, 1999.

[28] Saccani S., Pantano S. and Natoli G. p38-Dependent marking of inflammatory genes for increased NF-kappa B recruitment. *Nat Immunol*, 3(1):69–75, 2002.

[29] Weiss D. S., Raupach B., Takeda K., Akira S. and Zychlinsky A. Toll-Like Receptors Are Temporally Involved in Host Defense. *The Journal of Immunology*, 172(7):4463–4469, 2004.

[30] Takeuchi O., Hoshino K. and Akira S. Cutting Edge: TLR2-Deficient and MyD88-Deficient Mice Are Highly Susceptible to Staphylococcus aureus Infection. *The Journal of Immunology*, 165(10):5392–5396, 2000.

[31] Picard C., Puel A., Bonnet M., Ku C.-L., Bustamante J., Yang K., Soudais C., Dupuis S., Feinberg J., Fieschi C., Elbim C., Hitchcock R., Lammas D., Davies G., Al-Ghonaium A., Al-Rayes H., Al-Jumaah S., Al-Hajjar S., Al-Mohsen I. Z., Frayha H. H., Rucker R., Hawn T. R., Aderem A., Tufenkeji H., Haraguchi S., Day N. K., Good R. A., Gougerot-Pocidalo M.-A., Ozinsky A. and Casanova J.-L. Pyogenic Bacterial Infections in Humans with IRAK-4 Deficiency. *Science*, 299(5615):2076–2079, 2003.

[32] von Bernuth H., Picard C., Jin Z., Pankla R., Xiao H., Ku C.-L., Chrabieh M., Mustapha I. B., Ghandil P., Camcioglu Y., Vasconcelos J., Sirvent N., Guedes M., Vitor A. B., Herrero-Mata M. J., Aróstegui J. I., Rodrigo C., Alsina L., Ruiz-Ortiz E., Juan M., Fortuny C., Yagüe J., Antón J., Pascal M., Chang H.-H., Janniere L., Rose Y., Garty B.-Z., Chapel H., Issekutz A., Maródi L., Rodriguez-Gallego C., Banchereau J., Abel L., Li X., Chaussabel D., Puel A. and Casanova J.-L. Pyogenic Bacterial Infections in Humans with MyD88 Deficiency. *Science*, 321(5889):691–696, 2008.

[33] Casanova J.-L., Abel L. and Quintana-Murci L. Human TLRs and IL-1Rs in Host Defense: Natural Insights from Evolutionary, Epidemiological, and Clinical Genetics. *Annual Review of Immunology*, 29(1):447–491, 2011.

[34] Fritz J. H., Girardin S. E., Fitting C., Werts C., Mengin-Lecreulx D., Caroff M., Cavaillon J.-M., Philpott D. J. and Adib-Conquy M. Synergistic stimulation of human monocytes and dendritic cells by Toll-like receptor 4 and NOD1- and NOD2-activating agonists. *European Journal of Immunology*, 35(8):2459–2470, 2005.

[35] Fritz J. H., Ferrero R. L., Philpott D. J. and Girardin S. E. Nod-like proteins in immunity, inflammation and disease. *Nat Immunol*, 7(12):1250–1257, 2006.

[36] Elinav E., Strowig T., Henao-Mejia J. and Flavell R. Regulation of the Antimicrobial Response by NLR Proteins. *Immunity*, 34(5):665–679, 2011.

[37] Bauernfeind F., Ablasser A., Bartok E., Kim S., Schmid-Burgk J., Cavlar T. and Hornung V. Inflammasomes: current understanding and open questions. *Cellular and Molecular Life Sciences*, 68:765–783, 2011.

[38] Werts C., Rubino S., Ling A., Girardin S. E. and Philpott D. J. Nod-like receptors in intestinal homeostasis, inflammation, and cancer. *Journal of Leukocyte Biology*, 90(3):471–482, 2011.

[39] Ting J. P.-Y., Lovering R. C., Alnemri E. S., Bertin J., Boss J. M., Davis B. K., Flavell R. A., Girardin S. E., Godzik A., Harton J. A., Hoffman H. M., Hugot J.-P., Inohara N., MacKenzie A., Maltais L. J., Nunez G., Ogura Y., Otten L. A., Philpott D., Reed J. C., Reith W., Schreiber S., Steimle V. and Ward P. A. The NLR Gene Family: A Standard Nomenclature. *Immunity*, 28(3):285–287, 2008.

[40] Bertin J., Nir W.-J., Fischer C. M., Tayber O. V., Errada P. R., Grant J. R., Keilty J. J., Gosselin M. L., Robison K. E., Wong G. H. W., Glucksmann M. A. and DiStefano P. S. Human CARD4 Protein Is a Novel CED-4/Apaf-1 Cell Death Family Member That Activates NF-kappaB. *Journal of Biological Chemistry*, 274(19):12955–12958, 1999.

[41] Inohara N., Koseki T., del Peso L., Hu Y., Yee C., Chen S., Carrio R., Merino J., Liu D., Ni J. and Núñez G. Nod1, an Apaf-1-like Activator of Caspase-9 and Nuclear Factor-kappaB. *Journal of Biological Chemistry*, 274(21):14560–14567, 1999.

[42] Ogura Y., Bonen D. K., Inohara N., Nicolae D. L., Chen F. F., Ramos R., Britton H., Moran T., Karaliuskas R., Duerr R. H., Achkar J. P., Brant S. R., Bayless T. M., Kirschner B. S., Hanauer S. B., Nunez G. and Cho J. H. A frameshift mutation in NOD2 associated with susceptibility to Crohn's disease. *Nature*, 411(6837):603–6, 2001.

[43] Girardin S. E., Tournebize R., Mavris M., Page A. L., Li X., Stark G. R., Bertin J., DiStefano P. S., Yaniv M., Sansonetti P. J. and Philpott D. J. CARD4/Nod1 mediates NF-kappaB and JNK activation by invasive Shigella flexneri. *EMBO Rep*, 2(8):736–42, 2001.

[44] Girardin S. E., Boneca I. G., Carneiro L. A., Antignac A., Jehanno M., Viala J., Tedin K., Taha M. K., Labigne A., Zahringer U., Coyle A. J., DiStefano P. S., Bertin J., Sansonetti P. J. and Philpott D. J. Nod1 detects a unique muropeptide from gram-negative bacterial peptidoglycan. *Science*, 300(5625):1584–7, 2003.

[45] Chamaillard M., Hashimoto M., Horie Y., Masumoto J., Qiu S., Saab L., Ogura Y., Kawasaki A., Fukase K., Kusumoto S., Valvano M. A., Foster S. J., Mak T. W., Nunez G. and Inohara N. An essential role for NOD1 in host recognition of bacterial peptidoglycan containing diaminopimelic acid. *Nat Immunol*, 4(7):702–707, 2003.

[46] Girardin S. E., Boneca I. G., Viala J., Chamaillard M., Labigne A., Thomas G., Philpott D. J. and Sansonetti P. J. Nod2 is a general sensor of peptidoglycan through muramyl dipeptide (MDP) detection. *J Biol Chem*, 278(11):8869–72, 2003.

[47] Inohara N., Ogura Y., Fontalba A., Gutierrez O., Pons F., Crespo J., Fukase K., Inamura S., Kusumoto S., Hashimoto M., Foster S. J., Moran A. P., Fernandez-Luna J. L. and Núñez G. Host Recognition of Bacterial Muramyl Dipeptide Mediated through NOD2. *Journal of Biological Chemistry*, 278(8):5509–5512, 2003.

[48] Kobayashi K. S., Chamaillard M., Ogura Y., Henegariu O., Inohara N., Núñez G. and Flavell R. A. Nod2-Dependent Regulation of Innate and Adaptive Immunity in the Intestinal Tract. *Science*, 307(5710):731–734, 2005.

[49] Opitz B., Püschel A., Beermann W., Hocke A. C., Förster S., Schmeck B., van Laak V., Chakraborty T., Suttorp N. and Hippenstiel S. Listeria monocytogenes Activated p38 MAPK and Induced IL-8 Secretion in a Nucleotide-Binding Oligomerization Domain 1-Dependent Manner in Endothelial Cells. *The Journal of Immunology*, 176(1):484–490, 2006.

[50] Viala J., Chaput C., Boneca I. G., Cardona A., Girardin S. E., Moran A. P., Athman R., Memet S., Huerre M. R., Coyle A. J., DiStefano P. S., Sansonetti P. J., Labigne A., Bertin J., Philpott D. J. and Ferrero R. L. Nod1 responds to peptidoglycan delivered by the Helicobacter pylori cag pathogenicity island. *Nat Immunol*, 5(11):1166–1174, 2004.

[51] Lee J., Tattoli I., Wojtal K. A., Vavricka S. R., Philpott D. J. and Girardin S. E. pH-dependent Internalization of Muramyl Peptides from Early Endosomes Enables Nod1 and Nod2 Signaling. *Journal of Biological Chemistry*, 284(35):23818–23829, 2009.

[52] Marina-García N., Franchi L., Kim Y.-G., Hu Y., Smith D. E., Boons G.-J. and Núñez G. Clathrin- and Dynamin-Dependent Endocytic Pathway Regulates Muramyl Dipeptide Internalization and NOD2 Activation. *The Journal of Immunology*, 182(7):4321–4327, 2009.

[53] Vavricka S. R., Musch M. W., Chang J. E., Nakagawa Y., Phanvijhitsiri K., Waypa T. S., Merlin D., Schneewind O. and Chang E. B. hPepT1 transports muramyl dipeptide, activating NF-kappaB and stimulating IL-8 secretion in human colonic Caco2/bbe cells. *Gastroenterology*, 127(5):1401–1409, 2004.

[54] Swaan P. W., Bensman T., Bahadduri P. M., Hall M. W., Sarkar A., Bao S., Khantwal C. M., Ekins S. and Knoell D. L. Bacterial Peptide Recognition and Immune Activation Facilitated by Human Peptide Transporter PEPT2. *Am J Respir Cell Mol Biol*, 39(5):536–542, 2008.

[55] Kufer T. A., Kremmer E., Adam A. C., Philpott D. J. and Sansonetti P. J. The pattern-recognition molecule Nod1 is localized at the plasma membrane at sites of bacterial interaction. *Cell Microbiol*, 10(2):477–86, 2008.

[56] Barnich N., Aguirre J. E., Reinecker H.-C., Xavier R. and Podolsky D. K. Membrane recruitment of NOD2 in intestinal epithelial cells is essential for nuclear factor-kappaB activation in muramyl dipeptide recognition. *The Journal of Cell Biology*, 170(1):21–26, 2005.

[57] Ogura Y., Inohara N., Benito A., Chen F. F., Yamaoka S. and Núñez G. Nod2, a Nod1/Apaf-1 Family Member That Is Restricted to Monocytes and Activates NF-kappaB. *Journal of Biological Chemistry*, 276(7):4812–4818, 2001.

[58] Park J.-H., Kim Y.-G., McDonald C., Kanneganti T.-D., Hasegawa M., Body-Malapel M., Inohara N. and Núñez G. RICK/RIP2 Mediates Innate Immune Responses Induced through Nod1 and Nod2 but Not TLRs. *The Journal of Immunology*, 178(4):2380–2386, 2007.

[59] Hasegawa M., Fujimoto Y., Lucas P. C., Nakano H., Fukase K., Nunez G. and Inohara N. A critical role of RICK/RIP2 polyubiquitination in Nod-induced NF-kappaB activation. *EMBO J*, 27(2):373–83, 2008.

[60] Krieg A., Correa R. G., Garrison J. B., Le Negrate G., Welsh K., Huang Z., Knoefel W. T. and Reed J. C. XIAP mediates NOD signaling via interaction with RIP2. *Proceedings of the National Academy of Sciences*, 106(34):14524–14529, 2009.

[61] Bertrand M. J., Doiron K., Labbé K., Korneluk R. G., Barker P. A. and Saleh M. Cellular Inhibitors of Apoptosis cIAP1 and cIAP2 Are Required for Innate Immunity Signaling by the Pattern Recognition Receptors NOD1 and NOD2. *Immunity*, 30(6):789–801, 2009.

[62] McCarthy J. V., Ni J. and Dixit V. M. RIP2 Is a Novel NF-kappaB-activating and Cell Death-inducing Kinase. *Journal of Biological Chemistry*, 273(27):16968–16975, 1998.

[63] Strober W., Murray P. J., Kitani A. and Watanabe T. Signalling pathways and molecular interactions of NOD1 and NOD2. *Nat Rev Immunol*, 6(1):9–20, 2006.

[64] Allison C. C., Kufer T. A., Kremmer E., Kaparakis M. and Ferrero R. L. Helicobacter pylori Induces MAPK Phosphorylation and AP-1 Activation via a NOD1-Dependent Mechanism. *The Journal of Immunology*, 183(12):8099–8109, 2009.

[65] Welter-Stahl L., Ojcius D. M., Viala J., Girardin S., Liu W., Delarbre C., Philpott D., Kelly K. A. and Darville T. Stimulation of the cytosolic receptor for peptidoglycan, Nod1, by infection with Chlamydia trachomatis or Chlamydia muridarum. *Cellular Microbiology*, 8(6):1047–1057, 2006.

[66] Masumoto J., Yang K., Varambally S., Hasegawa M., Tomlins S. A., Qiu S., Fujimoto Y., Kawasaki A., Foster S. J., Horie Y., Mak T. W., Núñez G., Chinnaiyan A. M., Fukase K. and Inohara N. Nod1 acts as an intracellular receptor to stimulate chemokine production and neutrophil recruitment in vivo. *The Journal of Experimental Medicine*, 203(1):203–213, 2006.

[67] Uehara A., Fujimoto Y., Fukase K. and Takada H. Various human epithelial cells express functional Toll-like receptors, NOD1 and NOD2 to produce anti-microbial peptides, but not proinflammatory cytokines. *Molecular Immunology*, 44(12):3100–3111, 2007.

[68] Sabbah A., Chang T. H., Harnack R., Frohlich V., Tominaga K., Dube P. H., Xiang Y. and Bose S. Activation of innate immune antiviral responses by Nod2. *Nat Immunol*, 10(10):1073–1080, 2009.

[69] Watanabe T., Asano N., Fichtner-Feigl S., Gorelick P. L., Tsuji Y., Matsumoto Y., Chiba T., Fuss I. J., Kitani A. and Strober W. NOD1 contributes to mouse host defense against Helicobacter pylori via induction of type I IFN and activation of the ISGF3 signaling pathway. *The Journal of Clinical Investigation*, 120(5):1645–1662, 2010.

[70] Watanabe T., Asano N., Kitani A., Fuss I. J., Chiba T. and Strober W. NOD1-Mediated Mucosal Host Defense against Helicobacter pylori. *International Journal of Inflammation*, 2010:476–482, 2010.

[71] Hitotsumatsu O., Ahmad R.-C., Tavares R., Wang M., Philpott D., Turer E. E., Lee B. L., Shiffin N., Advincula R., Malynn B. A., Werts C. and Ma A. The Ubiquitin-Editing Enzyme A20 Restricts Nucleotide-Binding Oligomerization Domain Containing 2-Triggered Signals. *Immunity*, 28(3):381–390, 2008.

[72] Rosenstiel P., Huse K., Till A., Hampe J., Hellmig S., Sina C., Billmann S., von Kampen O., Waetzig G. H., Platzer M., Seegert D. and Schreiber S. A short isoform of NOD2/CARD15, NOD2-S, is an endogenous inhibitor of NOD2/receptor-interacting protein kinase 2-induced signaling pathways. *Proceedings of the National Academy of Sciences of the United States of America*, 103(9):3280–3285, 2006.

[73] McDonald C., Chen F. F., Ollendorff V., Ogura Y., Marchetto S., Lécine P., Borg J.-P. and Núñez G. A Role for Erbin in the Regulation of Nod2-dependent NF-kappaB Signaling. *Journal of Biological Chemistry*, 280(48):40301–40309, 2005.

[74] LeBlanc P. M., Yeretssian G., Rutherford N., Doiron K., Nadiri A., Zhu L., Green D. R., Gruenheid S. and Saleh M. Caspase-12 Modulates NOD Signaling and Regulates Antimicrobial Peptide Production and Mucosal Immunity. *Cell Host Microbe*, 3(3):146–157, 2008.

[75] Clark N. M., Marinis J. M., Cobb B. A. and Abbott D. W. MEKK4 Sequesters RIP2 to Dictate NOD2 Signal Specificity. *Curr Biol*, 18(18):1402–1408, 2008.

[76] Franchi L., Warner N., Viani K. and Núñez G. Function of Nod-like receptors in microbial recognition and host defense. *Immunological Reviews*, 227(1):106–128, 2009.

[77] Travassos L. H., Carneiro L. A. M., Ramjeet M., Hussey S., Kim Y.-G., Magalhaes J. G., Yuan L., Soares F., Chea E., Le Bourhis L., Boneca I. G., Allaoui A., Jones N. L., Nunez G., Girardin S. E. and Philpott D. J. Nod1 and Nod2 direct autophagy by recruiting ATG16L1 to the plasma membrane at the site of bacterial entry. *Nat Immunol*, 11(1):55–62, 2010.

[78] Cooney R., Baker J., Brain O., Danis B., Pichulik T., Allan P., Ferguson D. J. P., Campbell B. J., Jewell D. and Simmons A. NOD2 stimulation induces autophagy in dendritic cells influencing bacterial handling and antigen presentation. *Nat Med*, 16(1):90–97, 2010.

[79] Clarke T. B., Davis K. M., Lysenko E. S., Zhou A. Y., Yu Y. and Weiser J. N. Recognition of peptidoglycan from the microbiota by Nod1 enhances systemic innate immunity. *Nat Med*, 16(2):228–231, 2010.

[80] Ogawa T., Kotani S. and Shimauchi H. Enhancement of serum antibody production in mice by oral administration of lipophilic derivatives of muramylpeptides and bacterial lipopolysaccharides with bovine serum albumin. *Methods Find Exp Clin Pharmacol*, 8(1):19–26, 1986.

[81] Heinzelmann M., Jr. H. C. P., Chernobelsky A., Stites T. P. and Gordon L. E. Endotoxin and muramyl dipeptide modulate surface receptor expression on human mononuclear cells. *Immunopharmacology*, 48(2):117–128, 2000.

[82] Todate A., Suda T., Kuwata H., Chida K. and Nakamura H. Muramyl dipeptide-Lys stimulates the function of human dendritic cells. *Journal of Leukocyte Biology*, 70(5):723–729, 2001.

[83] Fritz J. H., Bourhis L. L., Sellge G., Magalhaes J. G., Fsihi H., Kufer T. A., Collins C., Viala J., Ferrero R. L., Girardin S. E. and Philpott D. J. Nod1-Mediated Innate Immune Recognition of Peptidoglycan Contributes to the Onset of Adaptive Immunity. *Immunity*, 26(4):445–459, 2007.

[84] da Silva Correia J., Miranda Y., Austin-Brown N., Hsu J., Mathison J., Xiang R., Zhou H., Li Q., Han J. and Ulevitch R. J. Nod1-dependent control of tumor growth. *Proceedings of the National Academy of Sciences of the United States of America*, 103(6):1840–1845, 2006.

[85] Cruickshank S. M., Wakenshaw L., Cardone J., Howdle P. D., Murray P. J. and Carding S. R. Evidence for the involvement of NOD2 in regulating colonic epithelial cell growth and survival. *World J Gastroenterol*, 14(38):5834–5841, 2008.

[86] Martinon F., Burns K. and Tschopp J. The Inflammasome: A Molecular Platform Triggering Activation of Inflammatory Caspases and Processing of proIL-beta. *Molecular Cell*, 10(2):417–426, 2002.

[87] Davis B. K., Roberts R. A., Huang M. T., Willingham S. B., Conti B. J., Brickey W. J., Barker B. R., Kwan M., Taxman D. J., Accavitti-Loper M., Duncan J. A. and Ting J. P.-Y. Cutting Edge: NLRC5-Dependent Activation of the Inflammasome. *The Journal of Immunology*, 186(3):1333–1337, 2011.

[88] Schroder K. and Tschopp J. The Inflammasomes. *Cell*, 140(6):821–832, 2010.

[89] Boyden E. D. and Dietrich W. F. Nalp1b controls mouse macrophage susceptibility to anthrax lethal toxin. *Nat Genet*, 38(2):240–244, 2006.

[90] Bruey J.-M., Bruey-Sedano N., Luciano F., Zhai D., Balpai R., Xu C., Kress C. L., Bailly-Maitre B., Li X., Osterman A., ichi Matsuzawa S., Terskikh A. V., Faustin B. and Reed J. C. Bcl-2 and Bcl-XL Regulate Proinflammatory Caspase-1 Activation byăInteraction with NALP1. *Cell*, 129(1):45–56, 2007.

[91] Franchi L., Amer A., Body-Malapel M., Kanneganti T.-D., Ozoren N., Jagirdar R., Inohara N., Vandenabeele P., Bertin J., Coyle A., Grant E. P. and Nunez G. Cytosolic flagellin requires Ipaf for activation of caspase-1 and interleukin 1[beta] in salmonella-infected macrophages. *Nat Immunol*, 7(6):576–582, 2006.

[92] Miao E. A., Mao D. P., Yudkovsky N., Bonneau R., Lorang C. G., Warren S. E., Leaf I. A. and Aderem A. Innate immune detection of the type III secretion apparatus through the NLRC4 inflammasome. *Proceedings of the National Academy of Sciences*, 107(7):3076–3080, 2010.

[93] Zhao Y., Yang J., Shi J., Gong Y.-N., Lu Q., Xu H., Liu L. and Shao F. The NLRC4 inflammasome receptors for bacterial flagellin and type III secretion apparatus. *Nature*, 477(7366):596–600, 2011.

[94] Mariathasan S., Weiss D. S., Newton K., McBride J., O'Rourke K., Roose-Girma M., Lee W. P., Weinrauch Y., Monack D. M. and Dixit V. M. Cryopyrin activates the inflammasome in response to toxins and ATP. *Nature*, 440(7081):228–232, 2006.

[95] Martinon F., Petrilli V., Mayor A., Tardivel A. and Tschopp J. Gout-associated uric acid crystals activate the NALP3 inflammasome. *Nature*, 440(7081):237–241, 2006.

[96] Dostert C., Pétrilli V., Van Bruggen R., Steele C., Mossman B. T. and Tschopp J. Innate Immune Activation Through Nalp3 Inflammasome Sensing of Asbestos and Silica. *Science*, 320(5876):674–677, 2008.

[97] Hornung V., Ablasser A., Charrel-Dennis M., Bauernfeind F., Horvath G., Caffrey D. R., Latz E. and Fitzgerald K. A. AIM2 recognizes cytosolic dsDNA and forms a caspase-1-activating inflammasome with ASC. *Nature*, 458(7237):514–518, 2009.

[98] Fernandes-Alnemri T., Yu J.-W., Datta P., Wu J. and Alnemri E. S. AIM2 activates the inflammasome and cell death in response to cytoplasmic DNA. *Nature*, 458(7237):509–513, 2009.

[99] Arend W. P., Palmer G. and Gabay C. IL-1, IL-18, and IL-33 families of cytokines. *Immunological Reviews*, 223(1):20–38, 2008.

[100] Faustin B., Lartigue L., Bruey J.-M., Luciano F., Sergienko E., Bailly-Maitre B., Volkmann N., Hanein D., Rouiller I. and Reed J. C. Reconstituted NALP1 Inflammasome Reveals Two-Step Mechanism of Caspase-1 Activation. *Molecular Cell*, 25(5):713–724, 2007.

[101] Hsu L.-C., Ali S. R., McGillivray S., Tseng P.-H., Mariathasan S., Humke E. W., Eckmann L., Powell J. J., Nizet V., Dixit V. M. and Karin M. A NOD2-NALP1 complex mediates caspase-1-dependent IL-1beta secretion in response to Bacillus anthracis infection and muramyl dipeptide. *Proceedings of the National Academy of Sciences*, 105(22):7803–7808, 2008.

[102] Mariathasan S., Newton K., Monack D. M., Vucic D., French D. M., Lee W. P., Roose-Girma M., Erickson S. and Dixit V. M. Differential activation of the inflammasome by caspase-1 adaptors ASC and Ipaf. *Nature*, 430(6996):213–218, 2004.

[103] Zamboni D. S., Kobayashi K. S., Kohlsdorf T., Ogura Y., Long E. M., Vance R. E., Kuida K., Mariathasan S., Dixit V. M., Flavell R. A., Dietrich W. F. and Roy C. R. The Birc1e cytosolic pattern-recognition receptor contributes to the detection and control of Legionella pneumophila infection. *Nat Immunol*, 7(3):318–325, 2006.

[104] Harder J., Franchi L., Muñoz-Planillo R., Park J.-H., Reimer T. and Núñez G. Activation of the Nlrp3 Inflammasome by Streptococcus pyogenes Requires Streptolysin O and NF-kappaB Activation but Proceeds Independently of TLR Signaling and P2X7 Receptor. *The Journal of Immunology*, 183(9):5823–5829, 2009.

[105] Mishra B. B., Moura-Alves P., Sonawane A., Hacohen N., Griffiths G., Moita L. F. and Anes E. Mycobacterium tuberculosis protein ESAT-6 is a potent activator of the NLRP3/ASC inflammasome. *Cellular Microbiology*, 12(8):1046–1063, 2010.

[106] Rathinam V. A. K., Jiang Z., Waggoner S. N., Sharma S., Cole L. E., Waggoner L., Vanaja S. K., Monks B. G., Ganesan S., Latz E., Hornung V., Vogel S. N., Szomolanyi-Tsuda E. and Fitzgerald K. A. The AIM2 inflammasome is essential for host defense against cytosolic bacteria and DNA viruses. *Nat Immunol*, 11(5):395–402, 2010.

[107] Lamkanfi M., Walle L. V. and Kanneganti T.-D. Deregulated inflammasome signaling in disease. *Immunological Reviews*, 243(1):163–173, 2011.

[108] Zaki M. H., Boyd K. L., Vogel P., Kastan M. B., Lamkanfi M. and Kanneganti T.-D. The NLRP3 Inflammasome Protects against Loss of Epithelial Integrity and Mortality during Experimental Colitis. *Immunity*, 32(3):379–391, 2010.

[109] Villani A.-C., Lemire M., Fortin G., Louis E., Silverberg M. S., Collette C., Baba N., Libioulle C., Belaiche J., Bitton A., Gaudet D., Cohen A., Langelier D., Fortin P. R., Wither J. E., Sarfati M., Rutgeerts P., Rioux J. D., Vermeire S., Hudson T. J. and Franchimont D. Common variants in the NLRP3 region contribute to Crohn's disease susceptibility. *Nat Genet*, 41(1):71–76, 2009.

[110] Schroder K., Zhou R. and Tschopp J. The NLRP3 Inflammasome: A Sensor for Metabolic Danger? *Science*, 327(5963):296–300, 2010.

[111] Larsen C. M., Faulenbach M., Vaag A., Vølund A., Ehses J. A., Seifert B., Mandrup-Poulsen T. and Donath M. Y. Interleukin-1–Receptor Antagonist in Type 2 Diabetes Mellitus. *New England Journal of Medicine*, 356(15):1517–1526, 2007.

[112] Jin Y., Mailloux C. M., Gowan K., Riccardi S. L., LaBerge G., Bennett D. C., Fain P. R. and Spritz R. A. NALP1 in Vitiligo-Associated Multiple Autoimmune Disease. *New England Journal of Medicine*, 356(12):1216–1225, 2007.

[113] Zurawek M., Fichna M., Januszkiewicz-Lewandowska D., Gryczynska M., Fichna P. and Nowak J. A coding variant in NLRP1 is associated with autoimmune Addison's disease. *Human Immunology*, 71(5):530–534, 2010.

[114] Pore D., Mahata N., Pal A. and Chakrabarti M. K. 34 kDa MOMP of Shigella flexneri promotes TLR2 mediated macrophage activation with the engagement of NF-kappaB and p38 MAP kinase signaling. *Molecular Immunology*, 47(9):1739–1746, 2010.

[115] Biswas A., Banerjee P., Mukherjee G. and Biswas T. Porin of Shigella dysenteriae activates mouse peritoneal macrophage through Toll-like receptors 2 and 6 to induce polarized type I response. *Molecular Immunology*, 44(5):812–820, 2007.

[116] Rallabhandi P., Awomoyi A., Thomas K. E., Phalipon A., Fujimoto Y., Fukase K., Kusumoto S., Qureshi N., Sztein M. B. and Vogel S. N. Differential Activation of Human TLR4 by Escherichia coli and Shigella flexneri 2a Lipopolysaccharide: Combined Effects of Lipid A Acylation State and TLR4 Polymorphisms on Signaling. *The Journal of Immunology*, 180(2):1139–1147, 2008.

[117] Nonaka T., Kuwabara T., Mimuro H., Kuwae A. and Imajoh-Ohmi S. Shigella-induced necrosis and apoptosis of U937 cells and J774 macrophages. *Microbiology*, 149(9):2513–2527, 2003.

[118] Suzuki T., Nakanishi K., Tsutsui H., Iwai H., Akira S., Inohara N., Chamaillard M., Nuñez G. and Sasakawa C. A Novel Caspase-1/Toll-like Receptor 4-independent Pathway of Cell Death Induced by Cytosolic Shigella in Infected Macrophages. *Journal of Biological Chemistry*, 280(14):14042–14050, 2005.

[119] Pédron T., Thibault C. and Sansonetti P. J. The invasive phenotype of Shigella flexneri directs a distinct gene expression pattern in the human intestinal epithelial cell line Caco-2. *J Biol Chem*, 278(36):33878–86, 2003.

[120] Fukazawa A., Alonso C., Kurachi K., Gupta S., Lesser C. F., McCormick B. A. and Reinecker H.-C. GEF-H1 Mediated Control of NOD1 Dependent NF-kB Activation by Shigella Effectors. *PLoS Pathog*, 4(11):e1000228, 2008.

[121] Wang C., Deng L., Hong M., Akkaraju G. R., Inoue J. and Chen Z. J. TAK1 is a ubiquitin-dependent kinase of MKK and IKK. *Nature*, 412(6844):346–51, 2001.

[122] Kohler H., Rodrigues S. P. and McCormick B. A. Shigella flexneri Interactions with the Basolateral Membrane Domain of Polarized Model Intestinal Epithelium: Role of Lipopolysaccharide in Cell Invasion and in Activation of the Mitogen-Activated Protein Kinase ERK. *Infect Immun*, 70(3):1150–8, 2002.

[123] Sansonetti P. J., Arondel J., Huerre M., Harada A. and Matsushima K. Interleukin-8 controls bacterial transepithelial translocation at the cost of epithelial destruction in experimental shigellosis. *Infect Immun*, 67(3):1471–80, 1999.

[124] Shim D.-H., Ryu S. and Kweon M.-N. Defensins play a crucial role in protecting mice against oral Shigella flexneri infection. *Biochemical and Biophysical Research Communications*, 401(4):554–560, 2010.

[125] Arbibe L., Kim D. W., Batsche E., Pedron T., Mateescu B., Muchardt C., Parsot C. and Sansonetti P. J. An injected bacterial effector targets chromatin access for transcription factor NF-kappaB to alter transcription of host genes involved in immune responses. *Nat Immunol*, 8(1):47–56, 2007.

[126] Li H., Xu H., Zhou Y., Zhang J., Long C., Li S., Chen S., Zhou J. M. and Shao F. The phosphothreonine lyase activity of a bacterial type III effector family. *Science*, 315(5814):1000–3, 2007.

[127] Trofa A. F., Ueno-Olsen H., Oiwa R. and Yoshikawa M. Dr. Kiyoshi Shiga: Discoverer of the Dysentery Bacillus. *Clinical Infectious Diseases*, 29(5):1303–1306, 1999.

[128] Shiga K. Sekiri byogen kenkyu hokoku dai-ichi (first report on etiologic research on dysentery). *Saikingaku Zasshi*, 25:790Ű810., 1897.

[129] Shiga K. Ueber den Erreger der Dysenterie in Japan. *Zentralbl Bakteriol Microbiol Hyg*, 23:599–600, 1898.

[130] Kotloff K., Winickoff J., Ivanoff B., Clemens J., Swerdlow D., Sansonetti P., Adak G. and MM. L. Global burden of Shigella infections: implications for vaccine development and implementation of control strategies. *Bull World Health Organ.*, 77(8):651–66, 1999.

[131] DuPont H. L., Levine M. M., Hornick R. B. and Formal S. B. Inoculum Size in Shigellosis and Implications for Expected Mode of Transmission. *The Journal of Infectious Diseases*, 159(6):pp. 1126–1128, 1989.

[132] Kosek M., Yori P. P. and Olortegui M. P. Shigellosis update: advancing antibiotic resistance, investment empowered vaccine development, and green bananas. *Current Opinion in Infectious Diseases*, 23(5):475–480, 2010.

[133] Levine M. M., Kotloff K. L., Barry E. M., Pasetti M. F. and Sztein M. B. Clinical trials of Shigella vaccines: two steps forward and one step back on a long, hard road. *Nat Rev Micro*, 5(7):540–553, 2007.

[134] Buchrieser C., Glaser P., Rusniok C., Nedjari H., d'Hauteville H., Kunst F., Sansonetti P. and Parsot C. The virulence plasmid pWR100 and the repertoire of proteins secreted by the type III secretion apparatus of Shigella flexneri. *Molecular Microbiology*, 38(4):760–771, 2000.

[135] Schroeder G. N. and Hilbi H. Molecular pathogenesis of Shigella spp.: controlling host cell signaling, invasion, and death by type III secretion. *Clin Microbiol Rev*, 21(1):134–56, 2008.

[136] Tobe T., Nagai S., Okada N., Adter B., Yoshikawa M. and Sasakawa C. Temperature-regulated expression of invasion genes in Shigella flexneri is controlled through the transcriptional activation of the virB gene on the large plasmid. *Molecular Microbiology*, 5(4):887–893, 1991.

[137] Le Gall T., Mavris M., Martino M. C., Bernardini M. L., Denamur E. and Parsot C. Analysis of virulence plasmid gene expression defines three classes of effectors in the type III secretion system of Shigella flexneri. *Microbiology*, 151(3):951–962, 2005.

[138] Parsot C., Ageron E., Penno C., Mavris M., Jamoussi K., D'Hauteville H., Sansonetti P. and Demers B. A secreted anti-activator, OspD1, and its chaperone, Spa15, are involved in the control of transcription by the type III secretion apparatus activity in Shigella flexneri. *Molecular Microbiology*, 56(6):1627–1635, 2005.

[139] Blocker A., Gounon P., Larquet E., Niebuhr K., Cabiaux V., Parsot C. and Sansonetti P. The Tripartite Type III Secreton of Shigella flexneri Inserts Ipab and Ipac into Host Membranes. *The Journal of Cell Biology*, 147(3):683–693, 1999.

[140] Cornelis G. R. The type III secretion injectisome. *Nat Rev Microbiol*, 4(11):811–25, 2006.

[141] Schuch R. and Maurelli A. T. The Mxi-Spa Type III Secretory Pathway of Shigella flexneri Requires an Outer Membrane Lipoprotein, MxiM, for Invasin Translocation. *Infection and Immunity*, 67(4):1982–1991, 1999.

[142] Schuch R. and Maurelli A. T. MxiM and MxiJ, Base Elements of the Mxi-Spa Type III Secretion System of Shigella, Interact with and Stabilize the MxiD Secretin in the Cell Envelope. *Journal of Bacteriology*, 183(24):6991–6998, 2001.

[143] Blocker A., Jouihri N., Larquet E., Gounon P., Ebel F., Parsot C., Sansonetti P. and Allaoui A. Structure and composition of the Shigella flexneri 'needle complex', a part of its type III secreton. *Molecular Microbiology*, 39(3):652–663, 2001.

[144] Morita-Ishihara T., Ogawa M., Sagara H., Yoshida M., Katayama E. and Sasakawa C. Shigella Spa33 Is an Essential C-ring Component of Type III Secretion Machinery. *Journal of Biological Chemistry*, 281(1):599–607, 2006.

[145] Venkatesan M. M., Buysse J. M. and Oaks E. V. Surface presentation of Shigella flexneri invasion plasmid antigens requires the products of the spa locus. *Journal of Bacteriology*, 174(6):1990–2001, 1992.

[146] Jouihri N., Sory M.-P., Page A.-L., Gounon P., Parsot C. and Allaoui A. MxiK and MxiN interact with the Spa47 ATPase and are required for transit of the needle components MxiH and MxiI, but not of Ipa proteins, through the type III secretion apparatus of Shigella flexneri. *Molecular Microbiology*, 49(3):755–767, 2003.

[147] Magdalena J., Hachani A., Chamekh M., Jouihri N., Gounon P., Blocker A. and Allaoui A. Spa32 Regulates a Switch in Substrate Specificity of the Type III Secreton of Shigella flexneri from Needle Components to Ipa Proteins. *Journal of Bacteriology*, 184(13):3433–3441, 2002.

[148] Tamano K., Katayama E., Toyotome T. and Sasakawa C. Shigella Spa32 Is an Essential Secretory Protein for Functional Type III Secretion Machinery and Uniformity of Its Needle Length. *Journal of Bacteriology*, 184(5):1244–1252, 2002.

[149] Akeda Y. and Galan J. E. Chaperone release and unfolding of substrates in type III secretion. *Nature*, 437(7060):911–915, 2005.

[150] Veenendaal A. K. J., Hodgkinson J. L., Schwarzer L., Stabat D., Zenk S. F. and Blocker A. J. The type III secretion system needle tip complex mediates host cell sensing and translocon insertion. *Molecular Microbiology*, 63(6):1719–1730, 2007.

[151] Sani M., Allaoui A., Fusetti F., Oostergetel G. T., Keegstra W. and Boekema E. J. Structural organization of the needle complex of the type III secretion apparatus of Shigella flexneri. *Micron*, 38(3):291–301, 2007.

[152] Jin Q., Yuan Z., Xu J., Wang Y., Shen Y., Lu W., Wang J., Liu H., Yang J., Yang F., Zhang X., Zhang J., Yang G., Wu H., Qu D., Dong J., Sun L., Xue Y., Zhao A., Gao Y., Zhu J., Kan B., Ding K., Chen S., Cheng H., Yao Z., He B., Chen R., Ma D., Qiang B., Wen Y., Hou Y. and Yu J. Genome sequence of Shigella flexneri 2a: insights into pathogenicity through comparison with genomes of Escherichia coli K12 and O157. *Nucleic Acids Research*, 30(20):4432–4441, 2002.

[153] Parsot C., Hamiaux C. and Page A. L. The various and varying roles of specific chaperones in type III secretion systems. *Curr Opin Microbiol*, 6(1):7–14, 2003.

[154] Johnson S., Roversi P., Espina M., Olive A., Deane J. E., Birket S., Field T., Picking W. D., Blocker A. J., Galyov E. E., Picking W. L. and Lea S. M. Self-chaperoning of the Type III Secretion System Needle Tip Proteins IpaD and BipD. *Journal of Biological Chemistry*, 282(6):4035–4044, 2007.

[155] Ogawa M., Handa Y., Ashida H., Suzuki M. and Sasakawa C. The versatility of Shigella effectors. *Nat Rev Microbiol*, 6(1):11–6, 2008.

[156] Parsot C. Shigella type III secretion effectors: how, where, when, for what purposes? *Curr Opin Microbiol*, 12(1):110–6, 2009.

[157] Mounier J., Vasselon T., Hellio R., Lesourd M. and Sansonetti P. J. Shigella flexneri enters human colonic Caco-2 epithelial cells through the basolateral pole. *Infection and Immunity*, 60(1):237–248, 1992.

[158] Sansonetti P. J., Arondel J., Cantey J. R., Prevost M. C. and Huerre M. Infection of rabbit Peyer's patches by Shigella flexneri: effect of adhesive or invasive bacterial phenotypes on follicle-associated epithelium. *Infect Immun*, 64(7):2752–64, 1996.

[159] High N., Mounier J., Prévost M. and Sansonetti P. IpaB of Shigella flexneri causes entry into epithelial cells and escape from the phagocytic vacuole. *EMBO J*, 11(5):1991–1999, 1992.

[160] Ashida H., Ogawa M., Mimuro H. and Sasakawa C. Shigella Infection of Intestinal Epithelium and Circumvention of the Host Innate Defense System. In Sasakawa C., editor, *Molecular Mechanisms of Bacterial Infection via the Gut*, volume 337 of *Current Topics in Microbiology and Immunology*, pages 231–255. Springer Berlin Heidelberg, 2009.

[161] Gouin E., Welch M. D. and Cossart P. Actin-based motility of intracellular pathogens. *Current Opinion in Microbiology*, 8(1):35–45, 2005.

[162] Ogawa M., Suzuki T., Tatsuno I., Abe H. and Sasakawa C. IcsB, secreted via the type III secretion system, is chaperoned by IpgA and required at the post-invasion stage of Shigella pathogenicity. *Molecular Microbiology*, 48(4):913–931, 2003.

[163] Ogawa M., Yoshimori T., Suzuki T., Sagara H., Mizushima N. and Sasakawa C. Escape of Intracellular Shigella from Autophagy. *Science*, 307(5710):727–731, 2005.

[164] Gorden J. and Small P. L. Acid resistance in enteric bacteria. *Infection and Immunity*, 61(1):364–367, 1993.

[165] Lin J., Lee I. S., Frey J., Slonczewski J. L. and Foster J. W. Comparative analysis of extreme acid survival in Salmonella typhimurium, Shigella flexneri, and Escherichia coli. *Journal of Bacteriology*, 177(14):4097–104, 1995.

[166] Jennison A. V. and Verma N. K. The acid-resistance pathways of Shigella flexneri 2457T. *Microbiology*, 153(8):2593–2602, 2007.

[167] Sansonetti P. J., Arondel J., Fontaine A., d'Hauteville H. and Bernardini M. L. OmpB (osmo-regulation) and icsA (cell-to-cell spread) mutants of Shigella flexneri: vaccine candidates and probes to study the pathogenesis of shigellosis. *Vaccine*, 9(6):416–422, 1991.

[168] Miller H., Zhang J., Kuolee R., Patel G. and W. C. Intestinal M cells: the fallible sentinels? *World J Gastroenterol.*, 13(10):1477–86, 2007.

[169] Wassef J. S., Keren D. F. and Mailloux J. L. Role of M cells in initial antigen uptake and in ulcer formation in the rabbit intestinal loop model of shigellosis. *Infection and Immunity*, 57(3):858–863, 1989.

[170] Zychlinsky A., Fitting C., Cavaillon J. M. and Sansonetti P. J. Interleukin 1 is released by murine macrophages during apoptosis induced by Shigella flexneri. *J Clin Invest*, 94(3):1328–32, 1994.

[171] Zychlinsky A., Prevost M. C. and Sansonetti P. J. Shigella flexneri induces apoptosis in infected macrophages. *Nature*, 358(6382):167–169, 1992.

[172] Hilbi H., Moss J. E., Hersh D., Chen Y., Arondel J., Banerjee S., Flavell R. A., Yuan J., Sansonetti P. J. and Zychlinsky A. Shigella-induced Apoptosis Is Dependent on Caspase-1 Which Binds to IpaB. *Journal of Biological Chemistry*, 273(49):32895–32900, 1998.

[173] Fink S. L. and Cookson B. T. Apoptosis, Pyroptosis, and Necrosis: Mechanistic Description of Dead and Dying Eukaryotic Cells. *Infection and Immunity*, 73(4):1907–1916, 2005.

[174] Willingham S. B., Bergstralh D. T., O'Connor W., Morrison A. C., Taxman D. J., Duncan J. A., Barnoy S., Venkatesan M. M., Flavell R. A., Deshmukh M., Hoffman H. and Ting J. P.-Y. Microbial Pathogen-Induced Necrotic Cell Death Mediated by the Inflammasome Components CIAS1/Cryopyrin/NLRP3 and ASC. *Cell Host & Microbe*, 2(3):147 – 159, 2007.

[175] Perdomo J. J., Gounon P. and Sansonetti P. J. Polymorphonuclear leukocyte transmigration promotes invasion of colonic epithelial monolayer by Shigella flexneri. *The Journal of Clinical Investigation*, 93(2):633–643, 1994.

[176] Weinrauch Y., Drujan D., Shapiro S. D., Weiss J. and Zychlinsky A. Neutrophil elastase targets virulence factors of enterobacteria. *Nature*, 417(6884):91–94, 2002.

[177] Brinkmann V., Reichard U., Goosmann C., Fauler B., Uhlemann Y., Weiss D. S., Weinrauch Y. and Zychlinsky A. Neutrophil Extracellular Traps Kill Bacteria. *Science*, 303(5663):1532–1535, 2004.

[178] Way S. S., Borczuk A. C., Dominitz R. and Goldberg M. B. An Essential Role for Gamma Interferon in Innate Resistance to Shigella flexneri Infection. *Infection and Immunity*, 66(4):1342–1348, 1998.

[179] Clerc P. and Sansonetti P. J. Entry of Shigella flexneri into HeLa cells: evidence for directed phagocytosis involving actin polymerization and myosin accumulation. *Infection and Immunity*, 55(11):2681–2688, 1987.

[180] Romero S., Grompone G., Carayol N., Mounier J., Guadagnini S., Prevost M.-C., Sansonetti P. and TranăVanăNhieu G. ATP-Mediated Erk1/2 Activation Stimulates Bacterial Capture by Filopodia, which Precedes Shigella Invasion of Epithelial Cells. *Cell Host & Microbe*, 9(6):508–519, 2011.

[181] Hayward R. D., Cain R. J., McGhie E. J., Phillips N., Garner M. J. and Koronakis V. Cholesterol binding by the bacterial type III translocon is essential for virulence effector delivery into mammalian cells. *Molecular Microbiology*, 56(3):590–603, 2005.

[182] van der Goot F. G., van Nhieu G. T., Allaoui A., Sansonetti P. and Lafont F. Rafts Can Trigger Contact-mediated Secretion of Bacterial Effectors via a Lipid-based Mechanism. *Journal of Biological Chemistry*, 279(46):47792–47798, 2004.

[183] Lafont F., Tran Van Nhieu G., Hanada K., Sansonetti P. and van der Goot F. G. Initial steps of Shigella infection depend on the cholesterol/sphingolipid raft-mediated CD44-IpaB interaction. *EMBO J*, 21(17):4449–57, 2002.

[184] Oliferenko S., Paiha K., Harder T., Gerke V., Schwärzler C., Schwarz H., Beug H., Günthert U. and Huber L. A. Analysis of Cd44-Containing Lipid Rafts. *The Journal of Cell Biology*, 146(4):843–854, 1999.

[185] Skoudy A., Mounier J., Aruffo A., Ohayon H., Gounon P., Sansonetti P. and Tran Van Nhieu G. CD44 binds to the Shigella IpaB protein and participates in bacterial invasion of epithelial cells. *Cell Microbiol*, 2(1):19–33, 2000.

[186] Parsot C., Ménard R., Gounon P. and Sansonetti P. J. Enhanced secretion through the Shigella flexneri Mxi-Spa translocon leads to assembly of extracellular proteins into macromolecular structures. *Molecular Microbiology*, 16(2):291–300, 1995.

[187] Watarai M., Funato S. and Sasakawa C. Interaction of Ipa proteins of Shigella flexneri with alpha5beta1 integrin promotes entry of the bacteria into mammalian cells. *The Journal of Experimental Medicine*, 183(3):991–999, 1996.

[188] Watarai M., Tobe T., Yoshikawa M. and Sasakawal C. Contact of Shigella with host cells triggers release of Ipa invasins and is an essential function of invasiveness. *EMBO J*, 14(11):2461–2470, 1995.

[189] Menard R., Prevost M. C., Gounon P., Sansonetti P. and Dehio C. The secreted Ipa complex of Shigella flexneri promotes entry into mammalian cells. *Proc Natl Acad Sci U S A*, 93(3):1254–8, 1996.

[190] Watarai M., Tobe T., Yoshikawa M. and Sasakawa C. Disulfide oxidoreductase activity of Shigella flexneri is required for release of Ipa proteins and invasion of epithelial cells. *Proceedings of the National Academy of Sciences*, 92(11):4927–4931, 1995.

[191] Boquet P. and Lemichez E. Bacterial virulence factors targeting Rho GTPases: parasitism or symbiosis? *Trends in Cell Biology*, 13(5):238–246, 2003.

[192] Mounier J., Laurent V., Hall A., Fort P., Carlier M., Sansonetti P. and Egile C. Rho family GTPases control entry of Shigella flexneri into epithelial cells but not intracellular motility. *Journal of Cell Science*, 112(13):2069–2080, 1999.

[193] Dumenil G., Sansonetti P. and Tran Van Nhieu G. Src tyrosine kinase activity down-regulates Rho-dependent responses during Shigella entry into epithelial cells and stress fibre formation. *Journal of Cell Science*, 113(1):71–80, 2000.

[194] Tran Van Nhieu G., Caron E., Hall A. and Sansonetti P. J. IpaC induces actin polymerization and filopodia formation during Shigella entry into epithelial cells. *EMBO J*, 18(12):3249–62, 1999.

[195] Adam T., Arpin M., Prévost M. C., Gounon P. and Sansonetti P. J. Cytoskeletal rearrangements and the functional role of T-plastin during entry of Shigella flexneri into HeLa cells. *The Journal of Cell Biology*, 129(2):367–381, 1995.

[196] Dehio C., Prevost M. C. and Sansonetti P. J. Invasion of epithelial cells by Shigella flexneri induces tyrosine phosphorylation of cortactin by a pp60c-src-mediated signalling pathway. *EMBO J*, 14(11):2471–82, 1995.

[197] Francis C. L., Ryan T. A., Jones B. D., Smith S. J. and Falkow S. Ruffles induced by Salmonella and other stimuli direct macropinocytosis of bacteria. *Nature*, 364(6438):639–642, 1993.

[198] Sasakawa C. A new paradigm of bacteria-gut interplay brought through the study of Shigella. *Proceedings of the Japan Academy, Series B*, 86(3):229–243, 2010.

[199] Dumenil G., Olivo J. C., Pellegrini S., Fellous M., Sansonetti P. J. and Nhieu G. T. Interferon alpha inhibits a Src-mediated pathway necessary for Shigella-induced cytoskeletal rearrangements in epithelial cells. *J Cell Biol*, 143(4):1003–12, 1998.

[200] Mounier J., Popoff M. R., Enninga J., Frame M. C., Sansonetti P. J. and Van Nhieu G. T. The IpaC Carboxyterminal Effector Domain Mediates Src-Dependent Actin Polymerization during Shigella Invasion of Epithelial Cells. *PLoS Pathog*, 5(1):e1000271, 2009.

[201] Burton E. A., Plattner R. and Pendergast A. M. Abl tyrosine kinases are required for infection by Shigella flexneri. *EMBO J*, 22(20):5471–9, 2003.

[202] O'Dwyer M. E., Mauro M. J. and Druker B. J. STI571 as a Targeted Therapy for CML. *Cancer Investigation*, 21(3):429–438, 2003.

[203] Vepachedu R., Karim Z., Patel O., Goplen N. and Alam R. Unc119 Protects from Shigella Infection by Inhibiting the Abl Family Kinases. *PLoS ONE*, 4(4):e5211, 2009.

[204] Tegtmeyer N. and Backert S. Role of Abl and Src family kinases in actin-cytoskeletal rearrangements induced by the Helicobacter pylori CagA protein. *European Journal of Cell Biology*, 90(11):880–890, 2011.

[205] Abassi Y. A. and Vuori K. Tyrosine 221 in Crk regulates adhesion-dependent membrane localization of Crk and Rac and activation of Rac signaling. *EMBO J*, 21(17):4571–4582, 2002.

[206] Bougneres L., Girardin S. E., Weed S. A., Karginov A. V., Olivo-Marin J. C., Parsons J. T., Sansonetti P. J. and Van Nhieu G. T. Cortactin and Crk cooperate to trigger actin polymerization during Shigella invasion of epithelial cells. *J Cell Biol*, 166(2):225–35, 2004.

[207] Ohya K., Handa Y., Ogawa M., Suzuki M. and Sasakawa C. IpgB1 Is a Novel Shigella Effector Protein Involved in Bacterial Invasion of Host Cells. *Journal of Biological Chemistry*, 280(25):24022–24034, 2005.

[208] Hachani A., Biskri L., Rossi G., Marty A., Ménard R., Sansonetti P., Parsot C., Nhieu G. T. V., Bernardini M. L. and Allaoui A. IpgB1 and IpgB2, two homologous effectors secreted via the Mxi-Spa type III secretion apparatus, cooperate to mediate polarized cell invasion and inflammatory potential of Shigella flexenri. *Microbes and Infection*, 10(3):260–268, 2008.

[209] Handa Y., Suzuki M., Ohya K., Iwai H., Ishijima N., Koleske A. J., Fukui Y. and Sasakawa C. Shigella IpgB1 promotes bacterial entry through the ELMO–Dock180 machinery. *Nat Cell Biol*, 9(1):121–128, 2007.

[210] Brugnera E., Haney L., Grimsley C., Lu M., Walk S. F., Tosello-Trampont A.-C., Macara I. G., Madhani H., Fink G. R. and Ravichandran K. S. Unconventional Rac-GEF activity is mediated through the Dock180-ELMO complex. *Nat Cell Biol*, 4(8):574–582, 2002.

[211] Alto N. M., Shao F., Lazar C. S., Brost R. L., Chua G., Mattoo S., McMahon S. A., Ghosh P., Hughes T. R., Boone C. and Dixon J. E. Identification of a Bacterial Type III Effector Family with G Protein Mimicry Functions. *Cell*, 124(1):133–145, 2006.

[212] Huang Z., Sutton S. E., Wallenfang A. J., Orchard R. C., Wu X., Feng Y., Chai J. and Alto N. M. Structural insights into host GTPase isoform selection by a family of bacterial GEF mimics. *Nat Struct Mol Biol*, 16(8):853–860, 2009.

[213] Klink B. U., Barden S., Heidler T. V., Borchers C., Ladwein M., Stradal T. E. B., Rottner K. and Heinz D. W. Structure of Shigella IpgB2 in Complex with Human RhoA. *Journal of Biological Chemistry*, 285(22):17197–17208, 2010.

[214] Orchard R. C. and Alto N. M. Mimicking GEFs: a common theme for bacterial pathogens. *Cellular Microbiology*, 14(1):10–18, 2012.

[215] Bulgin R., Raymond B., Garnett J. A., Frankel G., Crepin V. F., Berger C. N. and Arbeloa A. Bacterial Guanine Nucleotide Exchange Factors SopE-Like and WxxxE Effectors. *Infection and Immunity*, 78(4):1417–1425, 2010.

[216] Truttmann M. C., Guye P. and Dehio C. BID-F1 and BID-F2 Domains of Bartonella henselae Effector Protein BepF Trigger Together with BepC the Formation of Invasome Structures. *PLoS ONE*, 6(10):e25106, 2011.

[217] Adam T., Giry M., Boquet P. and Sansonetti P. Rho-dependent membrane folding causes Shigella entry into epithelial cells. *EMBO J*, 15(13):3315–21, 1996.

[218] Watarai M., Kamata Y., Kozaki S. and Sasakawa C. rho, a Small GTP-Binding Protein, Is Essential for Shigella Invasion of Epithelial Cells. *The Journal of Experimental Medicine*, 185(2):281–292, 1997.

[219] Skoudy A., Nhieu G., Mantis N., Arpin M., Mounier J., Gounon P. and Sansonetti P. A functional role for ezrin during Shigella flexneri entry into epithelial cells. *Journal of Cell Science*, 112(13):2059–2068, 1999.

[220] Hirao M., Sato N., Kondo T., Yonemura S., Monden M., Sasaki T., Takai Y., Tsukita S. and Tsukita S. Regulation mechanism of ERM (ezrin/radixin/moesin) protein/plasma membrane association: possible involvement of phosphatidylinositol turnover and Rho-dependent signaling pathway. *The Journal of Cell Biology*, 135(1):37–51, 1996.

[221] Tran Van Nhieu G., Ben-Ze'ev A. and Sansonetti P. Modulation of bacterial entry into epithelial cells by association between vinculin and the Shigella IpaA invasin. *EMBO J*, 16(10):2717–2729, 1997.

[222] Izard T., Tran Van Nhieu G. and Bois P. R. Shigella applies molecular mimicry to subvert vinculin and invade host cells. *The Journal of Cell Biology*, 175(3):465–475, 2006.

[223] Hamiaux C., van Eerde A., Parsot C., Broos J. and Dijkstra B. W. Structural mimicry for vinculin activation by IpaA, a virulence factor of Shigella flexneri. *EMBO Rep*, 7(8):794–799, 2006.

[224] Bourdet-Sicard R., Rudiger M., Jockusch B. M., Gounon P., Sansonetti P. J. and Nhieu G. T. Binding of the Shigella protein IpaA to vinculin induces F-actin depolymerization. *EMBO J*, 18(21):5853–62, 1999.

[225] Ramarao N., Clainche C. L., Izard T., Bourdet-Sicard R., Ageron E., Sansonetti P. J., Carlier M.-F. and Nhieu G. T. V. Capping of actin filaments by vinculin activated by the Shigella IpaA carboxyl-terminal domain. *FEBS Letters*, 581(5):853–857, 2007.

[226] DeMali K. A., Jue A. L. and Burridge K. IpaA Targets beta1 Integrins and Rho to Promote Actin Cytoskeleton Rearrangements Necessary for Shigella Entry. *Journal of Biological Chemistry*, 281(51):39534–39541, 2006.

[227] Hänisch J., Kölm R., Wozniczka M., Bumann D., Rottner K. and Stradal T. Activation of a RhoA/Myosin II-Dependent but Arp2/3 Complex-Independent Pathway Facilitates Salmonella Invasion. *Cell Host & Microbe*, 9(4):273–285, 2011.

[228] Sousa S., Cabanes D., El-Amraoui A., Petit C., Lecuit M. and Cossart P. Unconventional myosin VIIa and vezatin, two proteins crucial for Listeria entry into epithelial cells. *Journal of Cell Science*, 117(10):2121–2130, 2004.

[229] Ezratty E. J., Partridge M. A. and Gundersen G. G. Microtubule-induced focal adhesion disassembly is mediated by dynamin and focal adhesion kinase. *Nat Cell Biol*, 7(6):581–590, 2005.

[230] Pentecost M., Kumaran J., Ghosh P. and Amieva M. R. Listeria monocytogenes Internalin B Activates Junctional Endocytosis to Accelerate Intestinal Invasion. *PLoS Pathog*, 6(5):e1000900, 2010.

[231] Niebuhr K., Giuriato S., Pedron T., Philpott D. J., Gaits F., Sable J., Sheetz M. P., Parsot C., Sansonetti P. J. and Payrastre B. Conversion of PtdIns(4,5)P(2) into PtdIns(5)P by the S.flexneri effector IpgD reorganizes host cell morphology. *EMBO J*, 21(19):5069–78, 2002.

[232] Raucher D., Stauffer T., Chen W., Shen K., Guo S., York J. D., Sheetz M. P. and Meyer T. Phosphatidylinositol 4,5-Bisphosphate Functions as a Second Messenger that Regulates Cytoskeleton–Plasma Membrane Adhesion. *Cell*, 100(2):221–228, 2000.

[233] Sechi A. and Wehland J. The actin cytoskeleton and plasma membrane connection: PtdIns(4,5)P(2) influences cytoskeletal protein activity at the plasma membrane. *Journal of Cell Science*, 113(21):3685–3695, 2000.

[234] Konradt C., Frigimelica E., Nothelfer K., Puhar A., Salgado-Pabon W., diăBartolo V., Scott-Algara D., Rodrigues C., Sansonetti P. and Phalipon A. The Shigella flexneri Type Three Secretion System Effector IpgD Inhibits T Cell Migration by Manipulating Host Phosphoinositide Metabolism. *Cell Host & Microbe*, 9(4):263–272, 2011.

[235] Pendaries C., Tronchere H., Arbibe L., Mounier J., Gozani O., Cantley L., Fry M. J., Gaits-Iacovoni F., Sansonetti P. J. and Payrastre B. PtdIns(5)P activates the host cell PI3-kinase/Akt pathway during Shigella flexneri infection. *EMBO J*, 25(5):1024–1034, 2006.

[236] Uchiya K.-i., Tobe T., Komatsu K., Suzuki T., Watarai M., Fukuda I., Yoshikawa M. and Sasakawa C. Identification of a novel virulence gene, virA, on the large plasmid of Shigella, involved in invasion and intercellular spreading. *Molecular Microbiology*, 17(2):241–250, 1995.

[237] Demers B., Sansonetti P. J. and Parsot C. Induction of type III secretion in Shigella flexneri is associated with differential control of transcription of genes encoding secreted proteins. *EMBO J*, 17(10):2894–2903, 1998.

[238] Yoshida S., Katayama E., Kuwae A., Mimuro H., Suzuki T. and Sasakawa C. Shigella deliver an effector protein to trigger host microtubule destabilization, which promotes Rac1 activity and efficient bacterial internalization. *EMBO J*, 21(12):2923–2935, 2002.

[239] Yoshida S., Handa Y., Suzuki T., Ogawa M., Suzuki M., Tamai A., Abe A., Katayama E. and Sasakawa C. Microtubule-Severing Activity of Shigella Is Pivotal for Intercellular Spreading. *Science*, 314(5801):985–989, 2006.

[240] Davis J., Wang J., Tropea J. E., Zhang D., Dauter Z., Waugh D. S. and Wlodawer A. Novel fold of VirA, a type III secretion system effector protein from Shigella flexneri. *Protein Science*, 17(12):2167–2173, 2008.

[241] Germane K. L., Ohi R., Goldberg M. B. and Spiller B. W. Structural and Functional Studies Indicate That Shigella VirA Is Not a Protease and Does Not Directly Destabilize Microtubules. *Biochemistry*, 47(39):10241–10243, 2008.

[242] Matsuzawa T., Kuwae A., Yoshida S., Sasakawa C. and Abe A. Enteropathogenic Escherichia coli activates the RhoA signaling pathway via the stimulation of GEF-H1. *EMBO J*, 23(17):3570–3582, 2004.

[243] Germane K. L. and Spiller B. W. Structural and Functional Studies Indicate That the EPEC Effector, EspG, Directly Binds p21-Activated Kinase. *Biochemistry*, 50(6):917–919, 2011.

[244] Selyunin A. S., Sutton S. E., Weigele B. A., Reddick L. E., Orchard R. C., Bresson S. M., Tomchick D. R. and Alto N. M. The assembly of a GTPase-kinase signalling complex by a bacterial catalytic scaffold. *Nature*, 469(7328):107–111, 2011.

[245] Picking W. L., Nishioka H., Hearn P. D., Baxter M. A., Harrington A. T., Blocker A. and Picking W. D. IpaD of Shigella flexneri Is Independently Required for Regulation of Ipa Protein Secretion and Efficient Insertion of IpaB and IpaC into Host Membranes. *Infection and Immunity*, 73(3):1432–1440, 2005.

[246] Harrington A., Darboe N., Kenjale R., Picking W. L., Middaugh C. R., Birket S. and Picking W. D. Characterization of the Interaction of Single Tryptophan Containing Mutants of IpaC from Shigella flexneri with Phospholipid Membranes. *Biochemistry*, 45(2):626–636, 2006.

[247] Osiecki J. C., Barker J., Picking W. L., Serfis A. B., Berring E., Shah S., Harrington A. and Picking W. D. IpaC from Shigella and SipC from Salmonella possess similar biochemical properties but are functionally distinct. *Molecular Microbiology*, 42(2):469–481, 2001.

[248] Bernardini M. L., Mounier J., d'Hauteville H., Coquis-Rondon M. and Sansonetti P. J. Identification of icsA, a plasmid locus of Shigella flexneri that governs bacterial intra- and intercellular spread through interaction with F-actin. *Proc Natl Acad Sci U S A*, 86(10):3867–71, 1989.

[249] Goldberg M. B., Bârzu O., Parsot C. and Sansonetti P. J. Unipolar localization and ATPase activity of IcsA, a Shigella flexneri protein involved in intracellular movement. *Journal of Bacteriology*, 175(8):2189–2196, 1993.

[250] Egile C., D'Hauteville H., Parsot C. and Sansonetti P. J. SopA, the outer membrane protease responsible for polar localization of IcsA in Shigella flexneri. *Molecular Microbiology*, 23(5):1063–1073, 1997.

[251] Santapaola D., Del Chierico F., Petrucca A., Uzzau S., Casalino M., Colonna B., Sessa R., Berlutti F. and Nicoletti M. Apyrase, the Product of the Virulence Plasmid-Encoded phoN2 (apy) Gene of Shigella flexneri, Is Necessary for Proper Unipolar IcsA Localization and for Efficient Intercellular Spread. *Journal of Bacteriology*, 188(4):1620–1627, 2006.

[252] Egile C., Loisel T. P., Laurent V., Li R., Pantaloni D., Sansonetti P. J. and Carlier M. F. Activation of the CDC42 effector N-WASP by the Shigella flexneri IcsA protein promotes actin nucleation by Arp2/3 complex and bacterial actin-based motility. *J Cell Biol*, 146(6):1319–32, 1999.

[253] Rathman M., de Lanerolle P., Ohayon H., Gounon P. and Sansonetti P. Myosin light chain kinase plays an essential role in S. flexneri dissemination. *Journal of Cell Science*, 113(19):3375–3386, 2000.

[254] Page A.-L., Ohayon H., Sansonetti P. J. and Parsot C. The secreted IpaB and IpaC invasins and their cytoplasmic chaperone IpgC are required for intercellular dissemination of Shigella flexneri. *Cellular Microbiology*, 1(2):183–193, 1999.

[255] Mostowy S., Bonazzi M., Hamon M. A., Tham T. N., Mallet A., Lelek M., Gouin E., Demangel C., Brosch R., Zimmer C., Sartori A., Kinoshita M., Lecuit M. and Cossart P. Entrapment of Intracytosolic Bacteria by Septin Cage-like Structures. *Cell Host & Microbe*, 8(5):433–444, 2010.

[256] Mizushima N. Autophagy: process and function. *Genes & Development*, 21(22):2861–2873, 2007.

[257] Deretic V. Autophagy in infection. *Current Opinion in Cell Biology*, 22(2):252 – 262, 2010.

[258] Ogawa M. and Sasakawa C. Shigella and Autophagy. *Autophagy*, 2(1554-8627):171–174, 2006.

[259] Lucchini S., Liu H., Jin Q., Hinton J. C. D. and Yu J. Transcriptional Adaptation of Shigella flexneri during Infection of Macrophages and Epithelial Cells: Insights into the Strategies of a Cytosolic Bacterial Pathogen. *Infect. Immun.*, 73(1):88–102, 2005.

[260] Reeves S. A., Torres A. G. and Payne S. M. TonB Is Required for Intracellular Growth and Virulence of Shigella dysenteriae. *Infection and Immunity*, 68(11):6329–6336, 2000.

[261] Noriega F. R., Losonsky G., Lauderbaugh C., Liao F. M., Wang J. Y. and Levine M. M. Engineered deltaguaB-A deltavirG Shigella flexneri 2a strain CVD 1205: construction, safety, immunogenicity, and potential efficacy as a mucosal vaccine. *Infection and Immunity*, 64(8):3055–61, 1996.

[262] Cersini A., Salvia A. M. and Bernardini M. L. Intracellular Multiplication and Virulence of Shigella flexneri Auxotrophic Mutants. *Infection and Immunity*, 66(2):549–557, 1998.

[263] Cersini A., Martino M. C., Martini I., Rossi G. and Bernardini M. L. Analysis of Virulence and Inflammatory Potential of Shigella flexneri Purine Biosynthesis Mutants. *Infection and Immunity*, 71(12):7002–7013, 2003.

[264] Runyen-Janecky L. J. and Payne S. M. Identification of Chromosomal Shigella flexneri Genes Induced by the Eukaryotic Intracellular Environment. *Infect. Immun.*, 70(8):4379–4388, 2002.

[265] Daugherty A., Suvarnapunya A. E. and Runyen-Janecky L. The role of OxyR and SoxRS in oxidative stress survival in Shigella flexneri. *Microbiological Research*, page In press, 2011.

[266] Ramel D., Lagarrigue F., Pons V., Mounier J., Dupuis-Coronas S., Chicanne G., Sansonetti P. J., Gaits-Iacovoni F., Tronchere H. and Payrastre B. Shigella flexneri Infection Generates the Lipid PI5P to Alter Endocytosis and Prevent Termination of EGFR Signaling. *Sci. Signal.*, 4(191):ra61, 2011.

[267] Osmani N., Peglion F., Chavrier P. and Etienne-Manneville S. Cdc42 localization and cell polarity depend on membrane traffic. *The Journal of Cell Biology*, 191(7):1261–1269, 2010.

[268] Misselwitz B., Dilling S., Vonaesch P., Sacher R., Snijder B., Schlumberger M., Rout S., Stark M., Mering C. v., Pelkmans L. and Hardt W.-D. RNAi screen of Salmonella invasion shows role of COPI in membrane targeting of cholesterol and Cdc42. *Mol Syst Biol*, 7:–, 2011.

[269] Page A.-L., Sansonetti P. and Parsot C. Spa15 of Shigella flexneri, a third type of chaperone in the type III secretion pathway. *Molecular Microbiology*, 43(6):1533–1542, 2002.

[270] Faherty C. S. and Maurelli A. T. Spa15 of Shigella flexneri Is Secreted through the Type III Secretion System and Prevents Staurosporine-Induced Apoptosis. *Infection and Immunity*, 77(12):5281–5290, December 2009.

[271] Cliffe L. J., Humphreys N. E., Lane T. E., Potten C. S., Booth C. and Grencis R. K. Accelerated Intestinal Epithelial Cell Turnover: A New Mechanism of Parasite Expulsion. *Science*, 308(5727):1463–1465, 2005.

[272] Kim M., Ogawa M., Fujita Y., Yoshikawa Y., Nagai T., Koyama T., Nagai S., Lange A., Fassler R. and Sasakawa C. Bacteria hijack integrin-linked kinase to stabilize focal adhesions and block cell detachment. *Nature*, 459(7246):578–582, 2009.

[273] Iwai H., Kim M., Yoshikawa Y., Ashida H., Ogawa M., Fujita Y., Muller D., Kirikae T., Jackson P. K., Kotani S. and Sasakawa C. A bacterial effector targets Mad2L2, an APC inhibitor, to modulate host cell cycling. *Cell*, 130(4):611–23, 2007.

[274] Carneiro L. A., Travassos L. H., Soares F., Tattoli I., Magalhaes J. G., Bozza M. T., Plotkowski M. C., Sansonetti P. J., Molkentin J. D., Philpott D. J. and Girardin S. E. Shigella Induces Mitochondrial Dysfunction and Cell Death in Nonmyleoid Cells. *Cell Host & Microbe*, 5(2):123–136, 2009.

[275] Lembo-Fazio L., Nigro G., Noel G., Rossi G., Chiara F., Tsilingiri K., Rescigno M., Rasola A. and Bernardini M. L. Gadd45[alpha] activity is the principal effector of Shigella mitochondria-dependent epithelial cell death in vitro and ex vivo. *Cell Death and Dis*, 2:e122–, 2011.

[276] Ninomiya-Tsuji J., Kishimoto K., Hiyama A., Inoue J., Cao Z. and Matsumoto K. The kinase TAK1 can activate the NIK-I kappaB as well as the MAP kinase cascade in the IL-1 signalling pathway. *Nature*, 398(6724):252–6, 1999.

[277] Ashida H., Ogawa M., Mimuro H., Kobayashi T., Sanada T. and Sasakawa C. Shigella are versatile mucosal pathogens that circumvent the host innate immune system. *Current Opinion in Immunology*, 23(4):448–455, 2011.

[278] Kim D. W., Lenzen G., Page A. L., Legrain P., Sansonetti P. J. and Parsot C. The Shigella flexneri effector OspG interferes with innate immune responses by targeting ubiquitin-conjugating enzymes. *Proc Natl Acad Sci U S A*, 102(39):14046–51, 2005.

[279] Newton H. J., Pearson J. S., Badea L., Kelly M., Lucas M., Holloway G., Wagstaff K. M., Dunstone M. A., Sloan J., Whisstock J. C., Kaper J. B., Robins-Browne R. M., Jans D. A., Frankel G., Phillips A. D., Coulson B. S. and Hartland E. L. The Type III Effectors NleE and NleB from Enteropathogenic E. coli and OspZ from Shigella Block Nuclear Translocation of NF-kappaB p65. *PLoS Pathog*, 6(5):e1000898, 2010.

[280] Ashida H., Kim M., Schmidt-Supprian M., Ma A., Ogawa M. and Sasakawa C. A bacterial E3 ubiquitin ligase IpaH9.8 targets NEMO/IKK[gamma] to dampen the host NF-[kappa]B-mediated inflammatory response. *Nat Cell Biol*, 12(1):66–73, 2010.

[281] Okuda J., Toyotome T., Kataoka N., Ohno M., Abe H., Shimura Y., Seyedarabi A., Pickersgill R. and Sasakawa C. Shigella effector IpaH9.8 binds to a splicing factor U2AF(35) to modulate host immune responses. *Biochem Biophys Res Commun*, 333(2):531–9, 2005.

[282] Rohde J. R., Breitkreutz A., Chenal A., Sansonetti P. J. and Parsot C. Type III Secretion Effectors of the IpaH Family Are E3 Ubiquitin Ligases. *Cell Host & Microbe*, 1(1):77–83, 2007.

[283] Ashida H., Toyotome T., Nagai T. and Sasakawa C. Shigella chromosomal IpaH proteins are secreted via the type III secretion system and act as effectors. *Molecular Microbiology*, 63(3):680–693, 2007.

[284] Zurawski D. V., Mumy K. L., Faherty C. S., McCormick B. A. and Maurelli A. T. Shigella flexneri type III secretion system effectors OspB and OspF target the nucleus to downregulate the host inflammatory response via interactions with retinoblastoma protein. *Mol Microbiol*, 71(2):350–68, 2009.

[285] Jupp O. J., Vandenabeele P. and MacEwan D. J. Distinct regulation of cytosolic phospholipase A2 phosphorylation, translocation, proteolysis and activation by tumour necrosis factor-receptor subtypes. *Biochem J*, 374(Pt 2):453–61, 2003.

[286] Zurawski D. V., Mitsuhata C., Mumy K. L., McCormick B. A. and Maurelli A. T. OspF and OspC1 are Shigella flexneri type III secretion system effectors that are required for postinvasion aspects of virulence. *Infect Immun*, 74(10):5964–76, 2006.

[287] Zurawski D. V., Mumy K. L., Badea L., Prentice J. A., Hartland E. L., McCormick B. A. and Maurelli A. T. The NleE/OspZ family of effector proteins is required for polymorphonuclear transepithelial migration, a characteristic shared by enteropathogenic Escherichia coli and Shigella flexneri infections. *Infect Immun*, 76(1):369–79, 2008.

[288] Mumy K. L., Bien J. D., Pazos M. A., Gronert K., Hurley B. P. and McCormick B. A. Distinct isoforms of phospholipase A2 mediate the ability of Salmonella enterica serotype typhimurium and Shigella flexneri to induce the transepithelial migration of neutrophils. *Infect Immun*, 76(8):3614–27, 2008.

[289] Raqib R., Sarker P., Bergman P., Ara G., Lindh M., Sack D. A., Nasirul Islam K. M., Gudmundsson G. H., Andersson J. and Agerberth B. Improved outcome in shigellosis associated with butyrate induction of an endogenous peptide antibiotic. *Proceedings of the National Academy of Sciences*, 103(24):9178–9183, 2006.

[290] Islam D., Bandholtz L., Nilsson J., Wigzell H., Christensson B., Agerberth B. and Gudmundsson G. H. Downregulation of bactericidal peptides in enteric infections: A novel immune escape mechanism with bacterial DNA as a potential regulator. *Nat Med*, 7(2):180–185, 2001.

[291] Sperandio B., Regnault B., Guo J., Zhang Z., Stanley S. L., Sansonetti P. J. and Pédron T. Virulent Shigella flexneri subverts the host innate immune response through manipulation of antimicrobial peptide gene expression. *The Journal of Experimental Medicine*, 205(5):1121–1132, 2008.

[292] Eilers B., Mayer-Scholl A., Walker T., Tang C., Weinrauch Y. and Zychlinsky A. Neutrophil antimicrobial proteins enhance Shigella flexneri adhesion and invasion. *Cellular Microbiology*, 12(8):1134–1143, 2010.

[293] Reiterer V., Grossniklaus L., Tschon T., Kasper C. A., Sorg I. and Arrieumerlou C. Shigella flexneri type III secreted effector OspF reveals new crosstalks of proinflammatory signaling pathways during bacterial infection. *Cellular Signalling*, 23(7):1188–1196, 2011.

[294] Kim M. L., Sorg I. and Arrieumerlou C. Endocytosis-Independent Function of Clathrin Heavy Chain in the Control of Basal NF-kappaB Activation. *PLoS ONE*, 6(2):e17158, 2011.

[295] Sansonetti P. and Arondel J. Construction and evaluation of a double mutant of Shigella flexneri as a candidate for oral vaccination against shigellosis. *Vaccine*, 7(5):443–450, 1989.

[296] Sansonetti P. J., Hale T. L., Dammin G. J., Kapfer C., Collins H. H. and Formal S. B. Alterations in the pathogenicity of Escherichia coli K-12 after transfer of plasmid and chromosomal genes from Shigella flexneri. *Infection and Immunity*, 39(3):1392–1402, 1983.

[297] Serény B., Tenner C. and Rácz P. Immunogenicity of living attenuated shigellae. *Acta microbiologica Academiae Scientiarum Hungaricae*, 18(4):239–245, 1971.

[298] Fernandez M.-I., Regnault B., Mulet C., Tanguy M., Jay P., Sansonetti P. J. and Pédron T. Maturation of Paneth Cells Induces the Refractory State of Newborn Mice to Shigella Infection. *The Journal of Immunology*, 180(7):4924–4930, 2008.

[299] Fernandez M. I., Thuizat A., Pedron T., Neutra M., Phalipon A. and Sansonetti P. J. A newborn mouse model for the study of intestinal pathogenesis of shigellosis. *Cell Microbiol*, 5(7):481–91, 2003.

[300] Mallett C., VanDeVerg L., Collins H. and Hale T. Evaluation of Shigella vaccine safety and efficacy in an intranasally challenged mouse model. *Vaccine*, 11(2):190–196, 1993.

[301] Zhang Z., Jin L., Champion G., Seydel K. B. and Stanley S. L. Shigella Infection in a SCID Mouse-Human Intestinal Xenograft Model: Role for Neutrophils in Containing Bacterial Dissemination in Human Intestine. *Infection and Immunity*, 69(5):3240–3247, 2001.

[302] Shim D.-H., Suzuki T., Chang S.-Y., Park S.-M., Sansonetti P. J., Sasakawa C. and Kweon M.-N. New Animal Model of Shigellosis in the Guinea Pig: Its Usefulness for Protective Efficacy Studies. *The Journal of Immunology*, 178(4):2476–2482, 2007.

[303] Barman S., Kumar R., Chowdhury G., Rani Saha D., Wajima T., Hamabata T., Ramamurthy T., Balakrish Nair G., Takeda Y. and Koley H. Live non-invasive Shigella dysenteriae 1 strain induces homologous protective immunity in a guinea pig colitis model. *Microbiology and Immunology*, 55(10):683–693, 2011.

[304] Kasper C. A., Sorg I., Schmutz C., Tschon T., Wischnewski H., Kim M. L. and Arrieumerlou C. Cell-Cell Propagation of NF-kappaB Transcription Factor and MAP Kinase Activation Amplifies Innate Immunity against Bacterial Infection. *Immunity*, 33(5):804–816, 2010.

[305] Kadner R. J., Murphy G. P. and Stephens C. M. Two mechanisms for growth inhibition by elevated transport of sugar phosphates in Escherichia coli. *Journal of General Microbiology*, 138(10):2007–2014, 1992.

[306] Island M. D., Wei B. Y. and Kadner R. J. Structure and function of the uhp genes for the sugar phosphate transport system in Escherichia coli and Salmonella typhimurium. *Journal of Bacteriology*, 174(9):2754–2762, 1992.

[307] Mollenhauer H. H., Morre D. J. and Rowe L. D. Alteration of intracellular traffic by monensin; mechanism, specificity and relationship to toxicity. *Biochim Biophys Acta*, 1031(2):225–46, 1990.

[308] Carpenter A. E., Jones T. R., Lamprecht M. R., Clarke C., Kang I. H., Friman O., Guertin D. A., Chang J. H., Lindquist R. A., Moffat J., Golland P. and Sabatini D. M. CellProfiler: image analysis software for identifying and quantifying cell phenotypes. *Genome Biol*, 7(10):R100, 2006.

[309] Kittler R., Putz G., Pelletier L., Poser I., Heninger A.-K., Drechsel D., Fischer S., Konstantinova I., Habermann B., Grabner H., Yaspo M.-L., Himmelbauer H., Korn B., Neugebauer K., Pisabarro M. T. and Buchholz F. An endoribonuclease-prepared siRNA screen in human cells identifies genes essential for cell division. *Nature*, 432(7020):1036–1040, 2004.

[310] Bauch A., Adamczyk I., Buczek P., Elmer F.-J., Enimanev K., Glyzewski P., Kohler M., Pylak T., Quandt A., Ramakrishnan C., Beisel C., Malmstrom L., Aebersold R. and Rinn B. openBIS: a flexible framework for managing and analyzing complex data in biology research. *BMC Bioinformatics*, 12(1):468, 2011.

[311] Snijder B., Sacher R., Ramo P., Damm E.-M., Liberali P. and Pelkmans L. Population context determines cell-to-cell variability in endocytosis and virus infection. *Nature*, 461(7263):520–523, 2009.

[312] Rämö P., Sacher R., Snijder B., Begemann B. and Pelkmans L. CellClassifier: supervised learning of cellular phenotypes. *Bioinformatics*, 25(22):3028–3030, 2009.

[313] Yang L., Cranson D. and Trinkaus-Randall V. Cellular injury induces activation of MAPK via P2Y receptors. *J Cell Biochem*, 91(5):938–50, 2004.

[314] Block E. R. and Klarlund J. K. Wounding Sheets of Epithelial Cells Activates the Epidermal Growth Factor Receptor through Distinct Short- and Long-Range Mechanisms. *Molecular Biology of the Cell*, 19(11):4909–4917, 2008.

[315] Hamada N., Matsumoto H., Hara T. and Kobayashi Y. Intercellular and intracellular signaling pathways mediating ionizing radiation-induced bystander effects. *J Radiat Res (Tokyo)*, 48(2):87–95, 2007.

[316] Patel S. J., King K. R., Casali M. and Yarmush M. L. DNA-triggered innate immune responses are propagated by gap junction communication. *Proc Natl Acad Sci U S A*, 106(31):12867–72, 2009.

[317] Solan J. L. and Lampe P. D. Connexin phosphorylation as a regulatory event linked to gap junction channel assembly. *Biochimica et Biophysica Acta (BBA) - Biomembranes*, 1711(2):154–163, 2005.

[318] Tran Van Nhieu G., Clair C., Bruzzone R., Mesnil M., Sansonetti P. and Combettes L. Connexin-dependent inter-cellular communication increases invasion and dissemination of Shigella in epithelial cells. *Nat Cell Biol*, 5(8):720–6, 2003.

[319] Kiefer P., Delmotte N. and Vorholt J. A. Nanoscale Ion-Pair Reversed-Phase HPLC–MS for Sensitive Metabolome Analysis. *Analytical Chemistry*, 83(3):850–855, 2011.

[320] Stork P. J. and Schmitt J. M. Crosstalk between cAMP and MAP kinase signaling in the regulation of cell proliferation. *Trends in Cell Biology*, 12(6):258–266, 2002.

[321] Ghosh S. and Baltimore D. Activation in vitro of NF-kappaB by phosphorylation of its inhibitor IkappaB. *Nature*, 344(6267):678–682, 1990.

[322] Mehta P. P., Yamamoto M. and Rose B. Transcription of the gene for the gap junctional protein connexin43 and expression of functional cell-to-cell channels are regulated by cAMP. *Molecular Biology of the Cell*, 3(8):839–50, 1992.

[323] Kanemitsu M. Y. and Lau A. F. Epidermal growth factor stimulates the disruption of gap junctional communication and connexin43 phosphorylation independent of 12-0-tetradecanoylphorbol 13-acetate-sensitive protein kinase C: the possible involvement of mitogen-activated protein kinase. *Molecular Biology of the Cell*, 4(8):837–48, 1993.

[324] Kwak B. R., Sáez J. C., Wilders R., Chanson M., Fishman G. I., Hertzberg E. L., Spray D. C. and Jongsma H. J. Effects of cGMP-dependent phosphorylation on rat and human connexin43 gap junction channels. *Pflügers Archiv European Journal of Physiology*, 430:770–778, 1995.

[325] Lampe P. D., TenBroek E. M., Burt J. M., Kurata W. E., Johnson R. G. and Lau A. F. Phosphorylation of Connexin43 on Serine368 by Protein Kinase C Regulates Gap Junctional Communication. *The Journal of Cell Biology*, 149(7):1503–1512, 2000.

[326] TenBroek E. M., Lampe P. D., Solan J. L., Reynhout J. K. and Johnson R. G. Ser364 of connexin43 and the upregulation of gap junction assembly by cAMP. *The Journal of Cell Biology*, 155(7):1307–1318, 2001.

[327] Sáez J. C., Berthoud V. M., Brañes M. C., Martínez A. D. and Beyer E. C. Plasma Membrane Channels Formed by Connexins: Their Regulation and Functions. *Physiological Reviews*, 83(4):1359–1400, 2003.

[328] Neijssen J., Herberts C., Drijfhout J. W., Reits E., Janssen L. and Neefjes J. Cross-presentation by intercellular peptide transfer through gap junctions. *Nature*, 434(7029):83–8, 2005.

[329] Handel A., Yates A., Pilyugin S. S. and Antia R. Sharing the burden: antigen transport and firebreaks in immune responses. *Journal of The Royal Society Interface*, 6(34):447–454, 2009.

[330] Matsue H., Yao J., Matsue K., Nagasaka A., Sugiyama H., Aoki R., Kitamura M. and Shimada S. Gap Junction-Mediated Intercellular Communication between Dendritic Cells (DCs) Is Required for Effective Activation of DCs. *The Journal of Immunology*, 176(1):181–190, 2006.

[331] Schajnovitz A., Itkin T., D'Uva G., Kalinkovich A., Golan K., Ludin A., Cohen D., Shulman Z., Avigdor A., Nagler A., Kollet O., Seger R. and Lapidot T. CXCL12 secretion by bone marrow stromal cells is dependent on cell contact and mediated by connexin-43 and connexin-45 gap junctions. *Nat Immunol*, 12(5):391–398, 2011.

[332] Patel S. J., Milwid J. M., King K. R., Bohr S., Iracheta-Velle A., Li M., Vitalo A., Parekkadan B., Jindal R. and Yarmush M. L. Gap junction inhibition prevents drug-induced liver toxicity and fulminant hepatic failure. *Nat Biotech*, 30(2):179–183, 2012.

[333] Fischer N. O., Mbuy G. N. and Woodruff R. I. HSV-2 disrupts gap junctional intercellular communication between mammalian cells in vitro. *Journal of Virological Methods*, 91(2):157–166, 2001.

[334] Ceelen L., Haesebrouck F., Vanhaecke T., Rogiers V. and Vinken M. Modulation of connexin signaling by bacterial pathogens and their toxins. *Cellular and Molecular Life Sciences*, 68:3047–3064, 2011.

[335] Eckmann L., Kagnoff M. F. and Fierer J. Epithelial cells secrete the chemokine interleukin-8 in response to bacterial entry. *Infect Immun*, 61(11):4569–74, 1993.

[336] Dolowschiak T., Chassin C., Ben Mkaddem S., Fuchs T. M., Weiss S., Vandewalle A. and Hornef M. W. Potentiation of Epithelial Innate Host Responses by Intercellular Communication. *PLoS Pathog*, 6(11):e1001194, 2010.

[337] Leybaert L., Paemeleire K., Strahonja A. and Sanderson M. J. Inositol-trisphosphate-dependent intercellular calcium signaling in and between astrocytes and endothelial cells. *Glia*, 24(4):398–407, 1998.

[338] Bleasdale J. E., Bundy G. L., Bunting S., Fitzpatrick F. A., Huff R. M., Sun F. F. and Pike J. E. Inhibition of phospholipase C dependent processes by U-73, 122. *Adv Prostaglandin Thromboxane Leukot Res*, 19:590–3, 1989.

[339] Cohen-Saidon C., Cohen A. A., Sigal A., Liron Y. and Alon U. Dynamics and Variability of ERK2 Response to EGF in Individual Living Cells. *Molecular Cell*, 36(5):885–893, 2009.

[340] Schmid J. A., Birbach A., Hofer-Warbinek R., Pengg M., Burner U., Furtmüller P. G., Binder B. R. and de Martin R. Dynamics of NF-kappaB and I-kappaB Studied with Green Fluorescent Protein (GFP) Fusion Proteins. *Journal of Biological Chemistry*, 275(22):17035–17042, 2000.

[341] Ramanan S. and Brink P. Exact solution of a model of diffusion in an infinite chain or monolayer of cells coupled by gap junctions. *Biophysical Journal*, 58(3):631–639, 1990.

[342] Christ G., Brink P. and Ramanan S. Dynamic gap junctional communication: a delimiting model for tissue responses. *Biophysical Journal*, 67(3):1335–1344, 1994.

[343] Olesen N. E., Hofgaard J. P., Holstein-Rathlou N.-H., Nielsen M. S. and Jacobsen J. C. B. Estimation of the effective intercellular diffusion coefficient in cell monolayers coupled by gap junctions. *European Journal of Pharmaceutical Sciences*, page In press, 2011.

[344] Hardt W.-D. Infected Cell in Trouble: Bystander Cells Ring the Bell. *Immunity*, 33(5):652–654, 2010.

[345] Mrsny R. J., Gewirtz A. T., Siccardi D., Savidge T., Hurley B. P., Madara J. L. and McCormick B. A. Identification of hepoxilin A3 in inflammatory events: a required role in neutrophil migration across intestinal epithelia. *Proc Natl Acad Sci U S A*, 101(19):7421–6, 2004.

# Acknowledgements

I owe deep gratitude to...

- ... my supervisor Cécile Arrieumerlou for giving me the opportunity to do my PhD in her lab and for getting the chance to work on exciting projects. I really appreciated the encouraging discussions and all the brilliant ideas for experiments.
- ... my committee members Prof. Christoph Dehio and Prof. Dirk Bumann for their interest in my projects and the valuable inputs provided during our meetings.
- ... the group members Isabel Sorg, Therese Tschon, Michaela Hanisch, Christoph Schmutz, Roland Dreier and Klaus Handloser for a cheerful working atmosphere, coffee breaks, numerous chats, countless laughs and lengthy discussions (not only about soccer!).
- ... the former group members Hyun Gyeong Jeong, Veronika Reiterer, Sonja Weichsel, Harry Wischnewski, Gregory Melroe, Man Lyang Kim and Lars Grossniklaus for the great time we had together.
- ... the members of the Basel InfectX team for a joyful and supportive lab atmosphere "upstairs". A special thank goes to Mario Emmenlauer and Pauli Rämö for assisting me in my relentless pursuit of data.
- ... the people from research IT: Michael Podvinec, Eva Pujadas and Vincent Rouilly for a fantastic work in progress.
- ... the floor managers Roger Sauder, Marina Kuhn and their team for making sure that we can truly focus on science.
- ... the Swiss National Science Foundation and especially the Werner Siemens Foundation for funding.
- ... Angie Klarer, Prof. Urs Jenal and Prof. Joachim Seelig for providing opportunities for excellence and for memorable city trips.
- ... my family for the interest in my work and the continuous support along my way.
- ... my girlfriend, Claudia Lenz, for her understanding when lab work was taking a little longer (again), for cheering me up when things didn't work out as planned and simply for being there for me at all times.

# List of Publications

- Boehm A, Kaiser M, Li H, Spangler C, **Kasper CA**, Ackermann M, Kaever V, Sourjik V, Roth V, Jenal U. Second messenger-mediated adjustment of bacterial swimming velocity. *Cell*, 141(1):107–16, 2010.
- Kim ML, Jeong HG, **Kasper CA**, Arrieumerlou C. IKK$\alpha$ contributes to canonical NF-$\kappa$B activation downstream of Nod1-mediated peptidoglycan recognition. *PLoS One*, 5(10):e15371, 2010.
- **Kasper CA**, Sorg I, Schmutz C, Tschon T, Wischnewski H, Kim ML, Arrieumerlou C. Cell-cell propagation of NF-$\kappa$B transcription factor and MAP kinase activation amplifies innate immunity against bacterial infection. *Immunity*, 33(5):804–16, 2010.
- Reiterer V, Grossniklaus L, Tschon T, **Kasper CA**, Sorg I, Arrieumerlou C. *Shigella flexneri* type III secreted effector OspF reveals new crosstalks of proinflammatory signaling pathways during bacterial infection. *Cell Signal*, 23(7):1188–96, 2011.

# Curriculum vitae

## Personal data

| | |
|---|---|
| Name: | Christoph Kasper |
| Date of birth: | 4th of October, 1984 |
| Place of birth: | Langenthal BE |
| Place of citizenship: | Zetzwil AG |

## Education

| | |
|---|---|
| Mar. 2008 - present: | PhD Thesis<br>Thesis committee: Prof. Dr. Cécile Arrieumerlou (PI),<br>Prof. Dr. Christoph Dehio, Prof. Dr. Dirk Bumann<br>Focal Area Infection Biology<br>Biozentrum, University of Basel |
| Sep. 2006 - Feb. 2008: | Master of Science in Molecular Biology<br>Major in Infection Biology<br>Thesis committee: Prof. Dr. Cécile Arrieumerlou (PI),<br>Prof. Dr. Guy Cornelis<br>Focal Area Infection Biology<br>Biozentrum, University of Basel |
| Oct. 2003 - Jul. 2006: | Bachelor of Science in Biology<br>Major in Molecular Biology<br>University of Basel |
| Aug. 1996 - Sep. 2003: | Grammar school Olten SO<br>Higher education entrance qualification<br>Main subjects mathematics and natural sciences |